

**Identification and Determination of Selected Pharmaceuticals and Their Dead
End Degradation Products in Degradation Testing and the Aquatic
Environment**

Kumulative Dissertationsschrift zur Erlangung des akademischen Grades
Doktor der Naturwissenschaften
(Dr. rer. nat.)

Angefertigt am Institut für Nachhaltige Chemie und Umweltchemie
Leuphana Universität Lüneburg

vorgelegte Dissertation von

Waleed Mohamed Mamdouh Mahmoud Ahmed

geb. October 01.1981 in: Ismailia, Ägypten

Eingereicht am: 05.08.2013

Betreuer und Erstgutachter: Prof. Dr. rer. nat. Klaus Kümmerer

Zweitgutachter: Prof. Dr. Benoit Roig

Drittgutachter: PD Dr. Wolfgang Ahlf

Tag der Disputation: 04.12.2013

Die einzelnen Beiträge des kumulativen Dissertationsvorhabens sind oder werden wie folgt in Zeitschriften veröffentlicht:

1. **Waleed M. M. Mahmoud**, Klaus Kümmerer (2012) Captopril and its dimer captopril disulfide: photodegradation, aerobic biodegradation and identification of transformation products by HPLC-UV and LC-ion trap-MSⁿ. Chemosphere 88(10): 1170–1177. DOI: 10.1016/j.chemosphere.2012.03.064.
2. Marcelo L Wilde, **Waleed M. M. Mahmoud**, Klaus Kümmerer, Ayrton Figueiredo Martins (2013) Oxidation–coagulation of β -blockers by $K_2Fe^{VI}O_4$ in hospital wastewater: Assessment of degradation products and biodegradability. Science of the Total Environment 452–453: 137–147. DOI: 10.1016/j.scitotenv.2013.01.059
3. **Waleed M. M. Mahmoud**, Nareman D. H. Khaleel, Ghada M. Hadad, Randa A. Abdel- Salam, Annette Haiß, Klaus Kümmerer (2013) Simultaneous determination of 11 sulfonamides by HPLC–UV and application for fast screening of their aerobic elimination and biodegradation in a simple test. CLEAN – Soil, Air, Water. DOI: 10.1002/clen.201200508
4. Nareman D. H. Khaleel, **Waleed M. M. Mahmoud**, Ghada M. Hadad, Randa A. Abdel- Salam, Klaus Kümmerer (2013) Photolysis of sulfamethoxypyridazine in various aqueous media: aerobic biodegradation and photoproducts identification by LC-UV-MS/MS. Journal of Hazardous Materials 244–245: 654–661. DOI:10.1016/j.jhazmat.2012.10.059
5. Faten Sleman, **Waleed M. M. Mahmoud**, Rolf Schubert, Klaus Kümmerer (2012) Photodegradation, photocatalytic and aerobic biodegradation of sulfisomidine and identification of transformation products By LC–UV-MS/MS. CLEAN – Soil, Air, Water 40 (11) 1244–1249. DOI: 10.1002/clen.201100485.
6. **Waleed M. M. Mahmoud**, Christoph Trautwein, Christoph Leder, Klaus Kümmerer (2013) Aquatic photochemistry, abiotic and aerobic biodegradability of thalidomide: identification of stable transformation products by LC-UV-MSⁿ. Science of the Total Environment. 463–464: 140–150. DOI: 10.1016/j.scitotenv.2013.05.082
7. **Waleed M. M. Mahmoud**, Anju P. Toolaram, Jakob Menz, Christoph Leder, Mandy Schneider, Klaus Kümmerer (2013) Identification of phototransformation products of Thalidomide and mixture toxicity assessment: an experimental and quantitative structural activity relationships (QSAR) approach. Water Research. DOI: 10.1016/j.watres.2013.11.014.

Nachdruck mit freundlicher Genehmigung des Chemosphere (Elsevier), Journal of Hazardous Materials (Elsevier), Science of the Total Environment (Elsevier), Water Research (Elsevier), und CLEAN – Soil, Air, Water (Wiley-VCH Verlag GmbH & Co. KGaA).

Gedruckt mit Unterstützung des Deutschen Akademischen Austauschdienstes.

**Identification and Determination of Selected Pharmaceuticals and Their Dead
End Degradation Products in Degradation Testing and the Aquatic
Environment**

This cumulative thesis and the publications listed on the following page are
submitted to the Faculty of Sustainability of Leuphana University Lüneburg to earn
the academic degree of
Doctor of Natural Science (Dr. rer. nat.)

Carried out at the Institute of Sustainable and Environmental Chemistry
Leuphana University of Lüneburg

Dissertation submitted by

Waleed Mohamed Mamdouh Mahmoud Ahmed

Born on October 01.1981 in: Ismailia, Egypt

Submitted on: 05.08.2013

Doctoral advisor and first reviewer: Prof. Dr. rer. nat. Klaus Kümmerer

Second reviewer: Prof. Dr. Benoit Roig

Third reviewer: PD Dr. Wolfgang Ahlf

Date of disputation: 04.12.2013

The individual articles constituting this cumulative doctoral dissertation meet the formal requirements for a cumulative dissertation. The PhD thesis consists of the following publications:

1. **Waleed M. M. Mahmoud**, Klaus Kümmerer (2012) Captopril and its dimer captopril disulfide: photodegradation, aerobic biodegradation and identification of transformation products by HPLC-UV and LC-ion trap-MSⁿ. *Chemosphere* 88(10): 1170–1177. DOI: 10.1016/j.chemosphere.2012.03.064.
2. Marcelo L Wilde, **Waleed M. M. Mahmoud**, Klaus Kümmerer, Ayrton Figueiredo Martins (2013) Oxidation-coagulation of β -blockers by $K_2Fe^{VI}O_4$ in hospital wastewater: Assessment of degradation products and biodegradability. *Science of the Total Environment* 452–453: 137–147. DOI: 10.1016/j.scitotenv.2013.01.059
3. **Waleed M. M. Mahmoud**, Nareman D. H. Khaleel, Ghada M. Hadad, Randa A. Abdel-Salam, Annette Haiß, Klaus Kümmerer (2013) Simultaneous determination of 11 sulfonamides by HPLC–UV and application for fast screening of their aerobic elimination and biodegradation in a simple test. *CLEAN – Soil, Air, Water*. DOI: 10.1002/clen.201200508
4. Nareman D. H. Khaleel, **Waleed M. M. Mahmoud**, Ghada M. Hadad, Randa A. Abdel-Salam, Klaus Kümmerer (2013) Photolysis of sulfamethoxypyridazine in various aqueous media: aerobic biodegradation and photoproducts identification by LC-UV-MS/MS. *Journal of Hazardous Materials* 244–245: 654–661. DOI:10.1016/j.jhazmat.2012.10.059
5. Faten Sleman, **Waleed M. M. Mahmoud**, Rolf Schubert, Klaus Kümmerer (2012) Photodegradation, photocatalytic and aerobic biodegradation of sulfisomidine and identification of transformation products By LC–UV-MS/MS. *CLEAN – Soil, Air, Water* 40 (11) 1244–1249. DOI: 10.1002/clen.201100485.
6. **Waleed M. M. Mahmoud**, Christoph Trautwein, Christoph Leder, Klaus Kümmerer (2013) Aquatic photochemistry, abiotic and aerobic biodegradability of thalidomide: identification of stable transformation products by LC-UV-MSⁿ. *Science of the Total Environment*. 463–464: 140–150. DOI: 10.1016/j.scitotenv.2013.05.082
7. **Waleed M. M. Mahmoud**, Anju P. Toolaram, Jakob Menz, Christoph Leder, Mandy Schneider, Klaus Kümmerer (2013) Identification of phototransformation products of Thalidomide and mixture toxicity assessment: an experimental and quantitative structural activity relationships (QSAR) approach. *Water Research*. DOI: 10.1016/j.watres.2013.11.014.

Reprinted with the permission of *Chemosphere* (Elsevier), *Journal of Hazardous Materials* (Elsevier), *Science of the Total Environment* (Elsevier), *Water Research* (Elsevier), and *CLEAN – Soil, Air, Water* (Wiley-VCH Verlag GmbH & Co. KGaA).

Acknowledgements

I would like to express my gratitude to all those people who gave me the possibility to complete this thesis. The success of any project depends largely on the encouragement and guidelines of many others.

No word can express my gratitude for my supervisor Prof. Dr. Klaus Kümmerer for all he has done with me and my family. I am deeply indebted to Prof. Dr. Kümmerer for all the support, advice, motivation and help during my whole PhD studies. He is always able to increase my enthusiasm and give me unlimited inspirations and valuable guidance on scientific work.

I submit my highest appreciation to all the coauthors who had contributed to this PhD project as their contributions, guidance and support was vital for the success of the project. I also would like to express my gratitude to my former and present colleagues of Prof. Kümmerer's group in the Institute of Sustainable and Environmental Chemistry and formerly in the Institute of Environmental Health Science, University Medical Center Freiburg for their help, advice, scientific discussions, valuable hints, mutual encouragements and coffee breaks. Thanks for the good times and for becoming friends. I would like to personally thank (in alphabetical order) Anju, Armin, Andreas, Annette, Carlos, Christoph, Evgenia, Ewelina, Jakob, Janin, Kham Dieu, Karen, Lukasz, Mandy, Manuel, Marco, Marcelo, Matthias, Muhammet, Natalie, Richard, Oliver, Philipp, Stefanie, Tarek, and Tushar.

Many thanks go to Dr. Christoph Rücker and Dr. Annette Haiß for their help, advice, and answers to my questions. I also wish to thank Evgenia Logunova and Janin Westphal for all the help in the lab.

Special thanks go to Prof. Wolfgang Ruck and his entire group, Leuphana University Lüneburg, Institute of Sustainable and Environmental Chemistry for their friendly neighborhood atmosphere. Thanks to Dr. Jan Sebastian Mänz, Leuphana University Lüneburg, Institute of Sustainable and Environmental Chemistry for his assistance and help in measuring some environmental samples. Thanks to Dr. Wolf-Ulrich Palm, Leuphana University Lüneburg, Institute of Sustainable and Environmental Chemistry for his valuable discussion regarding photodegradation experiments. I hope I didn't forget any people I knew during my PhD work here in Germany.

I would also like to convey thanks to the Ministry of Higher Education and Scientific Research of the Arab Republic of Egypt (MHESR) and the German Academic Exchange Service (DAAD) for their scholarship (German-Egyptian Research Long Term Scholarship (GERLS)).

I must express my special gratitude to my wife Nareman Dahshan Henedaq Khaleel for her support, her continuous inspiration and support on the scientific research work, sharing of my stresses and burdens and suffering from my bad temper, taking care of the children and giving me the strength to go through with this thesis. Also, I would like to acknowledge my mother, brother, family and friends for their understandings, encouragement and supports for me in completing this project.

Finally, no word can express my gratitude to Allah (God) for providing me the blessings to complete this work.

Dedication

I would like to dedicate this thesis to my Family, source of inspiration to my life. I would like to dedicate it to all people that stood beside me throughout my studies and to all my friends.

Table of contents

Acknowledgements	I
Dedication	III
Table of contents	IV
List of symbols and abbreviations.....	VI
Summary	1
Zusammenfassung	4
1. Introduction and motivation.....	8
2. Aims and objectives	11
3. Research approach	11
4. Results and Discussion	14
5. Synopsis	18
6. Concluding remarks and future outlook	19
References	21
Curriculum Vitae.....	25
Declaration 1	29
Authors' contributions to the articles and articles publication status:	30
Declaration of Authorship: Authors' contributions to the articles:.....	32
Appendices	33
Paper I: Captopril and its dimer captopril disulfide: photodegradation, aerobic biodegradadation and identification of transformation products by HPLC-UV and LC-ion trap-MS ⁿ . Chemosphere 88(10): 1170–1177 (2012). DOI: 10.1016/j.chemosphere.2012.03.064.	
Paper II: Oxidation–coagulation of β -blockers by $K_2Fe^{VI}O_4$ in hospital wastewater: Assessment of degradation products and biodegradability. Science of the Total Environment 452–453: 137-147 (2013). DOI: 10.1016/j.scitotenv.2013.01.059	
Paper III: Simultaneous determination of 11 sulfonamides by HPLC–UV and application for fast screening of their aerobic elimination and biodegradation in a simple test (2013). CLEAN – Soil, Air, Water. DOI: 10.1002/clen.201200508	
Paper IV: Photolysis of sulfamethoxypyridazine in various aqueous media: aerobic biodegradation and photoproducts identification by LC-UV-MS/MS. Journal of Hazardous Materials 244-245: 654–661(2013). DOI:10.1016/j.jhazmat.2012.10.059	
Paper V: Photodegradation, photocatalytic and aerobic biodegradation of sulfisomidine and identification of transformation products By LC–UV-MS/MS. CLEAN – Soil, Air, Water 40 (11) 1244-1249 (2012). DOI: 10.1002/clen.201100485.	

Paper VI: Aquatic photochemistry, abiotic and aerobic biodegradability of thalidomide: identification of stable transformation products by LC-UV-MSⁿ. *Science of the Total Environment*. 463–464: 140–150(2013). DOI: 10.1016/j.scitotenv.2013.05.082

Paper VII: Identification of phototransformation products of Thalidomide and mixture toxicity assessment: an experimental and quantitative structural activity relationships (QSAR) approach(2013). *Water Research*. DOI: 10.1016/j.watres.2013.11.014.

List of symbols and abbreviations

2-AA	2-Aminoanthracene
2-NF	2-Nitrofluorene
4-NQO	4-Nitroquinoline-N-oxide
ACE	Angiotensin converting enzyme
Ames MPF	Ames microplate format aqua assay
ANOVA	Analysis of variance
AOPs	Advanced oxidation processes
ATE	Atenolol
BDW	Buffered demineralized water pH 7.4
BOD	Biological Oxygen Demand
CBT	Closed Bottle Test
CFU	Colony forming units
COD	Chemical oxygen demand
CP	Captopril
CPDS	Captopril disulphide
deg	Degradation
DMSO	Dimethylsulphoxide
DOC	Dissolved Organic Carbon
DPs	Degradation products
EIC	Extracted ion chromatogram
EPV	Ecopharmacovigilance
ESI-IT-MSⁿ	Mass spectrometry with electrospray ionization and ion trap detector in tandem
FDA	Food and Drug Administration
FL (FLD)	Fluorescence detector
GI	Growth inhibition
HO[•]	Hydroxyl radical
HPLC (LC)	High Performance Liquid Chromatography
HTPs	Hydrolysis transformation products
HWW	Hospital wastewater

IC	Inhibitory concentration
ICH	The International Conference on Harmonisation of Technical Requirements for Registration of Pharmaceuticals for Human Use
K'	Capacity factor or retention factor
K₂Fe^{VI}O₄	Potassium ferrate (VI)
LC (HPLC)	High Performance Liquid Chromatography
LC-MS/MS (LC-MSⁿ)	Liquid Chromatography Tandem Mass Spectrometry
LI	Luminescence inhibition
LOD	Limit of detection
LOEC	Lowest observed effect concentration
LOQ	Limit of quantification
m/z	Mass to charge ratio
MET	Metoprolol
min	Minute
MP	Millipore water
MRT	Manometric Respirometry test
MS	Mass spectrometry
n	The number of samples
NPOC	Non Purgeable Organic Carbon
OD	Optical density
OECD	Organization for Economic Co-operation and Development
PRO	Propranolol
PTP	Phototransformation product
QSAR	Quantitative structure activity relationship(s)
R²	Coefficient of determination
Red_{COD}	Reduction of the chemical oxygen demand
Red_{UV254}	Removal of UV absorption measured at the wavelength of 254 nm
Rs	Resolution
RSD	Relative standard deviation
RSM	Response surface methodology
S/N	Signal to noise ratio

SAM	Sulfanilamide
SAs or SNs	Sulfonamides
SCP	Sulfachloropyridazine
SDX	Sulfadimethoxine
SDZ	Sulfadiazine
SGD-MH	Sulfaguanidine monohydrate
SMP	Sulfamethoxypyridazine
SMR	Sulfamerazine
SMT	Sulfamethazine
SMX	Sulfamethoxazole
SPE	Solid phase extraction
SPY	Sulfapyridine
STP	Sewage treatment plant
STZ	Sulfathiazole
SUI	Sulfisomidine
TD	Thalidomide
ThOD	Theoretical oxygen demand
TIC	Total ion chromatogram
TOC	Total Organic Carbon
TP	Transformation product
t_R	Retention time
UP	Ultrapure water
UV	Ultraviolet
<i>V. fischeri</i>	<i>Vibrio fischeri</i>
WWTP	Waste water treatment plant
ZWT	Zahn–Wellens test
α	Selectivity or separation factor
λ	Wavelength

Summary

Emerging contaminants such as pharmaceutical compounds and their metabolites and transformation products (TPs) are unregulated contaminants. Over the past few years they are considered to be an emerging environmental issue. In recent years, there has been an increasing interest in gathering knowledge on sources, occurrence, fate, and possible effects of human and veterinary pharmaceuticals in the environment. The negative impact of pharmaceuticals in the environment might not only affect our water resources, but in fact it can also influence the favorable conditions that are suitable for flora and fauna. Pharmaceuticals may be transformed through the abiotic and biotic processes in the environment and during the treatment processes applied at the sewage and drinking water treatment plants. In recent years, there has been a growing interest in advanced oxidation processes (AOPs) as a promising and efficient treatment in the remediation of wastewater and for general water treatment because of their abilities to degrade a wide range of organic pollutants, or / and mineralized them to carbon dioxide and water, such as treatment with ozone, TiO₂ heterogeneous photocatalysis, and others such as treatment in the presence of potassium ferrate (K₂Fe^{VI}O₄). Recently, TPs have become a topic of interest not only due to their formation during water treatment processes, but also in the environment. Transformation processes can lead to TPs which can have more or less toxic effects than the parent compound. Moreover, some TPs are more abundant than their parent compounds in the aquatic environment. Therefore, it is important to gather more information about environmental impact of pharmaceuticals and their TPs by investigating their toxicity for different toxicological endpoints such as mutagenicity and ecotoxicity. The identification of TPs has heightened the need for *in silico* software based on quantitative structure activity relationships (QSAR) models. These QSAR models are gaining importance because these TPs are usually only formed in low concentrations within complex matrices so that isolation and purification is very difficult. Further, many of these TPs are not available commercially, which makes the individual analysis of their environmental fate impossible. Thus, with increasing concern for green chemistry for sustainable development, data on their environmental fate, behavior, ecological effects, potential health effects and monitoring data regarding their occurrence are needed urgently. Therefore, the main objectives for this thesis are assessment of the efficiency of these various photodegradation and biodegradation processes for the selected pharmaceuticals in the laboratory, identification of degradation products and their preliminary

assessment (e.g. bacterial toxicity, mutagenicity and genotoxicity using experimental systems as well as computer based ones such as (QSAR)).

The present thesis includes seven research papers (I-VII). Selection criteria for the investigated compounds were a) little knowledge up to now (such as Captopril (CP)), b) high sales volume (such as CP, atenolol, metoprolol, propranolol, sulfonamides), c) high side effects (such as thalidomide (TD)) and d) with respect to usage of pharmaceuticals in Egypt and Germany as far as data are available.

The first paper focuses on photodegradation, aerobic biodegradation of CP and its dimer captopril disulphide and identification of TPs by HPLC-UV and LC-ion trap-MSⁿ. The second paper deals with the degradation behavior of β -blockers (atenolol, metoprolol and propranolol) in hospital wastewater and in aqueous solution by $K_2Fe^{VI}O_4$, identification of the formed degradation products, and the assessment of biodegradability of the degradation product mixtures.

Paper III-V focus on the sulfonamides (SAs). The third paper focuses on the aerobic biodegradability assessment of eleven SAs (sulfanilamide, sulfaguanidine monohydrate, sulfadiazine, sulfathiazole, sulfapyridine, sulfamerazine, sulfamethoxypyridazine, sulfachloropyridazine, sulfamethazine, sulfamethoxazole, and sulfadimethoxine) in the Closed Bottle test, and the development and validation of a HPLC method for the simultaneous determination of these eleven SAs in ultrapure water with respect to the range, linearity, precision, detection and quantitation limits, selectivity, specificity, robustness, and analytical solution stability. The fourth paper focuses on degradation and removal efficiencies of sulfamethoxypyridazine by photolysis in three different aqueous media: Millipore water pH 6.1 (MW), effluent from sewage treatment plant pH 7.6 (STP), and buffered demineralized water pH 7.4 (BDW) in order to investigate any possible effect of the water matrix to the photolysis of SMP. Moreover, the aerobic biodegradation of SMP was studied. Identification of TPs was performed by LC-UV-MS/MS. The fifth paper focuses on photolysis, photocatalytic and aerobic biodegradation of sulfisomidine and identification of TPs by LC-UV-MS/MS.

Paper VI-VII focus on TD. The sixth paper deals with the assessment of environmental fate of TD experimentally and by *in silico* prediction programs based on QSAR. TD fate was monitored during photolysis, abiotic and aerobic biodegradability as well as the stable TPs was identified by LC-UV-MSⁿ. The seventh paper focuses on the identification and initial toxicity

assessment of TD, its photo-transformation products (PTPs) and its hydrolysis TPs experimentally and/or by *in silico* prediction programs based on QSAR. In addition, toxicity of phthalimide (one of TD PTPs) was investigated in a modified luminescent bacteria test.

Based on the obtained results from the studies, it can be concluded that photolysis plays an important role for the removal of the investigated pharmaceuticals in the aquatic environment, however, often without complete mineralization leading to formation of TPs. However, photolysis might not always be a green technology as in case of TD photodegradation because the acute and chronic toxicity towards *Vibrio fischeri* was increasing during the photolytic process. Therefore, AOP might be more preferable than photolysis if it leads to complete mineralization as in case of photocatalytic degradation of sulfisomidine with TiO₂.

Moreover, biodegradation and abiotic degradation play an important role in the removal of some of the investigated pharmaceuticals as in case of CP in Zahn–Wellens test. All the tested pharmaceuticals were not readily biodegradable. Therefore, they are expected to reach or accumulate in the aquatic environment such as SAs are frequently detected in surface water at concentrations up to the $\mu\text{g L}^{-1}$. Combinations of biodegradation and other treatment techniques such as photolysis or AOP might have a synergistic or additive effect in removal of pharmaceuticals, for example propranolol samples after 120 min of K₂Fe^{VI}O₄ treatment was readily biodegradable in closed bottle test.

Turning now to the predicted results from the different *in silico* software as an important tool to predict the environmental fate and risk for the TPs. In case of TD UV-treatment, the number of PTPs within the reaction mixture that might be responsible for the acute and chronic toxicity towards *Vibrio fischeri* was successfully narrowed down by correlating the formation kinetics of PTPs with QSAR predictions and experimental toxicity data.

Taken together, these results contribute in enhancing the existing knowledge about the life cycle and behavior of pharmaceuticals in the environment including the environmental fate and risk of these pharmaceuticals. The investigated pharmaceuticals and / or their TPs might have been present for decades in the aquatic environment without any knowledge of their environmental fate or connected risk. Therefore, further work needs to be done including analysis of environmental samples (e.g., surface waters), as well as toxicity tests in order to know its environmental impact.

Zusammenfassung

Aufkommende Verunreinigungen wie pharmazeutische Wirkstoffe und deren Metaboliten und Transformationsprodukte (TPs) sind unregulierte Verunreinigungen. Daher sind sie in den letzten paar Jahren zu einem zunehmenden ökologischen Problem geworden. In den letzten Jahren gab es ein wachsendes Interesse an Zusammentragen von Wissen über Quellen, Vorkommen, Verbleib und möglichen Auswirkungen der Human- und Tierarzneimittelstoffe in der Umwelt. Arzneimittel können in der Umwelt nicht nur auf unsere Wasserressourcen negative Auswirkungen haben sondern auch die Bedingungen für Flora und Fauna beeinträchtigen. Pharmazeutika verändern sich durch abiotische und biotische Prozesse in der Umwelt und während der Behandlungsprozesse während der Abwasser- und Trinkwasseraufbereitung. In den letzten Jahren gab es ein wachsendes Interesse an „Advanced Oxidation Processes (AOPs)“ als vielversprechende und wirksame Methode bei der Behandlung von Abwasser und allgemein bei der Wasseraufbereitung wegen ihrer Fähigkeiten eine breiten Palette von organischen Schadstoffen abzubauen, und / oder sie zu Kohlendioxid und Wasser zu mineralisieren. Beispiele für AOPs wären eine Behandlung mit Ozon, heterogene Photokatalyse mit TiO_2 oder eine Behandlung mit Kalium-Ferrat ($\text{K}_2\text{Fe}^{\text{VI}}\text{O}_4$).

Vor kurzem sind TPs zu einem Thema von steigendem Interesse geworden, nicht nur aufgrund ihrer Bildung während der Wasseraufbereitungsprozesse, sondern auch aufgrund ihres Entstehens in der Umwelt. Aus Transformationsprozessen entstandene TPs können mehr oder weniger toxische Wirkungen als die Stammverbindung haben. Darüber hinaus sind einige TPs häufiger als ihre Muttersubstanz in der aquatischen Umwelt zu finden. Daher ist es wichtig, mehr Informationen über Umweltauswirkungen von Arzneimitteln und deren TPs durch die Untersuchung ihrer Toxizität für verschiedene toxikologische Endpunkte wie Mutagenität und Ökotoxizität zu sammeln. Die Identifizierung von TPs hat die Notwendigkeit für *in silico* Software auf „quantitative structure activity relationships (QSAR)“ Modellen erhöht. Diese QSAR Modelle gewinnen an Bedeutung, da in der Regel TPs nur in geringen Konzentrationen in komplexen Matrices gebildet werden, so dass die Isolierung und Reinigung sehr schwierig ist. Darüber hinaus sind viele dieser TPs nicht im Handel erhältlich, wodurch die individuelle Analyse ihres Umweltverhaltens nicht möglich ist. So werden mit zunehmender Sorge für „green chemistry“ für eine nachhaltige Entwicklung, Daten auf ihren Verbleib in der Umwelt, Verhalten,

Ökologie, mögliche gesundheitliche Auswirkungen und Daten zur Überwachung ihres Auftretens dringend benötigt. Daher sind die Hauptziele für dieser Arbeit die Bewertung der Effizienz dieser verschiedenen photochemischen und biologischen Abbauprozesse für die gewählten Arzneimittel im Labor, die Identifizierung von Abbauprodukten und ihre vorläufige Einschätzung (z.B. bakterielle Toxizität, Mutagenität und Genotoxizität mit experimentellen Systemen sowie Computer basiert sind, wie QSAR).

Die vorliegende Arbeit umfasst sieben Forschungsarbeiten (I-VII). Auswahlkriterien für die untersuchten Verbindungen waren a) wenig bereits vorhandenes Wissen (wie Captopril (CP)), b) hohe Umsatzvolumen (wie CP, Atenolol, Metoprolol, Propranolol, Sulfonamide), c) hohe Nebenwirkungen (wie Thalidomid (TD)) und d) in Bezug auf Nutzung von Pharmazeutika in Ägypten und Deutschland soweit Daten verfügbar sind.

Die erste Forschungsarbeit konzentriert sich auf Photoabbau und aeroben Bioabbau von CP und seinem Dimer Captoprildisulfid und Identifizierung von TPs durch HPLC-UV und LC-Ionenfallen-MSⁿ.

Die zweite Forschungsarbeit beschäftigt sich mit dem Abbauverhalten β -Blockern (Atenolol, Metoprolol und Propranolol) im Krankenhausabwasser und in wässriger Lösung durch $K_2Fe^{VI}O_4$, Identifizierung der gebildeten Abbauprodukte und Bewertung der biologischen Abbaubarkeit der Abbauproduktmischungen.

Die Forschungsarbeiten III-V fokussieren sich auf die Sulfonamide (SAs). Der dritte Arbeit konzentriert sich auf die biologische Abbaubarkeit von elf SAs (Sulfanilamid, Sulfaguanidin Monohydrat, Sulfadiazin, Sulfathiazol, Sulfapyridin, Sulfamerazin, Sulfamethoxypyridazin, sulfachloropyridazin, Sulfamethazin, Sulfamethoxazol und Sulfadimethoxin) im „Closed Bottle test“ und die Entwicklung und Validierung einer HPLC-Methode für die simultane Bestimmung dieser elf SAs in Reinstwasser in Bezug auf die Auswahl, Linearität, Präzision, Nachweis- und Bestimmungsgrenzen, Selektivität, Spezifität, Robustheit und Stabilität analytischer Lösung. Der vierte Beitrag konzentriert sich auf den Abbau und die Abbaurate von Sulfamethoxypyridazin durch Photolyse in drei verschiedenen wässrigen Medien: Millipore Wasser pH 6,1 (MW), Abwasser aus Kläranlagen pH 7,6 (STP), und gepufferten vollentsalzten Wasser pH 7,4 (BDW), zur Untersuchung möglicher Wirkung der Wassermatrix auf die Photolyse von SMP. Darüber hinaus wurde die aerobe biologische Abbaubarkeit von SMP untersucht. Die TPs wurden mittels

LC-UV-MS/MS identifiziert. Die fünfte Arbeit konzentriert sich auf Photolyse, photokatalytische und aerobe biologische Abbaubarkeit von Sulfisomidin und der Identifizierung von entstandenen TPs durch LC-UV-MS/MS.

Die Forschungsarbeiten VI-VII fokussieren sich auf TD. Die sechste Arbeit befasst sich mit der Bewertung der Umweltauswirkungen durch TD sowohl experimentell und als auch durch *in silico* auf QSAR basierte Vorhersageprogramme. Das Abbauverhalten von TD wurde während der Photolyse sowie den abiotischen und aeroben biologischen Abbauteests beobachtet. Des Weiteren wurden die stabilen TPs mittels LC-UV-MSⁿ identifiziert. Der siebte Arbeit konzentriert sich auf die Identifizierung und erste Beurteilung der Toxizität von TD, seine Phototransformationsprodukte (PTPs) und dessen Hydrolyse TPs experimentell und / oder durch *in silico* auf QSAR basierte Vorhersageprogramme. Darüber hinaus wurde die Toxizität von Phthalimid (eines TD PTPs) in einem modifizierten Leuchtbakterientest untersucht. Auf der Basis der erhaltenen Ergebnisse aus den Versuchen kann geschlossen werden, dass Photolyse eine wichtige Rolle für die Entfernung der untersuchten Pharmaka in Gewässern spielt, jedoch häufig ohne vollständige Mineralisierung sondern unter Bildung von TPs werden. Allerdings ist Photolyse nicht immer eine „Green Technology“, da z.B. bei TD die akute und chronische Toxizität gegenüber *Vibrio fischeri* durch das photolytische Verfahren erhöht wurde. Daher könnte AOP stärker als Photolyse bevorzugt werden, da es zu vollständiger Mineralisierung wie im Falle des photokatalytischen Abbaus von Sulfisomidin mit TiO₂ führt.

Darüber hinaus spielt biologischer und abiotischer Abbau eine wichtige Rolle bei der Beseitigung von einigen der untersuchten Pharmaka wie im Fall von CP in Zahn-Wellens-Test. Alle getesteten Arzneimittel waren nicht leicht biologisch abbaubar. Deshalb werden sie voraussichtlich in die aquatische Umwelt gelangen oder sich dort anreichern, wie beispielsweise SAs, welche häufig in Oberflächengewässern in Konzentrationen bis zum µg L⁻¹ nachgewiesen werden. Kombinationen von biologischen und anderen Behandlungsverfahren wie Photolyse oder AOP könnte eine synergistische oder additive Wirkung bei der Entfernung von Pharmazeutika haben, beispielsweise waren Propranolol Proben nach 120 min von K₂Fe^{VI}O₄ Behandlung leicht biologisch abbaubar im „Closed Bottle Test“.

Wenden wir uns nun zu den vorhergesagten Ergebnissen aus den verschiedenen *in silico* Software als ein wichtiges Instrument der Vorhersagen des Verbleibs und des Risiko durch TPs

in der Umwelt, z.B. bei UV-Behandlung von TD wurde die Anzahl der PTPs innerhalb der Reaktionsmischung, die für die akute und chronische Toxizität gegenüber *Vibrio fischeri* verantwortlich sind, erfolgreich durch Korrelation der Kinetik der Bildung PTPs mit QSAR-Vorhersagen und experimenteller Daten zur Toxizität verringert.

Zusammengefasst tragen diese Ergebnisse zur Verbesserung der vorhandenen Kenntnisse über den Lebenszyklus und das Verhalten von Arzneimitteln in der Umwelt bei, einschließlich des Verbleibs in der Umwelt und den Risiken dieser Arzneimittel. Die untersuchten Arzneimittel und / oder deren TP's sind vielleicht seit Jahrzehnten in der aquatischen Umwelt vorhanden ohne Kenntnis ihres Umweltverhaltens oder den damit verbundenen Risiken. Daher muss zukünftig weitere Arbeit, einschließlich der Analyse von Umweltproben (z. B. Oberflächenwasser), sowie Prüfungen der Toxizität erfolgen, um ihre Auswirkungen auf die Umwelt festzustellen.

1. Introduction and motivation

Chemical substances including pharmaceuticals shape the world we live in, the air we breathe, the food we eat and the water we drink. Besides other micro-pollutants, drug residues have become a notable contaminant of surface water during recent years (Aherne, G. W. and Briggs, 1989; Bendz et al., 2005; García-Galána et al., 2011; Hirsch et al., 1999; Jongh et al., 2012; Kümmerer et al., 1997; Pailler et al., 2009; Richardson and Bowron, 1985). The prevalence of low concentrations of pharmaceutically active substances and their metabolites and transformation products (TPs) in the environment is an area of growing concern (Hao et al., 2006; Jongh et al., 2012; Kümmerer, 2008; Zwiener and Frimmel, 2004). The increasing use of pharmaceutical products is becoming a new environmental problem. Emerging contaminants such as pharmaceutical compounds are unregulated contaminants, which may be candidates for future regulation depending on research on their potential health effects and monitoring data regarding their occurrence.

Numerous studies have shown that some pharmaceutical compounds are not removed during wastewater treatment processes, being therefore discharged to receiving surface waters, and can subsequently be found in ground and drinking waters (Carballa et al., 2004; Gros et al., 2006; Kosjek and Heath, 2011; Vieno et al., 2007). These compounds along with their metabolites, which can be even more harmful than the parent compound, are continuously released into the environment, mainly through excreta, disposal of unused or expired drugs, veterinary use, and pharmaceuticals discharged e.g., from hospitals, households, and pharmaceuticals industries (Gros et al., 2006). Furthermore, in effluent treatment and/or the environment recalcitrant TPs can be formed. Once released into the environment via the discharge of treated or untreated wastewater, pharmaceuticals and their metabolites are subjected to processes (e.g., dilution, photolysis, biodegradation, and sorption to bed sediments) that contribute to their elimination from the environmental waters (Gartiser et al., 2007; Petrovic and Barceló, 2007) or lead to formation of TPs which have not been identified so far (Fatta-Kassinos et al., 2011; Mahmoud and Kümmerer, 2012; Trautwein and Kümmerer, 2011). Much attention has to be attributed to the fact that pharmaceuticals, pharmaceutical metabolites and TPs can be more bioaccumulative, harmful and toxic than their parent compound in aquatic and terrestrial ecosystems (Gros et al., 2006; Jongh et al., 2012; Santos et al., 2010; Wang and Lin, 2012).

With respect to pharmaceuticals, the main concern relates to their continual entry into water bodies as pollutants originating from permanent use of drugs in farming, aquaculture and human health, in addition to improper disposal of expired medication. Although their pharmacological effects are well characterized in humans and animals, whose health they are designed to improve, due to their inherent biological activity, the exposure of living organisms in environmental systems to drug residues can lead to adverse effects (La Farré et al., 2008; Pérez and Barceló, 2008). Therefore, a new science of great interest begins to develop which is pharmacovigilance for the environment or ecopharmacovigilance (EPV) (Velo and Moretti, 2010). As for EPV it not yet clear what it might mean in practice. EPV would describe the science and activities associated with the detection, evaluation, understanding and prevention of adverse effects of pharmaceuticals in the environment (Holm et al., 2013).

The presence of pharmaceuticals in the environment is an emerging environmental issue that provides a new challenge to develop new treatment systems for drinking water, wastewater and water reuse. Biotic degradation is the first line in the pharmaceuticals' degradation effluent treatment. Biodegradation is based exclusively on the activity of microorganisms, thus, it is important to carry out tests on the degradation of substances reaching STPs (Alexy et al., 2004). Abiotic elimination processes such as photolysis, hydrolysis, and sorption are also of great importance for the aquatic fate of pharmaceutical compounds. Photolysis is among the important abiotic degradation mechanisms for many pharmaceutical pollutants' degradation. Therefore, knowledge of the photodegradation pathways and kinetics is essential to predict the environmental fate of these pollutants in natural waters (Trovó et al., 2009).

Phototreatment for the removal of organic pollutants such as drugs e.g. from potable water, surface water or biologically treated sewage is a topic currently under discussion (Lam and Mabury, 2005; Tixier et al., 2003). Phototreatment with ultraviolet (UV) light irradiation is an established method for sterilization and water disinfection (Canonica et al., 2008), and a growing technology for wastewater purification (Kang et al., 2004; Liberti and Notarnicola, 1999; Meneses et al., 2010; U.S. EPA, 1998). Moreover, Photodegradation is one of the important removal mechanisms for pollutants in surface water with intense solar radiation such as in Egypt. However, photodegradation does not necessarily end up with the complete mineralization of a chemical resulting in the formation of TPs. Photodegradation mechanisms are often complex, involving various competing or parallel pathways, leading to multiple reaction photo-

transformation products (PTPs) which can have more toxic effect than the parent compound (Garcia-Käufer et al., 2012; Gómez et al., 2008; Wang and Lin, 2012) or less toxic than the parent compound (Ji et al., 2012). Elucidation of photolytic reaction pathways and identification of TPs are therefore of crucial importance in understanding the fate of emerging organic pollutants in the aquatic environment. Moreover, there has also been a growing interest in advanced oxidation processes (AOPs) as a promising and efficient treatment in the remediation of wastewater and for general water treatment, such as heterogeneous photocatalysis, ozonation and potassium ferrate ($\text{K}_2\text{Fe}^{\text{VI}}\text{O}_4$) (Esplugas et al., 2007; Jiang and Lloyd, 2002; Klavarioti et al., 2009). Titanium dioxide (TiO_2) has emerged as a powerful photocatalyst due to several properties such as its high photo-activity, stability, chemical inertness, and relatively low cost (Fujishima et al., 2000; Keane et al., 2011). As well as potassium Ferrate has attracted the attention of scientists owing to its dual character, since it is an oxidant–coagulant, with a higher oxidation potential (Jiang and Lloyd, 2002; Sharma, 2002). The pharmaceutical active compounds are mainly composed of products used in everyday life and for most of them ecotoxicological data are not yet available. Therefore, it is important to gather information about environmental properties of pharmaceuticals and their TPs and to consider this information in environmental risk assessment e.g., by identification of TPs, and toxicity assessment of photodegradation mixture (Escher and Fenner, 2011).

Thus, it is important to identify the structure of TPs by analytical methods such as LC–UV–MSⁿ. The simplified molecular input line entry specification (SMILES) codes from the identified molecular TP structures were taken as input in *in silico* prediction software based on quantitative structure activity relationships (QSAR). These *in silico* approaches are gaining importance especially for analyzing environmental fate and impact of these TPs because these TPs are usually formed in low concentrations within complex matrices so that isolation and purification is very difficult, tedious and expensive. Further, many of these TPs are not available commercially, which makes the individual analysis of their environmental fate impossible. Therefore, it can be helpful to apply QSAR models that estimate the potential for biodegradation, photodegradation, and toxicity in the environment (European Commission, 2003a, 2003b; Rucker and Kümmerer, 2012; Trautwein and Kümmerer, 2012; Walker et al., 2004).

A set of programs for predicting biodegradation, photodegradation, and toxicity was applied in order to take into account that the available programs might have individual strengths because of

different algorithms and training sets (Laboratory of Mathematical Chemistry, 2012; Roberts et al., 2000; Sedykh et al., 2001).

2. Aims and objectives

The main objectives for this PhD project were:

- Identification and determination of selected pharmaceuticals and their TPs.
- Investigation of photodegradation and biodegradation for the selected pharmaceuticals using experimental systems as well as computer based ones based on QSAR in order to gather knowledge on the fate of pharmaceuticals.
- Development of analytical methods used for the identification of TPs and elucidation of reaction pathways.
- Preliminary toxicity assessment (e.g. ecotoxicity and mutagenicity using experimental systems as well as computer based ones based on QSAR) for the identified TPs.

3. Research approach

In order to fulfill the above objectives, the following work tasks were addressed in the seven research papers. Selection criteria for the investigated compounds were: a) little knowledge up to now (such as captopril), b) high sales volume (such as captopril, atenolol, metoprolol, propranolol, sulfonamides), c) high side effect (such as thalidomide) and d) with respect to usage of pharmaceuticals in Egypt and Germany as far as data are available (Figure 1).

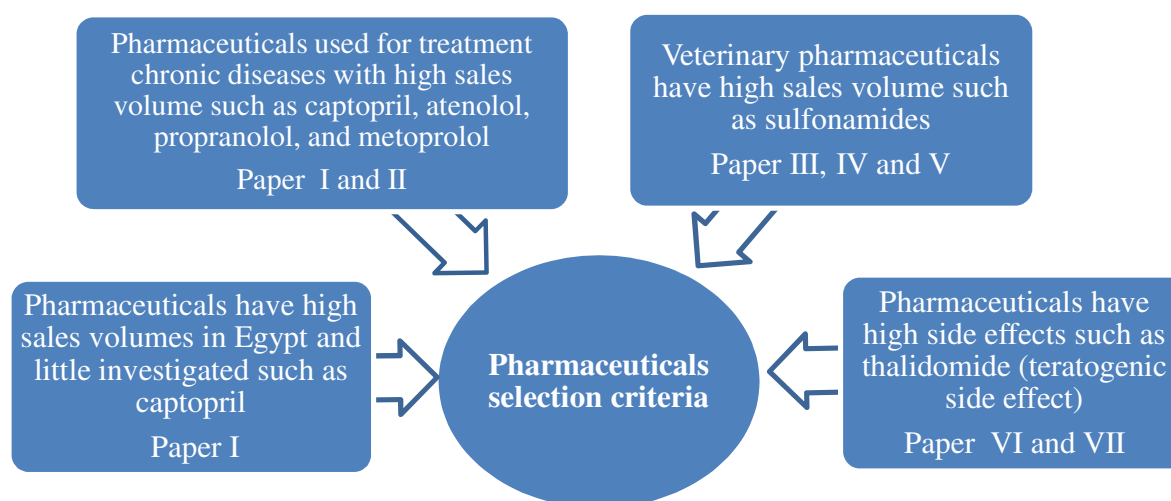


Figure 1: Selection criteria for the pharmaceuticals investigated in the papers of the thesis.

The first paper focuses on the environmental fate of captopril (CP). CP is used in this study as it is widely used in Egypt and stated as one of the essential drugs in Egypt for hypertension (Ministry of Health and Population (MOHP), 2006). Three tests from the OECD series were used for biodegradation testing: Closed Bottle test (CBT; OECD 301 D), Manometric Respirometry test (MRT; OECD 301 F) and the modified Zahn–Wellens test (ZWT; OECD 302 B). Photodegradation (150 W medium-pressure Hg-lamp) of CP was studied. Also CBT was performed for captopril disulphide (CPDS) and samples received after 64 min and 512 min of photolysis. The primary elimination of CP and CPDS was monitored by LC-UV at 210 nm and structures of photoproducts were assessed by LC-UV-MS/MS (ion trap).

The second paper deals with the application of an advanced oxidation process (AOP) for three pharmaceuticals of the β -blockers. β -blockers are one of the most important groups of prescription drugs used in the therapeutic treatment of hypertension and cardiac dysfunction. Atenolol and metoprolol together account for more than 80% of total β -blocker consumption in Europe, whereas atenolol and propranolol are as one of the essential drugs in Egypt for hypertension (Alder et al., 2010; Ministry of Health and Population (MOHP), 2006). The three most widely used β -blockers are atenolol (ATE), metoprolol (MET) and propranolol (PRO). This study investigated the degradation of ATE, MET and PRO by ferrate (K_2FeO_4) as a new approach in hospital wastewater and in aqueous solution. In the case of hospital wastewater, the effect of the independent variables pH and $[\text{Fe}^{(\text{VI})}]$ was evaluated by means of response surface methodology in order to use an optimized experimental setting, as there are many factors that can have an impact on oxidation of micro-pollutants by ferrate. In the aqueous solution, the TPs were identified and the ready biodegradability of the post-process samples was evaluated by using the CBT.

The third to the fifth paper focus on sulfonamides (SAs) which are one of the most commonly used group of antibiotics. In the third paper, the aerobic biodegradability of eleven SAs in the CBT and the development and validation of a high-performance liquid chromatography-ultraviolet (HPLC-UV) method for the simultaneous determination of these eleven SAs was investigated. The biodegradability of eleven SAs (sulfanilamide, sulfaguanidine monohydrate, sulfadiazine, sulfathiazole, sulfapyridine, sulfamerazine, sulfamethoxy-pyridazine, sulfachloropyridazine, sulfamethazine, sulfamethoxazole, and sulfadimethoxine) was studied using CBT. The HPLC–UV method performance was validated with respect to the range,

linearity, precision, detection and quantitation limits, selectivity, specificity, robustness, and analytical solution stability. The applicability of the method was assessed through the analysis of the selected SAs separately in the CBT samples.

The fourth paper focuses on the degradation and removal efficiencies of sulfamethoxypyridazine (SMP) by photodegradation and aerobic biodegradability. The photolysis of SMP using a medium pressure Hg-lamp was evaluated in three different media: Millipore water pH 6.1 (MW), effluent from sewage treatment plant pH 7.6 (STP), and buffered demineralized water pH 7.4 (BDW). Identification of TPs was performed by LC-UV-MS/MS. The biodegradation of SMP using two tests from the OECD series was studied: CBT and MRT.

The fifth paper focuses on degradation and removal efficiencies of sulfisomidine (SUI) by photodegradation and aerobic biodegradability. SUI behavior was monitored during photolysis and photocatalysis (catalyst TiO_2) using 150 W medium-pressure Hg-lamp. The TPs were identified by LC-UV-MS/MS. Also CBT for SUI was performed.

Yet, nothing was known about the environmental fate of TD. Therefore, the sixth and seventh papers focus on the fate of TD in the aquatic environment, and the toxicity assessments of TD and its PTPs and hydrolysis transformation products (HTPs). The sixth paper deals with the assessment of environmental fate of TD (“Contergan[®]”) experimentally and by *in silico* prediction software using QSAR models. TD, besides being notorious for its teratogenicity, became a promising drug for the treatment of different cancers and inflammatory diseases within recent years. Therefore, photolytic degradation of 10 mg/L TD was tested with two different light sources (medium-pressure mercury lamp and xenon lamp) and aerobic biodegradability was investigated with two OECD tests (CBT and MRT). An additional CBT was performed for TD samples after 16 min of UV-photolysis. The primary elimination of TD was monitored and the structures of its photo-, abiotic and biodegradation products were elucidated by HPLC-UV-Fluorescence-MSⁿ.

The seventh paper focuses on the evaluation of the environmental risk of TD - experimentally and by using *in silico* prediction software using QSAR models. The fate of 47 mg/L and 10 mg/L TD in different reactor size was monitored during irradiation with a medium-pressure Hg-lamp. For this purpose, the primary elimination of TD was monitored and structures of PTPs were assessed by LC-UV-FL-MS/MS. The estimation of the relevant properties of TD and its PTPs and HTPs was performed using *in silico* QSAR models. Mutagenicity of TD and its PTPs was

assessed in the Ames microplate format (MPF) aqua assay (Xenometrix, AG). Furthermore, a modified luminescent bacteria test (kinetic luminescent bacteria test (kinetic LBT)), using the luminescent bacteria species *Vibrio fischeri*, was applied for the initial assessment of environmental toxicity. Additionally, toxicity of phthalimide, one of the identified PTPs and which was commercially available, was investigated separately in the kinetic LBT due to the contradiction between different *in silico* software regarding the predicted phthalimide toxicity against *V. Fischeri*.

4. Results and Discussion

CP was completely degraded after 512 min of irradiation (Paper I). Photodegradation of CP did not lead to any mineralization or any obvious change in NPOC concentration. Analysis of CP photodegradation samples by LC-MS/MS revealed CP sulphonic acid as the major PTP. No biodegradation was observed for CP, CPDS and of the mixture resulting from photo-treatment after 64 min in CBT. In CBT, there was a primary elimination of CP to CPDS. Partial biodegradation in the CBT and MRT was observed in samples taken after 512 min photolysis and for CP itself in MRT. In MRT, CP was transformed to degradation products which are neither identical with CPDS nor the photo-transformation product. Complete biodegradation and mineralization of CP occurred in the ZWT. These results show that CP was not readily biodegradable but it was completely biodegradable in ZWT. Moreover, photolysis can play an important role in removal of CP without any mineralization.

It was found that $\text{Fe}^{(\text{VI})}$ plays an important role in the oxidation–coagulation process of the investigated β -blockers (Paper II). In the hospital wastewater, the treatment led to degradations above 90% for all the three β -blockers, reduction of UV absorption at 254 nm that is due to the loss or at least change in the aromaticity that were close to 60%, and removal of only 17% of the organic load (COD). In aqueous solution, the degradation of ATE, MET and PRO was 71.7%, 24.7% and 96.5%, respectively, when a ratio of 1:10 [β -blocker]: $[\text{Fe}^{(\text{VI})}]$ was used. No mineralization was achieved, which suggests that there was a conversion of the β -blockers to degradation products identified by LC-MSⁿ. Degradation pathways were proposed, which took account of the role of $\text{Fe}^{(\text{VI})}$. Thus, it is suggested that ATE should follow two main degradation pathways: (1) electrophilic attack on the aromatic ring, and (2) electrophilic attack on secondary amine moiety and elimination of the isopropyl moiety. MET should follow three main

degradation pathways: (1) hydroxylation of MET, (2) attack on the ether side chain, and (3) N-dealkylation by oxidative attack on the α -C of the dimethylamine moiety. PRO have a large number of TPs identified showing how complex this kind of process can be and suggests that there are different reductive and oxidative degradation routes, resulting in multistep and interconnected pathways.

Furthermore, an increase in ready biodegradability of the formed TPs mixture in the samples treated by $\text{Fe}^{(\text{VI})}$ was observed in the CBT. Therefore, it can be concluded that the use application of the $\text{Fe}^{(\text{VI})}$ seems could be a useful means of ensuring the remediation of hospital and similar wastewater.

A simple, efficient, and reliable HPLC-UV method for the simultaneous determination of eleven SAs has been developed (paper III). The sufficient resolution, good sensitivity and acceptable analysis time for the developed liquid chromatographic separation of all studied SAs were obtained by adjusting different chromatographic factors mainly stationary-phase composition (column type and size), column oven temperature, flow rate, and optimum mobile phase compositions. In the CBT, none of these SAs was readily biodegradable. The validated HPLC-UV method was successfully applied for the quantitative determination of SAs separately in CBT. The HPLC-UV analysis confirmed that no primary elimination of any SA took place. In the toxicity control, these SAs showed no toxic effect in the used concentration of environmental bacteria applied in the test. In the Japanese National Institute of Technology and Evaluation (NITE) database, the benzene sulfonic acid (CAS-No.: 98-11-3) is readily biodegradable but the 4-aminobenzenesulfonic acid (CAS-No.: 121-57-3) is not biodegradable. Therefore, the presence of 4-aminobenzenesulfone in the skeleton of these SAs makes the biodegradation problematic.

One of the SAs was studied more in detail (paper IV) under different photodegradation and biodegradation conditions. It was found that SMP was not readily biodegradable in both CBT and MRT. SMP was removed completely within 128 min of irradiation in the three media, and the elimination rate was different for each investigated type of water. However, dissolved organic carbon (DOC) was not removed in BDW and only little DOC removal was observed in MW and STP effluent, thus indicating the formation of TPs. Analysis by LC-UV-MS/MS revealed TPs formed that have not yet been described in literature. It was found that the hydroxylation of SMP represented the main photodegradation pathway in all the investigated water type.

Another SA was studied which is SUI (paper V). SUI was not readily biodegradable in CBT. After 256 min of irradiation (treatment without catalyst), about 50% of SUI was eliminated without any decrease in NPOC concentration. On the other hand, photocatalytic degradation led to complete mineralization of the SUI sample after 256 min of treatment. Therefore, photocatalysis was more effective than photolysis in the removal of SUI. In both treatment types, SUI underwent photodegradation and several PTPs were identified. Accordingly, the photodegradation pathway of SUI was postulated. The formed TPs can occur by separation of a pyrimidine ring, or cleavage of the sulfonamide functional group, or by the addition of hydroxyl group.

The results, as shown in paper III-V, indicate that SAs are not readily biodegradable. Therefore, they are expected to reach or accumulate in the aquatic environment. Photodegradation can play an important role in elimination of SMP and SUI leading to formation of new TPs.

In addition to the presented already published results regarding SAs. Analysis of aquatic samples from the river Nile (Cairo, Egypt), Lake Fishermen (Ismailia, Egypt), tap water (Ismailia, Egypt), Ilmenau River (Upstream the STP, Lüneburg, Germany), Amelinghausen lake, tap water (Lüneburg, Germany) were done. LC-MS analysis revealed the presence of lot of SAs compounds in the environmental samples especially in the samples from Egypt. Some of these SAs were detected in samples from the tap water from Ismailia, Egypt at concentrations up to the ng L^{-1} . A limitation of this study is that the numbers of samples were small. On the other hand, only one SA at concentrations up to the ng L^{-1} was detected in the tap water from Lüneburg, Germany. This finding in tap water from Egypt and Germany was unexpected as SAs are rarely detected in tap water. Therefore, these results have not been published until now as further research needs to be done by collecting and analyzing more environmental samples from Egypt and Germany in order to validate and confirm this finding. This work contributes to existing knowledge about the SAs concentration in Egypt but further experimental investigations are needed to check if there were any cross-contamination for this tap water before final conclusion can be drawn.

Paper IV and VII deal with the fate of TD in the aquatic environment, and the toxicity assessments of TD and its PTPs and HTPs. TD underwent photolysis with mercury and xenon lamp (Paper IV). New PTPs were identified by LC-MSⁿ, among them two isomers of TD with the

same molecular mass. It was found that the main photo-degradation pathways are homolytic cleavage of the α -bond (α -cleavage; Norrish type I reaction), fragmentation between the phthalimide and the glutamiride ring, and hydroxylation of TD or the constitutional isomers. LC-MSⁿ revealed that these PTPs were different to the products formed by biodegradation. TD and its PTPs were not readily biodegradable. The experimental findings were compared with the results obtained from the *in silico* prediction programs where e.g. a good correlation for TD biodegradation in the CBT was confirmed. Moreover, some of the identified TPs were also structurally predicted by the MetaPC software. These results demonstrate that TD and its TPs are not readily biodegradable and not fully mineralized by photochemical treatment. Furthermore, *in silico* methods gave reliable results.

In the seventh paper, it was reported that the UV irradiation eliminated TD itself without complete mineralization and led to the formation of several PTPs. New PTPs were identified by LC-MSⁿ in addition to the reported PTPs in the sixth paper. TD and its PTPs did not exhibit mutagenic activities in the *Salmonella typhimurium* strains TA 98, and TA 100 with and without metabolic activation. In contrast, QSAR analysis of PTPs and HTPs provided evidence for mutagenicity, genotoxicity and carcinogenicity by investigating additional endpoints *in silico* compared with the experimental Ames MPF tests. QSAR analysis for ecotoxicity provided evidence for positive alerts in several identified PTPs and HTPs such as acute toxicity towards *V. fischeri*. This was confirmed by the modified LBT, in which a steady increase of acute and chronic toxicity with irradiation time was observed for the whole reaction mixtures. Moreover, PTPs within the reaction mixture that might be responsible for the toxification of TD during UV-treatment were successfully narrowed down by correlating the formation kinetics of PTPs with QSAR results and experimental data. There is a significant increase in toxicity after 16 min of photolysis which postulated to be related to the PTPs increased after 16 min. According to the kinetics of PTPs formation, PTP129, PTP173, PTP297, PTP313, PTP259, PTP291 and PTP245 are possible candidates that might be responsible for the toxification of TD during UV-treatment. Beyond that, further analysis of the phthalimide indicated that transformation of TD into phthalimide was not the cause for the toxification of TD during UV-treatment.

These results show the toxic potential of the PTPs and deserve further attention as UV irradiation might not always be a green technology. Beyond that, a more integrated approach for

the evaluation of environmental properties of unknown PTPs was successfully applied by combining *in silico* methods and conventional experimental testing.

5. Synopsis

Photodegradation can be an important transformation process for removal of the studied pharmaceuticals in the aquatic environment. All the investigated compounds underwent photodegradation, however without complete mineralization leading to formation of new TPs. The new TPs were identified by LC-MSⁿ analysis. Different photodegradation pathways for different pharmaceutical compounds are reported. Because of no or at least incomplete mineralization of CP, TD, SUI, SMP and their TPs, the introduction of these pharmaceuticals into the environment may therefore pose a risk to the aquatic environment due to their pharmacological activity and the unknown properties of their PTPs. The applied techniques within this study emphasize the importance of *in silico* approaches such as QSAR models and others as a tool for getting additional information on environmental fate and effects of PTPs.

The AOP was applied in the removal of β -blockers and SUI. The photocatalytic degradation of SUI with TiO₂ led to complete mineralization after 256 min of treatment. Regarding the removal of β -blockers, the ferrate could be a useful means of ensuring the remediation of hospital and similar wastewater. However, further research for the application of Fe^(VI) are needed as no mineralization of β -blockers was achieved in aqueous solution.

In CBT, whose conditions (low bacterial density and low concentration of the test substance) is comparable to the situation in surface water, all the investigated pharmaceuticals were not readily biodegradable except the post process ATE sample after 120 min from the Fe^(VI) treatment. Therefore, no biodegradation can be expected for the investigated compounds if they are introduced directly into surface water. The presence of these antibiotics such as SAs in the aquatic environment can lead to the development of bacterial resistance which cannot be ruled out. On the other hand, there was an increase in biodegradation in the CBT for CP samples taken after 512 min photolysis, MET sample after 120 min from the Fe^(VI) treatment, and PRO sample after 120 min from the Fe^(VI) treatment. This increase in biodegradation indicates that combinations of biodegradation and other treatment techniques such as photolysis or AOP might have in some cases a synergistic or additive effect in removal of pharmaceuticals. However, the finding for other compounds tests also show, that this is not a general rule. Moreover, the ready

biodegradability experimental findings of TD and its PTPs were compared with the results obtained from the *in silico* prediction programs where e.g. a good correlation for TD biodegradation in the CBT was confirmed.

CP, SMP, and TD were not readily biodegradable in MRT with higher concentrations of inoculum and test substance. In ZWT, biodegradation and full mineralization was found for CP after approximately 21 days. This demonstrates the impact of bacterial density and diversity on biodegradation. HPLC analysis of the CBT and MRT samples of the studied compounds revealed that only CP and TD were primary eliminated.

Although photolysis was able to remove TD within the photo-reactor, numerous PTPs were formed. The experimental results have proven that the mixture of PTPs possesses higher toxic properties than the parent compound and therefore the acute and chronic toxicity towards *V. fischeri* was increasing during the photolytic process. No mutagenic potential of the photolytic mixtures of TD was recognized with the Ames MPF test. In contrast, the QSAR predictions provided evidence that various PTPs and HTPs might have an increased genotoxic potential.

These results emphasize that not only the removal of parent pollutants is important but also the elimination of the PTPs from waste water. The combination of monitoring by LC–UV–MSⁿ, DOC monitoring, and QSAR predictions gave valuable insights into the transformation processes and the resulting TPs.

6. Concluding remarks and future outlook

The work presented here shows how important the assessment of environmental fate and risk for understanding the pharmaceuticals lifecycle is. Furthermore, the results demonstrated that there is a case by case approach and investigation necessary. This holds on the one hand with respect to the individual compounds – even the structurally highly related SAs showed different behavior and fate within the same treatment processes. On the other hand, these results show that treatment processes as well as the conditions applied have a high impact on the result of the processes. This confirmed some of the knowledge already reported in literature for other processes and compounds. However, the role of matrix composition is new knowledge as reported here.

The identification of TPs is one of the most difficult and challenging aspects in environmental chemicals analysis of micro-pollutants. The TPs of the investigated pharmaceuticals were

resulting from different transformation process such as photodegradation, AOP, abiotic and biotic degradation. It is important to underline the fact that knowledge on the TPs is still very little in general and especially when it comes to prediction of their formations and the assessment of their physico-chemical and (eco)toxicological properties. Therefore, it was important to identify these TPs by analytical methods such as LC–UV-MSⁿ and to characterize the behavior and fate of the unknown cocktail of TPs by different experiments and *in silico* prediction approaches. New knowledge was gained regarding the combination of the photodegradation process with the biodegradation process. The toxicity of the photo-treatment mixtures was investigated with the goal of prioritizing the relevant TPs in terms of their contribution to environmental risk by different experiments for different toxicological endpoints and *in silico* prediction approaches. The number of TPs within the reaction mixture that might be responsible for the toxification during UV-treatment can be successfully narrowed down by correlating the formation kinetics of PTPs with QSAR predictions and experimental toxicity data. The combination of the experimental data and the predicted data by *in silico* software gave valuable insights into the environmental fate, behavior and risk of the parent compound and the resulting TPs.

This research has led to many questions in need of further investigation. In order to fill this gap, future research should therefore concentrate on the investigation of TPs as well as parent pharmaceuticals in the aquatic environment especially in countries where little or no information is available up to now such as Egypt. Furthermore, these results call for the incorporation of these topics into the education of students.

References

- Aherne, G. W., Briggs, R., 1989. The relevance of the presence of certain synthetic steroids in the aquatic environment. *Journal of Pharmacy and Pharmacology* 41 (10), 735–736.
- Alder, A.C., Schaffner, C., Majewsky, M., Klasmeier, J., Fenner, K., 2010. Fate of β -blocker human pharmaceuticals in surface water: Comparison of measured and simulated concentrations in the Glatt Valley Watershed, Switzerland. *Water Research* 44 (3), 936–948.
- Alexy, R., Kümpel, T., Kümmerer, K., 2004. Assessment of degradation of 18 antibiotics in the Closed Bottle Test. *Chemosphere* 57 (6), 505–512.
- Bendz, D., Paxéus, N.A., Ginn, T.R., Loge, F.J., 2005. Occurrence and fate of pharmaceutically active compounds in the environment, a case study: Höje River in Sweden. *Journal of Hazardous Materials* 122 (3), 195–204.
- Canonica, S., Meunier, L., Gunten, U. von, 2008. Phototransformation of selected pharmaceuticals during UV treatment of drinking water. *Water Research* 42 (1–2), 121–128.
- Carballa, M., Omil, F., Lema, J.M., Llompart, M., García-Jares, C., Rodríguez, I., Gómez, M., Ternes, T., 2004. Behavior of pharmaceuticals, cosmetics and hormones in a sewage treatment plant. *Water Research* 38 (12), 2918–2926.
- Escher, B.I., Fenner, K., 2011. Recent Advances in Environmental Risk Assessment of Transformation Products. *Environmental Science & Technology* 45 (9), 3835–3847.
- Esplugas, S., Bila, D.M., Krause, L.G.T., Dezotti, M., 2007. Ozonation and advanced oxidation technologies to remove endocrine disrupting chemicals (EDCs) and pharmaceuticals and personal care products (PPCPs) in water effluents. *Journal of Hazardous Materials* 149 (3), 631–642.
- European Commission, 2003a. Technical Guidance Document on Risk Assessment Part II: Environmental Risk Assessment.
http://ec.europa.eu/environment/chemicals/exist_subst/pdf/tgdpart2_2ed.pdf.
- European Commission, 2003b. Technical Guidance Document on Risk Assessment Part III: Chapter 4: Use of (Quantitative) Structure Activity Relationships ((Q)SARs), Use Categories, Risk Assessment Report Format.
http://ec.europa.eu/environment/chemicals/exist_subst/pdf/tgdpart3_2ed.pdf.
- Fatta-Kassinos, D., Vasquez, M.I., Kümmerer, K., 2011. Transformation products of pharmaceuticals in surface waters and wastewater formed during photolysis and advanced oxidation processes – Degradation, elucidation of byproducts and assessment of their biological potency. *Chemosphere* 85 (5), 693–709.
- Fujishima, A., Rao, T.N., Tryk, D.A., 2000. Titanium dioxide photocatalysis. *Journal of Photochemistry and Photobiology C: Photochemistry Reviews* 1 (1), 1–21.
- García-Galána, M.J., Díaz-Cruza, M.S., Barceló, D., 2011. Occurrence of sulfonamide residues along the Ebro river basin: Removal in wastewater treatment plants and environmental impact assessment. *Environment International* 37 (2), 462–473.
- García-Käufer, M., Haddad, T., Bergheim, M., Gminski, R., Gupta, P., Mathur, N., Kümmerer, K., Mersch-Sundermann, V., 2012. Genotoxic effect of ciprofloxacin during photolytic

- decomposition monitored by the in vitro micronucleus test (MNvit) in HepG2 cells. *Environmental Science and Pollution Research* 19 (5), 1719-1727.
- Gartiser, S., Urich, E., Alexy, R., Kümmerer, K., 2007. Ultimate biodegradation and elimination of antibiotics in inherent tests. *Chemosphere* 67 (3), 604–613.
- Gómez, M.J., Sirtori, C., Mezcuca, M., Fernández-Alba, A.R., Agüera, A., 2008. Photodegradation study of three dipyrone metabolites in various water systems: Identification and toxicity of their photodegradation products. *Water Research* 42 (10–11), 2698–2706.
- Gros, M., Petrović, M., Barceló, D., 2006. Multi-residue analytical methods using LC-tandem MS for the determination of pharmaceuticals in environmental and wastewater samples: a review. *Analytical and Bioanalytical Chemistry* 386 (4), 941–952.
- Hao, C., Lissemore, L., Nguyen, B., Kleywegt, S., Yang, P., Solomon, K., 2006. Determination of pharmaceuticals in environmental waters by liquid chromatography/electrospray ionization/tandem mass spectrometry. *Analytical and Bioanalytical Chemistry* 384 (2), 505–513.
- Hirsch, R., Ternes, T., Haberer, K., Kratz, K.-L., 1999. Occurrence of antibiotics in the aquatic environment. *Science of The Total Environment* 225 (1–2), 109–118.
- Holm, G., Snape, J.R., Murray-Smith, R., Talbot, J., Taylor, D., Sörme, P., 2013. Implementing Ecopharmacovigilance in Practice: Challenges and Potential Opportunities. *Drug Safety* 36 (7), 533–546.
- Ji, Y., Zeng, C., Ferronato, C., Chovelon, J.-M., Yang, X., 2012. Nitrate-induced photodegradation of atenolol in aqueous solution: Kinetics, toxicity and degradation pathways. *Chemosphere* 88 (5), 644–649.
- Jiang, J.-Q., Lloyd, B., 2002. Progress in the development and use of ferrate(VI) salt as an oxidant and coagulant for water and wastewater treatment. *Water Research* 36 (6), 1397–1408.
- Jongh, C.M. de, Kooij, P.J., Voogt, P. de, ter Laak, T.L., 2012. Screening and human health risk assessment of pharmaceuticals and their transformation products in Dutch surface waters and drinking water. *Science of The Total Environment* 427-428, 70–77.
- Kang, S., Allbaugh, T., Reynhout, J., Erickson, T., Olmstead, K., Thomas, L., Thomas, P., 2004. Selection of an ultraviolet disinfection system for a municipal wastewater treatment plant. *Water science and technology* 50 (7), 163–169.
- Keane, D., Basha, S., Nolan, K., Morrissey, A., Oelgemöller, M., Tobin, J.M., 2011. Photodegradation of Famotidine by Integrated Photocatalytic Adsorbent (IPCA) and Kinetic Study. *Catalysis Letters* 141 (2), 300–308.
- Klavarioti, M., Mantzavinos, D., Kassinos, D., 2009. Removal of residual pharmaceuticals from aqueous systems by advanced oxidation processes. *Environment International* 35 (2), 402–417.
- Kosjek, T., Heath, E., 2011. Occurrence, fate and determination of cytostatic pharmaceuticals in the environment. *TrAC Trends in Analytical Chemistry* 30 (7), 1065–1087.
- Kümmerer, K. (Ed.), 2008. *Pharmaceuticals in the environment: Sources, fate, effects and risks*, 3.ed. ed. Springer, Berlin, Heidelberg.

- Kümmerer, K., Eitel, A., Braun, U., Hubner, P., Daschner, F., Mascart, G., Milandri, M., Reinthaler, F., Verhoef, J., 1997. Analysis of benzalkonium chloride in the effluent from European hospitals by solid-phase extraction and high-performance liquid chromatography with post-column ion-pairing and fluorescence detection. *Journal of Chromatography A* 774 (1-2), 281–286.
- La Farré, M., Pérez, S., Kantiani, L., Barceló, D., 2008. Fate and toxicity of emerging pollutants, their metabolites and transformation products in the aquatic environment. *TrAC Trends in Analytical Chemistry* 27 (11), 991–1007.
- Laboratory of Mathematical Chemistry, 2012. Oasis Catalogic software V.5.11.6TB. “Prof. Dr. Assen Zlatarov” University, Bourgas, Bulgaria.
- Lam, M.W., Mabury, S.A., 2005. Photodegradation of the pharmaceuticals atorvastatin, carbamazepine, levofloxacin, and sulfamethoxazole in natural waters. *Aquatic Sciences* 67 (2), 177–188.
- Liberti, L., Notarnicola, M., 1999. Advanced treatment and disinfection for municipal wastewater reuse in agriculture. *Water Science and Technology* 40 (4–5), 235–245.
- Mahmoud, W.M.M., Kümmerer, K., 2012. Captopril and its dimer captopril disulfide: Photodegradation, aerobic biodegradation and identification of transformation products by HPLC–UV and LC–ion trap–MSⁿ. *Chemosphere* 88 (10), 1170–1177.
- Meneses, M., Pasqualino, J., Castells, F., 2010. Environmental assessment of urban wastewater reuse: Treatment alternatives and applications. *Chemosphere* 81 (2), 266–272.
- Ministry of Health and Population (MOHP), 2006. National Essential Drug List. Ministry of Health and Population (MOHP) (accessed 17.03.2011). <http://www.mohp.gov.eg/sec/Drugs/Groups3.pdf>.
- Pailler, J.-Y., Krein, A., Pfister, L., Hoffmann, L., Guignard, C., 2009. Solid phase extraction coupled to liquid chromatography-tandem mass spectrometry analysis of sulfonamides, tetracyclines, analgesics and hormones in surface water and wastewater in Luxembourg. *Science of The Total Environment* 407 (16), 4736–4743.
- Pérez, S., Barceló, D., 2008. Applications of LC-MS to quantitation and evaluation of the environmental fate of chiral drugs and their metabolites. *TrAC Trends in Analytical Chemistry* 27 (10), 836–846.
- Petrovic, M., Barceló, D., 2007. LC-MS for identifying photodegradation products of pharmaceuticals in the environment: Pharmaceutical-residue analysis. *TrAC Trends in Analytical Chemistry* 26 (6), 486–493.
- Richardson, M.L., Bowron, J.M., 1985. The fate of pharmaceutical chemicals in the aquatic environment. *Journal of Pharmacy and Pharmacology* 37 (1), 1–12.
- Roberts, G., Myatt, G., Johnson, W., Cross, K., Blower, P., 2000. LeadScope: Software for Exploring Large Sets of Screening Data. *Journal of Chemical Information and Modeling* 40 (6), 1302–1314.
- Rücker, C., Kümmerer, K., 2012. Modeling and predicting aquatic aerobic biodegradation – a review from a user's perspective. *Green Chemistry* 14 (4), 875.

- Santos, L.H.M.L.M., Araújo, A.N., Fachini, A., Pena, A., Delerue-Matos, C., Montenegro, M.C.B.S.M., 2010. Ecotoxicological aspects related to the presence of pharmaceuticals in the aquatic environment. *Journal of Hazardous Materials* 175 (1–3), 45–95.
- Sedykh, A., Saiakhov, R., Klopman, G., 2001. META V. A model of photodegradation for the prediction of photoproducts of chemicals under natural-like conditions. *Chemosphere* 45 (6–7), 971–981.
- Sharma, V.K., 2002. Potassium ferrate(VI): an environmentally friendly oxidant. *Advances in Environmental Research* 6 (2), 143–156.
- Tixier, C., Singer, H.P., Oellers, S., Müller, S.R., 2003. Occurrence and Fate of Carbamazepine, Clofibric Acid, Diclofenac, Ibuprofen, Ketoprofen, and Naproxen in Surface Waters. *Environmental Science & Technology* 37 (6), 1061–1068.
- Trautwein, C., Kümmerer, K., 2011. Incomplete aerobic degradation of the antidiabetic drug Metformin and identification of the bacterial dead-end transformation product Guanylurea. *Chemosphere* 85 (5), 765–773.
- Trautwein, C., Kümmerer, K., 2012. Ready biodegradability of trifluoromethylated phenothiazine drugs, structural elucidation of their aquatic transformation products, and identification of environmental risks studied by LC-MSⁿ and QSAR. *Environmental Science and Pollution Research* 19 (8), 3162–3177.
- Trovó, A.G., Nogueira, Raquel F. P., Agüera, A., Sirtori, C., Fernández-Alba, A.R., 2009. Photodegradation of sulfamethoxazole in various aqueous media: Persistence, toxicity and photoproducts assessment. *Chemosphere* 77 (10), 1292–1298.
- U.S. EPA, 1998. United States Environmental Protection Agency, Wastewater Technology Fact Sheet Ultraviolet Disinfection 832-F99-064.
- Velo, G., Moretti, U., 2010. Ecopharmacovigilance for Better Health. *Drug Safety* 33 (11), 963–968.
- Vieno, N., Tuhkanen, T., Kronberg, L., 2007. Elimination of pharmaceuticals in sewage treatment plants in Finland. *Water Research* 41 (5), 1001–1012.
- Walker, J.D., Dimitrova, N., Dimitrov, S., Mekenyan, O., Plewak, D., 2004. Use of QSARs to promote more cost-effective use of chemical monitoring resources. 2. Screening chemicals for hydrolysis half-lives, Henry's Law constants, ultimate biodegradation potential, modes of toxic action and bioavailability. *Water Quality Research Journal of Canada* 39 (1), 40–49.
- Wang, X.-H., Lin, A.Y.-C., 2012. Phototransformation of Cephalosporin Antibiotics in an Aqueous Environment Results in Higher Toxicity. *Environmental Science & Technology* 46 (22), 12417–12426.
- Zwiener, C., Frimmel, F., 2004. LC-MS analysis in the aquatic environment and in water treatment technology – a critical review. *Analytical and Bioanalytical Chemistry* 378 (4), 862–874.

Curriculum Vitae

Waleed Mohamed Mamdouh Mahmoud Ahmed, Born on 01.10.1981 in Ismailia, Egypt.

Education:

- 12/2009-12/2013** Ph.D. candidate (Dr. rer. nat.) in Institute for Sustainable and Environmental Chemistry, Faculty of Sustainability Sciences at Leuphana University in Lüneburg, Germany. Former Ph.D. candidate (Dr. rer. nat.) in Department of Environmental Health Sciences, University Medical Center Freiburg and Institute of Pharmaceutical Sciences, Albert-Ludwigs-Universität Freiburg, Freiburg, Germany
- 2004-2007** Master in Pharmaceutical Sciences (Analytical Chemistry), Faculty of pharmacy of the Suez Canal University, Ismailia, Egypt
- 1998-2003** Bachelor (Excellent with Honors) in Pharmaceutical Sciences, Faculty of pharmacy of the Suez Canal University, Ismailia, Egypt
- 1995-1998** Secondary school certificate, El-Sadat secondary school, Ismailia, Egypt

Employment and Professional Experience

- 2011-2013** One of the supervisors of the practical experimental chemistry techniques sections for the bachelor students in the Faculty of Sustainability in the winter semester 2011-2012, summer semester 2012, and summer semester 2013.
- 6/2007- present** Assistant Lecturer of Analytical Chemistry at the Faculty of pharmacy of the Suez Canal University in Ismailia, Egypt.
- 11/2003 – 6/2007** Demonstrator of Analytical Chemistry at the Faculty of pharmacy of the Suez Canal University in Ismailia, Egypt.
- 2003-2004** Pharmacist in private pharmacies
- 09/2001** Practical at Medical Union Pharmaceuticals (M.U.P), Ismailia- Egypt.

Scholarships:

PhD scholarship from the German-Egyptian Research Long Term scholarship (GERLS) financed by the Ministry of Higher Education and Scientific Research (MHESR) and the German Academic Exchange Service (DAAD).

List of Publications:

1. **Waleed M. M. Mahmoud**, Anju P. Toolaram, Jakob Menz, Christoph Leder, Mandy Schneider, Klaus Kümmerer (2013) Identification of phototransformation products of Thalidomide and mixture toxicity assessment: an experimental and quantitative structural activity relationships (QSAR) approach. Water Research. DOI: 10.1016/j.watres.2013.11.014.

2. **Waleed M. M. Mahmoud**, Christoph Trautwein, Christoph Leder, Klaus Kümmerer, (2013) Aquatic photochemistry, abiotic and aerobic biodegradability of thalidomide: identification of stable transformation products by LC-UV-MSⁿ. *Science of the Total Environment* 463–464: 140–150. DOI: 10.1016/j.scitotenv.2013.05.082
3. **Waleed M. M. Mahmoud**, Nareman D. H. Khaleel, Ghada M. Hadad, Randa A. Abdel-Salam, Annette Haiß, Klaus Kümmerer.(2013) Simultaneous Determination of 11 Sulfonamides by HPLC–UV and Application for Fast Screening of Their Aerobic Elimination and Biodegradation in a Simple Test. *CLEAN – Soil, Air, Water*. DOI: 10.1002/clen.201200508
4. Marcelo L Wilde, **Waleed M. M. Mahmoud**, Klaus Kümmerer, Ayrton Figueiredo Martins, (2013) Oxidation–coagulation of β -blockers by $K_2Fe^{VI}O_4$ in hospital wastewater: Assessment of degradation products and biodegradability. *Science of the Total Environment* 452–453: 137-147. DOI: 10.1016/j.scitotenv.2013.01.059
5. Nareman D. H. Khaleel, **Waleed M. M. Mahmoud**, Ghada M. Hadad, Randa A. Abdel-Salam, Klaus Kümmerer, (2013) Photolysis of sulfamethoxypyridazine in various aqueous media: Aerobic biodegradation and photoproducts identification by LC-UV-MS/MS. *Journal of Hazardous Materials* 244-245: 654–661. doi:10.1016/j.jhazmat.2012.10.059
6. **Waleed M. M. Mahmoud**, Klaus Kümmerer, (2012) Captopril and its dimer captopril disulfide: photodegradation, aerobic biodegradation and identification of transformation products by HPLC-UV and LC–ion trap-MSⁿ. *Chemosphere* 88(10): 1170–1177. DOI: 10.1016/j.chemosphere.2012.03.064.
7. Faten Sleman, **Waleed M. M. Mahmoud**, Rolf Schubert, Klaus Kümmerer, (2012) Photodegradation, photocatalytic and aerobic biodegradation of sulfisomidine and identification of transformation products By LC–UV-MS/MS. *CLEAN – Soil, Air, Water* 40 (11) 1244-1249. DOI: 10.1002/clen.201100485.
8. Ghada M. Hadad, **Waleed M. M. Mahmoud**, (2011) The use of a monolithic column to improve the simultaneous determination of caffeine, paracetamol, pseudoephedrine, aspirin, dextromethorphan, chlorpheniramine in pharmaceutical formulations by HPLC-a comparison with a conventional reversed-phase silica-based column. *Journal of Liquid Chromatography & Related Technologies*. 34 (20): 2516–2532. DOI: 10.1080/10826076.2011.591031
9. Ghada M. Hadad, Samy Emara, **Waleed M. M. Mahmoud**, (2009) Optimization and Validation of High Performance Liquid Chromatographic Method for the Determination of Cefdinir in Dosage Form and Human Urine. *Chromatographia*, 70(11-12): 1593-1598.
10. Ghada M. Hadad, Samy Emara, **Waleed M. M. Mahmoud**, (2009) Development and validation of a stability-indicating RP-HPLC method for the determination of paracetamol with dantrolene or/and cetirizine and pseudoephedrine in two pharmaceutical dosage forms. *Talanta* 79(5):1360-1367.
11. Ghada M. Hadad, Alaa El-Gindy, **Waleed M. M. Mahmoud**, (2008) HPLC and chemometrics-assisted UV-spectroscopy methods for the simultaneous determination of

- ambroxol and doxycycline in capsule. *Spectrochimica Acta Part A: Molecular and Biomolecular Spectroscopy* 70(3): 655-663.
12. Ghada M. Hadad, Alaa El-Gindy and **Waleed M. M. Mahmoud**, (2008) New Validated Liquid Chromatography and Chemometrics-Assisted UV-Spectroscopic Methods for the Simultaneous Determination of Two Multicomponent cough Mixtures in Syrup. *Journal of AOAC International* 91(1): 39-51.
 13. Ghada M. Hadad, Alaa El-Gindy and **Waleed M. M. Mahmoud**, (2007) Optimization and validation of an HPLC-UV method for determination of tranexamic acid in a dosage form and in human urine. *Chromatographia*, 66(5/6): 311-317.
 14. Ghada M. Hadad, Alaa El-Gindy and **Waleed M. M. Mahmoud**, (2007) Development and validation of chemometrics-assisted spectrophotometry and liquid chromatography methods for the simultaneous determination of the active ingredients in two multicomponent mixtures containing chlorpheniramine maleate and phenylpropanolamine hydrochloride. *Journal of AOAC International* 90(4): 957-970.
 15. Alaa El-Gindy, Ghada M. Hadad and **Waleed M. M. Mahmoud**, (2007) High performance liquid chromatographic determination of etofibrate and its hydrolysis products. *Journal of Pharmaceutical and Biomedical Analysis* 43(1): 196–203.

Contributions to international conferences

Oral presentation:

Waleed M. M. Mahmoud, Anju Priya Toolaram, Mandy Schneider, Klaus Kümmerer (28.08.2012). Photodegradation of thalidomide: Identification of transformation products by LC-UV-FL-MS/MS, assessment of biodegradability, cytotoxicity and mutagenicity” presented in the presentation session of *Environmental Chemistry - Emerging contaminants, POPs, phototransformation* in the 4th EuCheMS Chemistry Congress, August 26 – 30, 2012, in Prague, Czech Republic. *Chem. Listy* 106, 650 (2012).

Poster presentation:

1. **Waleed M. M. Mahmoud**, Anju P. Toolaram, Jakob Menz, Christoph Leder, Mandy Schneider, Klaus Kümmerer. Identification and initial toxicity assessment of Thalidomide and its photo transformation products. The 14th EuCheMS International Conference on Chemistry and the Environment (ICCE 2013), Barcelona, Spain, June 25 – 28.06.2013.
2. Nareman D. H. Khaleel, **Waleed M. M. Mahmoud**, Ghada M. Hadad, Randa A. Abdel-Salam, Christoph Leder, Klaus Kümmerer, Photocatalytic degradation of sulfamethoxypyridazine with TiO₂, FeCl₃ and TiO₂/FeCl₃: Biodegradability, toxicity assessment, and LC-UV-MS/MS identification of the photodegradation products in aqueous and sewage treatment plant effluent. The 14th EuCheMS International Conference on Chemistry and the Environment (ICCE 2013), Barcelona, Spain, June 25 – 28.06.2013.
3. Nareman D. H. Khaleel, **Waleed M. M. Mahmoud**, Ghada M. Hadad, Randa A. Abdel-Salam, Klaus Kümmerer, Photolysis of sulfamethoxypyridazine in various aqueous media: Aerobic biodegradation and photoproducts identification by LC-UV-MS/MS. 4th

- EuCheMS Chemistry Congress, Prague, Czech Republic, 26 – 30.08.2012. Chem. Listy 106, 904 (2012).
4. **Waleed M. M. Mahmoud**, Christoph Trautwein, Klaus Kümmerer, Photodegradation, Aerobic Biodegradability and Identification of Transformation Products of Thalidomide by LC–MS/MS. Poster no. ACH 4. GDCh-Wissenschaftsforum Chemie 2011. Bremen, Germany: 4-7.9.2011.
 5. Marcelo L. Wilde, Francieli M. Mayer, **Waleed M. M. Mahmoud**, Klaus Kümmerer, Ayrton F. Martins, Degradation of the emerging contaminant Atenolol by $K_2Fe^{VI}O_4$: Assessment of biodegradability and degradation products. Poster, IX Latin American Symposium on Environmental and Sanitary Analytical Chemistry. Salvador – Brasil: 17-20.4.11.
 6. **Waleed M. M. Mahmoud**, Klaus Kümmerer, Photodegradation and aerobic biodegradability of angiotensin-converting enzyme inhibitor Captopril and identification of transformation products by LC MS/MS. Poster no. UMW_P 14, ANAKON 2011 (Analytical Chemistry Conference). Zürich, Switzerland: 22.-25.3.11.
 7. Ghada M. Hadad, Samy Emara, **Waleed M. M. Mahmoud**, Optimization and Validation of High Performance Liquid Chromatographic Method for the Determination of Cefdinir in Dosage Form and Human Urine. 1st International Pharmaceutical Science Conference “Pharmacy Education and Community Expectations” Faculty of Pharmacy, Tanta University, Tanta, Egypt, November 18-19, 2009.

Scientific Activities:

- Peer reviewer for 8 international journals for several times:
 1. Water Research
 2. Environmental Pollution
 3. Journal of AOAC INTERNATIONAL.
 4. Journal of Liquid Chromatography & Related Technologies.
 5. Journal of Chromatographic Science.
 6. E-Journal of Chemistry.
 7. Scientia Pharmaceutica (The Austrian Journal of Pharmaceutical Sciences).
 8. Current Pharmaceutical Analysis.
- An active member in the Higher Education Enhancement Project Fund (HEEPF) of Pharmacy Courses, Faculty of Pharmacy, Suez Canal University, Ismailia- Egypt.
- An active member in the Quality Assurance and Accreditation Project (QAAP), Faculty of Pharmacy, Suez Canal University, Ismailia- Egypt.

Engagement:

- Member in the German Chemical Society.
- Member in the General Syndicate of Pharmacists, Egypt.
- Member in the Suez Canal University Staff Club.

Declaration 1

I avouch that all information given in this appendix is true in each instance and overall.

Waleed Mohamed Mamdouh Mahmoud Ahmed
Lüneburg, 1st August 2013

Authors' contributions to the articles and articles publication status:

Article*	Short title	Specific contributions of all authors	Author status	Weighting factor	Publication status**	Conference contributions
1	Captopril and its dimer captopril disulfide: photodegradation, aerobic biodegradation and identification of transformation products by HPLC-UV and LC-ion trap-MS ⁿ	Waleed M. M. Mahmoud, Klaus Kümmerer	Co-author with predominant contribution [Überwiegender Anteil]	1.0	Chemosphere 2012; 88(10): 1170–1177. DOI: 10.1016/j.chemosphere.2012.03.064. (IF=3.137 (2012), Q1)	ANAKON 2011 (Analytical Chemistry Conference). Zürich, Switzerland: 22.-25.3.2011.
2	A HPLC-UV method for the simultaneous determination of eleven sulfonamides and its application for fast screening of their aerobic elimination and biodegradation in a simple test.	Waleed M. M. Mahmoud, Nareman D. H. Khaleel, Ghada M. Hadad, Randa A. Abdel-Salam, Annette Haiß, Klaus Kümmerer.	Co-author with predominant contribution [Überwiegender Anteil]	1.0	CLEAN – Soil, Air, Water. 2013; DOI: 10.1002/clen.201200508 (IF=2.046 (2012), Q2)	
3	Aquatic photochemistry, abiotic and aerobic biodegradability of thalidomide: identification of stable transformation products by LC-UV-MS ⁿ	Waleed M. M. Mahmoud, Christoph Trautwein, Christoph Leder, Klaus Kümmerer,	Co-author with predominant contribution [Überwiegender Anteil]	1.0	Science of the Total Environment. 2013; 463–464: 140–150. DOI: 10.1016/j.scitotenv.2013.05.082 (IF=3.258 (2012), Q1)	GDCh-Wissenschaftsforum Chemie 2011. Bremen, Germany: 4-7.9.2011. and The 4 th EuCheMS Chemistry Congress, August 26 – 30, 2012, in Prague, Czech Republic. Chem. Listy 106, 650 (2012).
4	Identification of phototransformation products of Thalidomide and mixture toxicity assessment: an	Waleed M. M. Mahmoud, Anju P. Toolaram, Jakob Menz, Christoph	Co-author with equal contribution [Gleicher	1.0	Water Research. 2013 DOI: 10.1016/j.watres.2013.11.014	The 4 th EuCheMS Chemistry Congress, August 26 – 30, 2012, in Prague, Czech Republic. Chem. Listy 106,

	experimental and quantitative structural activity relationships (QSAR) approach.	Leder, Mandy Schneider, Klaus Kümmerer.	Anteil]		(IF=4.655 (2012), Q1)	650 (2012). and the 14 th EuCheMS International Conference on Chemistry and the Environment (ICCE 2013), Barcelona, June 25 - 28, 2013
5	Photolysis of sulfamethoxypyridazine in various aqueous media: Aerobic biodegradation and photoproducts identification by LC-UV-MS/MS.	Nareman D. H. Khaleel, Waleed M. M. Mahmoud, Ghada M. Hadad, Randa A. Abdel- Salam, Klaus Kümmerer,	Co-author with important contribution [Wichtiger Anteil]	0.5	Journal of Hazardous Materials 2013; 244-245: 654–661. DOI:10.1016/j.jhazmat.2012.10.059 (IF=3.925 (2012), Q1)	4 th EuCheMS Chemistry Congress, Prague, Czech Republic, 26-30.08.2012. Chem. Listy 106, 904 (2012).
6	Photodegradation, photocatalytic and aerobic biodegradation of sulfisomidine and identification of transformation products By LC–UV-MS/MS.	Faten Sleman, Waleed M. M. Mahmoud, Rolf Schubert, Klaus Kümmerer,	Co-author with important contribution [Wichtiger Anteil]	0.5	CLEAN – Soil, Air, Water 2012; 40 (11) 1244-1249. DOI: 10.1002/clen.20110 0485. (IF=2.046 (2012), Q2)	
7	Oxidation–coagulation of β -blockers by $K_2Fe^{VI}O_4$ in hospital wastewater: Assessment of degradation products and biodegradability	Marcelo L Wilde, Waleed M. M. Mahmoud, Klaus Kümmerer, Ayrton Figueiredo Martins	Co-author with important contribution [Wichtiger Anteil]	0.5	Science of the Total Environment 2013; 452–453: 137-147. DOI: 10.1016/j.scitotenv.2013.01.059 (IF=3.258 (2012), Q1)	The IX Latin American Symposium on Environmental and Sanitary Analytical Chemistry. Salvador – Brasil: 17-20.4.2011.
Sum:				5.5		

* Articles order according to the weighting factor

****IF** = Impact Factor 2011, **Q** = Quartile in environmental sciences category 2011 from ISI Web of Science (Journal Citation Reports).

Declaration of Authorship: Authors' contributions to the articles:

	<u>Paper I</u>	<u>Paper II</u>	<u>Paper III</u>	<u>Paper IV</u>	<u>Paper V</u>	<u>Paper VI</u>	<u>Paper VII</u>
Conception of research approach	KK, WMA	AM, KK, MW, WMA	AH, GH, KK, NK, RA, WMA	GH, KK, NK, RA, WMA	FS, KK, RS, WMA	CL, CT, KK, WMA	AT, CL, JM, KK, MS, WMA
Development of research methods	KK, WMA	AM, KK, MW	AH, KK, NK, WMA	KK, NK, WMA	FS, KK, WMA	CT, KK, WMA	AT, CL, JM, KK, MS, WMA
Data collection and data preparation	WMA	MW, WMA	NK, WMA	NK, WMA	FS, KK	WMA	AT, CL, JM MS, WMA
Execution of research	WMA	MW, WMA	NK, WMA	NK, WMA	FS, WMA	CL, CT, WMA	AT, JM, WMA
Analysis/ interpretation of data	KK, WMA	MW	AH, KK, NK, WMA	KK, NK, WMA	FS, KK, WMA	CL, CT, KK, WMA	AT, CL, JM, KK, MS, WMA
Writing of the manuscript	WMA	AM, MW	NK, WMA	NK, WMA	FS, WMA	WMA	AT, JM, WMA
Internal revision of manuscript	KK, WMA	AM, KK, MW	AH, GH, KK, NK, RA, WMA	GH, KK, NK, RA, WMA	FS, KK, RS, WMA	CL, CT, KK, WMA	AT, CL, JM, KK, MS, WMA

Alphabetic order of the authors' names:

AH=Annette Haiß¹, AM= Ayrton Figueiredo Martins², AT = Anju P. Toolaram¹, CT = Christoph Trautwein¹, CL = Christoph Leder¹, FS = Faten Sleman³, GH = Ghada M. Hadad⁴, JM = Jakob Menz¹, KK = Klaus Kümmerer¹, MS = Mandy Schneider¹, MW= Marcelo L. Wilde², NK= Nareman D. H. Khaleel^{1,4}, RA = Randa A. Abdel-Salam⁴, RS = Rolf Schubert⁵, **WMA**= Waleed M. M. Mahmoud Ahmed^{1,4}.

Affiliations:

- 1- Sustainable Chemistry and Material Resources, Institute of Sustainable and Environmental Chemistry, Faculty of Sustainability Sciences, Leuphana University of Lüneburg, Scharnhorststraße 1/C13, DE-21335 Lüneburg, Germany.
- 2- Chemistry Department, Federal University of Santa Maria, 97105-900, Santa Maria, RS, Brazil.
- 3- Department of Environmental Health Sciences, University Medical Center Freiburg, Freiburg, Germany.
- 4- Pharmaceutical Analytical Chemistry Department, Faculty of Pharmacy, Suez Canal University, Ismailia 41522, Egypt.
- 5- Department of Pharmaceutical Technology and Biopharmacy, Albert- Ludwigs University, Freiburg, Germany.

Appendices

Paper I

Captopril and its dimer captopril disulfide:
photodegradation, aerobic biodegradation and
identification of transformation products by HPLC-UV
and LC-ion trap-MSⁿ

Chemosphere 88(10): 1170–1177 (2012)

DOI: 10.1016/j.chemosphere.2012.03.064



Captopril and its dimer captopril disulfide: Photodegradation, aerobic biodegradation and identification of transformation products by HPLC–UV and LC–ion trap–MSⁿ

Waleed M.M. Mahmoud^{a,b}, Klaus Kümmerer^{a,*}

^a Sustainable Chemistry and Material Resources, Institute of Sustainable Environmental Chemistry, Leuphana University Lüneburg, C13, DE-21335 Lüneburg, Germany

^b Pharmaceutical Analytical Chemistry Department, Faculty of Pharmacy, Suez Canal University, Ismailia 41522, Egypt

ARTICLE INFO

Article history:

Received 17 June 2011

Received in revised form 22 March 2012

Accepted 26 March 2012

Available online 24 April 2012

Keywords:

Photolysis

Biodegradation

Aquatic environment

Dead-end metabolite

UV treatment

Angiotensin converting enzyme (ACE) inhibitor

ABSTRACT

In some countries effluents from hospitals and households are directly emitted into open ditches without any further treatment and with very little dilution. Under such circumstances photo- and biodegradation in the environment can occur. However, these processes do not necessarily end up with the complete mineralization of a chemical. Therefore, the biodegradability of photoproduct(s) by environmental bacteria is of interest.

Cardiovascular diseases are the number one cause of death globally. Captopril (CP) is used in this study as it is widely used in Egypt and stated as one of the essential drugs in Egypt for hypertension. Three tests from the OECD series were used for biodegradation testing: Closed Bottle test (CBT; OECD 301 D), Manometric Respirometry test (MRT; OECD 301 F) and the modified Zahn–Wellens test (ZWT; OECD 302 B). Photodegradation (150 W medium-pressure Hg-lamp) of CP was studied. Also CBT was performed for captopril disulfide (CPDS) and samples received after 64 min and 512 min of photolysis.

The primary elimination of CP and CPDS was monitored by LC–UV at 210 nm and structures of photo-products were assessed by LC–UV–MS/MS (ion trap). Analysis of photodegradation samples by LC–MS/MS revealed CP sulfonic acid as the major photodegradation product of CP. No biodegradation was observed for CP, CPDS and of the mixture resulting from photo-treatment after 64 min in CBT. Partial biodegradation in the CBT and MRT was observed in samples taken after 512 min photolysis and for CP itself in MRT. Complete biodegradation and mineralization of CP occurred in the ZWT.

© 2012 Elsevier Ltd. All rights reserved.

1. Introduction

A variety of different pharmaceutical substances have been found in several environmental compartments (Halling-Sørensen et al., 1998; Heberer et al., 2002; Nikolaou et al., 2007; Kümmerer, 2008, 2009a,b,c; Jiang et al., 2011). Some cardiovascular pharmaceuticals have been detected in the environment e.g. β -blockers (Gros et al., 2007; Valcárcel et al., 2011), which have an ecotoxicological effect on zooplankton (*Daphnia magna*) and benthic organisms (Fent et al., 2006).

Pharmaceutical compounds are released into the environment in a variety of ways: via waste water effluent as a result of incomplete metabolism in the body after use in human therapy, through improper disposal by private households or hospitals or through insufficient removal by water treatment plants (Al-Rifai et al.,

2007; Gomez et al., 2007). Many pharmaceuticals are not completely metabolized, and they are excreted unchanged or either slightly transformed as metabolites such as conjugated polar molecules, e.g. glucuronides. These conjugates can easily be cleaved during sewage treatment and the original drugs might then be released into the aquatic environment (Heberer, 2002). By effluent treatment and metabolism new compounds can result, so called transformation products (Kümmerer, 2009c).

Once pharmaceuticals and their transformation products have been released into the effluent and the aquatic environment they are subjected to many processes (e.g., dilution, hydrolysis, oxidation, photolysis, biodegradation, and sorption to bed sediments and sewage sludge) that contribute to their elimination from the environmental waters (Gartiser et al., 2007; Petrovic and Barceló, 2007). Elimination of drugs during the waste water treatment and their biodegradation is often being limited, so they can persist in the environment (Heberer, 2002).

Photochemical degradation is one of the potentially significant removal mechanisms for pharmaceuticals in aquatic environments. Phototreatment such as photolysis and photocatalysis for

* Corresponding author. Address: Nachhaltige Chemie und Ressourcen, Institut für Nachhaltige Chemie und Umweltchemie, Leuphana Universität Lüneburg, C.13, Scharnhorststraße 1, D-21335 Lüneburg, Germany. Tel.: +49 4131 677 2893.

E-mail address: Klaus.Kuemmerer@uni.leuphana.de (K. Kümmerer).

the removal of pharmaceuticals in effluents is currently under discussion as the data on the photochemical transformation of pharmaceuticals in the aquatic environment are still largely missing (Boreen et al., 2003; Lin and Reinhard, 2005; Konstantinou et al., 2010).

Furthermore photolysis can take place when compounds reach surface water. Photolytic reactions are often complex involving various competing parallel pathways thus leading to multiple reaction products that may be more toxic than the parent compound or lose antimicrobial activity and/or toxicity (Petrovic and Barceló, 2007). Although manufacturers rigorously test the stability of pharmaceuticals, photo-induced and biodegradation of these compounds in the environment has not been widely investigated. Elucidation of photolysis-reaction pathways and identification of transformation products are therefore of crucial importance in understanding the fate of these compounds in the aquatic environment. In some countries effluents from hospitals and households are directly emitted into open ditches without any further treatment and with very little dilution. Under such circumstances photo-degradation in the environment can occur. However, photo-degradation does not necessarily end up with the complete mineralization of a pharmaceutical.

Cardiovascular diseases (CVDs) are the number one cause of death globally. CVDs are the world's largest killers, claiming 29% (17.1 million people) of all global deaths. Low- and middle-income countries are disproportionately affected: 82% of CVDs deaths take place in low- and middle-income countries according to World Health Organization (2011). Hypertension is a major health problem throughout the world because of its high prevalence and its association with increased risk of CVDs. In the Eastern Mediterranean Region, the prevalence of hypertension averages 29% and it affects approximately 125 million individuals. Of greater concern is that cardiovascular complications of high blood pressure are on the increase, including the incidence of stroke, end-stage renal disease and heart failure according to World health organization Regional Office for the Eastern Mediterranean (World Health Organization, 2009). Hypertension is a major health problem in Egypt with a prevalence rate of 26.3% among the adult population (>25 years). Its prevalence increases with aging, approximately 50% of Egyptians above the age of 60 years suffer from hypertension according to Egyptian Hypertension Society (Ibrahim, 2004).

Captopril (CP; 1-[(2S)-3-Mercapto-2-methylpropionyl]-l-proline) is a sulfhydryl-containing angiotensin converting enzyme (ACE) inhibitor. It is used in the management of hypertension, in heart failure, after myocardial infarction, and in diabetic nephropathy. It is largely excreted in the urine, 40–50% as unchanged drug, the rest as disulfide and other metabolites (Sweetman, 2009). Disulfide products of captopril metabolism are all in vivo and in vitro reversibly formed. However, the dynamic interconversion of captopril and largely inactive disulfide metabolites distinguishes captopril from other anti-hypertensive agents and probably contributes to the prolonged pharmacological effect of captopril in the absence of detectable blood levels of captopril. Renal failure results in only small increases in blood levels of captopril but large increases in circulating metabolites which are largely not dialyzable. Some studies demonstrated that CP disulfides may contribute in the antihypertensive action of CP and have weak but significant inhibition of angiotensin converting enzyme activity. Therefore, it is of high importance to assess the impact of these metabolites on the environment (Drummer and Jarrott, 1986). CP aqueous solutions are subject to oxidative degradation, mainly to Captopril Disulfide (CPDS), which increases with increase at pH above 4 (Sweetman, 2009). Captopril is widely used in Egypt and stated as one of the essential drugs in Egypt for hypertension in the pharmacological group ACE Inhibitors according to Egyptian Ministry of Health and Population (Ministry of Health and Population (MOHP),

2006). Nile River suffers from pollution due to direct and indirect sanitation of the villages and cities along its stream leading to pollution arising from mixing water with sewage as a result of random drainage from villages. So many pharmaceuticals such as CP and its metabolite CPDS can reach surface water i.e. Nile River. Due to that it is important to assess the photodegradability and biodegradability of CP and its possible microbial degradation products.

Therefore, we report here on the photodegradability and biodegradability of CP and CPDS and the identification of stable dead-end transformation products. To assess the biodegradability of CP and the possible formation of potential microbial degradation products, three tests of the OECD series were used in the present study: the widely used Closed Bottle test (CBT, OECD 301 D) working with low bacterial density, the manometric respirometry test (MRT, OECD 301 F) working with medium bacterial density and the modified Zahn–Wellens test (ZWT, OECD 302 B) working with high bacterial density thus simulating surface water and effluent, respectively.

The CBT is recommended as a first, simple test for the assessment of the biodegradability of organic compounds in the environment. Substances that pass the test are classified as readily biodegradable. Compounds are also assumed to be readily biodegradable in sewage treatment plants and therefore are expected not to reach or accumulate in the aquatic environment (Nyholm, 1991). Accordingly, the CBT was performed for CP, CPDS, and photodegradation samples taken after 64 min contain CP & photodegradation products and after 512 min contain photodegradation products only.

Additional to mineralization the primary elimination of CP was monitored by HPLC–UV at 210 nm and structures of photoproducts were assessed by liquid chromatography ion trap mass spectrometry (LC–UV–MS/MS).

2. Experimental

2.1. Chemicals

All the chemicals used were of analytical grade. Acetonitrile (LiChrosolv[®], gradient grade) and formic acid (analytical grade) were purchased from Merck (Darmstadt, Germany). HPLC-grade water was generated using a Milli-Q water-purification system from Millipore (Molsheim, France). Captopril (CP) (CAS number 62571-86-2) from Fluka (Sigma–Aldrich, Steinheim, Germany), and Captopril Disulfide (CPDS) (CAS number 64806-05-9) from VWR International GmbH, Hannover, Germany.

2.2. Photodegradation

The experiments were conducted in a 1L batch photoreactor. The photolysis was performed using a medium-pressure mercury lamp (TQ150, UVConsulting Peschl, Mainz) with ilmasil quartz immersion tube. The lamp emits polychromatic radiation in the range from 200 to 600 nm. The maximal intensities were at 254, 265, 302, 313, 366, 405/408, 436, 546, and 577/579 nm. Radiation flux Φ from 200–600 nm is 47 W. During the photoreaction it is necessary to ensure a constant mixing of the solution. The mixture was stirred with a magnetic stirrer. The temperature was maintained by a circulating cooler (WKL230, LAUDA, Berlin) between 18–20 °C. Prior to each experiment, the lamp was warmed up for 5 min. CP samples (20 ml) were taken at different reaction times (0, 2, 4, 8, 16, 32, 64, 128, 256, and 512 min) for the analysis of the CP concentration by LC–UV–MS/MS and by non-purgeable organic carbon (NPOC).

The samples from 0–256 min after irradiation were stored at 3 different temperatures 20, 12 and 4 °C in order to monitor their

storage stability by LC–MS/MS. All experiments were performed at 20 °C and Milli-Q purified water was used to prepare all the solutions. In order to reach the adequate theoretical oxygen demand conditions for the Closed Bottle test (CBT), photoprocesses were carried out using high CP concentration 10 mg L⁻¹. Three experiments were run in order to get 576 ml of each at three different time points (0, 64 and 512 min).

2.3. Biodegradation testing

2.3.1. Closed Bottle test (OECD 301 D) (CBT)

The CBT was performed according to test guidelines (Organisation for Economic Co-operation and Development, 1992a) with a low nutrient content, low bacterial density (10²–10⁵ colony forming units (CFU) mL⁻¹) and at room temperature (20 ± 1 °C) in the dark (Kümmerer et al., 1996; Trautwein et al., 2008). According to the guidelines, at least 60% decomposition of the reference substance sodium acetate is required within 14 d.

The test consisted of four different series. The blank series contained only mineral medium and inoculum. The actual test series contained the respective test substance, while the quality control series contained readily biodegradable sodium acetate as the only respective carbon sources beside the inoculum. The amount of sodium acetate and of each test compounds corresponded to a theoretical oxygen demand (ThOD) of 5 mg L⁻¹ (Table S1, Supplementary material). The fourth series was the toxicity control, which in addition to the test compound also contained sodium acetate at an amount corresponding to 5 mg L⁻¹ ThOD. The toxicity control monitors a possible inhibitory effect to the bacteria used or the presence of a co-metabolism, i.e. the bacteria need a more easily biodegradable substance in order to be able to degrade the test substance. This allows for the recognition of false negative results caused toxicity of the test compound against the degrading bacteria. All tests were run as duplicates. Toxicity was assessed by comparing oxygen consumption as measured in the toxicity control bottles with the predicted level computed from the oxygen consumption in the quality control and in the test vessel containing only the test compound, respectively. A compound is labelled toxic if the difference between the predicted amount of oxygen consumption and the measured one exceeds 25% (OECD, 1992a).

Each test vessel contained the same mineral salt solution. Test compounds were obtained from our laboratory stocks as supplied by the manufacturers. All test vessels were inoculated with an aliquot from the effluent of a local municipal sewage treatment plant (Kenzingen, Germany, 13000 inhabitant equivalents). Two drops of inoculum were added to 1 L of medium, which resulted in approximately 500 CFU mL⁻¹.

According to the test guidelines a test compound is classified as “readily biodegradable” if biodegradability, expressed as a percentage of oxygen consumed in the test vessel (ThOD), exceeds 60% within a period of ten d after the oxygen consumption reached 10% ThOD. The process of aerobic biodegradation was monitored for 28 d by measuring oxygen concentration in the test vessels with Fibox 3 (Fiber-optic oxygen meter connected with Temperature sensor PT 1000) (PreSens, Precision Sensing GmbH, D-93053 Regensburg, Germany). For qualitative reasons pH values were also monitored at 0 and 28 d.

2.3.2. Manometric Respiratory test (OECD 301 F) (MRT)

Another method for assessing the degradability of chemicals is MRT (Organisation for Economic Co-operation and Development, 1992b) which can be performed in the dark at room temperature (20 ± 1 °C) under gentle stirring by use of the Oxitop system (WTW, Weilheim, Germany). It consists of measuring heads that are put on top of the test vessels and monitor the oxygen partial pressure in the system. No opening and closure of the test system

during the test procedure is necessary and possible. The sample scheme is equivalent to that of the CBT, although the test is performed with higher inoculum densities (5–10 × 10⁶ CFU mL⁻¹) and a higher sodium acetate and test compound concentration (Table S2, Supplementary material). They corresponded to a theoretical oxygen demand (ThOD) of 30 mg L⁻¹. All test bottles were inoculated with an aliquot from the effluent of a local municipal sewage treatment plant (Kenzingen, Germany, 13000 inhabitant equivalents). 80 mL of inoculum were added to 1 L of medium. Measurements were made in duplicate, i.e. for every data point in a curve, two individual bottles were used. The validity criteria are the same as for the CBT.

2.3.3. Zahn–Wellens test (OECD 302 B) (ZWT)

ZWT was performed according to test guidelines (Organisation for Economic Co-operation and Development, 1992c) with a high nutrient content and high bacterial diversity (~10⁷ CFU mL⁻¹) (Trautwein et al., 2008). All the chemicals were of analytical grade purchased from Merck (Darmstadt, Germany). The test was conducted at 22–26.5 °C; each consisting of five different 2 L Erlenmeyer Duran containers (Table S3, Supplementary material). In the flask for the “blank” set-up, only inoculum and mineral medium were present. With a concentration of 100.5 mg L⁻¹ CP (=50.0 mg dissolved organic carbon (DOC) L⁻¹) was added to two “test” containers as the only source of carbon. A set-up containing ethylene glycol at a concentration equivalent to a DOC of 50 mg L⁻¹ was chosen as “quality control”. The “negative control” vessel contained sodium azide (NaN₃) instead of the inoculum. Sodium azide is highly toxic to bacteria and therefore allows determining the degree of potential non-biotic elimination, e.g. caused by hydrolysis, non-biotic oxidation, photodegradation or volatilization. To account for the latter, a stripping control was applied. The sludge required as inoculum was obtained from a local municipal sewage treatment plant (Kenzingen, Germany, 13000 inhabitant equivalents). The dry matter content was 3.90 g L⁻¹. The final dry matter content of sludge in all the test vessels was 1 g L⁻¹. Prior to the experiments, the sludge was stored in the laboratory at room temperature and aerated until use. Shortly before the experiments the sludge was washed three times with tap water in order to reduce the DOC background. pH was adjusted to 6.5 ≤ pH ≤ 8.0 with sodium hydroxide (NaOH 0.1N) or sulfuric acid (H₂SO₄ 0.1N). The test was performed for 28 d under continuous gentle stirring and aeration.

Samples for DOC measurements were taken continually over the course of the extended test period of 28 d. DOC was determined according to European standard procedure EN 1484 with a TOC (TOC = total organic carbon) analyzer (TOC 5000, Shimadzu GmbH, Duisburg, Germany) in three replicates. First samples were taken and analyzed before adding the sludge, immediately after adding the sludge (0 h) and 3 h after start of the experiments. Elimination by sorption was accounted for by the DOC measured after 3 h. Prior to the chemical analysis, samples were filtered (using cellulose nitrate, cut-off 0.45 μm, Sartorius, Göttingen, Germany) in order to meet the conditions for DOC measurements. After sampling and filtering, DOC (released by the filtration process) of all samples were directly analyzed.

2.4. Monitoring of primary elimination by HPLC–UV and LC–MS/MS

The samples were measured for their primary elimination using HPLC–UV (210 nm) and ESI–LC–MS/MS (ion trap) was applied to get further structure related information.

Stock solutions of CP (100 μg mL⁻¹) and CPDS (150 μg mL⁻¹) were prepared in water. Standard solutions were prepared by further dilution with diluent to get the concentration range of linearity. Triplicate 100 μL and 50 μL for CP and CPDS injections,

respectively, were made for each concentration and chromatographed under the specified chromatographic conditions as described below. The peak areas were plotted against corresponding concentrations. Linear relationships were obtained.

A HPLC apparatus (Shimadzu, Duisburg, Germany) was used. Chromatographic separation was performed on an RP-18 column (CC 70/3 NUCLEODUR 100-3 C18 ec, Macherey and Nagel, Düren, Germany) protected by a CC 8/4 HYPERSIL 100-3 C18 ec, guard column. An isocratic system with a mobile phase consisting 0.1% formic acid in water (CH₂O₂: solution A) and 100% acetonitrile (CH₃CN: solution B) (80:20 v/v). The sample injection volume was 100 µL and 50 µL for CP and CPDS, respectively. The flow rate was set at 0.6 mL min⁻¹ and the oven temperature was set to 40 °C. Total run time was 10 min.

LC-MS/MS quantification and detection was performed on a Bruker Daltonic Esquire 6000 plus ion-trap mass spectrometer (IT-MS) equipped with a Bruker data analysis system and atmospheric pressure electrospray ionization (API-ESI) interface (Bruker Daltonic GmbH, Bremen, Germany). The MS was connected to the Agilent Technologies HPLC system (Agilent Technologies, Böblingen, Germany, HPLC 1100 series). Chromatographic separation was performed on the same RP-18 column previously described. For chromatography, 2 methods were used: (i) isocratic elution as previously described Total run time was 15 min. The retention time for CP and CPDS were 2.8 and 9.5 min, respectively. (ii) Gradient elution: 0.1% formic acid in water (CH₂O₂: solution A) and 100% acetonitrile (CH₃CN: solution B) were used by applying the following linear gradient: 0 min 5% B, 5 min 5% B, 20 min 40% B, 23 min 40% B, 26 min 5% B, 30 min 5% B. The flow rate was set at 0.6 mL min⁻¹ and the oven temperature was set to 40 °C. The molecule ion for CP and CPDS were *m/z* 218 and 433 at a retention time of 12.9 and 18.2 min, respectively.

The IT-MS was operated in positive polarity. The scan range was determined from *m/z* 40 to 1000 and the scan time was 200 ms (S4, Supplementary material). A typical chromatogram is presented in Fig. 1.

3. Results and discussion

The general objective of this study was to assess photodegradability and biodegradability of CP and biodegradability of its dimer CPDS and its photoproducts solutions and to correlate this information with data obtained from the photoproducts analysis.

3.1. Photo degradation

Photodegradation of CP did not lead to any mineralization or any obvious change in NPOC concentration. The LC-UV chromatogram demonstrated that most compounds formed by photolysis up have a polarity higher than CP (*t*_{RCP} = 2.3 min) (Fig. 1). CP was not detectable anymore after 512 min of irradiation.

The total ion current chromatograms (TICs) obtained for the irradiated samples show only one peak at the retention times of photodegradation products. The most intense peak, *m/z* = 266.1, was found at *t*_r = 1.8 min, is increased until 256 min irradiation time, after which they then decreased until 512 min (Fig 1c). For structural elucidation, this peak was isolated and fragmented (Table 1). The fragmentation pattern of mass *m/z* 266 was the same in all CP photodegradation samples which indicate that there is no photo isomerisation for this mass occurs. The specific mass *m/z* 266 can be assumed to be the molecular mass peak of 1-(3-sulpho-2-methyl-1-oxopropyl)-proline (Fig. 2).

During CP storage, a new transformation product (*t*_R = 2.6 min) with *m/z* 232 was formed in all stored samples in addition to CPDS

(Fig 1d–f). For structural elucidation, this peak was isolated and fragmented (Table 1). The specific mass *m/z* 232 could be the molecular mass peak of S-methyl captopril (Fig. 2). But it is very difficult that methylation occurred without any bacteria or methylating agent in the media.

3.2. Biodegradability

The CBT experiments were valid according to the test guidelines. No biodegradation was found for CP and CPDS in the CBT, classifying them as not readily biodegradable. Samples after 64 min irradiation of CP were not biodegradable in the CBT. However, the sample after 512 min irradiation, which contained photoproducts only, was about 28% biodegraded, demonstrating that the photoprocess increased the biodegradability. The toxicity control for CP, CPDS and samples after 64 and 512 min irradiation did not indicate toxicity against the bacteria present. The CP content in the samples was controlled by LC-MS/MS to monitor any primary CP elimination without significant oxygen consumption or abiotic reactions as hydrolysis. The results of these measurements confirmed the ones described above.

CP was stable in the MRT for the first 20 d, and then followed by some biodegradation. The quality control was valid according to the test guidelines. The measured toxicity control showed a good accordance with the calculated curve. From d 20 to d 28 the oxygen demand for the sample containing CP increased from 3.6% to 38.8%. NPOC (without any sample filtration) and elimination reached 54.6% in all the test flasks after 28 d. The toxicity control did not indicate toxicity against the bacteria present. To get more information on the partial elimination of CP revealed by the NPOC measurement, the samples were investigated for their primary elimination by LC-MS/MS.

The ZWT performed was valid according to the criteria stated in the OECD 302 B guideline. Based on DOC monitoring, no elimination of CP by sorption to the sewage sludge was found within the first 3 h of the ZWT. In the quality control samples the ethylene glycol was eliminated within less than 4 d. In contrast to the CBT, elimination of CP could be observed in the ZWT. The ZWT is a batch test, i.e. the adaptation of biocenosis to the test compound is enforced, which is also the case in the CBT. The results of DOC measurements and the primary elimination of CP in the ZWT showed that CP was totally eliminated. DOC elimination started after a time lag of 7 d. DOC elimination reached 96.9% in all the test flasks after approximately 21 d (Fig. 3).

According to the test guideline, a compound is classified as inherently biodegradable if at least 70% DOC elimination is reached after 28 d, which is the testing period prescribed by the test guideline. According to the results presented here, CP can thus be classified as inherent biodegradable. DOC elimination was not observed in the non-biotic controls, indicating that non-biological processes were not of significance for mineralization of CP. The samples were investigated for their primary elimination by LC-MS/MS. The LC-MS/MS data can give more detailed information about the chronological sequence of the CP degradation and the formed transformation products.

3.3. LC-UV and LC-MS/MS analysis

The calibration range for CP and CPDS were established through consideration of the practical range necessary to give accurate, precise and linear results. The linearity of the calibration graphs were validated by the high value of the correlation coefficient.

Precision was validated based on the evaluation of intra-day and inter-day repeatability of the method. Intra-day and inter-day repeatabilities were determined by analyzing three replicates of the standards at three concentration levels. Inter-day precision

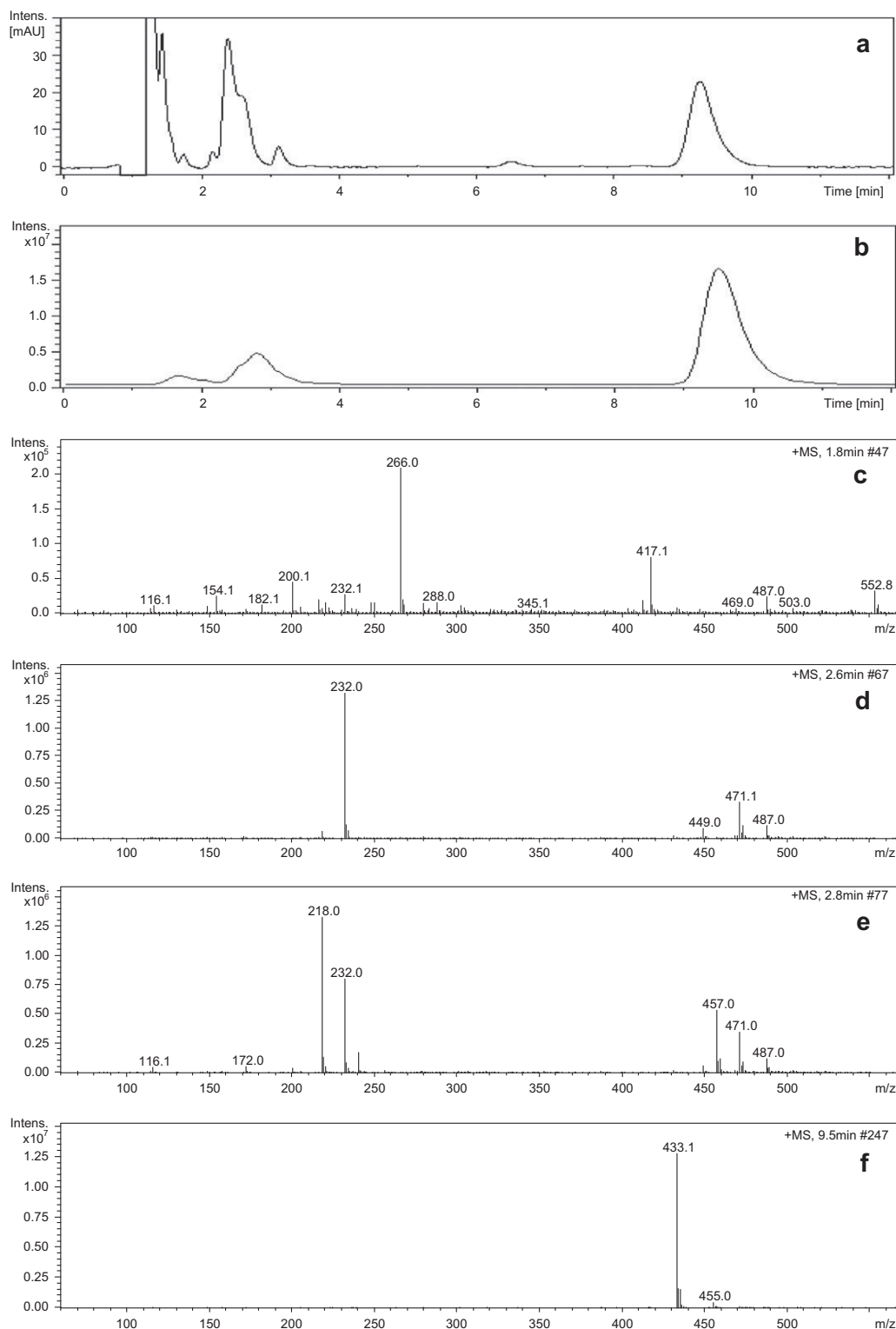


Fig. 1. Mass spectra of CP sample after 64 min photolysis after 1 month storage at 20 °C using isocratic method. Showing (a) LC-UV at 210 nm, (b) total ion chromatogram (TIC), (c) peak at 266 m/z (main photodegradation product), (d) peak at 232 m/z (new degradation product during storage), (e) CP at 218 m/z , and (f) CPDS (abiotic degradation) at 433.1 m/z .

were determined by analyzing the standards on three consecutive days. Intra-day and inter-day precision were expressed as relative standard deviations (RSDs). Satisfactory results were achieved for all analytes. The intraday repeatability was ranged from 0.03–0.68 and 0.01–0.13 for CP and CPDS, respectively. The interday repeatability was ranged from 0.3–2.38 and 0.32–1.14 for CP and CPDS, respectively.

In the Closed Bottle test, there was a primary elimination of CP to CPDS by oxidation which is abiotic transformation under aerobic condition forming a disulfide bridge. There is no CP detected at the end of the biodegradability test in samples of 0 min irradiation time. However, CP was still detected in the sample of 64 min irradiation time. CPDS was not degraded; the concentration was the same after 28 d in CBT. The photoproduct with mass 266 m/z was

Table 1

Chromatographic and mass spectrometer parameters for the CP analysis in LC/MS–MS using gradient method (Positive mode; relative abundance in brackets; no data if <10%).

Compound, specific mass (<i>m/z</i>)	Retention time (min)	Precursor ions (<i>m/z</i>) (relative intensity in brackets)	Product ions (<i>m/z</i>)
CP standard	13	218.1(100), 457.6(18.4).	218 → 172.1 (100), 116.1 (80.4), 200 (44.3), 70.3 (30.5)
CPDS standard	18.2	433.2(100)	433.2 → 216(100), 387.1(14.2).
Photoproduct <i>m/z</i> 266 in 128 min sample	4.1	266.1(100), 219.2(37.1), 158.1(19.2), 373.1(17.1), 93.3(14.4)	266.1 → 220.1(100), 248(13.6)
Transformation products peak 1 Day 28 (MRT)	10.8	171(100), 394.1(45.9), 210(30.8), 188(28.6), 123.1(18.9),	171 → 123.1(100), 93.2(10.2) 394.1 → 346.8(100) 313.4(89.5) 300.6 (69) 210 → 242.7(100), 264.4(68), 210(59.8), 229.9(56), 239(55), 396.1(50.7), 169.2(47.8), 592.4 (42.7), 447.1(37.9), 190(36.88), 225(21.9), 136.2(14.9)
Transformation products peak 2 Day 28 (MRT)	24.8	279.1(100), 301.1(28.1), 578.8(26.1)	279.1 → 171(100), 123.1 (12.5)
Transformation products peak 1 Day 11 (ZWT)	4.7	216.4(100), 453.4(56.6), 254(39), 238(37.3), 174.1(15.5), 198.1(13.8)	216.4 → 198.1(100), 170.1(55.4). 453.4 → 238(100), 194(17.26)
Transformation products peak 2 Day 11 (ZWT)	18.1	433.2(100).	433.2 → 216
Transformation products peak 3 Day 11 (ZWT)	19.9	465.2 (100), 487.5(11.5)	465.2 → 216.1(100), 419.1(83.5) 487.5 → 272.1(100), 390.1(96.8), 238 (28.8), 206.1(15.4) 216.4 → 198.1(100), 170.1(59.38)
Transformation products peak 1 Day 14 (ZWT)	4.7	216.4(100), 453.4(79), 254(51), 238(47.2), 198.1(17.6), 174.1(10)	453.4 → 238(100), 194(11.35) 261 → 652.5(100), 631(63.2), 295.1(37.3), 243.1(28.9), 140.9(64.5)
Transformation products peak 2 Day 14 (ZWT)	18.1	261(100), 175(54.3), 221(40.9), 193(28.2), 135(13.7), 277(10.3)	175 → 147(100), 109.1(24.8), 73.3(34.6)
Transformation products peak 3 Day 14 (ZWT)	19.5	454.5(100), 476.1(32.2), 200.1(15.7)	454.5 → 200.1(100), 154.1(17.6)
Transformation products peak 4 Day 14 (ZWT)	20.4	293.3(100), 225(24.9), 253(15.2), 119.1(11.1), 93.2(10.4)	293.3 → 224.9(100), 226(96.9) 272.9(97.1), 254.9(59.2), 175(77.8), 134.1(72.3), 172.9(64.9), 336(58.2), 356.6(51), 308.9(24.7), 113.1(27.1)
Transformation products peak 1 Day 28 negative control (ZWT)	14.6	232(100), 471.4(10.5)	232 → 114.2(100), 146(36.7), 70.3(18.3), 186(14.3)

not degraded in the samples of 64 min irradiation time but degraded in the samples of 512 min irradiation time. The *m/z* and *t_R* of CP and identified transformation products are listed in Table 1.

In MRT, CP was transformed to degradation products which are neither identical with CPDS and photodegradation products. The total ion chromatograms of the test samples at 28 d showed 2 peaks (Table 1).

In ZWT, primary elimination of CP occurred immediately from the beginning of the test. CP completely degraded in the tests vessels and negative control after 1 and 4 d, respectively. In the biologically active test vessel, CP was rapidly degraded to its dimer CPDS (*t_R* = 18.2 min) (Major product), product *m/z* 465.2 (*t_R* = 19.9 min) and other minor degradation products (Table 1). CPDS was completely degraded after 11 d. New degradation products (more than 10-fold lower signal intensity than CPDS) *m/z* 465.2 and *m/z* 487.1 (*t_R* = 19.9 min) were formed on day 14. All these degradation products were completely degraded and mineralized on 21 d.

There are 2 degradation products with the *m/z* 465.2 (*t_R* = 16.4 min and 19.9 min). In order to get further information about these isomers products, the ions at 465.2 (*t_R* = 16.4 min and 19.9 min) were isolated and investigated by mass spectrometry using the MS³ mode. The product ions (216.1(100), 248(35.7)) and (216.1(100), 419.1(83.5)) were obtained by MS² of the mass *m/z* 465.2 at *t_R* = 16.4 min and 19.9 min, respectively. One of these 2 isomers with the specific mass *m/z* 465.2 could be the oxidative product of captopril disulfide which is captopril disulfide S-dioxide (Fig. 2). Captopril disulfide S-dioxide was synthesized by iron- or methyltrioxorhenium (VII)-catalyzed oxidation of CP with H₂O₂ (Huang et al., 2007).

In the “negative control” vessel, CP completely degraded to CPDS after 4 d. A New degradation products were formed with the mass *m/z* 232 (*t_R* = 14.6 min), *m/z* 465.2 and *m/z* 487.1 (*t_R* = 19.9 min) from day 7 and increased until day 11. CPDS and

the other degradation products were present in the negative control vessel until 28 d unchanged.

In conclusion, CP underwent fast abiotic transformation to CPDS. Then CPDS was further biodegraded and mineralized biotically. All these degradation products except mass *m/z* 232 (*t_R* = 14.6 min) in the negative control were formed in traces only compared to CPDS. In order to get further information about this product, the ion at 232 was isolated and investigated by mass spectrometry using the MS³ mode (Table 1). The specific mass *m/z* 232 could be the molecular mass peak of S-methyl captopril (Fig. 2) which stated previously under Section 2.2.

4. Conclusion

CP was stable for 28 d under CBT conditions with a relatively low density of test substance and bacteria from a wastewater treatment plant's effluent but for only 20 d under the conditions of the MRT with higher concentrations of inoculum and test substance. After 20 d in MRT, gradual decay of the CP was observed. In ZWT biodegradation and full mineralization was found for CP after approximately 21 d. This demonstrates the impact of bacterial density and diversity on biodegradation. If CP is introduced directly into surface water no biodegradation can be expected. Neither CP, CPDS nor samples after 64 min and 512 min irradiation were readily biodegraded or transformed under conditions of low bacterial density (CBT), which is the situation in surface water. This indicates that photolysis does not necessarily result in better biodegradable transformation products.

The combination of monitoring by LC–MS/MS, HPLC–UV, and DOC monitoring gave valuable insights into the transformation processes and the resulting products. The authors recommend further research on this drug and its transformation products, including toxicity tests and measurement of environmental samples. The

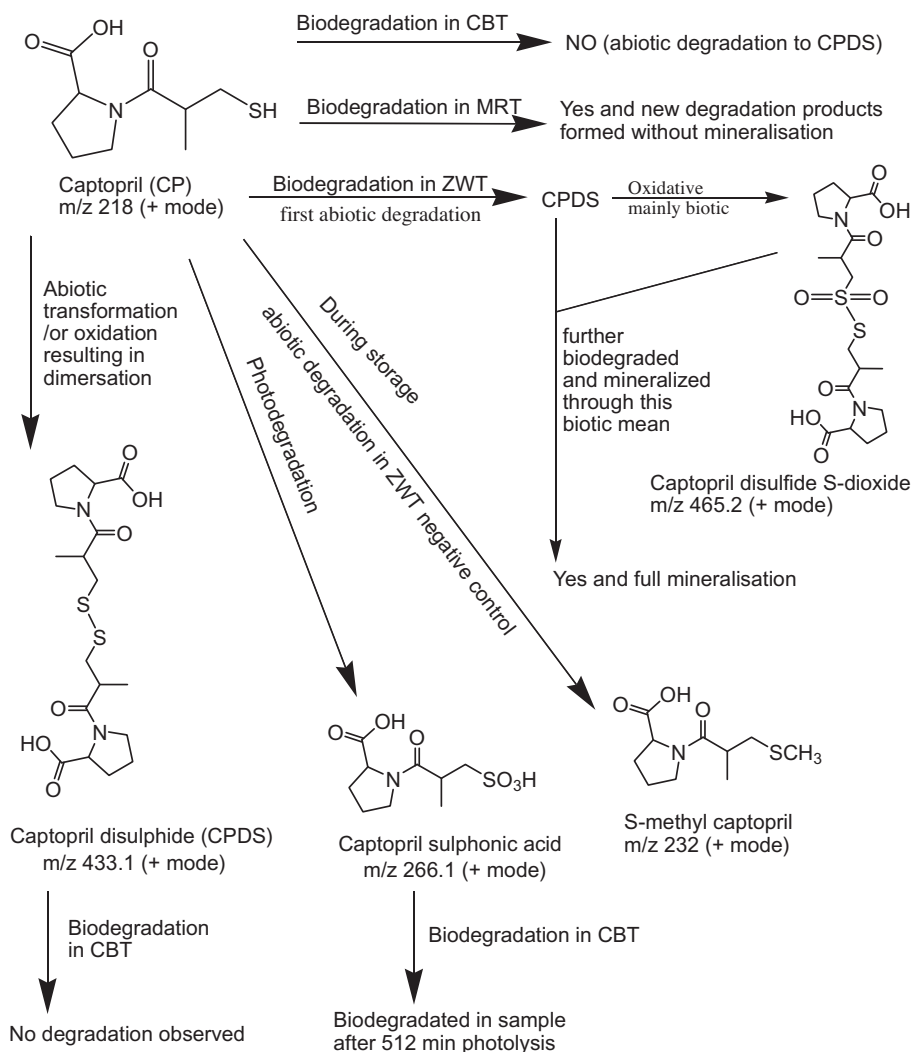


Fig. 2. Suggested abiotic, photo- and bio-degradation pathways for CP.

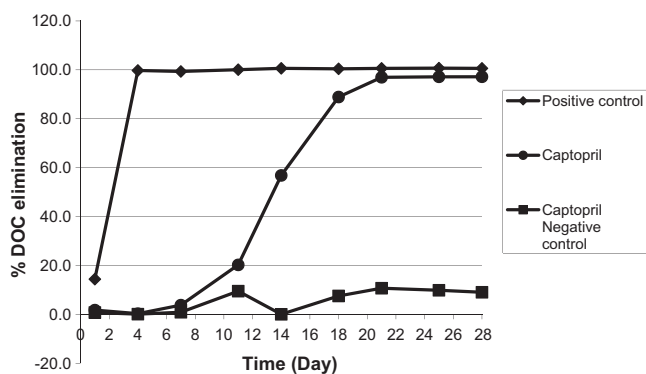


Fig. 3. ZWT experiment showing DOC elimination of CP in test vessels and negative control.

applied test concentration was necessary in order to be able to evaluate the biodegradation in the biological process of CP, CPDS and its photoproducts. If it were lower biodegradation could not have been monitored in accordance of the test guidelines for the biodegradation test. In this respect the applied tests and concentration of test compounds proved to be a useful research tool despite the fact that they are not exactly simulating environmental and sewage treatment plant conditions. The results demonstrate

that the fate of pharmaceuticals and other chemicals needs to be assessed on a case-by-case basis. As CP is not biodegradable in the presence of low bacterial density i.e. surface water photo transformation and degradation by sun light after input into the River Nile is of importance and deserves further investigation under real world conditions.

Acknowledgements

The authors wish to thank Armin Koenig and Andreas Längin (Department of Environmental Health Sciences, University Medical Center Freiburg, Germany), Natalie Hoehn (Material Resources, Institute of Environmental Chemistry, Leuphana University Lüneburg, Germany) for their help with the experiments. Waleed M.M. Mahmoud Ahmed thanks the Ministry of Higher Education and Scientific Research of the Arab Republic of Egypt (MHESR) and the German Academic Exchange Service (DAAD) for their sponsorship and financial support (GERLS Program).

Appendix A. Supplementary material

Supplementary data associated with this article can be found, in the online version, at <http://dx.doi.org/10.1016/j.chemosphere.2012.03.064>.

References

- Al-Rifai, J.H., Gabelish, C.L., Schäfer, A.I., 2007. Occurrence of pharmaceutically active and non-steroidal estrogenic compounds in three different wastewater recycling schemes in Australia. *Chemosphere* 69 (5), 803–815.
- Boreen, A.L., Arnold, W.A., McNeill, K., 2003. Photodegradation of pharmaceuticals in the aquatic environment: a review. *Aquatic Sciences – Research Across Boundaries* 65, 320–341.
- Drummer, O.H., Jarrott, B., 1986. The disposition and metabolism of captopril. *Medicinal Research Reviews* 6 (1), 75–97. <http://dx.doi.org/10.1002/med.2610060104>.
- Fent, K., Weston, A.A., Caminada, D., 2006. Ecotoxicology of human pharmaceuticals. *Aquatic Toxicology* 76 (2), 122–159.
- Gartiser, S., Urich, E., Alexy, R., Kümmerer, K., 2007. Ultimate biodegradation and elimination of antibiotics in inherent tests. *Chemosphere* 67 (3), 604–613.
- Gomez, M.J., Martinez Bueno, M.J., Lacorte, S., Fernandez-Alba, A.R., Agüera, A., 2007. Pilot survey monitoring pharmaceuticals and related compounds in a sewage treatment plant located on the Mediterranean coast. *Chemosphere* 66 (6), 993–1002.
- Gros, M., Petrović, M., Barceló, D., 2007. Wastewater treatment plants as a pathway for aquatic contamination by pharmaceuticals in the Ebro river basin (Northeast Spain). *Environmental Toxicology and Chemistry* 26 (8), 1553. <http://dx.doi.org/10.1897/06-495R.1>.
- Halling-Sørensen, B., Nors Nielsen, S., Lanzky, P.F., Ingerslev, F., Holten Lützhøft, H.C., Jørgensen, S.E., 1998. Occurrence, fate and effects of pharmaceutical substances in the environment – a review. *Chemosphere* 36 (2), 357–393.
- Heberer, T., 2002. Occurrence, fate, and removal of pharmaceutical residues in the aquatic environment: a review of recent research data. *Toxicology Letters* 131 (1–2), 5–17.
- Heberer, T., Reddersen, K., Mechlinski, A., 2002. From municipal sewage to drinking water: fate and removal of pharmaceutical residues in the aquatic environment in urban areas. *Water Science and Technology* 46 (3), 81–88.
- Huang, K.-P., Huang, F.L., Shetty, P.K., Yergey, A.L., 2007. Modification of protein by disulfide S-monoxide and disulfide S-dioxide: distinctive effects on PKC. *Biochemistry* 46 (7), 1961–1971. <http://dx.doi.org/10.1021/bi061955i>.
- Ibrahim, M.M., 2004. Management of hypertension in Egypt and developing countries guidelines. <http://www.ehs-egypt.net/pdf/HTNGuidelines.pdf> (retrieved 17.03.11.).
- Jiang, L., Hu, X., Yin, D., Zhang, H., Yu, Z., 2011. Occurrence, distribution and seasonal variation of antibiotics in the Huangpu River, Shanghai, China. *Chemosphere* 82 (6), 822–828.
- Konstantinou, I.K., Lambropoulou, D.A., Albanis, T.A., 2010. Photochemical transformation of pharmaceuticals in the aquatic environment: reaction pathways and intermediates. In: Fatta-Kassinos, D., Bester, K., Kümmerer, K. (Eds.), *Xenobiotics in the Urban Water Cycle*, vol. 16. Springer, Netherlands, pp. 179–194.
- Kümmerer, K., 2009a. Antibiotics in the aquatic environment – a review – Part I. *Chemosphere* 75 (4), 417–434.
- Kümmerer, K., 2009b. Antibiotics in the aquatic environment – a review – Part II. *Chemosphere* 75 (4), 435–441.
- Kümmerer, K., 2009c. The presence of pharmaceuticals in the environment due to human use – present knowledge and future challenges. *Journal of Environmental Management* 90 (8), 2354–2366.
- Kümmerer, K., 2008. *Pharmaceuticals in the Environment: Sources, Fate, Effects and Risks*, third ed. Springer, Berlin, Heidelberg, pp. 85–86.
- Kümmerer, K., Al-Ahmad, A., Steger-Hartmann, Thomas, 1996. Epirubicin hydrochloride in the aquatic environment – biodegradation and bacterial toxicity. *Umweltmed Forsch Prax* 1 (3), 133–137.
- Lin, A.Y.-C., Reinhard, M., 2005. Photodegradation of common environmental pharmaceuticals and estrogens in river water. *Environmental Toxicology and Chemistry* 24 (6), 1303–1309. <http://dx.doi.org/10.1897/04-236R.1>.
- Ministry of Health and Population (MOHP), 2006. National Essential Drug List. <http://www.mohp.gov.eg/sec/Drugs/Groups3.pdf> (retrieved 17.03.11.).
- Nikolaou, A., Meric, S., Fatta, D., 2007. Occurrence patterns of pharmaceuticals in water and wastewater environments. *Analytical and Bioanalytical Chemistry* 387 (4), 1225–1234. <http://dx.doi.org/10.1007/s00216-006-1035-8>.
- Nyholm, N., 1991. The European system of standardized legal tests for assessing the biodegradability of chemicals. *Environmental Toxicology and Chemistry* 10 (10), 1237–1246. <http://dx.doi.org/10.1002/etc.5620101002>.
- Organisation for Economic Co-operation and Development, 1992a. OECD Guideline for Testing of Chemicals 301 D: Ready Biodegradability. Closed Bottle Test. OECD Publishing, Paris.
- Organisation for Economic Co-operation and Development, 1992b. OECD Guideline for Testing of Chemicals 301F: Ready Biodegradability. Manometric respiratory test. OECD Publishing, Paris.
- Organisation for Economic Co-operation and Development, 1992c. OECD Guideline for Testing of Chemicals 302 B: Inherent Biodegradability. Zahn–Wellens Test. OECD Publishing, Paris.
- Petrović, M., Barceló, D., 2007. LC–MS for identifying photodegradation products of pharmaceuticals in the environment: pharmaceutical-residue analysis. *TrAC Trends in Analytical Chemistry* 26 (6), 486–493.
- Sweetman, S.C., 2009. *Martindale: The Complete Drug Reference*, thirty sixth ed. Pharmaceutical Press, London, Chicago (pp. 1239–1240).
- Trautwein, C., Kümmerer, K., Metzger, J.W., 2008. Aerobic biodegradability of the calcium channel antagonist verapamil and identification of a microbial dead-end transformation product studied by LC–MS/MS. *Chemosphere* 72 (3), 442–450.
- Valcárcel, Y., Alonso, S.G., Rodríguez-Gil, J.L., Maroto, R.R., Gil, A., Catalá, M., 2011. Analysis of the presence of cardiovascular and analgesic/anti-inflammatory/antipyretic pharmaceuticals in river- and drinking-water of the Madrid Region in Spain. *Chemosphere* 82 (7), 1062–1071.
- World Health Organization, 2009. WHO EMRO – noncommunicable diseases. <http://www.emro.who.int/ncd/hypertension.htm> (retrieved 25.05.11.).
- World Health Organization, 2011. WHO | Cardiovascular diseases (CVDs): Cardiovascular diseases (CVDs) January 2011. <http://www.who.int/mediacentre/factsheets/fs317/en/index.html> (retrieved 17.03.11.).

Supplementary materials

Table S1: Test system of the Closed Bottle test (“x” = addition, “-“ = no addition).

	Blank	Quality control	Test	Toxicity control
Mineral medium	x	x	x	x
Inoculum (2 drops L ⁻¹)	x	x	x	x
Test Substance ^a (ThOD = 5 mg L ⁻¹)	-	-	x	x
Sodium acetate (6.4 mg L ⁻¹) (ThOD = 5 mg L ⁻¹)	-	x	-	x

^a CP conc. = 2.88 mg L⁻¹, and CPDS conc.=2.83 mg L⁻¹

Table S2: Test system of the manometric respiratory test (“x” = addition, “-” = no addition).

	Blank	Quality control	Test	Toxicity control	Sterile control
Mineral medium	x	x	x	x	x
Inoculum (80 mL L ⁻¹)	x	x	x	x	-
CP (17.01 mg L ⁻¹) (ThOD = 30mg L ⁻¹)	-	-	x	x	x
Sodium acetate (ThOD = 30mg L ⁻¹)	-	x	-	x	x
Sodium azide (160.09 mg L ⁻¹)	-	-	-	-	x

Table S3: Test system of the Zahn-Wellens test (“x” = addition, “-“ = no addition).

	Blank	Quality control	Test vessel 1	Test vessel 2	Negative control
Mineral medium	x	x	x	x	x
Inoculum (TS = 1g L ⁻¹)	x	x	x	x	-
CP (100.51 mg L ⁻¹) (DOC = 50 mg L ⁻¹)	-	-	x	x	x
Ethylene glycol (129.2 mg L ⁻¹) (DOC = 50 mg L ⁻¹)	-	x	-	-	-
Sodium azide (160.02 mg L ⁻¹)	-	-	-	-	x

The Esquire 6000 plus mass spectrometer was operated in positive polarity.

The operating conditions of the source were: -500 V end plate, +3300 V capillary voltage, 30.00 Psi (206 kPa) nebulizer pressure, 12 L min⁻¹ dry gas flow at a dry temperature of 350 °C. The selected lens and block voltages were: +113.6 V capillary exit, +12 V octopole 1, +1.7 V octopole 2, 150 Vpp octopole reference amplitude, 40 V skimmer, 43.7 trap drive, -5.0 V lens one and -60.0 V lens two.

Paper II

Oxidation–coagulation of β -blockers by $\text{K}_2\text{Fe}^{\text{VI}}\text{O}_4$ in
hospital wastewater: Assessment of degradation
products and biodegradability

Science of the Total Environment 452–453: 137-147 (2013)

DOI: [10.1016/j.scitotenv.2013.01.059](https://doi.org/10.1016/j.scitotenv.2013.01.059)



Oxidation–coagulation of β -blockers by $K_2Fe^{VI}O_4$ in hospital wastewater: Assessment of degradation products and biodegradability

Marcelo L. Wilde ^a, Waleed M.M. Mahmoud ^{b,c}, Klaus Kümmerer ^b, Ayrton F. Martins ^{a,*}

^a Chemistry Department, Federal University of Santa Maria, 97105-900, Santa Maria, RS, Brazil

^b Sustainable Chemistry and Material Resources, Institute of Sustainable Environmental Chemistry, Leuphana University Lüneburg, C13, DE-21335 Lüneburg, Germany

^c Pharmaceutical Analytical Chemistry Department, Faculty of Pharmacy, Suez Canal University, Ismailia 41522, Egypt

HIGHLIGHTS

- Degradation of β -blockers by Fe(VI) in real hospital wastewater.
- Fe(VI) oxidized more than 90% of the β -blockers and reduced the aromaticity by 60%.
- 34 different degradation products were identified by means of LC-ESI-IT-MS.
- Degradation pathways were charted for atenolol, metoprolol and propranolol.
- The oxidation–coagulation increased the ready biodegradability of atenolol and propranolol.

ARTICLE INFO

Article history:

Received 3 December 2012

Received in revised form 17 January 2013

Accepted 19 January 2013

Available online xxxx

Keywords:

β -Blockers

Ferrate advanced oxidation

Hospital wastewater

Degradation pathways

Response surface methodology

ABSTRACT

This study investigated the degradation of atenolol, metoprolol and propranolol beta-blockers by ferrate (K_2FeO_4) in hospital wastewater and in aqueous solution. In the case of hospital wastewater, the effect of the independent variables pH and $[Fe(VI)]$ was evaluated by means of response surface methodology. The results showed that Fe(VI) plays an important role in the oxidation–coagulation process, and the treatment of the hospital wastewater led to degradations above 90% for all the three β -blockers, and to reductions of aromaticity that were close to 60%. In addition, only 17% of the organic load was removed. In aqueous solution, the degradation of the β -blockers atenolol, metoprolol and propranolol was 71.7%, 24.7% and 96.5%, respectively, when a ratio of 1:10 [β -blocker]: $[Fe(VI)]$ was used. No mineralization was achieved, which suggests that there was a conversion of the β -blockers to degradation products identified by liquid chromatography/mass spectrometry tandem. Degradation pathways were proposed, which took account of the role of Fe(VI). Furthermore, the ready biodegradability of the post-process samples was evaluated by using the closed bottle test, and showed an increase in biodegradability. The use of the ferrate advanced oxidation technology seems to be a useful means of ensuring the remediation of hospital and similar wastewater.

© 2013 Elsevier B.V. All rights reserved.

Abbreviations: $[Fe(VI)]$, concentration of Fe(VI); [β -blocker], concentration of β -blocker; ANOVA, analysis of variance; ATE, atenolol; CBT, closed bottle test; CFU, colony formation units; COD, chemical oxygen demand; Deg_{ATE} , degradation of atenolol; Deg_{MET} , degradation of metoprolol; Deg_{PRO} , degradation of propranolol; DPs, degradation products; ERM, electron rich moiety; HO, hydroxyl radical; HPLC-FLD, high performance liquid chromatography with fluorescence detector; HWW, hospital wastewater; $K_2Fe^{VI}O_4$, potassium ferrate; LC-ESI-IT-MSⁿ, liquid chromatography mass spectrometry with electrospray ionization and ion trap detector in tandem; LC-MS, liquid chromatography tandem mass spectrometry; m/z, mass charge ratio; MET, metoprolol; MS, mass spectra; NPOC, non-purgeable organic carbon; OD, oxygen dissolved; OECD, Organization for Economic Co-operation and Development; PRO, propranolol; Red_{COD} , reduction of the chemical oxygen demand; Red_{UV254} , removal of aromaticity measured at the wavelength of 254 nm; RSM, response surface methodology; SI, supporting information; SPE, solid phase extraction; STP, sewage treatment plant; TOC, total organic carbon.

* Corresponding author. Tel.: +55 55 32208664; fax: +55 55 32208754.

E-mail addresses: martins@quimica.ufsm.br, ayrtoth@pq.cnpq.br (A.F. Martins).

1. Introduction

The presence of pharmaceuticals in the aquatic environment has become a subject of increasing concern. The constant release of drugs in the environment can upset the natural removal rate (Hernando et al., 2006; Kümmerer, 2009), leading to effects that are as harmful to aquatic organisms as humans, as a result of chronic exposure (Bendz et al., 2005; Escher et al., 2010; Khetan and Collins, 2007).

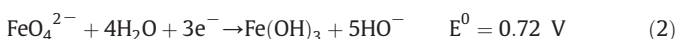
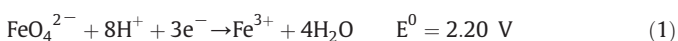
Hospitals are incontestable 'point sources' of pharmaceuticals (Kümmerer, 2009; Verlicchi et al., 2010) and can be considered 'hot spots' of contamination, particularly, when they are not properly connected to sewage treatment plants (STPs). Furthermore, hospital wastewater (HWW) constitutes a complex matrix containing microorganisms, disinfectants, detergents, contagious excretions (drugs and pathogens), biological fluids, pharmaceuticals, heavy metals, radioelements, etc. (Boillot et al., 2008). Thus, the release of this kind

of wastewater to the environment, or even to STP, carries potential risks.

One of the most important groups of prescription drugs used in the therapeutic treatment of cardiovascular diseases is the β -blockers, which are mainly used in hospitals, but also at home. As a result, β -blockers and their metabolites have been measured in sewage and surface waters up to $\mu\text{g L}^{-1}$ (Bendz et al., 2005; Gros et al., 2008; Hernandez et al., 2007; Huggett et al., 2003; Roberts and Thomas, 2006; Stolker et al., 2004; Ternes, 1998).

The three most widely used β -blockers are atenolol (ATE), metoprolol (MET) and propranolol (PRO) (Alder et al., 2010). These show polar characteristics in natural waters (pH 6–8), with pKa near to 9.6. Propranolol is more lipophilic and shows bioaccumulation potential, followed by metoprolol and atenolol (Escher et al., 2006).

There has also been a growing interest in 'green oxidants', such as hydroxyl radical ($\text{HO}\cdot$) and potassium ferrate ($\text{K}_2\text{Fe}^{\text{VI}}\text{O}_4$), in recent decades (Khetan and Collins, 2007; Sharma, 2002). Ferrate has attracted the attention of researchers owing to its dual character, since it is an oxidant-coagulant, with a higher oxidation potential (Reactions (1) and (2)) (Jiang and Lloyd, 2002; Sharma, 2002). Moreover, unlike other oxidants, Fe(VI) does not react with bromide ions forming carcinogenic species (Sharma et al., 2006).



The reduction of Fe(VI) does not generate toxic products; the hydrolysis produces pH dependent insoluble ferric species, such as $\text{Fe}(\text{OH})_3$, $\text{FeO}(\text{OH})$ and Fe_2O_3 , which are mainly responsible for coagulation. Hence, ferrate can be considered an environment-friendly oxidant (Sharma, 2002).

Most of the studies in the literature that have examined the application of Fe(VI) to mitigate the effects of micro-contamination have centered on analyzing the kinetic constants of degradation (Sharma, 2008). Only a few publications investigate the application of Fe(VI) to the degradation of pharmaceuticals and endocrine disruptors (Anquandah et al., 2011; Hu et al., 2009; Li et al., 2008; Sharma et al., 2006; Yang et al., 2011; Zimmermann et al., 2012). Likewise, there are relatively few studies which consider the degradation of drugs in HWW by advanced oxidation treatment (De Witte et al., 2010; Henriques et al., 2012; Martins et al., 2009, 2011; Vasconcelos et al., 2009).

As far as we know, this is the first study to investigate the application of ferrate to the degradation of a class of pharmaceuticals in HWW. Our main objective was to evaluate the degradation of ATE, MET and PRO by Fe(VI) in HWW by applying response surface methodology (RSM). Additionally, by carrying out experiments in aqueous solution, our aim was to evaluate the degradation of β -blockers and identify the degradation products (DPs), as well as to establish corresponding degradation pathways. The assessment of the ready biodegradability of the post-treatment samples was an additional objective.

2. Materials and methods

2.1. Chemicals

Atenolol (CAS Nr. 29122-68-7), metoprolol tartrate (CAS Nr. 56392-17-7) and propranolol hydrochloride (CAS Nr. 318-98-9) ($\geq 99.0\%$) were purchased from Sigma-Aldrich (Deisenhofen, Germany) and used as received. For the experiments in HWW, atenolol and propranolol hydrochloride (reference material, $>99.0\%$) were kindly provided by the Brazilian Pharmacopeia, while metoprolol tartrate (standard, $>98\%$) was purchased from a local provider. All the organic solvents were of HPLC grade and provided by Merck (Darmstadt, Germany), JT Baker

(Mexico City, Mexico) and Panreac (Barcelona, Spain). The aqueous solutions were prepared with ultra-pure water (Milli-Q, 18.2 m Ω cm).

For the experiments carried out in aqueous solution, K_2FeO_4 ($<98\%$) was purchased from Sigma-Aldrich (Deisenhofen, Germany) and used as received, while for experiments in HWW, K_2FeO_4 ($>85\%$) was prepared according to Delaude and Laszlo (1996) and used without extra purification, after careful storage in a desiccator. The characterization of the K_2FeO_4 was conducted by X-ray diffraction and the purity was determined by the chromite method according to Licht et al. (2001) (see supporting information, SI, Text S1). All the other chemicals used were of recognized analytical grade.

2.2. Oxidation-coagulation experiments of β -blockers by Fe(VI)

For the degradation experiments, samples of the HWW were collected from the sewage treatment system of the University Hospital of the Federal University of Santa Maria (Santa Maria, RS, Brazil). The composite samples were collected for one day, every hour, starting at 8 a.m. and finishing at 8 p.m. The collected samples were finally filtered (cellulose, 26 μm) and stored at 4–8 $^\circ\text{C}$, in the dark. All the degradation experiments were completed at a time interval lasting not longer than three days after sampling. The physical-chemical characteristics of the HWW can be seen in the SI (Text S2).

The HWW was spiked with the β -blockers to a final concentration of 200 $\mu\text{g L}^{-1}$. The experiments were carried out in a 1000 mL stirred tank glass reactor (800 mL HWW samples) under controlled temperature (20 ± 2 $^\circ\text{C}$) and reaction time of 120 min. The pH was adjusted with 6 mol L^{-1} NaOH and 1:1 v/v H_2SO_4 solutions. After the oxidation-coagulation with ferrate, 10 mL aliquots were taken, adjusted to pH 9, centrifuged (89 \times g, 1000 rpm) and filtered through syringe membrane filters of 0.45 μm (Chromafil® PTFE, Macherey-Nagel, Germany).

For HPLC analysis the samples were submitted to clean-up by solid phase extraction (SPE) using C18ec 200 mg/3 mL cartridge (Macherey-Nagel). The SPE procedure was conducted as follows: conditioning: 2 \times 3 mL of hexane, methanol and water (pH 9); loading: sample (pH 9); washing: 2 \times 3 mL of water (pH 9); drying: 5 min, with air; elution: 3 \times 2 mL of methanol:acetonitrile:formic acid mixture (90:9.9:0.1). Afterwards, the eluate was dried under gentle N_2 stream and reconstituted in mobile phase.

The experiments in aqueous solution (Milli-Q water, 18.2 m Ω cm) were also conducted as described above, but using initial pH 7 and β -blocker concentration of 10 mg L^{-1} , without buffering and under controlled temperature (20 ± 1 $^\circ\text{C}$). Two different ratios [β -blocker]:[Fe(VI)] were studied (1:1 and 1:10). For the determination by HPLC and LC-MS, the samples were taken from time to time and treated by adjusting the pH to 8–9, centrifuging (at 2863 \times g, 4000 rpm), and filtering through cellulose acetate membrane filter 0.22 μm (Millipore Millex-GP).

2.3. Experimental design

RSM, which consists of 4 factorial and 4 axial experiments (star points) and 3 replicates of the central point experiments (Bezerra et al., 2008), was chosen to evaluate the effects of the independent variables in the investigation, pH (2.8–11.2) and [Fe(VI)] (29.3 mg L^{-1} –170.7 mg L^{-1}). As dependent variables, the degradation of ATE (Deg_{ATE}), of MET (Deg_{MET}) and of PRO (Deg_{PRO}), as well as the reduction of the chemical oxygen demand (Red_{COD}) and the removal of aromaticity ($\text{Red}_{\text{UV254}}$) were chosen. The experiments were carried out in random order to avoid errors associated with the level of combinations.

The responses, the verification and the validation of the best fitted model were carried out with the aid of STATISTICA software 8.0 (StatSoft Inc., Tulsa, USA).

2.4. Determination of organic matter

The COD of the HWW samples was determined according to Standard Methods (APHA-AWWA, 1999). The initial COD of the HWW samples submitted to oxidation–coagulation treatment was $559.8 \pm 90.2 \text{ mg O}_2 \text{ L}^{-1}$ ($n=9$). The removal of aromaticity was monitored by measuring the centrifuged sample solutions at 254 nm with the aid of a Shimadzu UV 1800 spectrophotometer. In aqueous solution, the mineralization was measured as non-purgeable organic carbon (NPOC) in the centrifuged sample solutions using a Shimadzu TOC-5000 analyzer.

2.5. Chromatographic analysis by HPLC and LC–MSⁿ

The determination of ATE, MET and PRO in HWW was performed by HPLC–FLD using as mobile phase (A) formate buffer 0.02 mol L^{-1} at pH 4 and (B) acetonitrile as follows: 0–1 min isocratic flow with 5% of B, 1–4 min linear gradient flow of 5–40% B; 4–10 min isocratic flow at 40% B; 10–11 min linear gradient flow of 40–10% B; 11–15 min isocratic flow of 5% B, with flow rate of 1 mL min^{-1} and injection volume of $50 \mu\text{L}$.

The degradation products (DPs) were identified and further analyzed by LC–ESI–IT–MSⁿ until MS³ using an Agilent Technologies HPLC 1100 series (Agilent Technologies, Böblingen, Germany) tandem Mass Spectrometer Esquire 6000 plus Ion Trap with atmospheric pressure electrospray ionization (AP–ESI) interface (Bruker Daltonic GmbH, Bremen, Germany). The fragmentation of the DPs was performed by multiple reactions monitoring (MRM). The mobile phase used was (A) Milli-Q water acidified with 0.5% formic acid (*v/v*) and (B) acetonitrile, under a flow rate of 0.5 mL min^{-1} and injection volume of $20 \mu\text{L}$.

The chromatographic separation, in both HPLC and LC–MS, was performed using reverse phase column C18 ec (RP18 CC 125–4 mm Nucleodur 100–5) and guard column (RP18 CC 8–4 mm Nucleodur 100–5). Further information about the LC–MS method employed, such as linear gradient and MS work configuration, can be found in the SI (Text S3).

2.6. Assessment of biodegradability by means of the closed bottle test

Closed bottle test (CBT) was conducted in accordance with the OECD guidelines (1992) with low nutrient content and under low bacterial density conditions, at $20 \pm 1 \text{ }^\circ\text{C}$, in the dark, for 28 days (Längin et al., 2009; Trautwein and Kümmerer, 2012). The inoculum aliquot was sampled from the effluent of the STP Wyhl (Kaiserstuhl Nord, Germany), which covers a rural area without hospitals. It has been demonstrated, however, that the removal of selected pharmaceuticals by degradation or sorption in sewage treatment plants is an incomplete procedure (Bueno et al., 2012; Heberer, 2002; Längin et al., 2009; Kümmerer, 2008; Mahmoud and Kümmerer, 2012; Maurer et al., 2007; Trautwein and Kümmerer, 2011). Two drops of inoculum added to a 1000 mL solution resulted in circa 500 CFU mL^{-1} . The dissolved oxygen (OD) was monitored in the test vessels with Fibox 3 (PreSens, Regensburg, Germany) once a day, as well as the temperature.

Samples treated by Fe(VI) oxidation–coagulation (120 min) were submitted to a CBT test. To carry this out, the samples were adjusted to pH 7, and the COD was measured in order to make the necessary dilution for an initial concentration of $5 \text{ mg O}_2 \text{ L}^{-1}$. Substances in solution, which pass in the CBT, can be classified as ready biodegradability. Further information about CBT can be found in the SI (Text S4).

3. Results and discussion

3.1. Oxidation–coagulation of the hospital wastewater

The variable ranges, combination levels and obtained responses for Red_{COD}, Red_{UV254} and Deg_{ATE}, Deg_{MET} and Deg_{PRO} by the RSM experimental design, can be seen in Table 1.

Few studies have considered the use of ferrate in acidic conditions. The chosen initial pH varied from 2.8 to 11.2 so that it was possible to investigate the reaction at a high and low oxidation potential of the Fe(VI) species ($\approx 1.8\text{--}0.8 \text{ V}$) (Graham et al., 2004).

In Table 1, it can be seen that, in acidic pH, the best % COD removal from the HWW by Fe(VI) oxidation–coagulation was 17.5%, while in neutral conditions the absorbance removal at 254 nm, achieved a maximum of 67%. This provided evidence that the aromatic fraction of the HWW is generally degradable by Fe(VI), in accordance with Li et al. (2008).

As well as finding a poor COD removal, during the analysis of the degradation of each β -blocker, individually, degradations were detected above 90% for ATE, MET and PRO. Thus, even in a very complex matrix such as HWW, Fe(VI) is a very efficient oxidant–coagulant for the removal of micro-contaminants, like pharmaceuticals.

3.1.1. Model fitting and statistical analysis

Similar results found for triplicates of the central point provided evidence that the pure error was small. The replicate of the Red_{COD} showed a difference of only 2%, while the replicate of the each individual compound was 3.8 and 1.2% for Deg_{ATE} and Deg_{PRO}, respectively. Deg_{MET} and the Red_{UV254} showed a high pure error of 8.9% and 23%, respectively, indicating that these variables were susceptible to experimental variations. The *r*-squared of the adjusted model of each second-order polynomial equation was 0.8442, 0.844, 0.8448, 0.9537, and 0.889 for Red_{COD}, Red_{UV254}, Deg_{ATE}, Deg_{MET}, and Deg_{PRO}, respectively.

The Pareto chart of effects, ANOVA tables, regression equations and the adjusted plots, predicted vs. observed values, can be seen in the SI (Text S5).

3.1.2. Effect of the process variables

With the aid of RSM, the interaction between the studied variables, pH vs. [Fe(VI)], can be observed in Fig. 1.

As can be seen, the best results for COD removal were achieved in acidic pH and high [Fe(VI)]. Similarly, the aromaticity removal of the HWW improved when it passed from acidic to neutral pH by using high Fe(VI) concentrations. This behavior can be attributed to the high oxidation potential of Fe(VI), in acidic conditions (Graham et al., 2004).

The high degradation rates of ATE and MET were achieved in near neutral pH by 100 to 171 mg L^{-1} Fe(VI). At this pH, ATE and MET have the secondary amine moiety predominantly protonated, while the main Fe(VI) species are HFeO_4^- and FeO_4^{2-} (Noorhasan et al.,

Table 1

Experimental design with coded, natural values and the observed responses of HWW degradation by oxidation–coagulation with Fe(VI). Initial conditions: 800 mL, β -blocker $200 \mu\text{g L}^{-1}$, 120 min of treatment.

Coded Variables	Levels						
	−1.41	−1	0	+1	+1.41		
X ₁ pH	2.8	4	7	10	11.2		
X ₂ [Fe(VI)] mg L^{-1}	29.3	50	100	150	170.7		
Exp. pH	[Fe(VI)] (mg L^{-1})	Red _{COD} (%)	Red _{UV254} (%)	Deg _{ATE} (%)	Deg _{MET} (%)	Deg _{PRO} (%)	
1	4 (−1)	50 (−1)	4.54	47.69	10.09	21.75	86.14
2	4 (−1)	150 (1)	13.88	64.16	89.94	99.13	98.08
3	10 (1)	50 (−1)	5.44	12.06	65.41	11.73	66.08
4	10 (1)	150 (1)	11.44	48.02	96.71	87.86	86.03
5	2.8 (−1.41)	100 (0)	17.54	41.86	25.34	66.48	99.67
6	11.2 (1.41)	100 (0)	7.03	10.21	49.41	36.69	54.15
7	7 (0)	29.3 (−1.41)	3.37	7.01	14.90	25.11	60.07
8	7 (0)	170.7 (1.41)	11.65	53.73	69.22	94.73	99.55
9 (C)	7 (0)	100 (0)	8.08	56.46	84.62	81.54	81.42
10 (C)	7 (0)	100 (0)	9.88	67.23	88.41	83.71	81.62
11 (C)	7 (0)	100 (0)	9.30	44.43	85.77	74.85	80.47

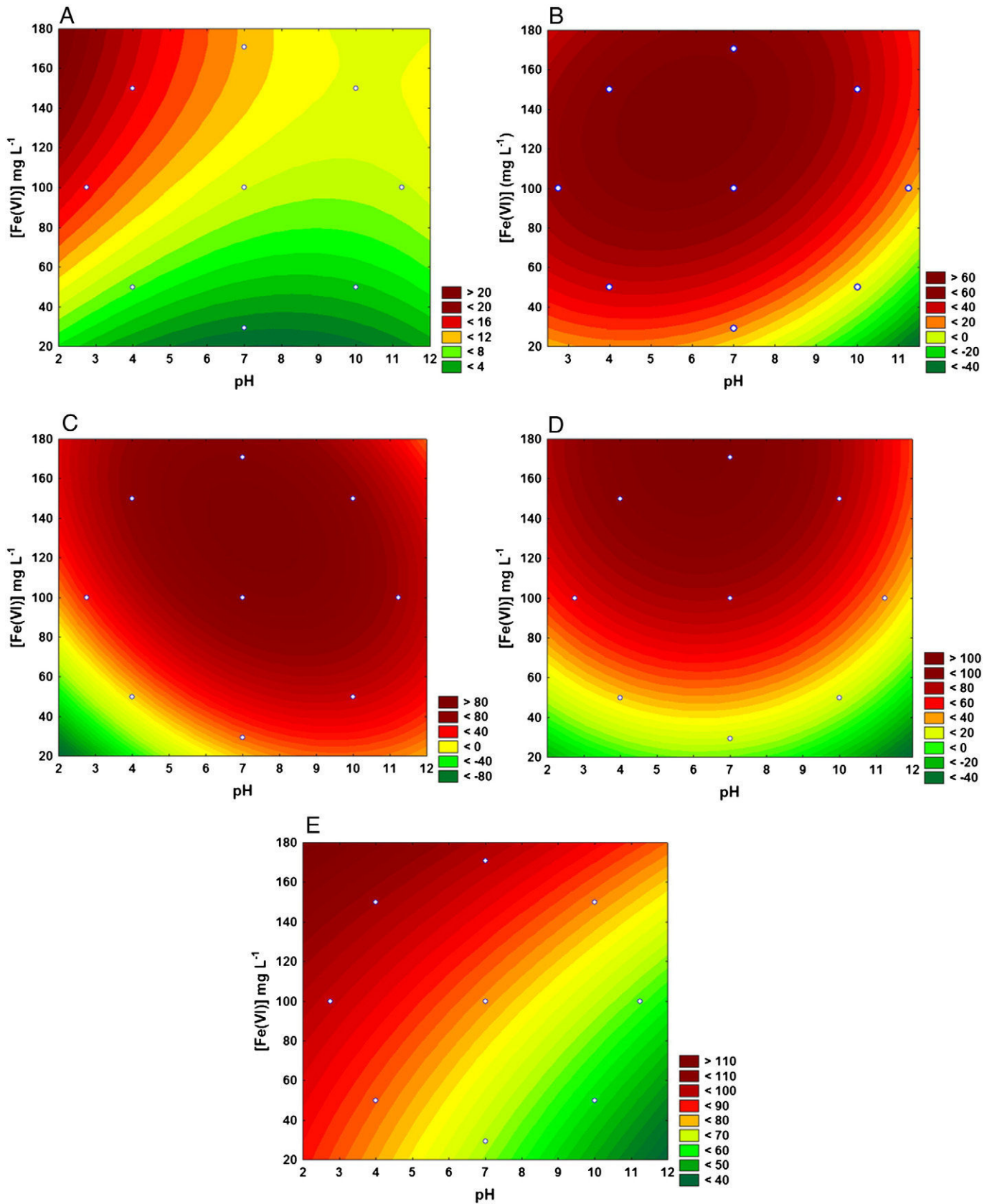


Fig. 1. Contour plot pH vs. [Fe(VI)] of the response surface from the oxidation–coagulation of HWW by Fe(VI). Initial conditions: 800 mL, [β -blocker] 200 $\mu\text{g L}^{-1}$, temp. 20 ± 1 °C; 120 min of treatment. (A) Red_{COD}, (B) Red_{UV254}, (C) Deg_{ATE}, (D) Deg_{MET} and (E) Deg_{PRO}.

2009; Sharma, 2002). In addition, in this condition, the ferrate maintains a partial free-radical character ($\text{Fe}^{\text{VI}} = \text{O} \rightleftharpoons \text{Fe}^{\text{V}}\text{-O}\cdot$) allowing protonation and resulting stabilization, which increases reactivity and, consequently, the efficiency of oxidation (Sharma and Mishra, 2006; Yuan et al., 2008).

The degradation of PRO was shown to be different from the other two β -blockers. In this case, the variable with the highest influence on the degradation, was the pH (acidic medium), by high Fe(VI) concentration. At this condition, ferrate shows high oxidation potential and reactivity, which increase oxidation efficiency. As PRO has a protonated secondary amine group and a naphthalene moiety in the structure, it is expected to degrade more rapidly in face of more potent oxidants, like Fe(VI) in more acidic pH rates (Song et al., 2008).

The predominant species of Fe(VI) in the pH range 4–7.2 is HFeO_4^- (Sharma, 2002); this shows a larger spin density on the oxo ligands than the unprotonated ferrate (FeO_4^{2-}), which increases its oxidation power (Li et al., 2008; Sharma and Mishra, 2006). Additionally, in acidic medium, ferrate acquires a partly free-radical character ($\text{Fe}^{\text{VI}} = \text{O} \rightleftharpoons \text{Fe}^{\text{V}}\text{-O}\cdot$), which makes it more reactive and increases the degradation efficiency (Sharma and Mishra, 2006; Sharma, 2002; Yuan et al., 2008).

In addition, in $\text{pH} < 9$, ATE, MET and PRO show the secondary moiety protonated. Thus, the main group that is able to react to Fe(VI) is the aromatic ring or the side chain $\text{NH}_2\text{C}(\text{O})\text{CH}_2^-$ /ATE, $\text{CH}_3\text{OCH}_2\text{CH}_2^-$ /MET. This means that ATE and MET would react preferentially in neutral conditions. The naphthalene group/PRO, an electron rich moiety (ERM), is more susceptible to react to Fe(VI) regardless of the pH.

3.2. Oxidation-coagulation of β -blockers in aqueous solution by Fe(VI)

As a result of the behavior described above, the [Fe(VI)] is the most important factor. In view of this, oxidation-coagulation experiments in aqueous solutions were carried out, using two different concentration ratios [β -blocker]:[Fe(VI)], 1:1 and 1:10, at initial pH 7.

Fig. 2(A) and (B) clearly shows that PRO was more susceptible to the degradation by Fe(VI) for both ratios studied, while MET was the least susceptible.

According to the profile, most of the degradation occurs in the first minutes, and the [Fe(VI)] appears to be the limiting factor of the process; once it is reduced to Fe(III), the degradation slows down.

As discussed earlier, the explanation for the different behavior of the β -blockers with respect to oxidation with Fe(VI) can be found in the structural differences. PRO has an electron rich moiety, and becomes more susceptible to an attack by the partial free-radical $\text{Fe}^{\text{VI}} = \text{O} \rightleftharpoons \text{Fe}^{\text{V}}\text{-O}\cdot$ (Sharma and Mishra, 2006).

However, ATE and MET have a phenolic moiety in the -p position. MET was less susceptible to oxidation, probably, because of the side chain $\text{CH}_3\text{OCH}_2\text{CH}_2^-$, which has a positive mesomeric effect caused by the free electron pair of the oxygen atom. This supplants the negative inductive effect, and results in an overall stabilization of the side chain in contrast with the $\text{NH}_2\text{C}(\text{O})\text{CH}_2^-$ moiety/ATE – which has a negative mesomeric effect, that results in an increase in electron density, and suggests that the reaction with Fe(VI) is preferable (Song et al., 2008). An electron-withdrawing substituent can increase the reaction rate of organic compounds with Fe(VI) (Audette et al., 1972). The mineralization, in terms of NPOC removal, was monitored by evaluating the process using two different concentrations ratios. As can be seen in Fig. 2(A) and (B), no mineralization was observed in aqueous solution, which suggests that the β -blockers were oxidized to DPs.

This singular behavior suggests that ferrate only partially oxidizes the parent compounds, revealing low potential for mineralization, probably due to the tendency to decompose generating insoluble ferric species, which in the absence of colloids do not coagulate providing efficient removal of compounds.

3.3. Identification of degradation products by oxidation with ferrate

The degradation products of the ATE, MET and PRO formed by the oxidation-coagulation process with Fe(VI) were identified by LC-ESI-IT-MSⁿ in positive ion mode. The mass spectra (MS) of the product ions, main fragments (m/z) and the relative abundances (%) of the identified DPs are summarized in Table 2. The m/z value of each peak that was found corresponds to the molecular ion $[\text{M} + \text{H}]^+$.

The MS² and MS³ product ion spectra of ATE, MET, PRO and their DPs were elucidated and can be seen in the SI (Text S6–S9).

3.3.1. Degradation pathway of atenolol by oxidation-coagulation with Fe(VI)

A pathway was proposed (Fig. 3) that was in accordance with the DPs that had been identified. The reaction between Fe(VI) and organic micro-contaminants, in aqueous solution, is not a simple process, owing to the direct oxidation by Fe(VI) iron-oxo species ($\text{Fe}^{\text{VI}} = \text{O} \rightleftharpoons \text{Fe}^{\text{V}} = \text{O}\cdot$) with a partial free-radical (Yuan et al., 2008).

Thus, it is suggested that ATE should follow two main degradation pathways: (I) electrophilic attack on the aromatic ring, which initially forms a phenoxy radical ($\text{C}_6\text{H}_5\text{-O}\cdot$) and then abstracts hydrogen from HFeO_4^- , forming hydroxylated DP 283. Following this, DP 283 can (I (a)) form benzoquinone (Huang et al., 2001a, 2001b) and a nitroso group in the acetamide moiety (DP 327) (Sharma et al., 2006; Yang et al., 2011), and (I (b)) suffer bond cleavage between the aromatic ring and the ether bond of the side chain 2-hydroxy-3-(isopropylamino) propoxy, forming the DP 152 and DP 134 or DP 132 according to the mechanism proposed by Yang et al. (2011).

The pathway (II) occurs in secondary amine moiety, and is based on electrophilic attack and elimination of the isopropyl moiety, forming the DP 225. In the same way as (I (a)), the DP 225 can form a nitroso intermediary by single electron-transfer mechanism (Huang et al., 2001a,b; Sharma et al., 2006), which is subsequently eliminated as NO_2 , forming DP 210.

Coupling reactions can form dimers of DP 210, such as DP 419, in a similar mechanism as proposed by Huang et al. (2001a,b). DP 210 or DP 225 can also generate DP 182 by eliminating $\text{NH}_2\text{-C}=\text{O}$ and $\text{C}=\text{O}$, respectively. In addition, DP 210 and its dimer, DP 410, can generate DP 208 by elimination of NH_4 or NO_2 and hydrogen abstraction, respectively (Anquandah et al., 2011). DP 194, probably, is originated from DP 208, DP 210 or DP 225 by eliminating H_2O and NH_4 or NO_2 , respectively (Anquandah et al., 2011; Noorhasan et al., 2009), and DP 194, can also undergo a coupling reaction similar as proposed by Huang et al. (2001a,b), and thus forming a dimer, DP 387.

The profile of the DPs was monitored during the oxidation-coagulation process and, once the DPs were formed, did not undergo any significant changes until the end of the process (SI, Text S10).

3.3.2. Degradation pathway of metoprolol by oxidation-coagulation with Fe(VI)

This study proposes three different pathways for the degradation of MET with Fe(VI), as can be seen in Fig. 4.

Pathway (I) characterizes the hydroxylation of MET, which can originate from two different DPs. A plausible explanation for the DP 284 (a), which can be given by with reactions with a ratio 1:1 [MET]:[Fe(VI)], involves electrophilic attack, as described earlier. On the other hand, the hydroxylation of the secondary amine moiety can occur, forming the DP 284 (b) (Zimmermann et al., 2012), that was only identified by carrying out the reactions with ratio 1:10, i.e. favored by alkaline pH (Noorhasan et al., 2009).

Degradation pathway (II) occurs via attack on the ether side chain and can be related to the action of oxygen as nucleophile, in HFeO_4^- , forming the intermediary $-\text{H}_2\text{C}\cdot$, followed by elimination of $\text{CH}_2=\text{O}$ (Zimmermann et al., 2012), which generates DP 254 and DP 240. On the other hand, the oxidation of alcohols to aldehydes and ketones by Fe(VI) (Delaude and Laszlo, 1996) can explain the formation of DP 238.

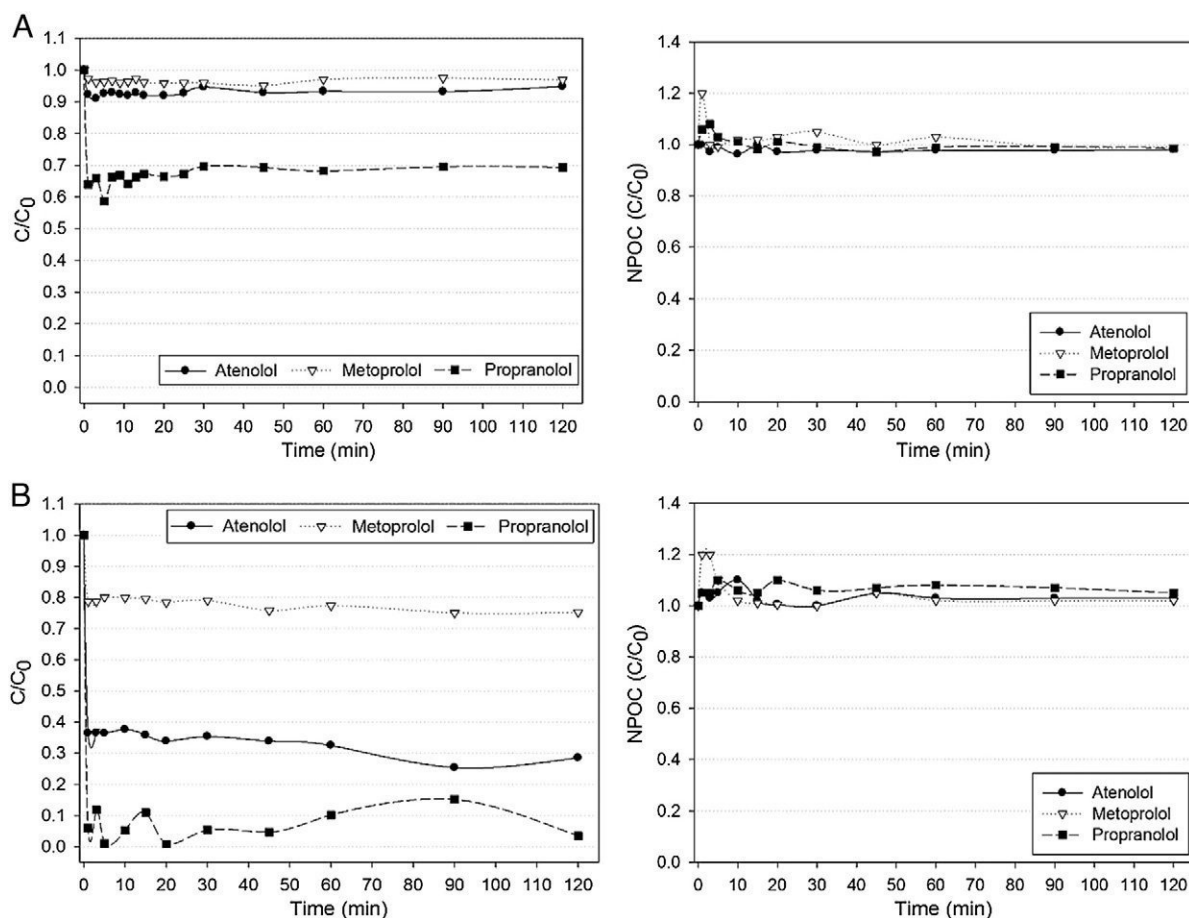


Fig. 2. Degradation of atenolol, metoprolol and propranolol and non-purgeable organic carbon (NPOC) removal by oxidation-coagulation using Fe(VI) in aqueous solution. (A) [β -blocker]:[Fe(VI)] 1:1 mol L⁻¹:mol L⁻¹ and (B) [β -blocker]:[Fe(VI)] 1:10 mol L⁻¹:mol L⁻¹. Initial conditions: 800 mL, pH 7, [β -blocker] 10 mg L⁻¹; temp. 20 ± 1 °C; 120 min of treatment.

Both pathways, (I) and (II), can lead to the formation of DP 134 by cleavage between the aromatic ring and the ether bond of the side chain 2-hydroxy-3-(isopropylamino)propoxy (Radjenovic et al., 2011; Yang et al., 2011).

Proposed pathway (III) occurs for N-dealkylation by oxidative attack on the α -C of the dimethylamine moiety and resulting cleavage forming DP 226 (Radjenovic et al., 2011; Zimmermann et al., 2012), which is assisted by raising the pH to ± 10 (SI, Text S11), where the secondary amine is neutral (Noorhasan et al., 2009). Following this, the degradation follows the pathway (II), forming DP 196, which undergoes hydrogen abstraction and elimination of water, forming possibly a carbonyl intermediary followed by intermolecular electron transference, generating a double bond and forming DP 175 (Anquandah et al., 2011; Noorhasan et al., 2009; Slegers et al., 2006).

Some DPs identified in this study were also identified in processes based on photolysis and in the generation of HO \cdot (Benner and Ternes, 2009b; Radjenovic et al., 2011; Slegers et al., 2006; Song et al., 2008).

3.3.3. Degradation pathway of propranolol by oxidation-coagulation with Fe(VI)

The large number of DPs identified in the degradation of PRO by Fe(VI) shows how complex this kind of process can be and suggests that there are different reductive and oxidative degradation routes, resulting in multi-step and interconnected pathways (Fig. 5).

Initially it was suggested that hydroxylation (I) occurs in the naphthalene group by action of the ion HFeO₄⁻ forming DP 276. Likewise, a new hydroxylation (II) occurs by ring opening, which forms isomers. Aromatic ring opening by FeO₄²⁻ was reported by Li et al. (2008) and Xu et al. (2009).

After the ring opening, a hydrogen abstraction process (III) can occur. The oxidation of alcohols to aldehydes and ketones by FeO₄²⁻ is very well known (Benner and Ternes, 2009a; Chen et al., 2011; Delaude and Laszlo, 1996; Liu and Williams, 2007; Marco-Urrea et al., 2009; Romero et al., 2011; Song et al., 2008; Yang et al., 2010).

A sequence follows the ring opening, involving decarboxylation (IV) of the DPs 292, 294 and 296, forming DP 266 and DP 268, followed by oxidation of the alcohol moiety (DP 268) to aldehyde (Delaude and Laszlo, 1996), which results in the formation of DP 266 (III).

A new hydroxylation (V) step occurs on DP 294 and DP 292, forming DP 308 and DP 310, or, similar to what is described above, there is an oxidation of the alcohol moiety (DP 310) to aldehyde DP 308 (III) (Delaude and Laszlo, 1996), followed by a new decarboxylation (IV) in the DP 308 or DP 310, forming DP 282.

Two other hydroxylation steps (VI and VII) were possible and, as a result of the ring opening, DP 340 was formed. As it was impossible to make a conclusive determination related to the hydroxylation in the naphthalene ring, and which ring was opened, this study suggests possible position isomers, as reported by Benner and Ternes (2009b). DPs of naphthalene cleavage (Yang et al., 2011), as well as of the side chain (VIII), forming DP 134, 132 and 116, were identified, as well.

The profile of the peak area of the DP, as a function of oxidation time, shows different behaviors for the two concentration ratios studied (SI, Text S10).

The structural differences in the R-group of the β -blockers led to different degradation pathways. ATE and MET mainly showed two sites of reaction; the ether and the acetamide side chains, respectively. The other reaction site was in the secondary amine moiety of the side chain 2-hydroxy-3-(isopropylamino)propoxy.

Table 2Degradation products of the oxidation–coagulation of atenolol, metoprolol and propranolol by Fe(VI) identified by LC-ESI-IT-MS^a.

DP	Rt (min)	Molecular formula	ESI(+) MS m/z ^a	ESI(+) MS ² m/z (relative abundance, %)
<i>Atenolol</i>	11.1	C ₁₄ H ₂₂ N ₂ O ₃	267.0	250.1 (6.47), 225.0 (67.83), 208.0 (41.48), 190.0 (100), 162.1 (13.04), 145.1 (40.64), 116.2 (23.75), 98.2 (3.75)
DP 419	14.3	C ₂₂ H ₃₀ N ₂ O ₆	419.0 ^c	401.2 (3.44), 300.5 (3.33), 209.9 (100), 182.0 (13.44), 164.0 (4.99), 146.9 (4.86)
DP 387	12.1	C ₂₂ H ₂₈ N ₂ O ₄	387.0 ^c	371.1 (63.52), 342.0 (9.05), 289.0 (2.38), 193.9 (100), 175.9 (33.29), 131.0 (47.53)
DP 327	14.5	C ₁₇ H ₃₀ N ₂ O ₄	327.2 ^c	309.9 (11.21), 279.1 (2.13), 267.8 (3.88), 236.9 (100), 221.8 (2.00), 193.8 (3.00), 132.0 (2.90)
DP 283	13.6	C ₁₄ H ₂₂ N ₂ O ₄	283.2 ^{b,c}	265.1 (100), 247.1 (38.39), 205.0 (7.94), 176.9 (10.06), 135.0 (13.26), 116.0 (38.0), 95.1 (7.32)
DP 225	7.4	C ₁₁ H ₁₆ N ₂ O ₃	225.1 ^{b,c}	207.0 (21.01), 189.0 (17.66), 164.9 (100), 147.0 (6.16), 121.0 (20.08)
DP 210	14.4	C ₁₁ H ₁₅ NO ₃	210.2 ^{b,c}	191.9 (13.24), 181.9 (100), 164.0 (38.23), 152.0 (16.26), 147.0 (15.16), 121.0 (4.45)
DP 208	5.5	C ₁₁ H ₁₃ NO ₃	207.8 ^{b,c}	191.9 (14.77), 181.9 (100), 164.0 (42.33), 151.9 (14.79), 121.0 (4.41)
DP 194	12.1	C ₁₁ H ₁₅ NO ₂	194.0 ^c	175.9 (100), 144.9 (3.63), 131.0 (60.42), 107.0 (2.86), 89.1 (2.96)
DP 182	14.4	C ₁₀ H ₁₅ NO ₂	182.1 ^c	163.9 (5.55), 151.9 (100), 107.1 (5.72)
DP 152	11.8	C ₈ H ₉ NO ₂	152.2 ^{b,c}	NF
DP 134	2.7	C ₆ H ₁₅ NO ₂	134.1 ^b	116.1 (100), 92.2 (42.37), 74.3 (32.50), 56.4 (16.75)
DP 132	12.1	C ₅ H ₁₃ NO ₂	131.8 ^c	113.9 (62.90), 100.1 (19.72), 86.3 (33.96), 57.2 (100)
<i>Metoprolol</i>	16.4	C ₁₅ H ₂₅ NO ₃	268.0	250.2 (1.53), 218.1 (9.59), 191.1 (26.75), 176.1 (4.80), 159.1 (19.30), 133.1 (4.96), 116.2 (100), 98.2 (4.05)
DP 284	13.1	C ₁₅ H ₂₅ NO ₄	284.2 ^{b,c}	265.1 (49.64), 247.1 (44.12), 239.0 (18.37), 204.9 (11.50), 176.9 (100), 149.0 (12.44), 133.0 (94.30), 121.0 (8.95), 107.1 (8.40), 89.1 (33.69)
DP 254	13.9	C ₁₄ H ₂₅ NO ₃	254.2 ^{b,c}	234.9 (54.28), 212.8 (68.46), 192.9 (100), 176.9 (38.29), 147.0 (32.17), 133.0 (27.12), 119.0 (18.26), 102.9 (12.42)
DP 240	13.6	C ₁₃ H ₂₁ NO ₃	240.4 ^c	219.9 (10.27), 197.9 (88.48), 177.0 (21.65), 160.9 (13.77), 132.9 (100), 116.0 (4.83), 89.0 (26.05), 74.1 (4.10)
DP 238	13.8	C ₁₃ H ₁₉ NO ₃	238.3 ^b	219.9 (17.68), 197.9 (100), 178.0 (5.10), 160.9 (18.05), 132.9 (61.12), 89.0 (27.98)
DP 226	14.2	C ₁₂ H ₁₉ NO ₃	226.2 ^{b,c}	208.8 (3.07), 193.9 (100), 176.0 (12.72), 158.9 (12.52), 133.0 (9.28), 121.0 (58.92), 93.1 (3.32), 74.2 (34.52)
DP 195	12.6	C ₁₁ H ₁₇ NO ₂	195.0 ^{b,c}	176.8 (100), 169.0 (35.47), 156.8 (14.57), 134.9 (18.55), 121.0 (14.15), 89.0 (6.90), 74.2 (5.00)
DP 175	18.0	C ₁₁ H ₁₃ NO	175.2 ^c	157.8 (41.48), 144.9 (100), 133.0 (6.21), 119.0 (4.61), 89.0 (8.74)
DP 134	2.8	C ₆ H ₁₅ NO ₂	134.1 ^{b,c}	116.1 (100), 92.2 (42.37), 74.3 (32.50), 56.4 (16.75)
<i>Propranolol</i>	21.6	C ₁₆ H ₂₁ NO ₂	260.1	242.0 (2.73), 218.0 (10.36), 183.0 (100), 157.0 (32.71), 116.2 (73.12), 98.2 (16.43), 86.3 (4.54)
DP 340	12.8	C ₁₆ H ₂₁ NO ₇	340.2 ^c	322.0 (100), 296.0 (21.00), 280.0 (32.89), 261.9 (15.51), 217.9 (17.12), 162.9 (18.24), 134.0 (51.40), 116.0 (37.06)
DP 326	12.5 and 13.3	C ₁₆ H ₂₃ NO ₆	326.2 ^{b,c}	308.1 (40.45), 282.9 (8.18), 264.0 (21.83), 221.0 (20.00), 194.8 (7.57), 177.0 (70.77), 133.0 (100), 116.0 (23.09)
DP 310	15.0	C ₁₆ H ₂₃ NO ₅	310.2 ^b	293.1 (100), 274.0 (29.80), 238.9 (12.31), 198.9 (11.50), 176.9 (10.23), 132.9 (14.20), 101.0 (2.59)
DP 308	15.1	C ₁₆ H ₂₁ NO ₅	308.2 ^{b,c}	290.0 (100), 265.0 (46.96), 230.0 (18.68), 192.0 (65.65), 174.9 (29.06), 149.9 (25.23), 134.0 (91.52), 116.0 (87.49), 98.1 (30.32)
DP 296	12.5	C ₁₆ H ₂₅ NO ₄	296.2 ^c	278.0 (100), 260.0 (27.39), 234.9 (14.80), 216.9 (5.90), 162.9 (8.05), 144.0 (6.08), 134.0 (6.53), 116.1 (19.10)
DP 294	13.9 and 15.2	C ₁₆ H ₂₃ NO ₄	294.3 ^{b,c}	276.0 (83.53), 233.9 (58.88), 205.9 (12.53), 161.9 (20.47), 132.9 (16.82), 116.0 (100), 98.1 (6.68)
DP 292	14.4 and 16.4	C ₁₆ H ₂₁ NO ₄	292.2 ^c	274.0 (22.02), 249.9 (2.51), 232.9 (5.70), 158.9 (5.55), 130.9 (21.04), 116.0 (100), 98.1 (11.94)
DP 282	14.0 and 22.5	C ₁₄ H ₁₉ NO ₅	282.2 ^{b,c}	264.0 (100), 221.9 (4.90), 148.9 (14.17), 134.0 (34.43), 116.1 (68.51), 98.1 (10.83)
DP 276	18.2	C ₁₆ H ₂₁ NO ₃	276.2 ^{b,c}	248.0 (100), 233.9 (18.24), 187.9 (4.07), 161.9 (9.25), 132.9 (5.11), 98.0 (2.60)
DP 268	16.5	C ₁₄ H ₂₁ NO ₄	268.4 ^c	249.0 (100), 206.9 (8.53), 190.9 (17.91), 158.9 (19.89), 133.0 (13.56), 116.0 (22.74), 81.1 (6.78)
DP 266	19.6	C ₁₄ H ₁₉ NO ₄	266.3 ^c	248.0 (100), 205.9 (11.50), 187.9 (6.64), 145.9 (2.77), 132.0 (4.20), 116.0 (5.29)
DP 134	3.0	C ₆ H ₁₅ NO ₂	134.2 ^b	116.0 (100), 107.9 (21.90), 89.1 (10.73), 72.3 (42.43)
DP 132	3.2	C ₅ H ₁₃ NO ₂	132.0 ^{b,c}	116.0 (100), 96.0 (57.15), 89.2 (24.62), 72.2 (12.34)
DP 116	2.7	C ₆ H ₁₃ NO	116.2 ^{b,c}	97.0 (100), 72.2 (26.44)

DP: degradation product; Rt: retention time; NF: not fragmented.

^a m/z values shown are for protonated molecular ions [M + H]⁺.^b Identified in the experiment using the ratio 1:1 [β-blocker]:[Fe(VI)].^c Identified in the experiment using the ratio 1:10 [β-blocker]:[Fe(VI)].

The reaction in the secondary amine moiety benefits from an increase of pH above 9 (SI, Text S11), which causes deprotonation of the secondary amine moiety, resulting in N-dealkylation from a further reaction with Fe(VI) (Romero et al., 2011). To a limited extent, hydroxylation on the aromatic ring was observed for both compounds. Concerning ATE, specific coupling reactions were identified in a similar mechanism, as proposed by Huang et al. (2001a,b).

On the other hand, PRO showed reactions in the naphthalene group, mainly, to further hydroxylation, ring opening, hydrogen abstraction and decarboxylation. In the case of PRO, no reaction was observed in the secondary amine moiety, which can be explained by the fact that it only occurs when the oxidized naphthalene group becomes less reactive (Romero et al., 2011).

A common degradation product found for the three β-blockers results from the cleavage of the side chain 2-hydroxy-3-(isopropylamino)

propoxy from the aromatic ring, forming the most polar DP that was identified (DP 134).

3.4. Assessment of the ready biodegradability by CBT

The biodegradability test conducted by CBT fulfilled the validation criteria of the OECD test. As can be observed in Fig. 6(A), ATE showed no biodegradation and the post-process sample showed 72.7% biodegradability, after 28 days. As in the post-treatment sample, the degradation resulting from the Fe(VI) treatment achieved 71.7% after 120 min; therefore, it can be concluded that about 30% of ATE is not degraded, and might be responsible for the non-biodegradable fraction in the CBT.

MET also proved to be not readily biodegradable, as shown in Fig. 6(B), and the degradation achieved by 120 min Fe(VI) treatment

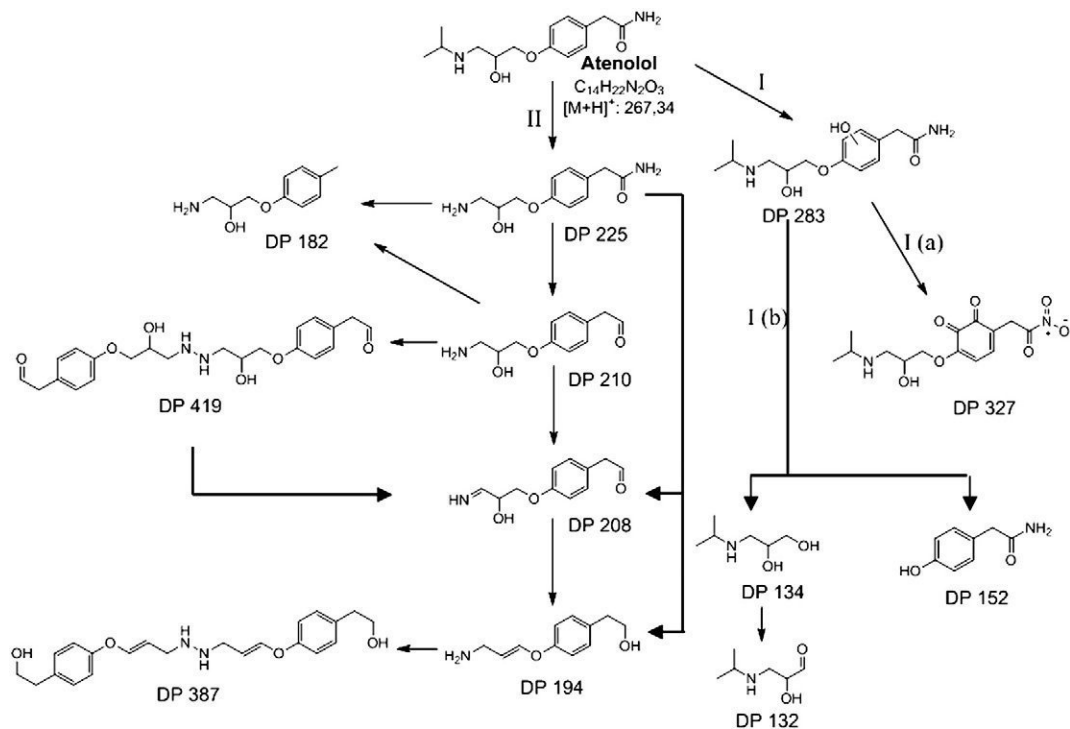


Fig. 3. Proposed degradation pathway of atenolol by oxidation-coagulation by Fe(VI) in aqueous solution.

was only 24.8%. As expected, the post-treatment mixture was not readily biodegradable, showing only 13.8% biodegradation after 28 days.

The ready biodegradability of PRO before and after Fe(VI) treatment can be observed in Fig. 6(C). As in the case of ATE and MET,

PRO was found to be not readily biodegradable. The post-treatment sample also proved to be not readily biodegradable after 28 days, achieving 44.4% biodegradation. As PRO was degraded 96.6% after 120 min of treatment, the content of the sample in CBT had a small proportion of non-degraded PRO and a mixture of non-biodegradable DPs.

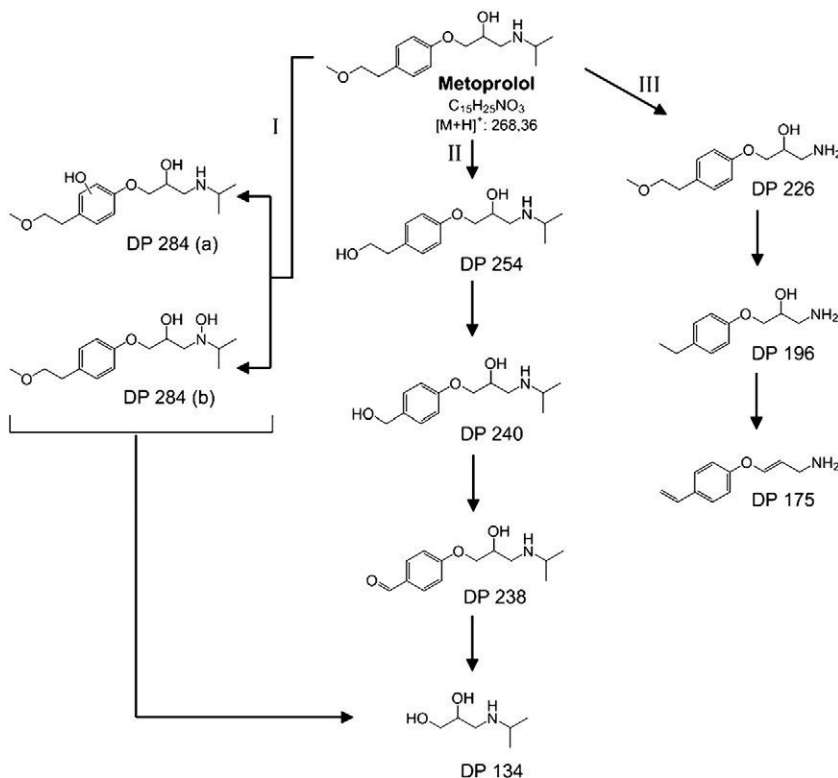


Fig. 4. Proposed degradation pathway of metoprolol by oxidation-coagulation by Fe(VI) in aqueous solution.

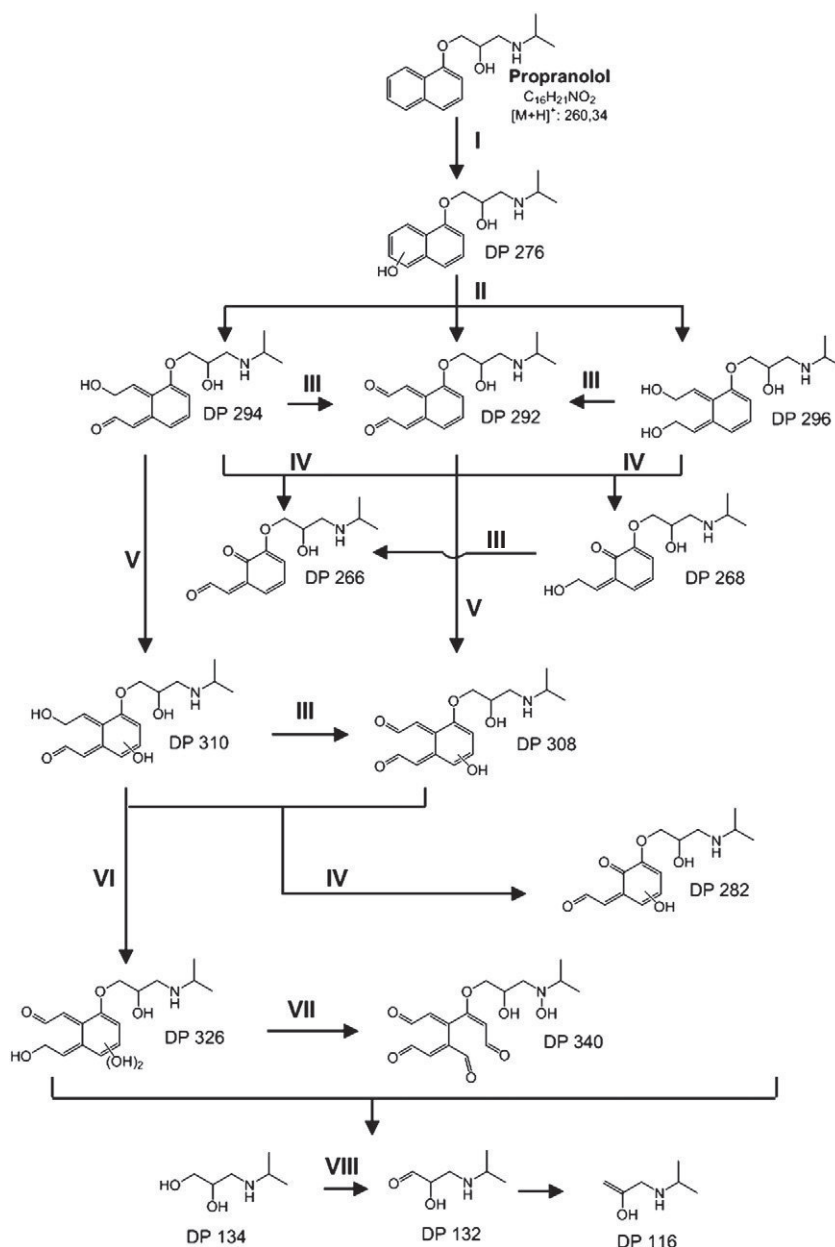


Fig. 5. Proposed degradation pathway of propranolol by oxidation-coagulation by Fe(VI) in aqueous solution.

4. Conclusion

This study demonstrated the applicability of K₂Fe^{VI}O₄ to the degradation of β-blockers in HWW by means of RSM; the findings indicate that the degradation process is mainly dependent on the [Fe(VI)].

Regardless of the high percent of aromaticity removal (>60%) and the degradation of β-blockers (>90%), the COD removal from HWW was found to be relatively low (only 17.5%). As well as belonging to the same pharmaceutical class, each β-blocker was shown to have a different behavior regarding the variables studied using RSM.

In aqueous solution, Fe(VI) treatment was found to be efficient for the degradation of ATE and PRO in both concentration ratios studied, but a singular non-mineralization behavior was observed, which led to a transformation to DPs. 34 different DPs were identified by LC/MS, which suggests the existence of multi-step and interconnected degradation pathways.

The assessment of the biodegradability showed that ATE, MET and PRO are not readily biodegradable. Post-treatment samples showed that ATE was converted into a mixture of readily biodegradable products, while with PRO, the oxidation-coagulation only led to a slight increase of biodegradability.

Even though the Fe(VI) treatment proved to be a suitable and useful option for the elimination of the parent compounds from wastewater, this investigation revealed many different degradation products and only a slight increase in biodegradability. This confirms that before it can be recommended for the treatment of real wastewater or even for handling drinking water, there is a need for more in-depth studies for a better understanding of the entire process.

Conflict of interest

The authors declare that there is no conflict of interest.

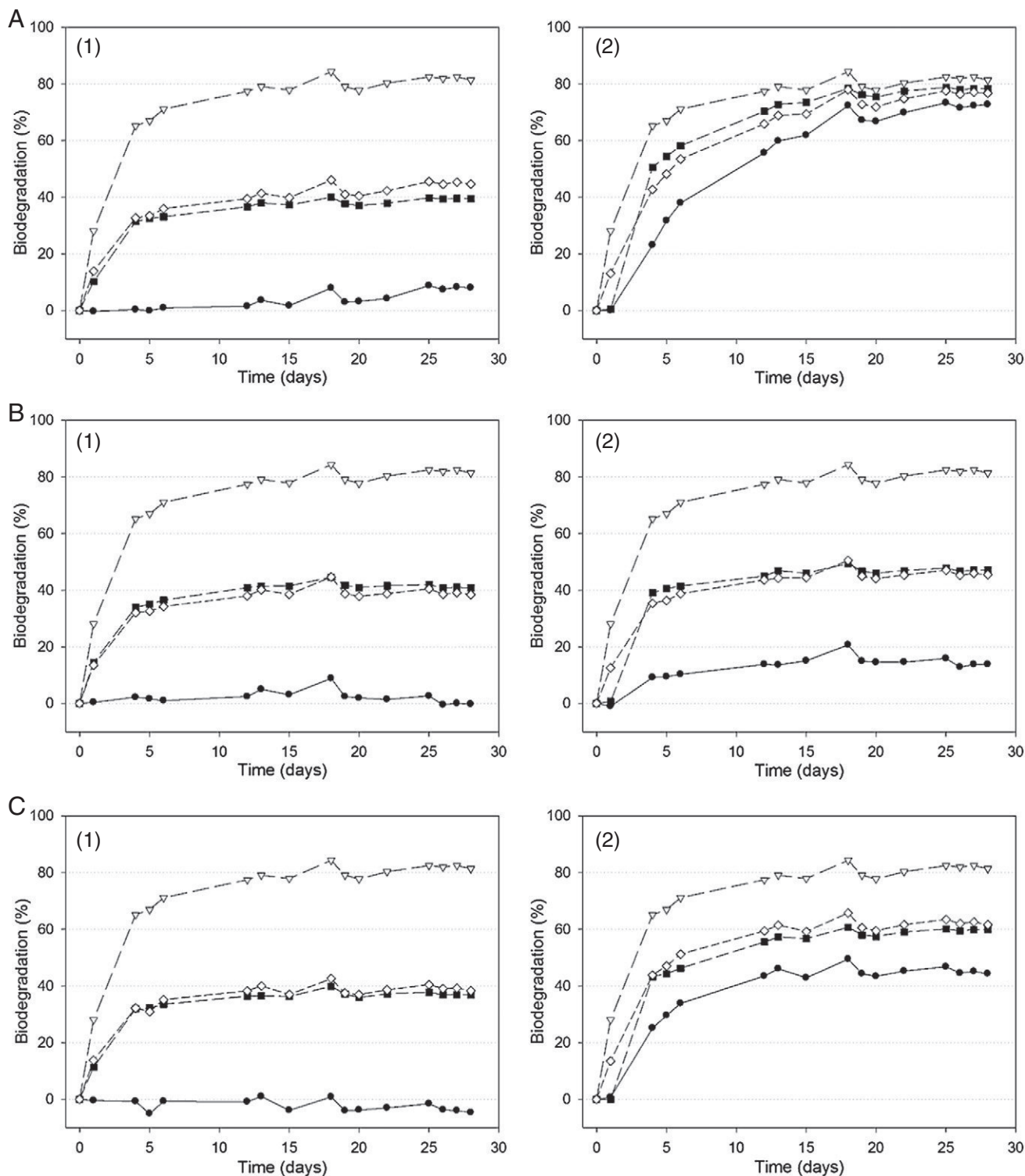


Fig. 6. Aerobic biodegradation of (A) atenolol, (B) metoprolol and (C) propranolol, (1) before and (2) post-treatment in the CBT by oxidation-coagulation using Fe(VI) in the ratio $[\beta\text{-blocker}]:[\text{Fe(VI)}] 1:10 \text{ mol L}^{-1}:\text{mol L}^{-1}$. (∇) Quality control ($n=2$), (\blacksquare) toxicity control (measured) ($n=2$), (\diamond) toxicity control (computed) and (\bullet) tested substance ($n=2$).

Acknowledgments

The authors would like to thank the CAPES Foundation – Ministry of Education of Brazil (BEX 2573/08-3) and the German Academic Exchange Service (DAAD, A/08/71780) for the scholarship granted to M.L. Wilde, as well as to the Brazilian National Council for Scientific and Technological Development (CNPq, Grant Nr. 27 303024/2009-7), for their financial support. Waleed M.M. Mahmoud is grateful to the

Ministry of Higher Education and Scientific Research of the Arab Republic of Egypt (MHESR) and the DAAD for their sponsorship and financial support (GERLS program).

Appendix A. Supplementary data

Supplementary data to this article can be found online at <http://dx.doi.org/10.1016/j.scitotenv.2013.01.059>.

References

- Alder AC, Schaffner C, Majewsky M, Klasmeyer J, Fenner K. Fate of β -blocker human pharmaceuticals in surface water: comparison of measured and simulated concentrations in the Glatt Valley Watershed, Switzerland. *Water Res* 2010;44:936–48.
- Anquandah GAK, Sharma VK, Knight DA, Batchu SR, Gardinali PR. Oxidation of trimethoprim by ferrate(VI): kinetics, products, and antibacterial activity. *Environ Sci Technol* 2011;45:10575–81.
- APHA-AWWA. Standard methods for the examination of water and wastewater, 5220-D. COD: closed reflux, colorimetric method. Public health 20th ed. American Public Health Association; 1999.
- Audette RJ, Quail JW, Smith PJ. Oxidation of substituted benzyl alcohols with ferrate(VI). *J Chem Soc, Chem Commun* 1972:38–9.
- Bendz D, Paxéus NA, Ginn TR, Loge FJ. Occurrence and fate of pharmaceutically active compounds in the environment, a case study: Høje River in Sweden. *J Hazard Mater* 2005;122:195–204.
- Benner J, Ternes TA. Ozonation of propranolol: formation of oxidation products. *Environ Sci Technol* 2009a;43:5086–93.
- Benner J, Ternes TA. Ozonation of metoprolol: elucidation of oxidation pathways and major oxidation products. *Environ Sci Technol* 2009b;43:5472–80.
- Bezerra MA, Santelli RE, Oliveira EP, Villar LS, Escalera LA. Response surface methodology (RSM) as a tool for optimization in analytical chemistry. *Talanta* 2008;76:965–77.
- Boillot C, Bazin C, Tissot-Guerraz F, Droguet J, Perraud M, Cetre JC, et al. Daily physico-chemical, microbiological and ecotoxicological fluctuations of a hospital effluent according to technical and care activities. *Sci Total Environ* 2008;403:113–29.
- Bueno MJM, Gomez MJ, Herrera S, Hernando MD, Agüera A, Fernández-Alba AR. Occurrence and persistence of organic emerging contaminants and priority pollutants in five sewage treatment plants of Spain: two years pilot survey monitoring. *Environ Pollut* 2012;164:267–73.
- Chen Y, Liu Z, Wang Z, Xue M, Zhu X, Tao T. Photodegradation of propranolol by Fe(III)-citrate complexes: kinetics, mechanism and effect of environmental media. *J Hazard Mater* 2011;194:202–8.
- De Witte B, Van Langenhove H, Demeestere K, Saerens K, De Wispelaere P, Dewulf J. Ciprofloxacin ozonation in hospital wastewater treatment plant effluent: effect of pH and H₂O₂. *Chemosphere* 2010;78:1142–7.
- Delaide L, Laszlo P. A novel oxidizing reagent based on potassium ferrate(VI). *J Org Chem* 1996;61:6360–70.
- Escher BI, Bramaz N, Richter M, Lienert J. Comparative ecotoxicological hazard assessment of beta-blockers and their human metabolites using a mode-of-action-based test battery and a QSAR approach. *Environ Sci Technol* 2006;40:7402–8.
- Escher BI, Baumgartner R, Koller M, Treyer K, Lienert J, Mcardell CS. Environmental toxicology and risk assessment of pharmaceuticals from hospital wastewater. *Water Res* 2010;45:75–92.
- Graham N, Jiang C, Li X-Z, Jiang J-Q, Ma J. The influence of pH on the degradation of phenol and chlorophenols by potassium ferrate. *Chemosphere* 2004;56:949–56.
- Gros M, Pizzolato T-M, Petrović M, Alda MJL, Barceló D. Trace level determination of beta-blockers in waste waters by highly selective molecularly imprinted polymers extraction followed by liquid chromatography-quadrupole-linear ion trap mass spectrometry. *J Chromatogr A* 2008;1189:374–84.
- Heberer T. Occurrence, fate, and removal of pharmaceutical residues in the aquatic environment: a review of recent research data. *Toxicol Lett* 2002;131:5–17.
- Henriques DM, Kümmerer K, Mayer FM, Vasconcelos TG, Martins AF. Nonylphenol polyethoxylate in hospital wastewater: a study of the subproducts of electrocoagulation. *J Environ Sci Health A Tox Hazard Subst Environ Eng* 2012;47:37–41.
- Hernando MD, Mezcua M, Fernández-Alba AR, Barceló D. Environmental risk assessment of pharmaceutical residues in wastewater effluents, surface waters and sediments. *Talanta* 2006;69:334–42.
- Hernando M, Gomez M, Agüera A, Fernandez-Alba AR. LC–MS analysis of basic pharmaceuticals (beta-blockers and anti-ulcer agents) in wastewater and surface water. *TrAC, Trends Anal Chem* 2007;26:581–94.
- Hu L, Martin HM, Arce-Bulted O, Sugihara MN, Keating KA, Strathmann TJ. Oxidation of carbamazepine by Mn(VII) and Fe(VI): reaction kinetics and mechanism. *Environ Sci Technol* 2009;43:509–15.
- Huang H, Sommerfeld D, Dunn BC, Eyring EM, Lloyd CR. Ferrate(VI) oxidation of aqueous phenol: kinetics and mechanism. *J Phys Chem A* 2001a;105:3536–41.
- Huang H, Sommerfeld D, Dunn BC, Lloyd CR, Eyring EM. Ferrate(VI) oxidation of aniline. *J Chem Soc Dalton Trans* 2001b:1301–5.
- Huggett DB, Khan IA, Foran CM, Schlenk D. Determination of beta-adrenergic receptor blocking pharmaceuticals in United States wastewater effluent. *Environ Pollut* 2003;121:199–205.
- Jiang J-Q, Lloyd B. Progress in the development and use of ferrate(VI) salt as an oxidant and coagulant for water and wastewater treatment. *Water Res* 2002;36:1397–408.
- Khetan SK, Collins TJ. Human pharmaceuticals in the aquatic environment: a challenge to green chemistry. *Chem Rev* 2007;107:2319–64.
- Kümmerer K. Pharmaceuticals in the environment: sources, fate, effects and risks. 3rd ed. Heidelberg: Springer-Verlag; 2008.
- Kümmerer K. The presence of pharmaceuticals in the environment due to human use – present knowledge and future challenges. *J Environ Manage* 2009;90:2354–66.
- Längin A, Alexy R, König A, Kümmerer K. Deactivation and transformation products in biodegradability testing of β -lactams amoxicillin and piperacillin. *Chemosphere* 2009;75:347–54.
- Li C, Li XZ, Graham N, Gao NY. The aqueous degradation of bisphenol A and steroid estrogens by ferrate. *Water Res* 2008;42:109–20.
- Licht S, Naschitz V, Halperin L, Halperin N, Lin L, Chen J, et al. Analysis of ferrate(VI) compounds and super-iron Fe(VI) battery cathodes: FTIR, ICP, titrimetric, XRD, UV/VIS, and electrochemical characterization. *J Power Sources* 2001;101:167–76.
- Liu Q-T, Williams HE. Kinetics and degradation products for direct photolysis of beta-blockers in water. *Environ Sci Technol* 2007;41:803–10.
- Mahmoud WMM, Kümmerer K. Captopril and its dimer captopril disulfide: photodegradation, aerobic biodegradation and identification of transformation products by HPLC–UV and LC-ion trap–MSn. *Chemosphere* 2012;88:1170–7.
- Marco-Urrea E, Radjenovic J, Caminal G, Petrovic M, Vicent T, Barceló D. Oxidation of atenolol, propranolol, carbamazepine and clofibrac acid by a biological Fenton-like system mediated by the white-rot fungus *Trametes versicolor*. *Water Res* 2009;1–12.
- Martins AF, Mayer F, Confortin EC, Frank CS. A study of photocatalytic processes involving the degradation of the organic load and amoxicillin in hospital wastewater. *Clean Soil, Air, Water* 2009;37:365–71.
- Martins AF, Mallmann CA, Arsand DR, Mayer FM, Brenner CGB. Occurrence of the antimicrobials sulfamethoxazole and trimethoprim in hospital effluent and study of their degradation products after electrocoagulation. *Clean Soil, Air, Water* 2011;39:21–7.
- Maurer M, Escher BI, Riehle P, Schaffner C, Alder AC. Elimination of β -blockers in sewage treatment plants. *Water Res* 2007;41:1614–22.
- Noorhasan N, Patel B, Sharma VK. Ferrate(VI) oxidation of glycine and glycyglycine: kinetics and products. *Water Res* 2009;1:1–9.
- OECD. Organisation for Economic Co-operation and Development, 2006. OECD Guideline for Testing of Chemicals 301 D: Ready Biodegradability. Closed Bottle Test. OECD Publishing, Paris. Organisation for Economic Co-operation and Development OECD; 1992.
- Radjenovic J, Escher BI, Rabaey K. Electrochemical degradation of the β -blocker metoprolol by Ti/RuO₂/IrO₃O₂ and Ti/SnO₂-Sb electrodes. *Water Res* 2011;45:3205–14.
- Roberts PH, Thomas KV. The occurrence of selected pharmaceuticals in wastewater effluent and surface waters of the lower Tyne catchment. *Sci Total Environ* 2006;356:143–53.
- Romero V, De Cruz N, Dantas RF, Marco P, Giménez J, Esplugas S. Photocatalytic treatment of metoprolol and propranolol. *Catal Today* 2011;161:115–20.
- Sharma VK. Potassium ferrate(VI): an environmentally friendly oxidant. *Adv Environ Res* 2002;6:143–56.
- Sharma VK. Oxidative transformations of environmental pharmaceuticals by Cl₂, ClO₂, O₃, and Fe(VI): kinetics assessment. *Chemosphere* 2008;73:1379–86.
- Sharma VK, Mishra SK. Ferrate(VI) oxidation of ibuprofen: a kinetic study. *Environ Chem Lett* 2006;3:182–5.
- Sharma VK, Mishra SK, Nesnas N. Oxidation of sulfonamide antimicrobials by ferrate(VI) [Fe^{VI}O₄²⁻]. *Environ Sci Technol* 2006;40:7222–7.
- Slegers C, Maquille A, Deridder V, Sonveaux E, Jivan J-LH, Tilquin B. LC–MS analysis in the e-beam and gamma radiolysis of metoprolol tartrate in aqueous solution: structure elucidation and formation mechanism of radiolytic products. *Radiat Phys Chem* 2006;75:977–89.
- Song W, Cooper WJ, Mezyk SP, Greaves J, Peake BM. Free radical destruction of β -blockers in aqueous solution. *Environ Sci Technol* 2008;42:1256–61.
- Stolker AAM, Niesing W, Hogendoorn EA, Versteegh JFM, Fuchs R, Brinkman UAT. Liquid chromatography with triple-quadrupole or quadrupole-time of flight mass spectrometry for screening and confirmation of residues of pharmaceuticals in water. *Anal Bioanal Chem* 2004;378:955–63.
- Ternes TA. Occurrence of drugs in German sewage treatment plants and rivers. *Water Res* 1998;32:3245–60.
- Trautwein C, Kümmerer K. Incomplete aerobic degradation of the antidiabetic drug Metformin and identification of the bacterial dead-end transformation product Guanylurea. *Chemosphere* 2011;85:765–763.
- Trautwein C, Kümmerer K. Degradation of the tricyclic antipsychotic drug chlorpromazine under environmental conditions, identification of its main aquatic biotic and abiotic transformation products by LC–MSn and their effects on environmental bacteria. *J Chromatogr B* 2012;889–890:24–38.
- Vasconcelos TG, Kümmerer K, Henriques DM, Martins AF. Ciprofloxacin in hospital effluent: degradation by ozone and photoprocesses. *J Hazard Mater* 2009;169:1154–8.
- Verlicchi P, Galletti A, Petrovic M, Barceló D. Hospital effluents as a source of emerging pollutants: an overview of micropollutants and sustainable treatment options. *J Hydrol* 2010;389:416–28.
- Xu GR, Zhang YP, Li GB. Degradation of azo dye active brilliant red X-3B by composite ferrate solution. *J Hazard Mater* 2009;161:1299–305.
- Yang H, An T, Li G, Song W, Cooper WJ, Luo H, et al. Photocatalytic degradation kinetics and mechanism of environmental pharmaceuticals in aqueous suspension of TiO₂: a case of β -blockers. *J Hazard Mater* 2010;179:834–9.
- Yang B, Ying G-G, Zhao J-L, Zhang L-J, Fang Y-X, Nghiem LD. Oxidation of triclosan by ferrate: reaction kinetics, products identification and toxicity evaluation. *J Hazard Mater* 2011;186:227–35.
- Yuan B, Li X, Graham N. Reaction pathways of dimethyl phthalate degradation in TiO₂-UV-O₂ and TiO₂-UV-Fe(VI) systems. *Chemosphere* 2008;72:197–204.
- Zimmerman SG, Schukat A, Schulz M, Benner J, Von Gunten U, Ternes TA. Kinetic and mechanistic investigations of the oxidation of tramadol by ferrate and ozone. *Environ Sci Technol* 2012;46:876–84.

Supplementary Material

Oxidation-coagulation of β -blockers by $\text{K}_2\text{Fe}^{\text{VI}}\text{O}_4$ in hospital wastewater: assessment of degradation products and biodegradability

Marcelo L. Wilde^a, Waleed M. M. Ahmed^{b,c}, Klaus Kümmerer^b and Ayrton F. Martins^{a*}

* Corresponding author:

Ayrton F. Martins – martins@quimica.ufsm.br; ayrton@pq.cnpq.br.

Phone/Fax: +55 55 3220 8664

Text S1. Characterization of synthesized $\text{K}_2\text{Fe}^{\text{VI}}\text{O}_4$

The purity of the synthesized K_2FeO_4 was determined by the chromite oxidation-reduction method in accordance with Licht et al. (2001), and the measured percent of K_2FeO_4 was 85.1% (w/w).

The identification and characterization was also carried out with X-ray diffraction (XRD, Bruker D8 Advance Diffractometer) in the range of 20 – 140° (2 θ) at room temperature. Figure S1 shows the main peaks of K_2FeO_4 [102], [111], [200], [112], [211] and [013]. The high intensity peak [013] was found to be 30.1° (2 θ), which is characteristic for K_2FeO_4 (Li et al., 2005; Wang et al., 2009), and indicates its high purity as well.

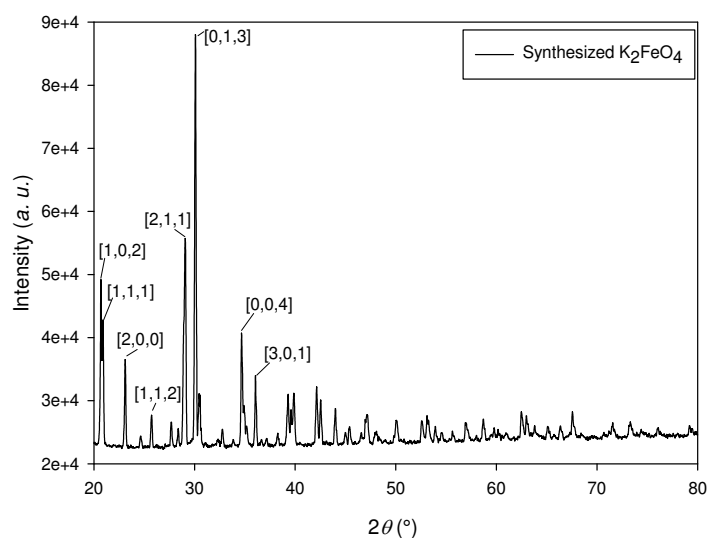


Figure S1. X-ray diffraction pattern of synthesized K_2FeO_4 .

Text S2. Characteristics of Hospital wastewater

The average physical-chemical parameters ($n = 3,4$) of samples collected from the sewage treatment plant of the University Hospital of the Federal University of Santa Maria can be seen in Table S1; even after the wastewater stream has passed through the septic tank-anaerobic filter system, it still retains high organic and inorganic content.

Table S1. Physical-chemical characteristics of the Hospital wastewater ($n = 3,4$) under study.

Parameter	Value
BOD ₅ (mg L ⁻¹)	303.7 ^a
COD (mg O ₂ L ⁻¹)	200-658 ^b
A _{UV 254}	1.2537 ^b
Organic matter (mg L ⁻¹)	130.5 ^a
Nitrogen as NH ₃ (mg L ⁻¹)	52.0 ^a
Total Nitrogen (mg L ⁻¹)	59.1 ^a
Alkalinity (HCO ₃ ⁻) (mg L ⁻¹)	200.0 ^b
NO ₃ ⁻ (μg L ⁻¹)	680 ^c
Cl ⁻ (mg L ⁻¹)	132 ^c
Total PO ₄ ³⁻ (mg L ⁻¹)	7.5 ^{a,c}
SO ₄ ²⁻ (mg L ⁻¹)	4.0 ^c
K ⁺ (mg L ⁻¹)	21.9 ^{c,d}
Na ²⁺ (mg L ⁻¹)	150.5 ^{a,d}
Total Suspended Solids (mg L ⁻¹)	57 ^a
Total Solids at 105 °C (mg L ⁻¹)	484 ^a
pH	7-8 ^b
Average Temperature (°C)	23 ^b

^a Martins et al. (2009); ^b This study; ^c Martins et al. (2008); ^d Vasconcelos et al. (2009)

Text S3. LC-ESI-IT-MSⁿ method

A chromatographic method was devised to determine the degradation products (DPs) of atenolol (ATE), metoprolol (MET) and propranolol (PRO) by oxidation-coagulation with Fe(VI). The sample injection volume was settled to 20 μ L and the LC was operated in three different gradient modes, one for each β -blocker, using Milli-Q water with 0.5 % formic acid (solvent A) and acetonitrile (solvent B) as mobile phase, with a flow rate of 0.5 mL min⁻¹. The gradient steps for ATE, MET and PRO are described in Table S2.

Table S2. Liquid chromatography gradient used for the identification of degradation products.

Atenolol		Metoprolol		Propranolol	
Time (min)	B (%)	Time (min)	B (%)	Time (min)	B (%)
0-2	1	0-3	1	0-3	1
2-3	1-5	3-10	1-20	3-5	1-5
3-10	5-20	10-11	20	5-10	5-20
10-11	20	11-15	20-50	10-13	20
11-15	20-50	15-18	50	13-23	20-50
15-18	50	18-20	50-1	23-28	50
18-20	50-1	20-25	1	28-29	50-1
20-25	1			29-35	1

The first 3 min of a chromatographic run was derived from waste to minimize the introduction of Fe ions into the ESI and, hence, in the mass spectrometer (MS). The operational conditions of the source were settled (as described in Table S3). The MS was operated in full scan, monitoring in positive and negative ion mode in the range of m/z 40-800 Da.

The chromatograms were analyzed with the aid of ESI Compass 1.3 software for HCT/Esquire (Bruker Daltonics, Bremen, Germany).

The fragmentation patterns of ATE, MET and PRO were used to optimize the conditions for the spectrometer, such as ionization, voltages and trapping condition by infusing standard aqueous solutions of 100 mg L⁻¹ using a syringe pump (Coler-Palmer

74900 series). The fragmentation pattern was used afterwards for the identification of the DPs.

The fragmentation of the DPs was carried out by means of multiple reaction monitoring (MRM) using the following characteristics: SmartFrag on, isolation mass MS/MS 210,00 m/z, fragmentation width 4,00 m/z, fragmentation time 40000 μ s, fragmentation delay 0 μ s, and fragmentation cutoff 57,00 m/z. The collision energy (fragmentation amplitude) was carried out from 0.2 to 1.0 V.

Table S3. Operational characteristics of the electrospray ionization Ion Trap-Mass Spectrometer (ESI-IT-MSⁿ).

Mode	Tune SPS			Tune Source		Trap	
Mass Range Mode	Std/Normal	Target Mass	400 m/z	Trap Drive	51.00	Rolling	On
Ion Polarity	Positive	Compound Stability	100%	Octopole RF Amplitude	150.0 Vpp	Rolling Averages	2 cts
Ion Source Type	ESI	Trap Drive Level	100%	Lens 2	60.0 V	Scan Begin	40 m/z
Alternating Ion Polarity	On	Optimize	Normal	Capillary Exit	-121.0 V	Scan End	800 m/z
Current Alternating Ion Polarity	Positive	Smart Parameter Setting	active	Dry Temp.	350 °C	Averages	6 Spectra
				Nebulizer	30.00 psi	Accumulation Time	200000 μ s
				Dry Gas	12.00 L/min	(Smart) ICC Target	40000
				HV Capillary HV End	-4000 V	ICC	On
				Plate Offset	-500 V	trap driver	37.2%
				Skimmer	-40 V		
				octopole one	12 V		
				octopole two	1.7 V		

Text S4. Closed Bottle Test (OECD 301D)

The test consists of four different series (Table S4), and was run in duplicates. The blank series only contained mineral medium and inoculum. The test series contained the respective tested substance, while the quality control series contained readily biodegradable sodium acetate as the only source of carbon, apart from the inoculum. The amount of sodium acetate and each test compound was chosen to correspond to a theoretical oxygen demand (ThOD) of 5 mg L^{-1} , with the exception of the post-process samples, which were measured in accordance with the chemical oxygen demand and diluted to reach a final concentration of $5 \text{ mg O}_2 \text{ L}^{-1}$. The fourth series was the toxicity control, which contains both the tested substance and the biodegradable sodium acetate, at an amount corresponding to 5 mg L^{-1} ThOD.

Table S4. Composition of the aerobic biodegradation test series in the CBT.

Test series	1	2	3	4
	Blank	Quality control	Test compound	Toxicity control
Mineral medium	+	+	+	+
Inoculum	+	+	+	+
Test substance			+	+
Sodium acetate		+		+

The toxicity series aims to control and monitor a possible inhibitory effect on the bacteria or the presence of a co-metabolism, i.e. the bacteria need a more easily biodegradable substance to be able to degrade the test substance (allowing the recognition of false negative results caused by toxicity of the tested substance). The toxicity was evaluated by comparing the dissolved oxygen (DO) consumption, (measured in the toxicity control bottles computed from the OD consumption in the quality control series), only with those containing the tested substance, respectively. A compound is considered to be toxic if the difference between the predicted amount of oxygen consumption and the amount measured exceeds 25% (OECD, 1992). The CBT test fulfilled the OECD criteria and no toxicity was observed for the bacteria.

Text S5. Model fitting and statistical analysis

The Pareto chart of standardized effects shows the main effects with 95% of confidence (Figure S2). As can be observed, the variable with most influence on the oxidation-coagulation process was the concentration of Fe(VI), while the pH exert some effect on the degradation of MET and PRO.

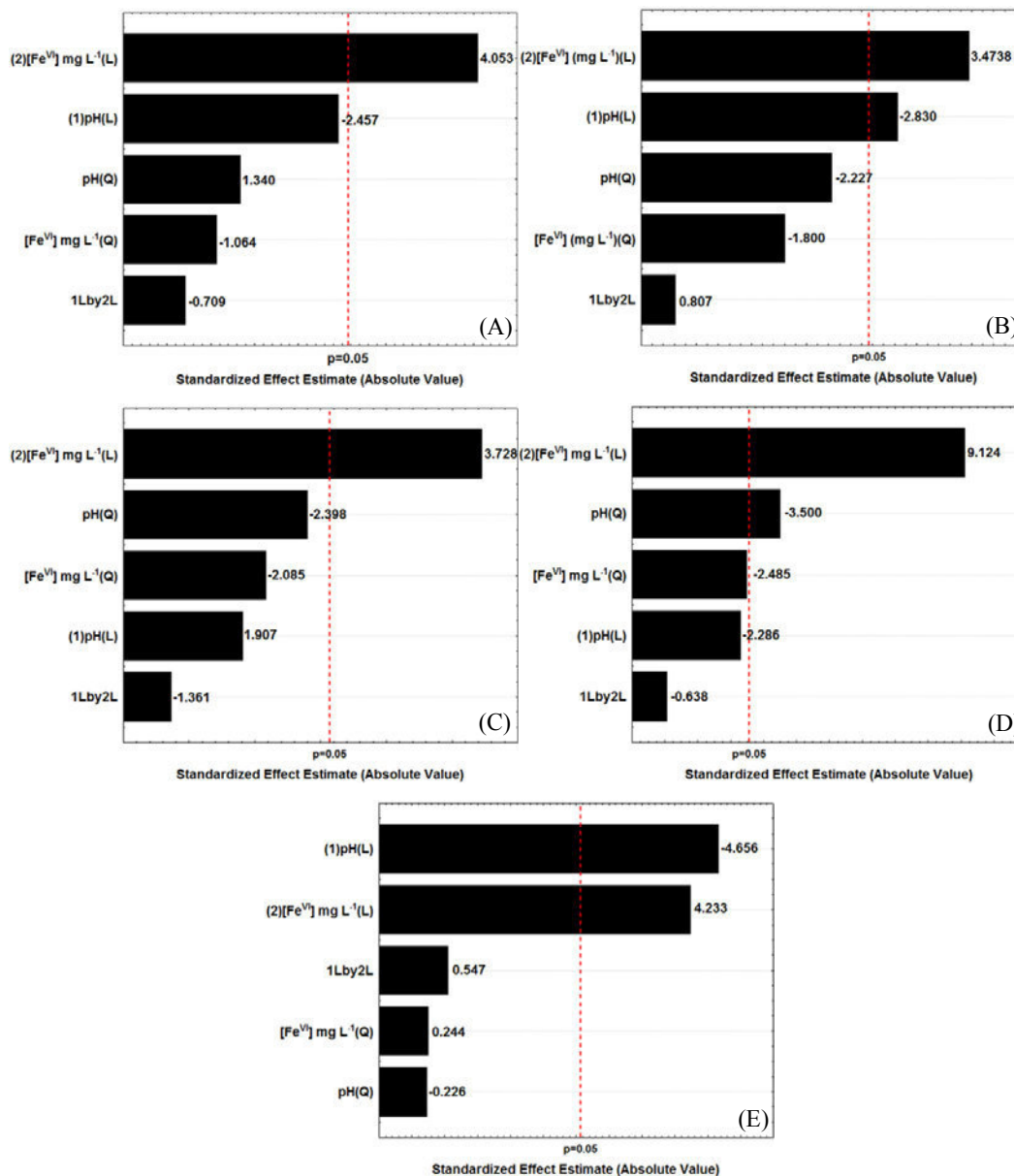


Figure S2. Pareto chart of standardized effect estimates (absolute values) of the oxidation-coagulation of Hospital wastewater with Fe(VI). (A) Red_{COD}, (B) Red_{UV254}, (C) Deg_{ATE}, (D) Deg_{MET} and (E) Deg_{PRO}. The vertical dashed line indicates a level of significance of 95% ($p = 0.05$), (L) stands for Linear variable and (Q) stands for Quadratic variable.

According to the Pareto chart, the empirical second-order polynomials expressing the responses of the model are given in equations 1-5. The equation only shows that the values of the independent variables have an influence on the process with 95% confidence.

$$Red_{COD}(\%) = 6,232 + 0,1912X_2 \quad (1)$$

$$Red_{UV_{254}}(\%) = -20,829 + 10,327X_1 + 0,80X_2 \quad (2)$$

$$Deg_{ATE}(\%) = -205,935 + 40,089X_1 + 2,287X_2 \quad (3)$$

$$Deg_{MET}(\%) = -85,12 + 19,958X_1 - 1,600X_1^2 + 1,461X_2 \quad (4)$$

$$Deg_{PRO}(\%) = 95,95 - 4,272X_1 + 0,065X_2 \quad (5)$$

Where X_1 and X_1^2 mean the coded linear (L) and quadratic (Q) variables of the pH and X_2 and X_2^2 mean the coded linear (L) and quadratic (Q) variables of the [Fe(VI)].

If the second order polynomial equations cannot satisfactorily define the results, it is necessary to find a more reliable way to evaluate the model fit. One suitable way of evaluating the significance of each variable is by using ANOVA, and comparing the variation sources with the *F*-test (Table S5).

This test makes it clear whether or not the model is suited to the data population that has been experimentally generated. It is based on the ratio between the sum of the squares (SS) from the regression model and the SS of the residues. The values obtained from the *F*-test were 5.4212, 5.432, 20.6229, and 8.0214 for Red_{COD} , $Red_{UV_{254}}$, Deg_{ATE} , Deg_{MET} and Deg_{PRO} , respectively, higher than the tabulated *F*-value (3.71 for 10 degrees of freedom).

Table S5. ANOVA of the quadratic model for the response surface of the Red_{COD}, Red_{UV254}, Deg_{GATE}, Deg_{MET} and Deg_{PRO} of the hospital wastewater by oxidation-coagulation with Fe(VI). (SS: sum of squares; df: degree of freedom; MS: media of the squares; F: Fischer-test; p: probability).

Red_{COD}	SS	df	MS	F	p
Regression	151	5	30.2	5.4212856	0.003
(1)pH (L)	33.6250	1	33.62501	6.03810	0.057422
pH (Q)	10.0033	1	10.00328	1.79630	0.237836
(2)[Fe ^{VI}] mg L ⁻¹ (L)	91.4914	1	91.49135	16.42924	0.009793
[Fe ^{VI}] mg L ⁻¹ (Q)	6.3095	1	6.30949	1.13301	0.335816
1L by 2L	2.7994	1	2.79945	0.50270	0.509997
Error	27.8441	5	5.56881		
Total SS	178.7239	10			
Red_{UV254}	SS	df	MS	F	p
Regression	3946	5	789	5.432077	0.0014
(1)pH (L)	1164.874	1	1164.874	8.00903	0.036674
pH (Q)	721.372	1	721.372	4.95976	0.076448
(2)[Fe ^{VI}] mg L ⁻¹ (L)	1755.117	1	1755.117	12.06723	0.017777
[Fe ^{VI}] mg L ⁻¹ (Q)	471.365	1	471.365	3.24085	0.131718
1L by 2L	94.863	1	94.863	0.65223	0.456003
Error	727.225	5	145.445		
Total SS	4672.466	10			
Deg_{GATE}	SS	df	MS	F	p
Regression	8652	5	1730	5.4532144	0.0002
(1)pH (L)	1155.14	1	1155.136	3.63512	0.114886
pH (Q)	1825.37	1	1825.374	5.74431	0.061870
(2)[Fe ^{VI}] mg L ⁻¹ (L)	4415.89	1	4415.892	13.89648	0.013602
[Fe ^{VI}] mg L ⁻¹ (Q)	1381.41	1	1381.414	4.34721	0.091479
1L by 2L	588.87	1	588.869	1.85313	0.231556
Error	1588.85	5	317.771		
Total SS	10237.21	10			
Deg_{MET}	SS	df	MS	F	p
Regression	9829	5	1966	20.622922	0.001
(1)pH (L)	502.74	1	502.742	5.27300	0.070095
pH (Q)	1168.10	1	1168.103	12.25163	0.017280
(2)[Fe ^{VI}] mg L ⁻¹ (L)	7936.54	1	7936.537	83.24225	0.000265
[Fe ^{VI}] mg L ⁻¹ (Q)	588.60	1	588.602	6.17355	0.055523
1L by 2L	0.39	1	0.388	0.00407	0.951581
Error	476.71	5	95.343		
Total SS	10305.76	10			
Deg_{PRO}	SS	df	MS	F	p
Regression	2150	5	430	8.0214418	0.00005
(1)pH (L)	1163.598	1	1163.598	21.67864	0.005552
pH (Q)	2.741	1	2.741	0.05107	0.830158
(2)[Fe ^{VI}] mg L ⁻¹ (L)	961.910	1	961.910	17.92106	0.008222
[Fe ^{VI}] mg L ⁻¹ (Q)	3.191	1	3.191	0.05945	0.817050
1L by 2L	16.070	1	16.070	0.29940	0.607785
Error	268.374	5	53.675		
Total SS	2418.347	10			

Text S6. Structural elucidation for Atenolol, Metoprolol and Propranolol

The first stage by the elucidation of degradation products (DP) implies in the determination of the fragmentation pattern of the parent compound. Thus, the fragmentation pattern of ATE $[M+H]^+$ 267,1 Da as precursor ion (PrI) can be seen in Figure S3.

Product ion (PI) m/z 250 results from the loss of 17 Da by neutral loss of ammonia from the acetamide moiety, and the PI of m/z 225 (loss of 42 Da), by cleavage of the isopropyl moiety. The PI of high intensity (m/z 190) is formed by the respective loss of hydroxyl and isopropyl moieties, generating a double bond.

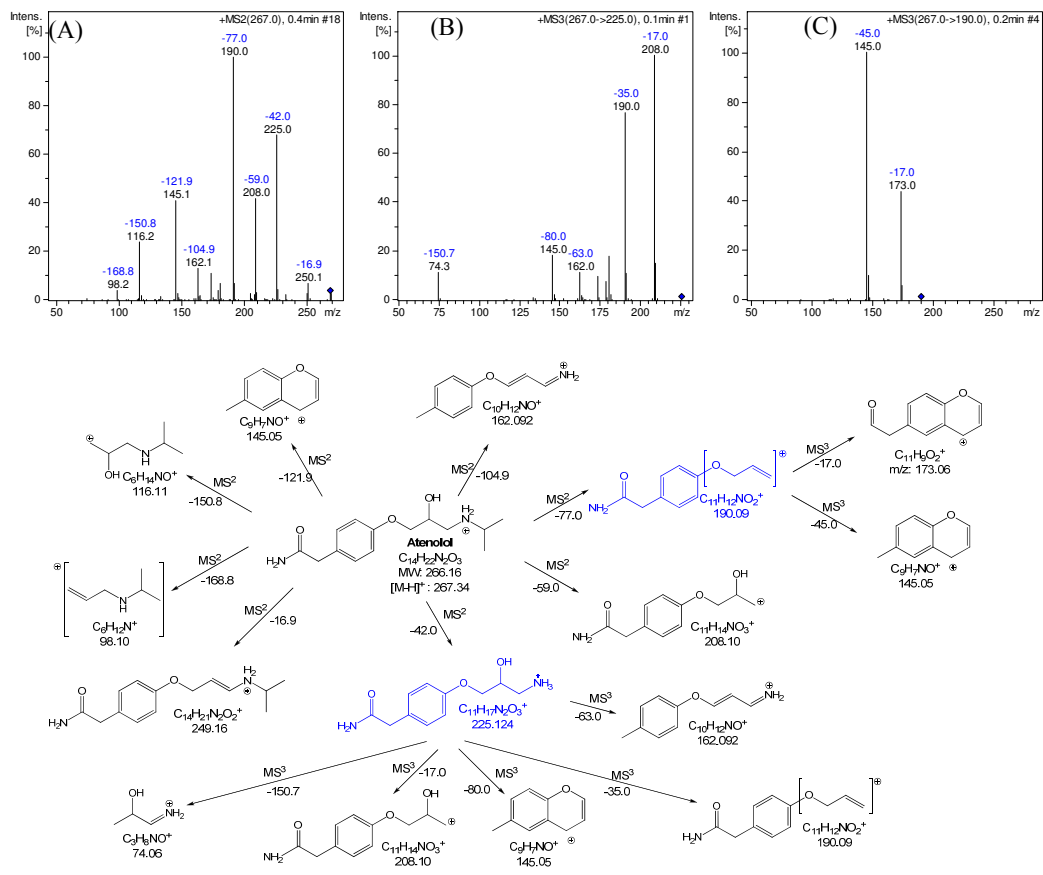


Figure S3. Mass spectra obtained by LC-ESI(+)-MS and the fragmentation pattern of ATE. (A) MS² of ATE m/z 267.0, (B) m/z 267.0 \rightarrow 225.0 MS³ and (C) m/z 267.0 \rightarrow 190.0 MS³.

The typical PIs of the side chain were m/z 116 Da and m/z 98 Da. The PIs m/z 162 and m/z 145 arise from fragmentation in different positions of the ATE molecule, with the remark that m/z 145 undergoes cyclization.

The main PI were used as PrI and further fragmented to MS3. The PrI of m/z 225 and m/z 190 originate similar PI to those of the parent compound. The fragmentation pattern proposed agree with that reported by Medana et al. (2008), Tay et al. (2011) and Radjenovic et al. (2008).

Similarly to ATE, the fragmentation pattern for MET was proposed (Figure S4). The PI found agree with those proposed by Benner and Ternes, 2009b, and Slegers et al., 2006. As can be seen, MET has a loss of 18 Da and 49 Da, which means loss of H_2O and CH_3OH from the ether side chain.

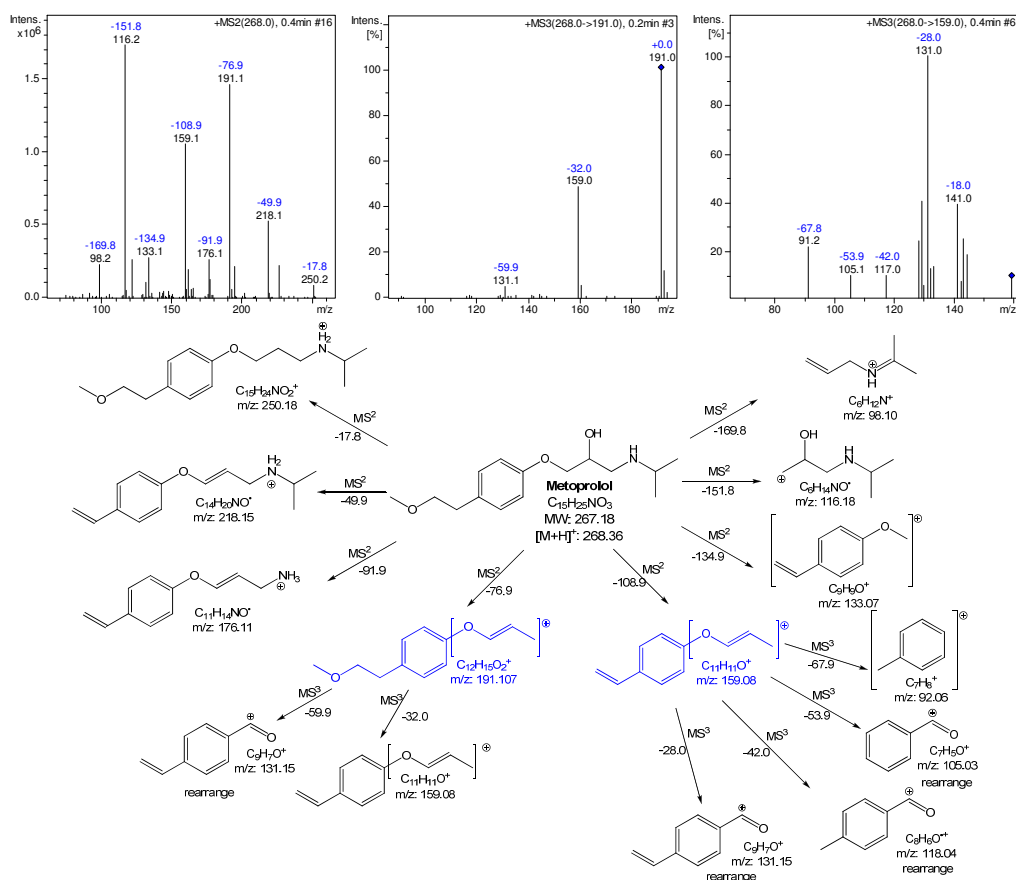


Figure S4. Mass spectra obtained by LC-ESI(+)-MS and the fragmentation pattern of MET. (A) MS² of MET m/z 268.0, (B) m/z 268.0 → 191.0 MS³ and (C) m/z 268.0 → 159.0 MS³.

The typical PI of the side chain 2-hydroxy-3-(isopropylamino)propoxy (m/z 133, 116 and 98.2) were also identified. For a better elucidation, the main fragments were used as PrI and further fragmented; the PI m/z 131 was found for both. It is proposed a rearrange of ether to ketone for it.

The fragmentation pattern of PRO can be seen in Figure S5. The loss of 18 Da and 42 Da reveals the loss of H_2O and isopropyl moieties, respectively. The PI m/z 183 results from cleavage of hydroxyl and propan-2-amine moieties. The PIs m/z 157 and m/z 141 keep the naphthalene group intact, occurring cleavage of the naphthalene-2-ol bond. Similarly to ATE and MET, PRO has typical PIs of the side chain 2-hydroxy-3-(isopropylamino)propoxy of m/z 116.2; 98.2 and 86.3. The fragmentation pattern found in this study is similar to that reported by Benner and Ternes (2009a).

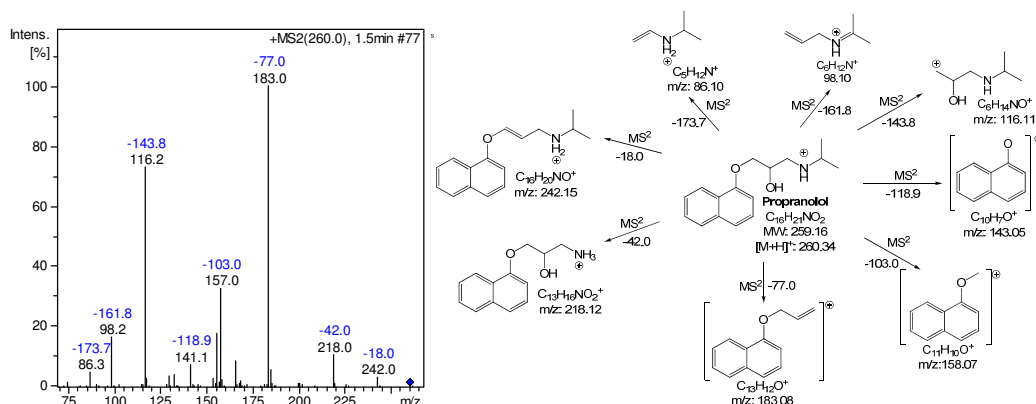


Figure S5. Mass spectra obtained by ESI(+)-MS² and the fragmentation pattern of PRO m/z 260.0

Text S7. Structural elucidation of degradation products from oxidation-coagulation of atenolol by Fe(VI)

The MS positive ion mode proved to be the most suitable way of analyzing the DPs of the β -blockers. The analyses involved comparing the m/z data of the samples

with the initial β -blockers in aqueous solution (blank). 12 DPs were identified by full scan (Figure S6), and were isolated and fragmented by MRM of the MSⁿ.

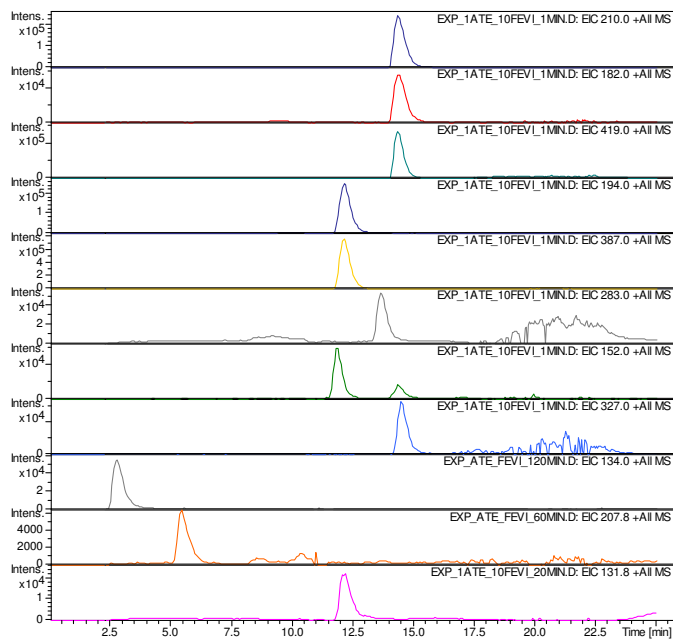


Figure S6. Extracted ion chromatograms of the DP identified by LC-ESI-IT-MS in the oxidation process carried out with the ratio of 1:10 [ATE]:[Fe(VI)].

4 DPs were found to have $[M+H]^+$ higher than ATE. The DPs with m/z 419.0 and 387.0 Da showed signs of dimerization, and were identified when the oxidation process was carried out with a concentration ratio of 1:10 [ATE]:[Fe(VI)].

The mass spectra and the fragmentation pattern of the hydroxylated DP 283 can be seen in Figure S7. This DP has the same fragment pattern as the one identified by the ozonation process of ATE (Tay et al., 2011).

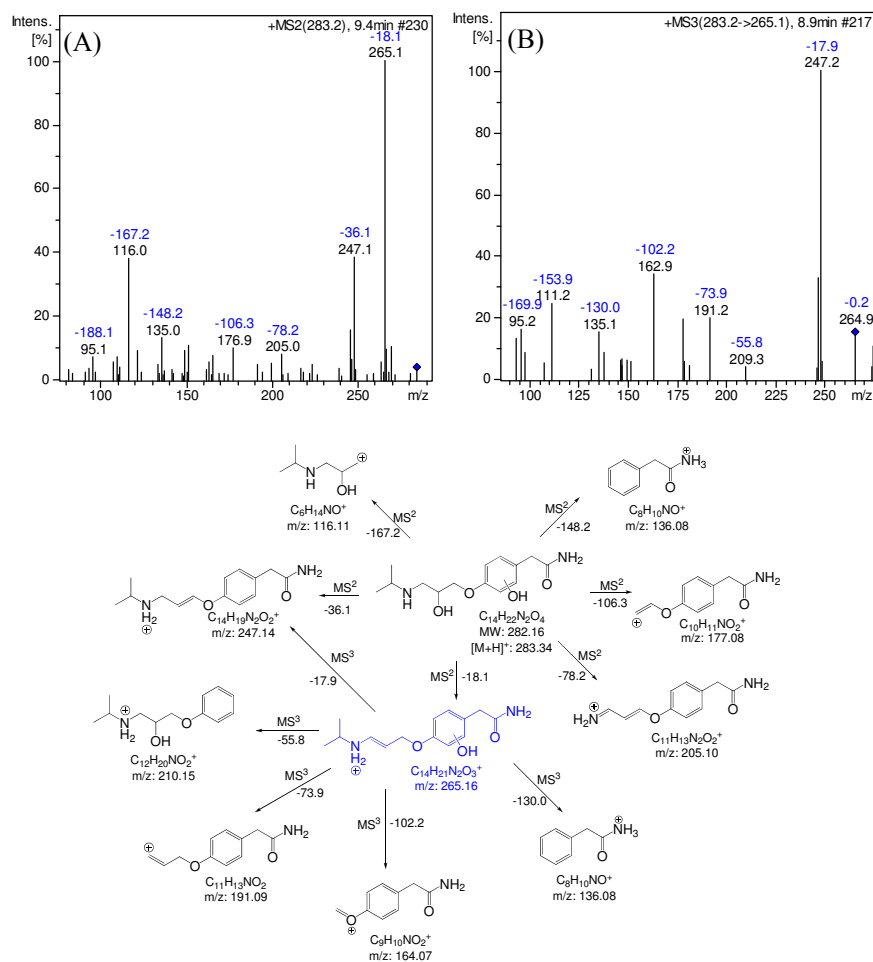


Figure S7. Mass spectra obtained by LC-ESI(+)-MS²/MS³ and the fragmentation pattern of DP 283. (A) MS² of m/z 283.2 and (B) m/z 283.2 → 265.1 MS³.

The oxidation-coagulation carried out in the ratio 1:1 [ATE]:[Fe(VI)] resulted in two peaks for the DP 283 with different retention times (Rt), 9.4 and 13.9 min, while in the process that was carried out with the ratio 1:10, only one peak was identified, (Rt 13.6 min), but no difference in the fragmentation pattern was observed.

Another DP identified with [M+H]⁺ higher than ATE was the DP 327. This study suggests that two different oxidation pathways occurred. The MS and the fragmentation pattern can be observed in Figure S8.

The product ion (PI) m/z 309.0 characterizes the loss of 18 Da (H₂O), while the m/z 279.1 characterizes the loss of NO₂. The m/z 132.0 suggests that the lateral chain 2-hydroxy-3-(isopropylamino)propoxy remains intact.

To confirm the characterization of the DP 327, the m/z 236.9 was used as a precursor ion and further fragmented. The PI resulting (MS^3) of m/z 221.1 characterizes the loss of H_2O or NH_3 , m/z 194.0 that results from the cleavage of the moiety $CH_2CH=O$, and the m/z 150.7 is formed by concomitant cleavage of $C=O$ and $NH_2CH_2CH(OH)CH_2$.

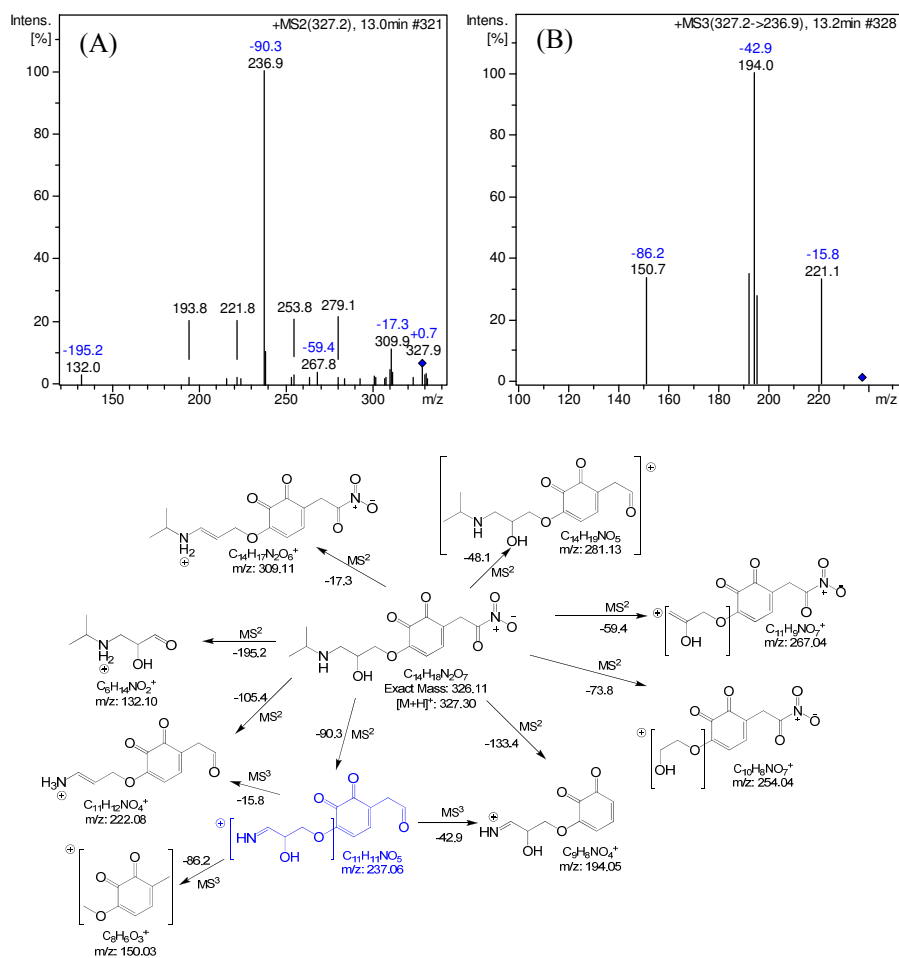


Figure S8. Mass spectra obtained by LC-ESI(+)-MS²/MS³ and the fragmentation pattern of DP 327. (A) MS² of m/z 297.2 and (B) m/z 327.2 \rightarrow 236.9 MS³.

8 DPs with lower $[M+H]^+$ than ATE were also found, which suggests the formation of low chain compounds. The DP 225 indicates that the ATE losses were 44 Da, and thus the elimination of isopropyl or acetamide moiety is proposed. When the MS² fragmentation pattern is analyzed (Figure S9), it is clear that the loss occurred in

the 2-hydroxy-3-(isopropylamino)propoxy side chain, since the fragmentation pattern does not show the PI characteristics of this moiety (m/z 132, 116 and 72).

The fragment ion of m/z 164.9 was used as the precursor ion and fragmented to MS^3 . The resulting PIs 120.9 and 93.2 are the same as those found in MS^2 , which confirms the proposed structure. The DP 225 was also cited as a DP of ozonation of ATE in alkaline medium (Tay et al., 2011).

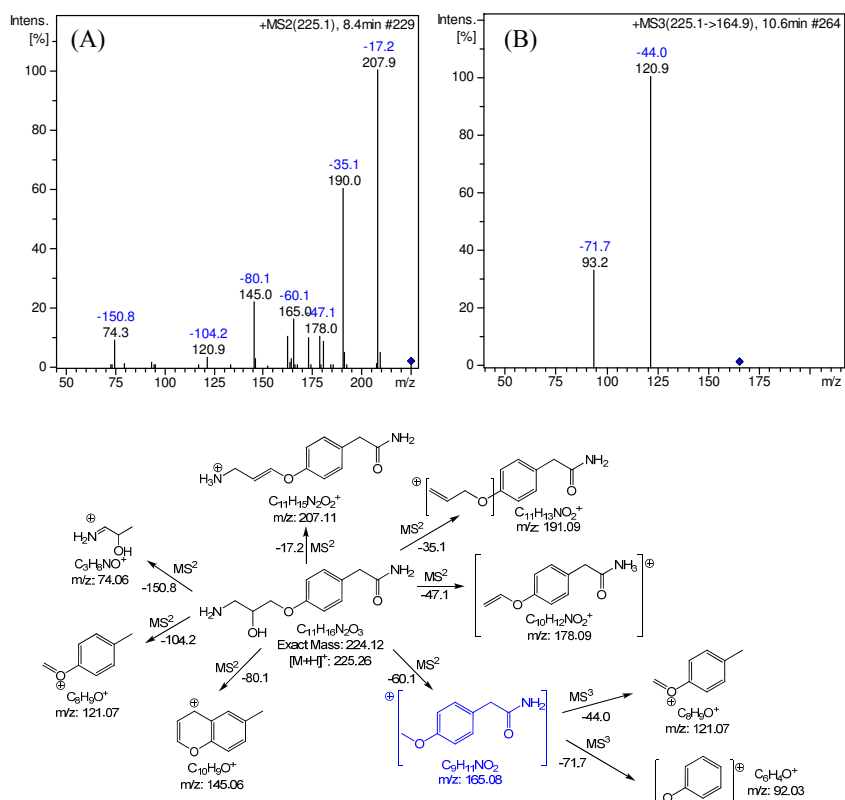


Figure S9. Mass spectra obtained by LC-ESI(+)- MS^2/MS^3 and the fragmentation pattern of DP 225. (A) MS^2 of m/z 225.1 and (B) m/z 225.1 \rightarrow 164.9 MS^3 .

The DP 210 shows a loss of 58 Da or 16 Da from ATE and DP 225, respectively. This study suggests that this DP results from both a loss of NH_3 and $-NH-CH(CH_3)_2$, respectively. When the fragmentation pattern (Figure S10) is examined, the

most intense fragment (m/z 182.0) can be observed, which refers to the loss of 28 Da by the cleavage of C=O moiety.

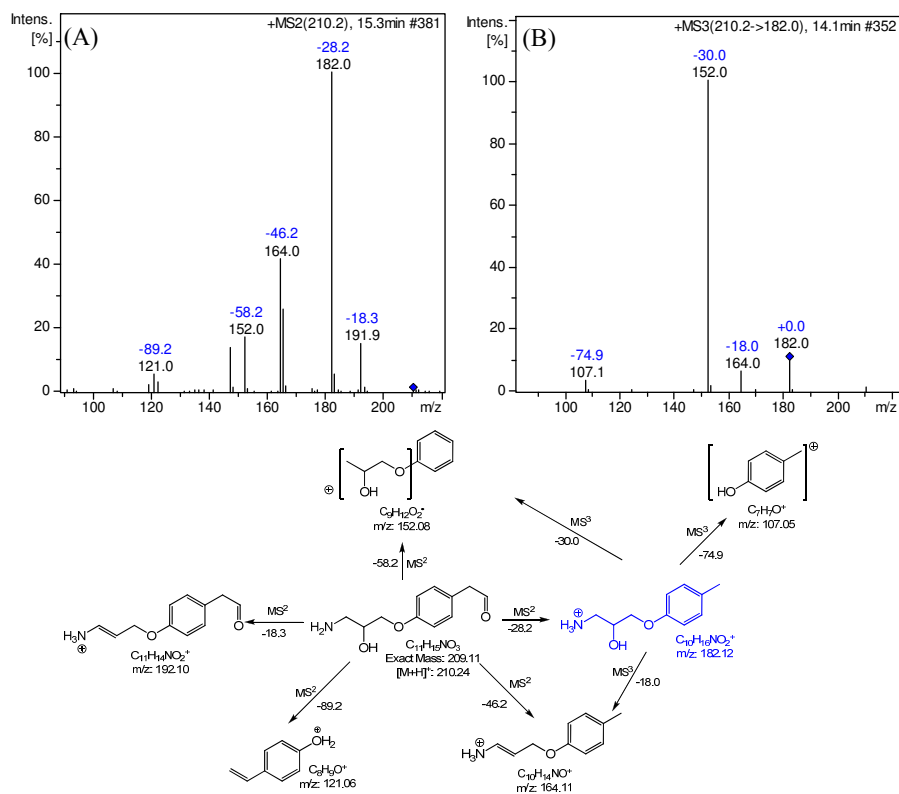


Figure S10. Mass spectra obtained by LC-ESI(+)-MS²/MS³ and the fragmentation pattern of DP 210. (A) MS² of m/z 210.2 and (B) m/z 210.2 → 182.0 MS³.

Since coupled reactions may also occur; it is proposed that the DP 210 forms a dimer DP 419. An analysis of the fragmentation pattern of the DP 419 (Figure S11) shows that the most abundant PI is m/z 209.9, which indicates the loss of exactly 209.1 Da, and other identical PIs that are shown by DP 210.

For a more accurate analysis, the m/z 209.9 was used as the precursor ion and further fragmented, resulting in the same PIs found for DP 210 (m/z : 192.1, 182.0, 164.1 e 152.0), Figure S11 (B).

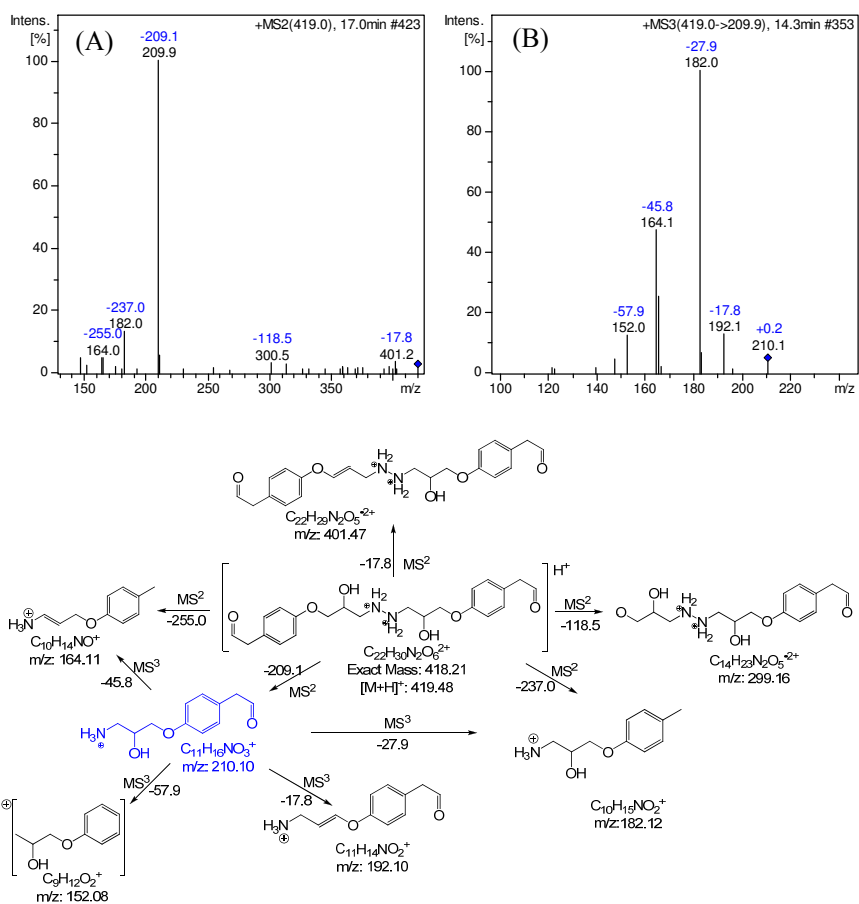


Figure S11. Mass spectra obtained by LC-ESI(+)-MS²/MS³ and the fragmentation pattern of DP 419. (A) MS² of m/z 419.0 and (B) m/z 419.0 → 209.9 MS³.

The DP 208 is 2 Da lower than DP 210 and was identified when the process was carried out with a 1:10 ratio [ATE]:[Fe(VI)]. Thus, a hydrogen abstraction from the amine moiety is proposed.

The fragmentation pattern of the DP 208 can be observed in Figure S12; thus, it is proposed that the hydrogen abstraction should not occur in the hydroxyl moiety because the PI of m/z 189.0 refers to the loss of H₂O. The PI 160.9 was used as precursor ion and further fragmented to confirm the proposed structure.

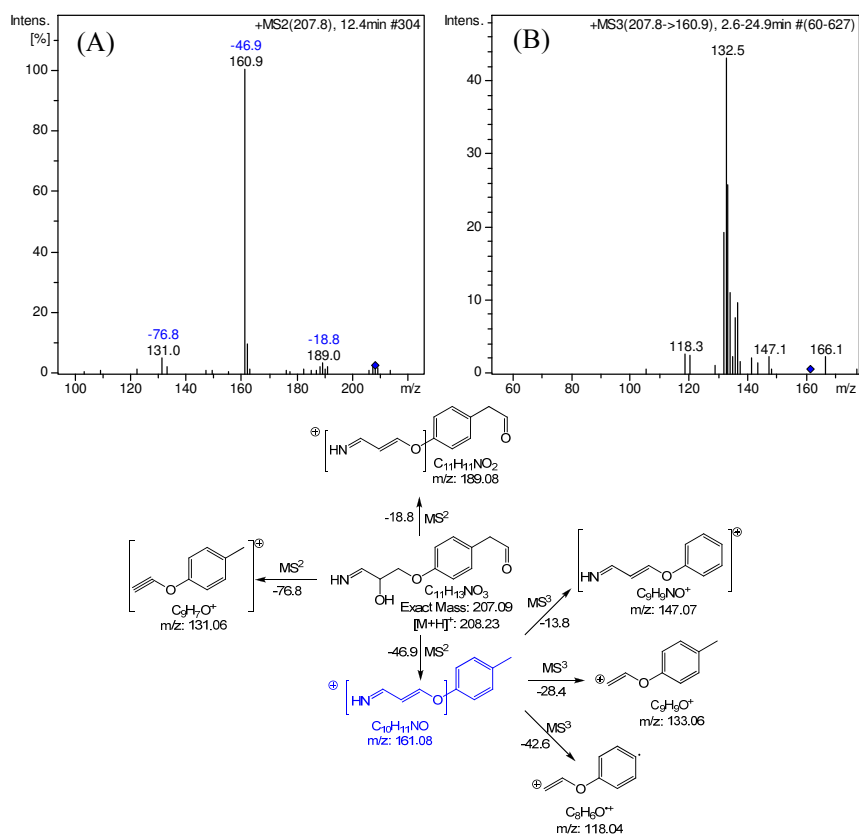


Figure S12. Mass spectra obtained by LC-ESI(+)-MS²/MS³ and the fragmentation pattern of DP 208. (A) MS² of m/z 207.8 and (B) m/z 207.8 → 160.9 MS³.

The DP 194 can also be derived from the DP 210 by the loss of H₂O and protonation of the C=O moiety. The fragmentation pattern (Figure S13) shows the loss of 18 Da (H₂O) and the characteristic ring fragment of m/z 144.9 (Medana et al., 2008; Tay et al., 2011; Radjenović et al., 2008).

Moreover, the most abundant PI (m/z 175.9) was used as precursor ion and further fragmented, resulting in the same PIs of DP 194 (m/z: 131.1, 107.1 and 89.2), with the exception of PI of m/z 159.0 (loss of 17 Da), which is proposed as the loss of a terminal amine moiety (NH₄⁺).

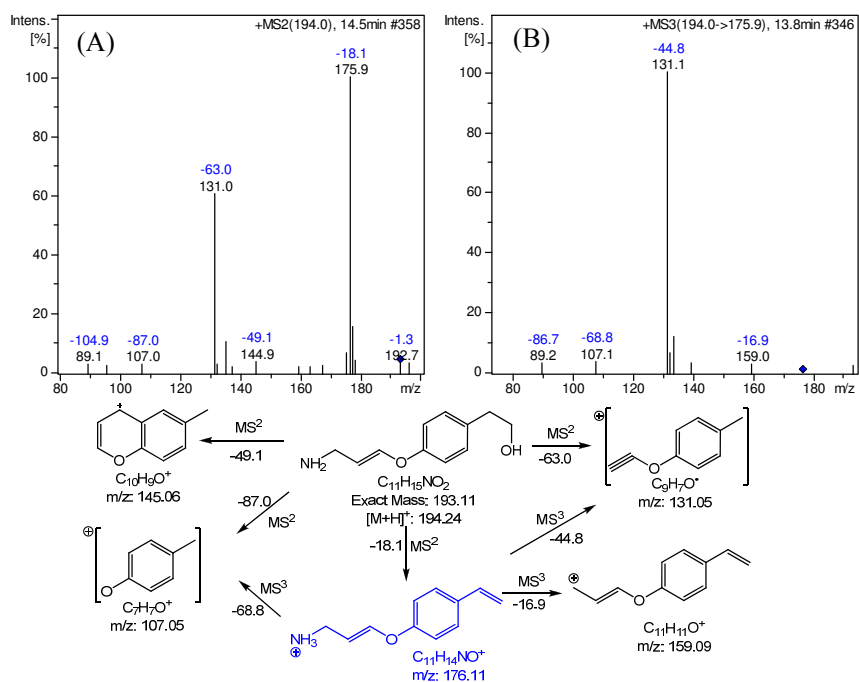


Figure S13. Mass spectra obtained by LC-ESI(+)-MS²/MS³ and the fragmentation pattern of DP 194. (A) MS² of m/z 194.0 and (B) m/z 194.0 → 175.9 MS³.

As in the case of DP 210, a coupled reaction of DP 194 may occur, resulting in a dimer with molecular ion $[M+H]^+$ of m/z 387.0 Da. The main fragment m/z 193.4 can be verified by neutral loss of 193.1 Da, and the fragmentation pattern (Figure S14) shows the same PI as for DP 194.

In a similar way to DP 419, this study proposes dimer formation by radical intermediation ($-NH\cdot$) or, in contrast, by the possible generation of an intermediary through the insertion of oxygen in the terminal amine $NH-O$ (intermediary not found), with a subsequent formation of a dimer, in accordance with the mechanism proposed by Huang et al. (2001).

The PI 193.9 was used as precursor ion and further fragmented (Figure S14 (B)) to confirm that the PI of the recommended dimer has the same fragmentation pattern as that of DP 194. The PI found were the same as for DP 194, which provides evidence that DP 387 is generated by coupled reaction.

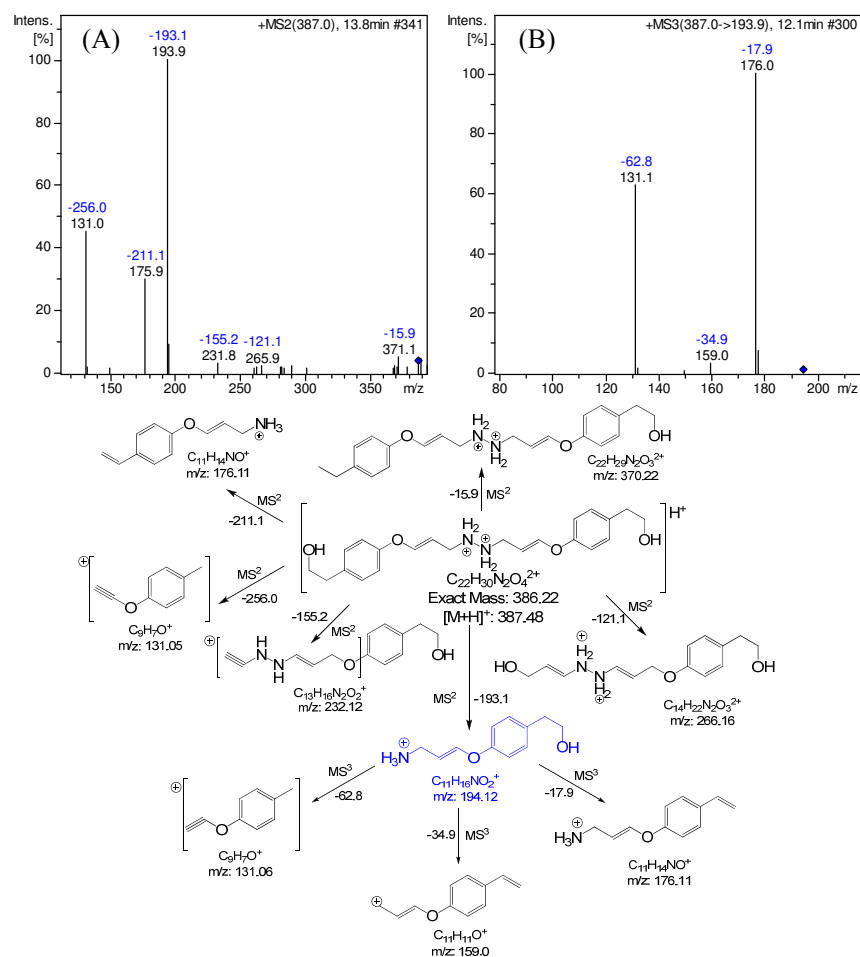


Figure S14. Mass spectra obtained by LC-ESI(+)-MS²/MS³ and the fragmentation pattern of DP 387. (A) MS² of m/z 387.0, (B) m/z 387.0 → 193.9 MS³.

The DP 182 is probably formed by the cleavage of the C=O moiety of the DPs 210 and 208. The fragmentation pattern can be seen in Figure S15 and the constant neutral loss of 18.1 Da (H₂O) characterizes the presence of hydroxyl moiety in the structure, while the loss of 30.1 Da can be referred to the cleavage of the terminal amine moiety (NH₂-CH₂·).

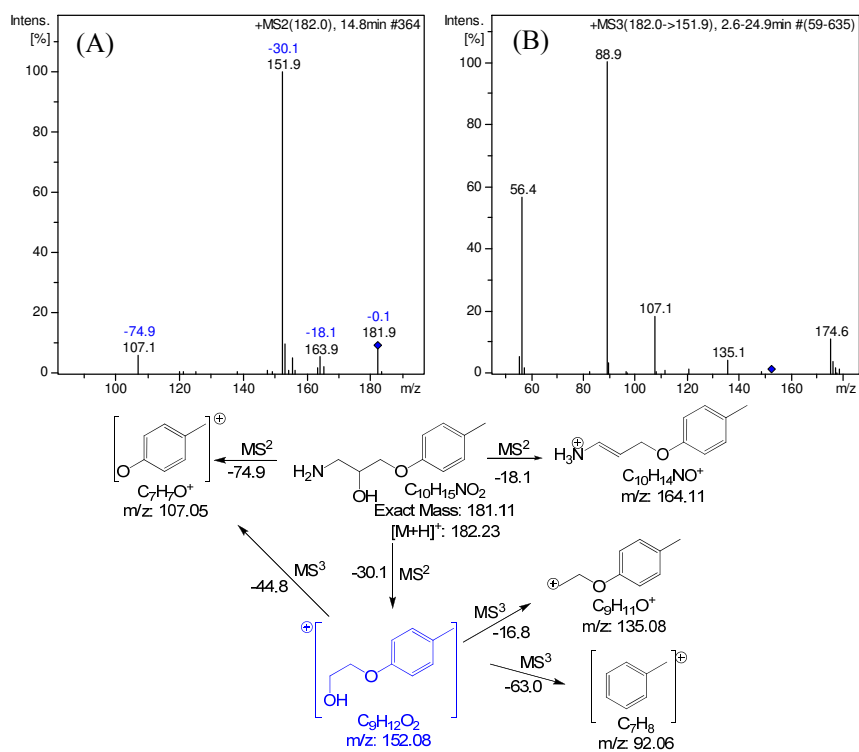


Figure S15. Mass spectra obtained by LC-ESI(+)-MS²/MS³ and fragmentation pattern of DP 182. (A) MS² of m/z 182.0 and (B) m/z 182.0 → 151.9 MS³.

DPs with molecular ion $[M+H]^+$ of m/z 152.2, 134.1 and 131.8 were also identified. DP 152 was identified as a result of the C₆H₅-O bond cleavage (Sirés et al., 2010; Isarain-Chávez et al., 2010), and this DP was found in both of the studied concentration ratios, while the DP 134 (Figure S16) was only identified when the process was carried out using a concentration ratio of 1:1.

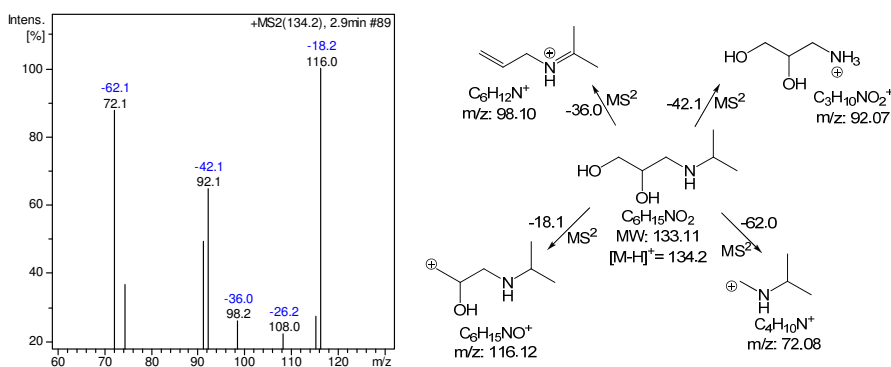


Figure S16. Mass spectra obtained by LC-ESI(+)-MS² and the fragmentation pattern of DP 134.

As can be seen, the DPs 134 and 132 (Figure S17) result from the oxidation of the 2-hydroxy-3-(isopropylamino)propoxy side chain. In addition, DP 132 was only identified in the process carried out with the ratio 1:10 [ATE]:[Fe^{VI}].

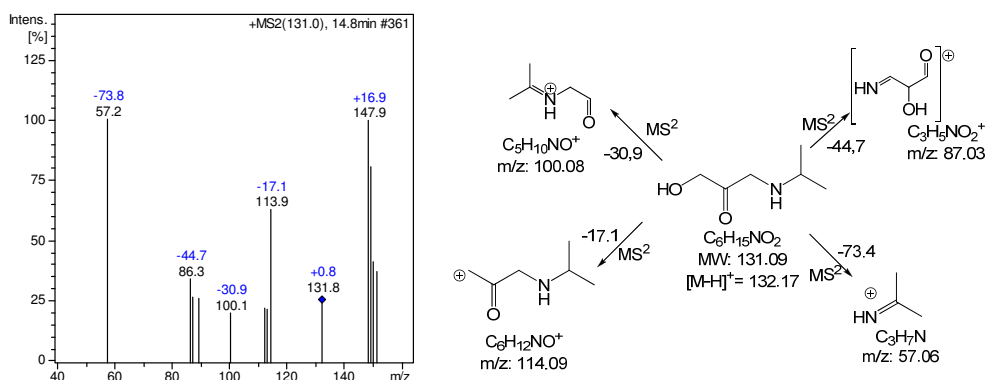


Figure S17. Mass spectra obtained by LC-ESI(+)-MS² and fragmentation pattern of DP 132.

Text S8. Structural elucidation of degradation products from oxidation-coagulation of Metoprolol with Fe(VI)

8 DPs for the oxidation-coagulation of MET with Fe(VI) were identified by means of full scan of LC-MS (Figure S18). These DPs were isolated and further fragmented to MS²/MS³.

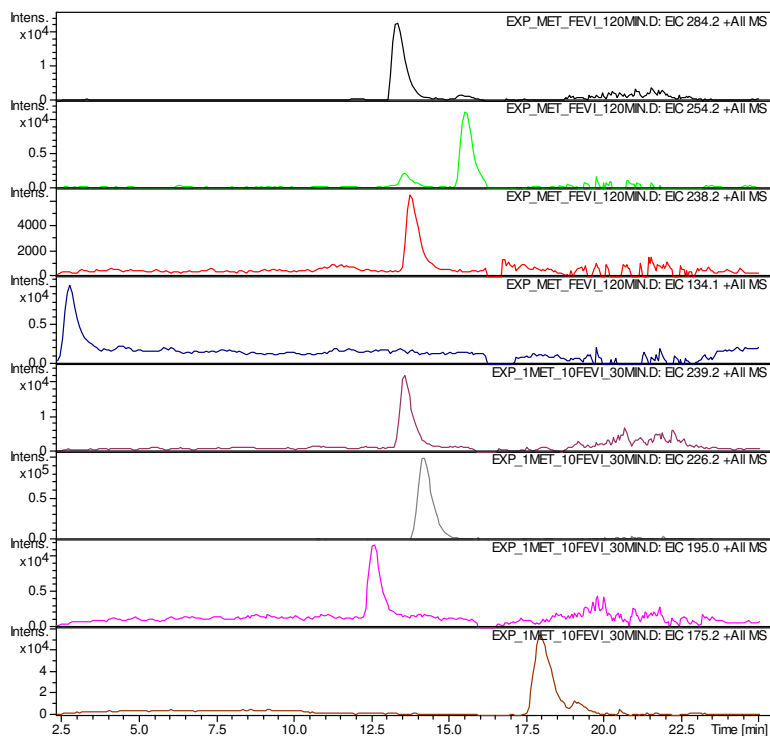


Figure S18. Extracted ion chromatograms of the DP identified by LC-ESI-IT-MS in the oxidation process carried out with the ratio of 1:10 [MET]:[Fe(VI)].

The LC-MS analysis showed only one DP with a molecular ion $[M+H]^+$ higher than MET (DP 284), in both of the concentration ratios studied. By means of the fragmentation pattern displayed in Figure S19, two different position isomers are proposed. In addition, the DP 284 has a similar fragmentation pattern to that obtained from the electrochemical degradation process, as discussed in the literature (Radjenovic et al., 2011).

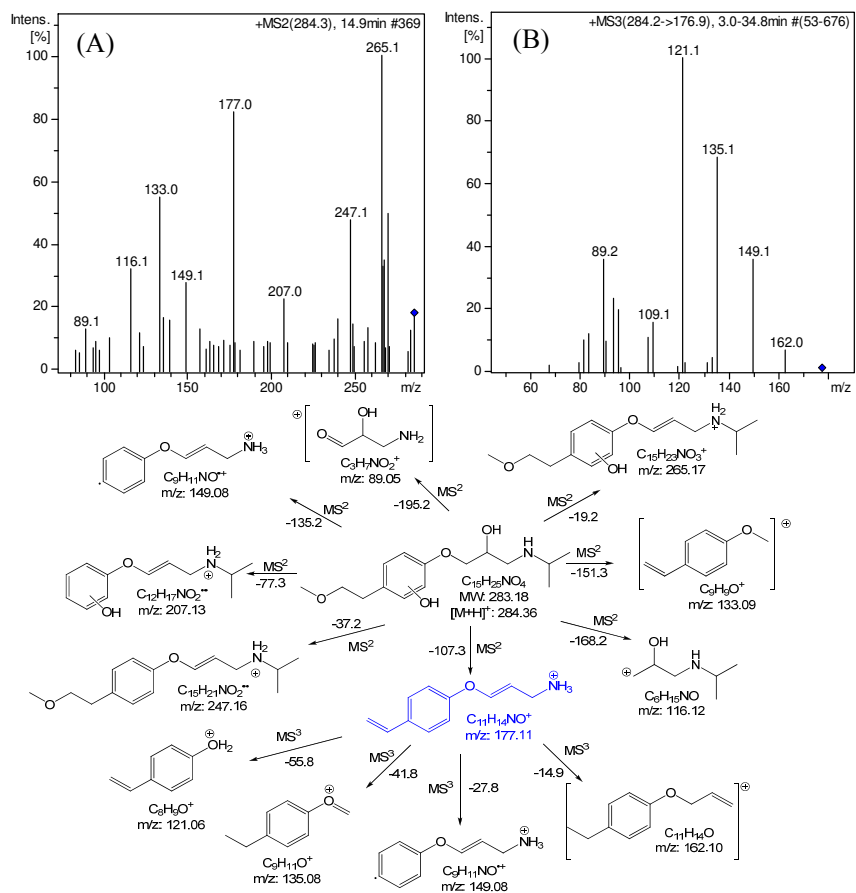


Figure S19. Mass spectra obtained by LC-ESI(+)-MS² and fragmentation pattern of DP 284 found in the oxidation-coagulation carried out by 1:1 concentration ratio [MET]:[Fe(VI)].

The position isomer DP 284, found in the process carried out in 1:10 ratio [MET]:[Fe(VI)], has the same characteristic fragments (Figure S20), but the hydroxylation occurred in the secondary amine moiety, since the PI characteristics of the 2-hydroxy-3-(isopropylamino)propoxy (m/z 116 and 74.2) side chain were not found.

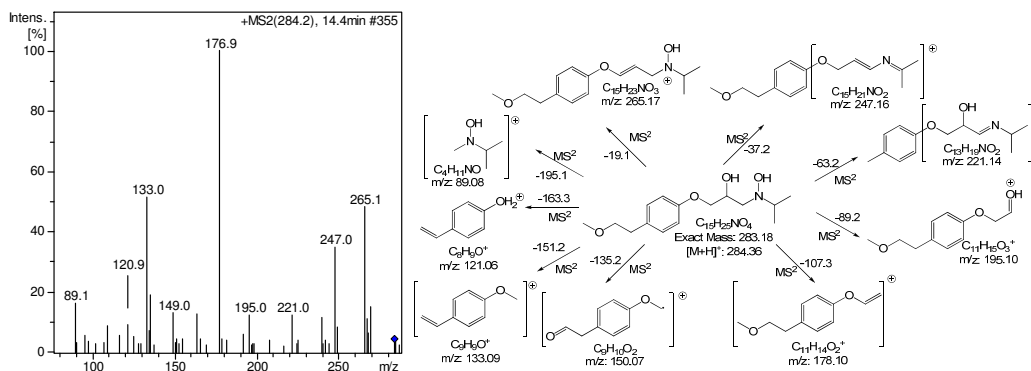


Figure S20. Mass spectra obtained by LC-ESI(+)-MS² and fragmentation pattern of DP 284 found in the oxidation-coagulation carried out by concentration 1:10 concentration ratio [MET]:[Fe(VI)].

DP 254 has similar fragmentation pattern (Figure S21) to that found in other degradation processes based on the generation of HO· radicals (Slegers et al., 2006; Benner and Ternes, 2009b; Radjenovic et al., 2011). The loss of CH₃OH may be due to the action of free radicals such as hydroxyl, or by oxidation with ferrate ion, as the terminal ether favors the reaction of ferrate to this moiety.

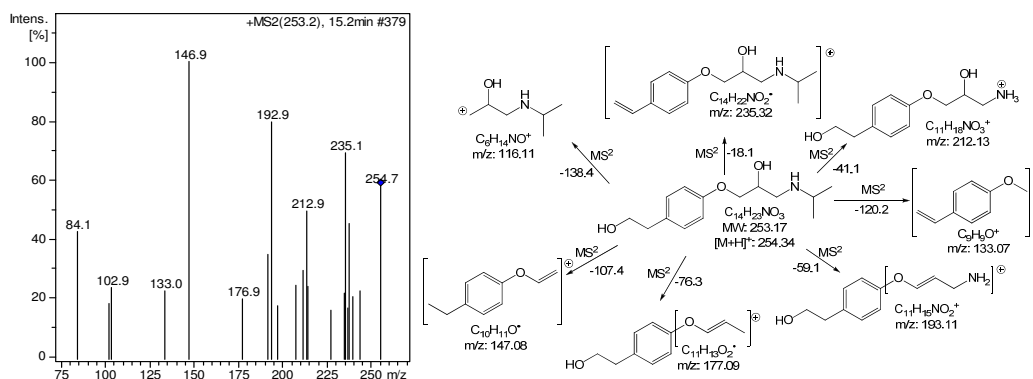


Figure S21. Mass spectra obtained by LC-ESI(+)-MS² and fragmentation pattern of DP 254.

Another DP identified in this study, and also in the HO· based degradation process, was DP 240 (Benner and Ternes, 2009b; Radjenovic et al., 2011; Song et al., 2008). This DP can arise from the DP 254 by the elimination of CH₃=O in a similar way to the formation of DP 254.

The fragmentation pattern of the DP 240 (Figure S22) shows clearly that the 2-hydroxy-3-(isopropylamino)propoxy side chain remained intact. The PI 219.9 is characterized by a loss of water, while the PI 197.9 arises from the loss of isopropyl moiety.

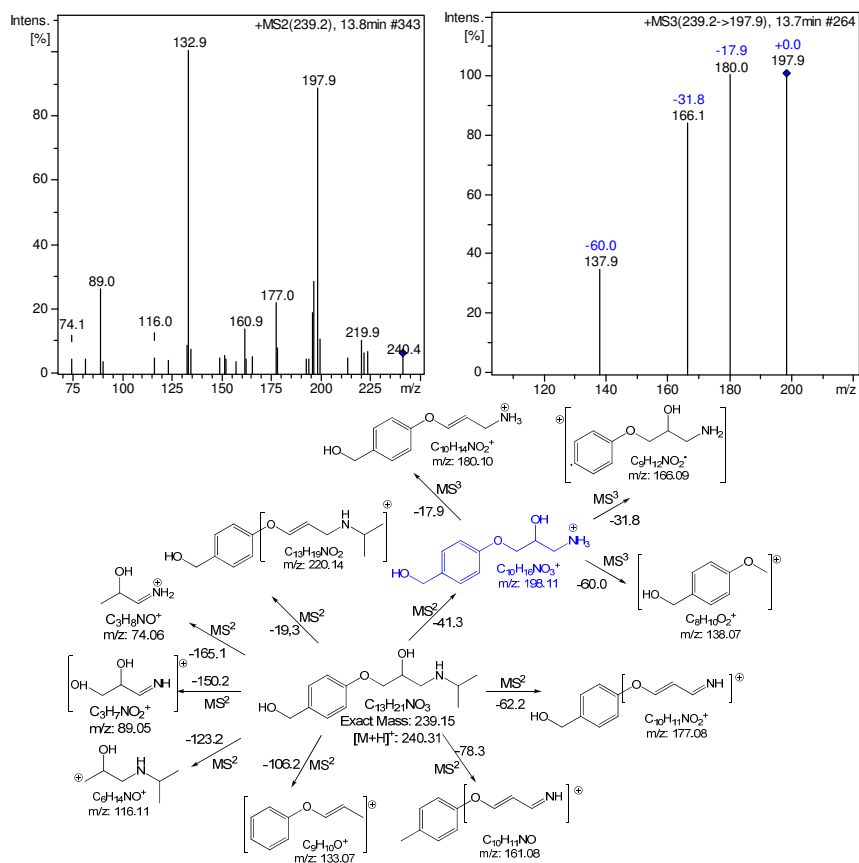


Figure S22. Mass spectra obtained by LC-ESI(+)-MS² and the fragmentation pattern of DP 240.

DP 238 was found as a result of the process carried out in 1:1ratio [MET]:[Fe^{VI}]. This DP has the same fragmentation pattern (Figure S23) as the intermediary found in the degradation process by γ -radiolysis (Slegers et al., 2006). A hydrogen abstraction of DP 254 is put forward involving free radicals such as hydroxyl, or even, the partial radical character of ferrate ($\text{Fe}^{\text{VI}}=\text{O} \rightleftharpoons \text{Fe}^{\text{V}}-\text{O}\cdot$).

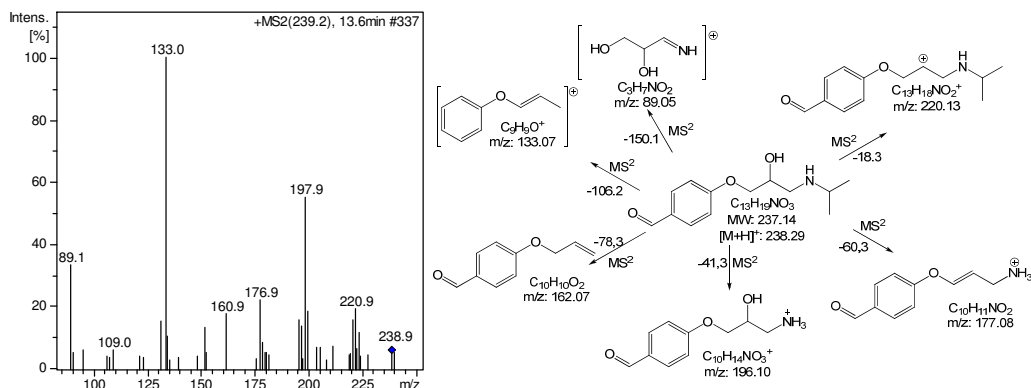


Figure S23. Mass spectra obtained by LC-ESI(+)-MS² and the fragmentation pattern of DP 238.

The DP 226 provides evidence that the reaction occurred in the secondary amine moiety by means of N-dealkylation. The structure of this intermediary was confirmed by the MS fragmentation pattern (Figure S24) and characterized by the elimination of the isopropyl moiety.

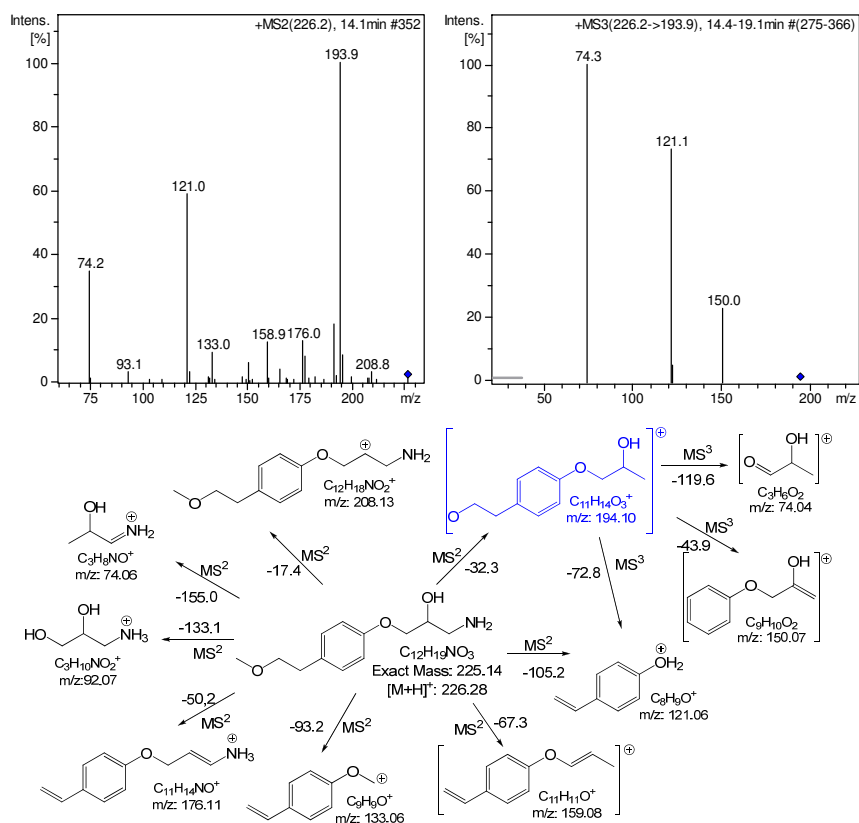


Figure S24. Mass spectra obtained by LC-ESI(+)-MS² and fragmentation pattern of DP 226.

Another DP found in both the studied concentration ratios was the molecular ion $[M+H]^+$ m/z 196. This DP can be generated by the degradation of DP 226 through the elimination of CH_3OH . According to the fragmentation pattern (Figure S25), it is characterized by the PIs 135.0 and 121.0, which are linked to the elimination of $CH(OH)CH_2-NH_2$ and $CH_2-CH(OH)CH_2-NH_2$ from the side chain, respectively.

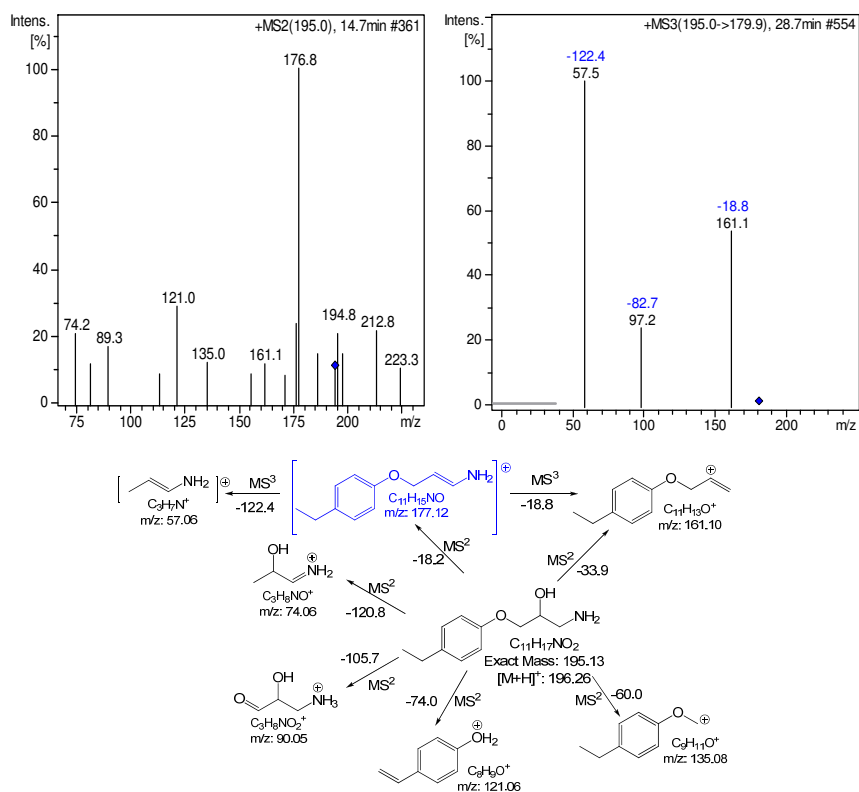


Figure S25. Mass spectra obtained by LC-ESI(+)-MS² and the fragmentation pattern of DP 196.

DP 175 (Figure S26) was identified by the ratio 1:10 [MET]:[Fe^{VI}], and, as can be observed in Figure S42, the relative area increase during the process. Therefore, it can be inferred that this DP results from DP 226, since its area decreases over a period of time. Thus, it is suggested that DP 175 can be formed by the elimination of CH_3OH from the ether chain.

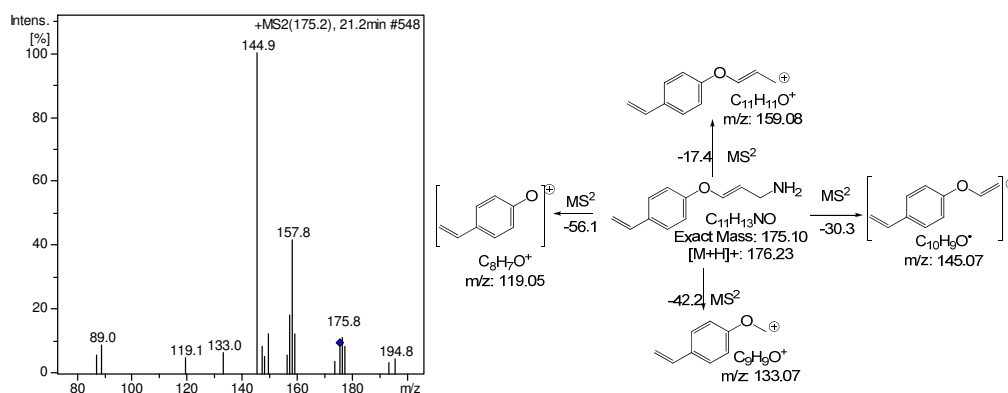


Figure S26. Mass spectra obtained by LC-ESI(+)-MS² and fragmentation pattern of DP 175.

Furthermore, DP 134 (m/z 134.2), which is a characteristic of the 2-hydroxy-3-(isopropylamino)propoxy side chain (Figure S27), was found, and is possibly formed by the cleavage of the C₆H₅-O bond.

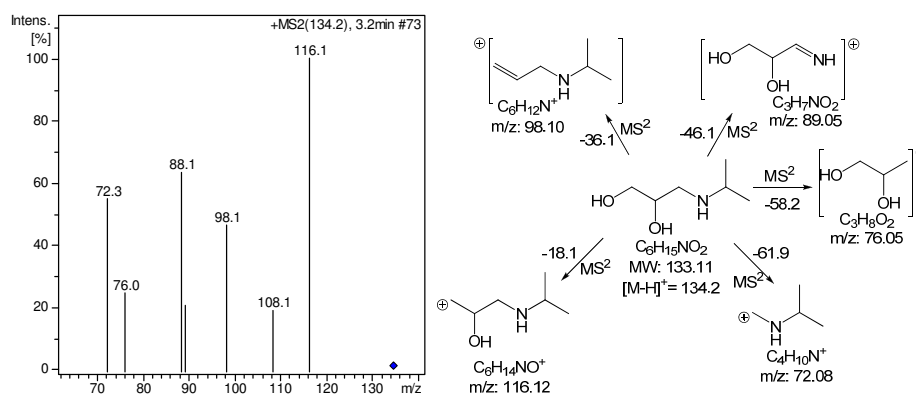


Figure S27. Mass spectra obtained by LC-ESI(+)-MS² and the fragmentation pattern of DP 134.

Text S9. Structural elucidation of degradation products through the oxidation-coagulation of propranolol with Fe(VI)

14 DPs were identified for PRO, with hydroxylation and decarboxylation being put forward as the main degradation pathways (Figure S28).

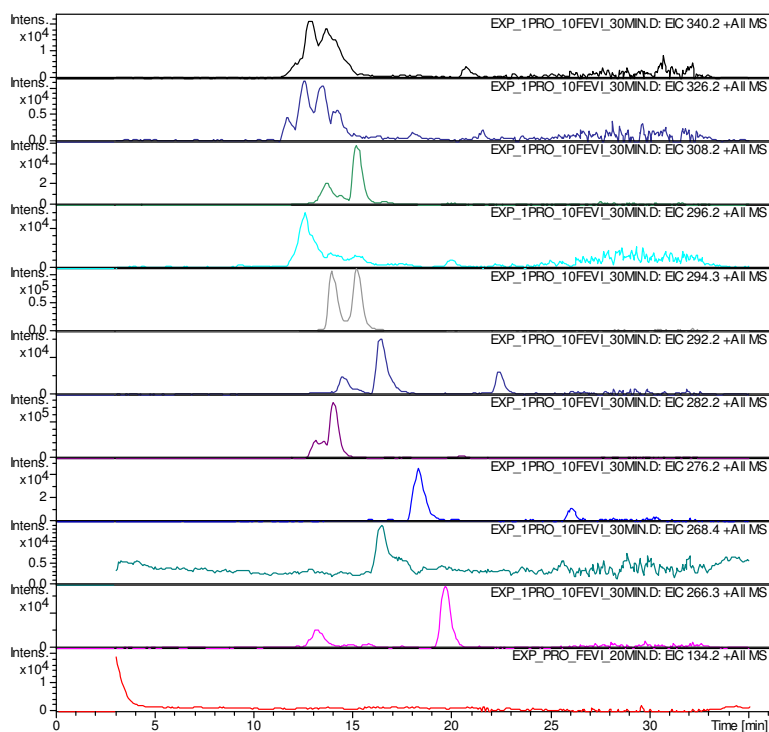


Figure S28. Extracted ion chromatograms of the DP identified by LC-ESI-IT-MS in the oxidation process carried out with the ratio of 1:10 [PRO]:[Fe(VI)].

DP 276 shows 16 Da higher than PRO, indicating a monohydroxylation on the naphthalene moiety (Figure S29). This DP was also referred to as an intermediary in many degradation processes based on hydroxyl radicals (Chen et al., 2011; Marco-Urrea et al., 2009; Song et al., 2008; Yang et al., 2010).

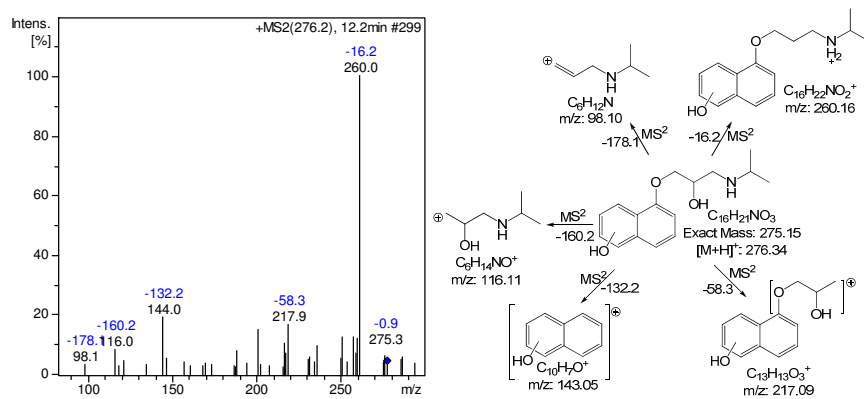


Figure S29. Mass spectra obtained by LC-ESI(+)-MS² and the fragmentation pattern of DP 276.

Further DPs are generated by new hydroxylation, and the ring opening of the naphthalene group is proposed as well. DP 292 (Figure S30) shows 32 Da higher than PRO and 16 Da higher than DP 276. This DP was only identified in the process carried out in the ratio of 1:10 [PRO]:[Fe(VI)], with two peaks with different Rt.

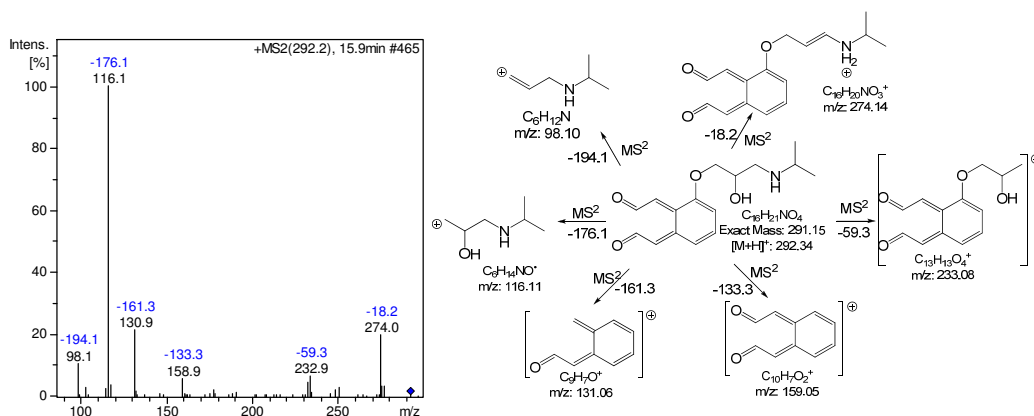


Figure S30. Mass spectra obtained by LC-ESI(+)-MS² and the fragmentation pattern of DP 292.

When the fragmentation pattern of both peaks was analyzed, no difference was found, which indicates the existence of isomers. It is suggested that hydroxylation may have occurred in different positions on the naphthalene moiety, or aromatic ring opening. This is indicated by the PI characteristic of the 2-hydroxy-3-(isopropylamino)propoxy side chain.

Additional indicators of the naphthalene moiety ring opening are DP 294 and 296. The fragmentation pattern of DP 294 can be seen in Figure S31. Two different peaks with Rt 13.9 and 15.2 min of DP 294 were identified, but no difference was found in the fragmentation pattern, which provides evidence of the formation of isomers.

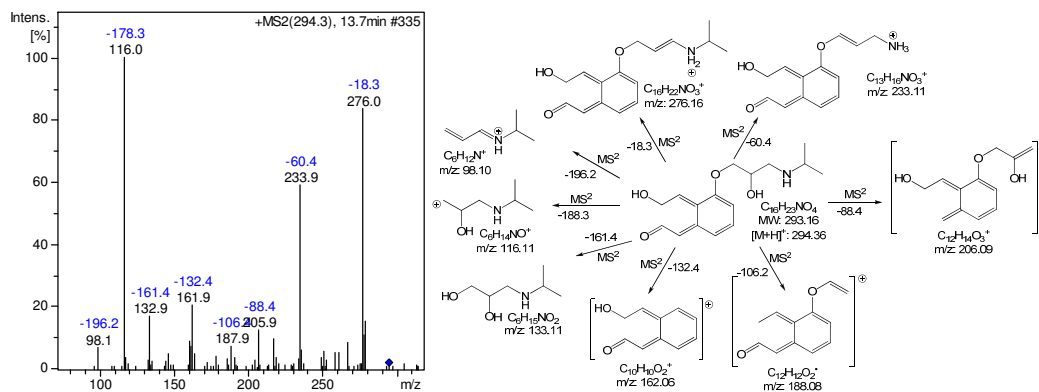


Figure S31. Mass spectra obtained by LC-ESI(+)-MS² and fragmentation pattern of DP 294.

DP 296 is 4 Da higher than DP 292 and 2 Da higher than DP 294, and the fragmentation pattern of DP 296 (Figure S32) confirms the ring opening.

As a means of improving the elucidation of the proposed structure, the PI 278.0 was used as precursor ion and further fragmented to MS³ (Figure S32 (B)), confirming the proposed structure.

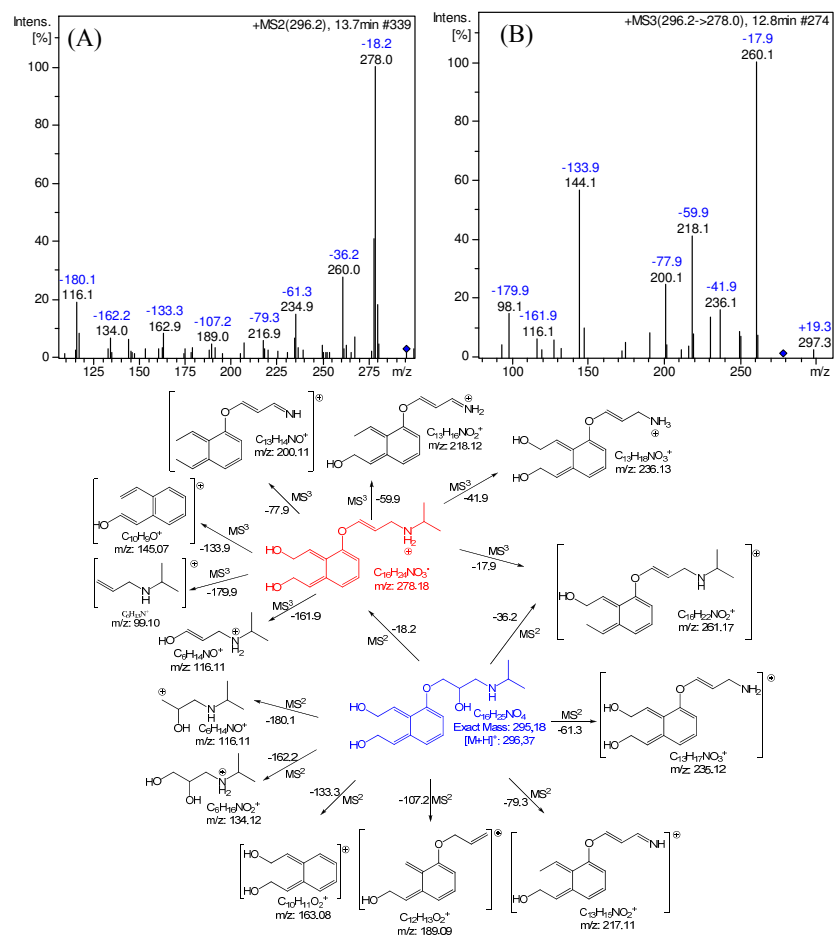


Figure S32. Mass spectra obtained by LC-ESI(+)-MS²/MS³ and the fragmentation pattern of DP 296. (A) MS² of m/z 296.2, (B) m/z 296.2 → 278.0 MS³.

DP 308 shows a new hydroxylation on PRO or on the DP 292. The fragmentation pattern indicates that the hydroxylation occurred on the aromatic ring (Figure S33), which is confirmed by the characteristic fragments of the side chain.

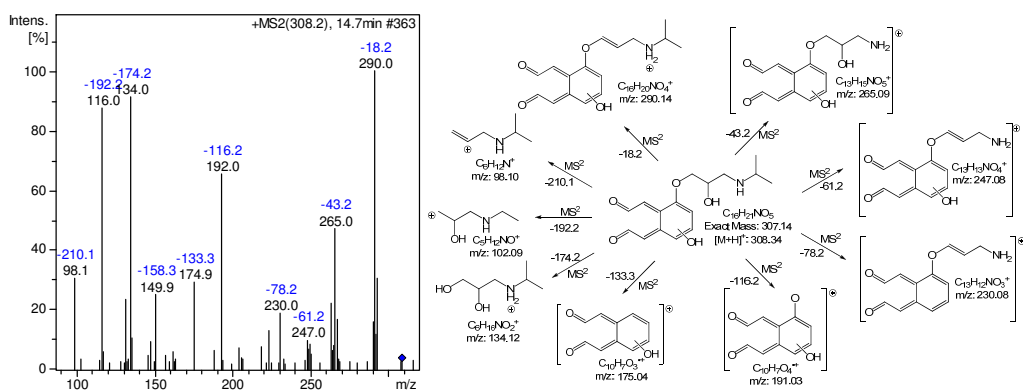


Figure S33. Mass spectra obtained by LC-ESI(+)-MS² and the fragmentation pattern of DP 308.

DP 310 (Figure S34) was only identified in the process carried out in 1:1 ratio [PRO]:[Fe(VI)], suggesting that the ring opening process occurs even in less oxidant conditions.

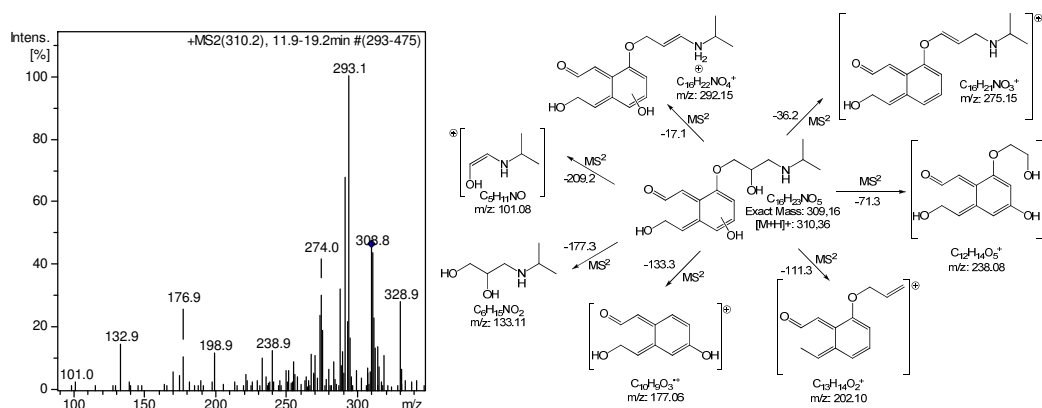


Figure S34. Mass spectra obtained by LC-ESI(+)-MS² and the fragmentation pattern of DP 310.

A further hydroxylation process occurs and this forms the DPs 326 and 340. DP 326 was identified in both the studied ratios, while DP 340 was only identified in 1:10 ratio [PRO]:[Fe^{VI}]. It is suggested that DP 326 should be generated by hydroxylation of the DP 308 in the aromatic ring (Figure S35).

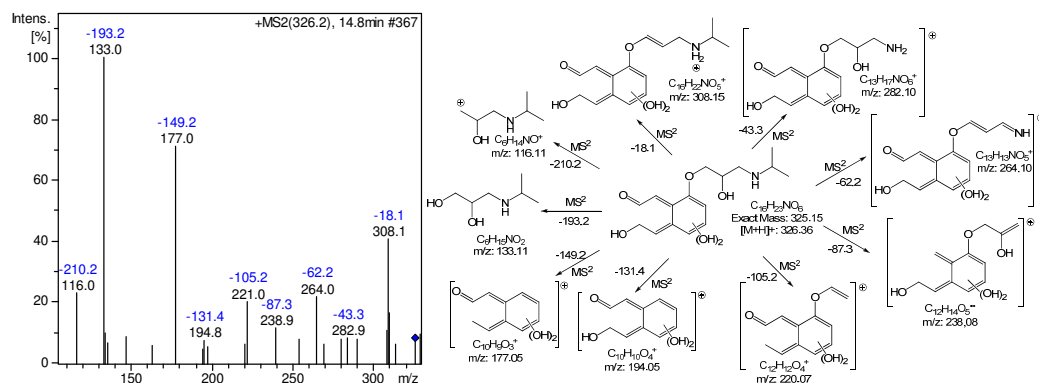


Figure S35. Mass spectra obtained by LC-ESI(+)-MS² and the fragmentation pattern of DP 326.

For DP 340, a hydroxylation on the secondary amine moiety is suggested to form a hydroxylamine. The fragmentation pattern (Figure S36) shows that both aromatic rings were opened by the degradation process.

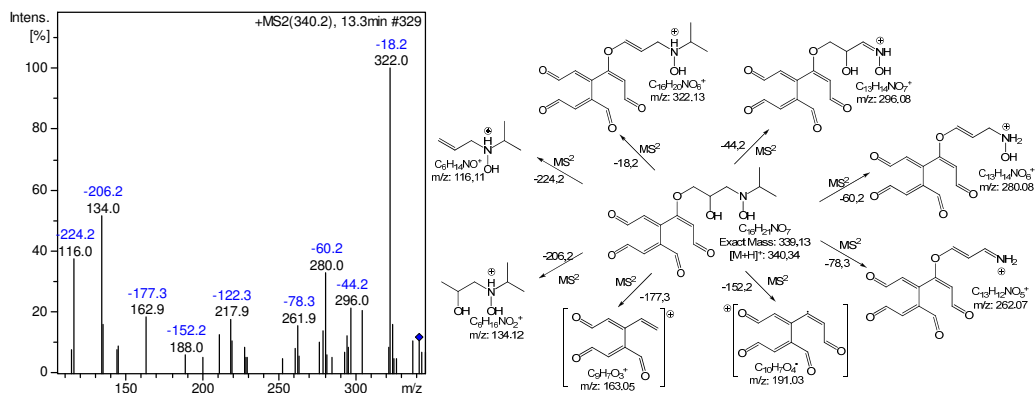


Figure S36. Mass spectra obtained by LC-ESI(+)-MS² and the fragmentation pattern of DP 340.

The fragmentation pattern of DP 282 (Figure S37) is characterized by the loss of 133.3 Da from the 2-hydroxy-3-(isopropylamino)propoxy side chain, indicating that decarboxylation has occurred on the naphthalene moiety.

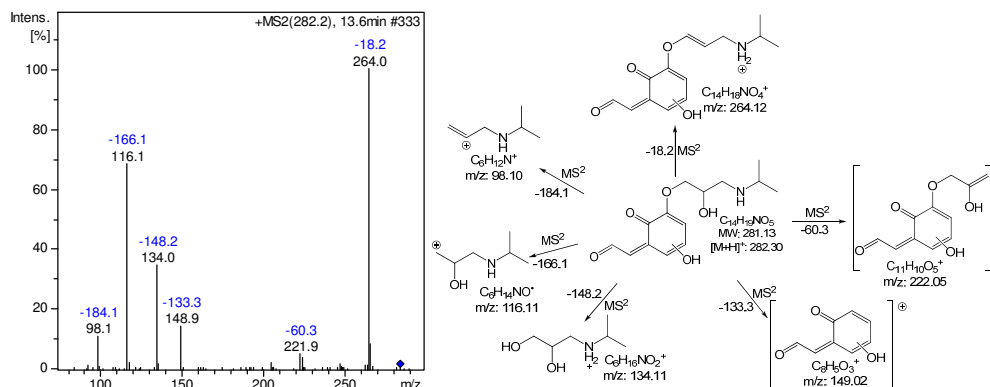


Figure S37. Mass spectra obtained by LC-ESI(+)-MS² and the fragmentation pattern of DP 282.

By means of the DP 268 fragmentation pattern (Figure S38), it is possible to see the PI 116 and 133 characteristics of the side chain, while PI 249.0 and 206.9 result from the loss of water and isopropyl, respectively.

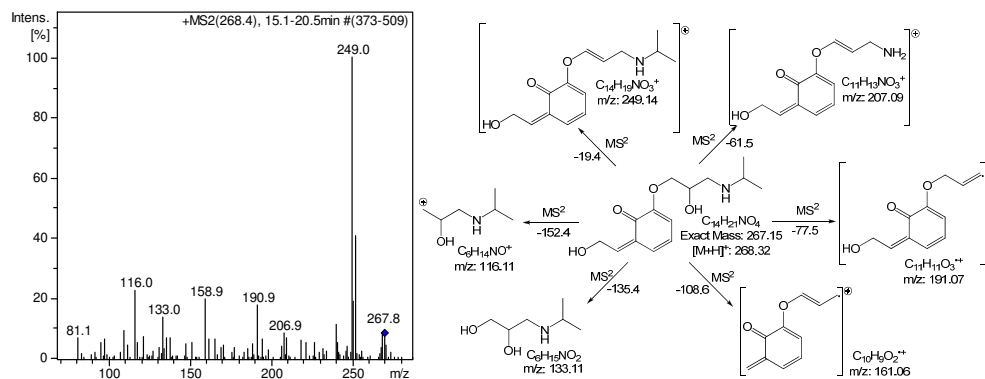


Figure S38. Mass spectra obtained by LC-ESI(+)-MS² and the fragmentation pattern of DP 268.

In the same way as for DP 268, DP 266 (Figure S39) results from decarboxylation of DP 294 or DP 292.

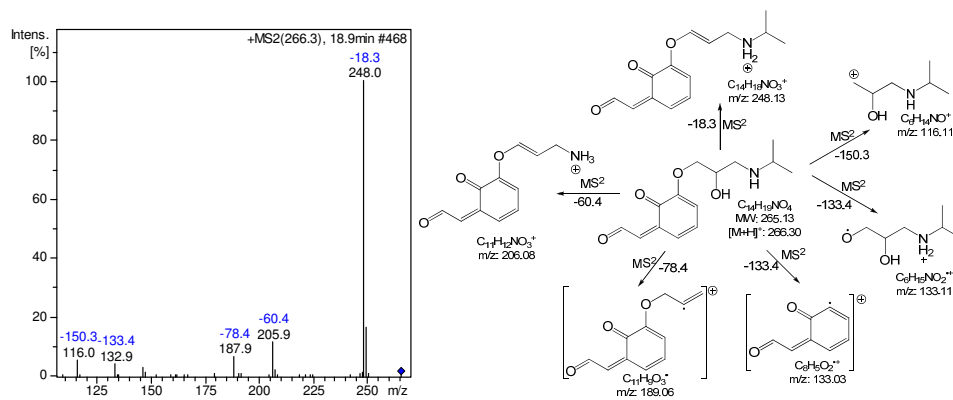


Figure S39. Mass spectra obtained by LC-ESI(+)-MS² and the fragmentation pattern of DP 266.

3 DPs were also identified that resulted from the side chain lateral 2-hydroxy-3-(isopropylamino)propoxy oxidation, DPs 134, 132 and 116 (Figure S40).

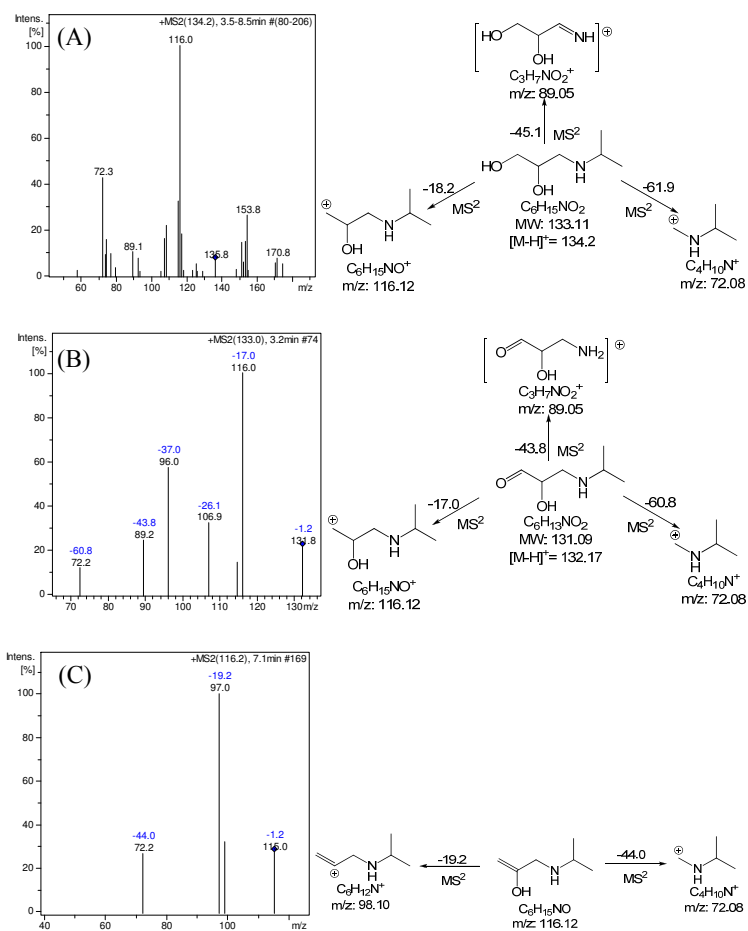


Figure S40. Mass spectra's obtained by LC-ESI(+)-MS² and fragmentation patterns of (A) DP 134, (B) DP 132 and (C) DP 116.

Text S10. Evolution of Degradation Products during the oxidation-coagulation process by Fe(VI).

The evolution of the relative area of the DPs resulting from the ATE, MET and PRO by oxidation-coagulation with Fe(VI), can be seen in Figures S41–S44, respectively.

As was observed in the case of ATE (Figure S38), the DPs can be regarded as persistent, since once they have been formed, they are not further degraded.

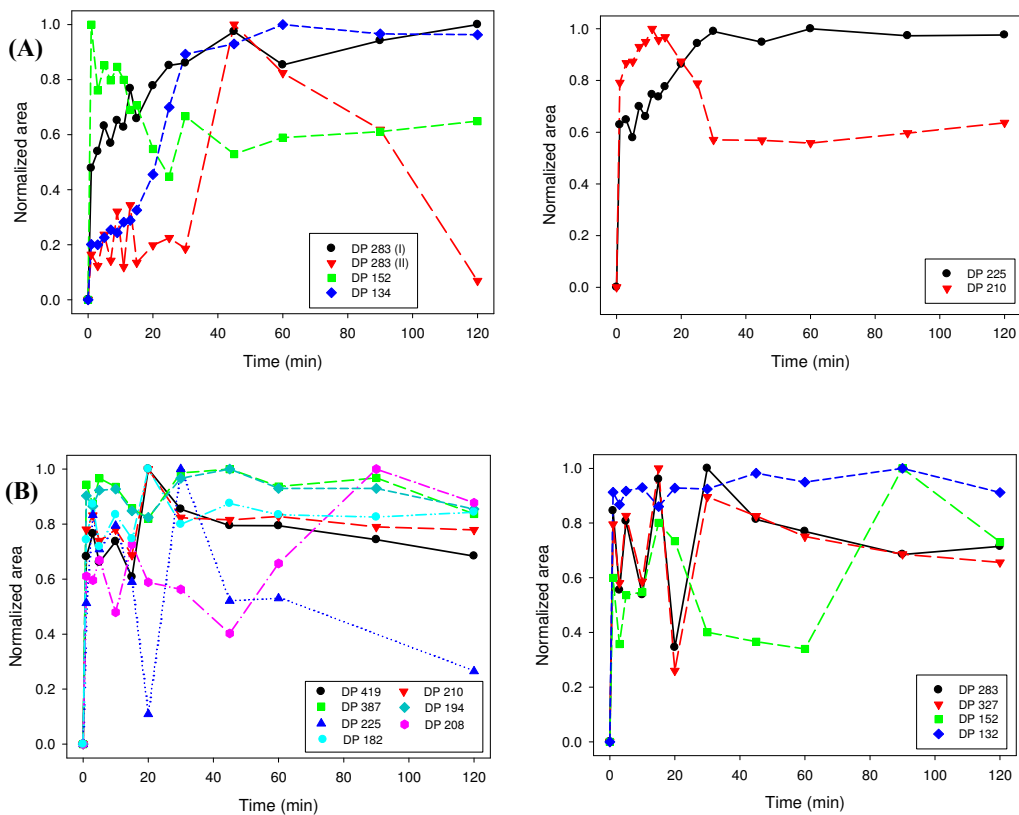


Figure S41. Time course of the normalized peak area of extracted degradation products during the oxidation coagulation of Atenolol by Fe(VI). (A) [ATE]:[Fe(VI)] 1:1 mol L⁻¹:mol L⁻¹, (B) [ATE]:[Fe(VI)] 1:10 mol L⁻¹:mol L⁻¹.

The relative area profiles of the MET DPs can be seen in Figure S42, and as observed they are also persistent, except for DP 226 which is further transformed.

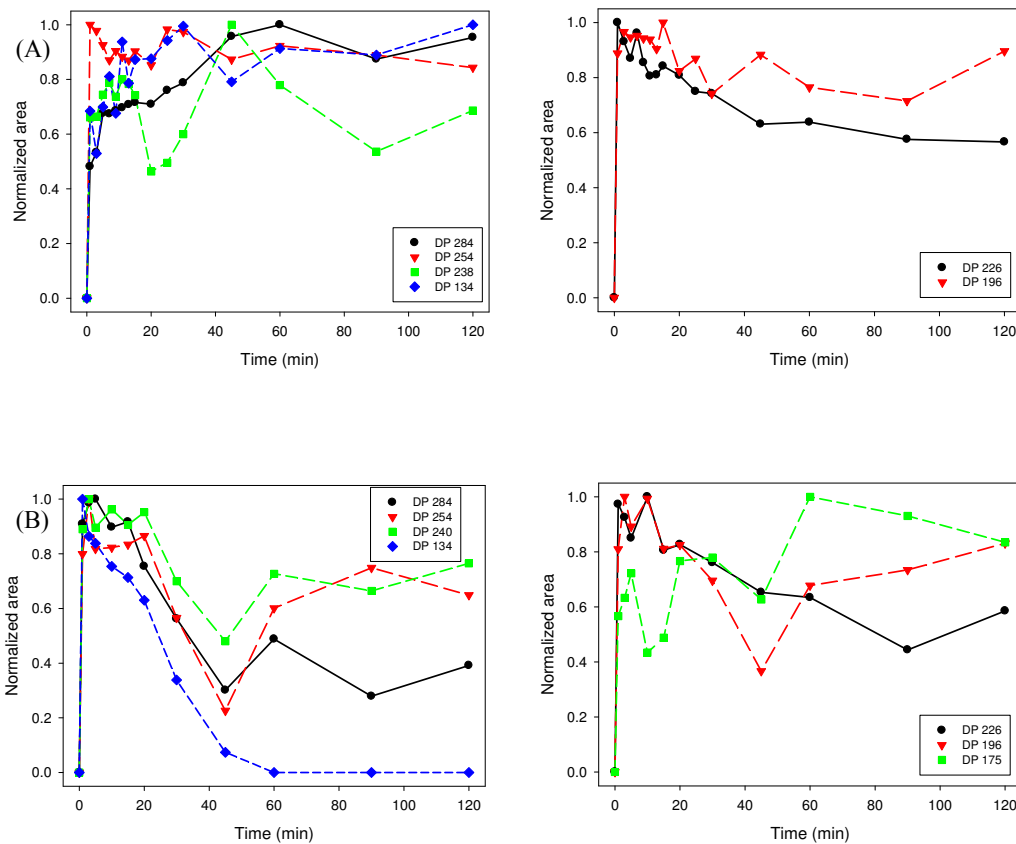


Figure S42. Time course of the normalized peak area of extracted degradation products during the oxidation coagulation of Metoprolol by Fe(VI). (A) [MET]:[Fe(VI)] 1:1 mol L⁻¹:mol L⁻¹, (B) [MET]:[Fe(VI)] 1:10 mol L⁻¹:mol L⁻¹.

In the same way as for ATE and MET, the DPs of PRO (Figure S43) also prove to be persistent in the process carried out in 1:1 ratio [PRO]:[Fe(VI)], while in 1:10 ratio [PRO]:[Fe(VI)], a further degradation was observed. This clearly shows that the reduction Fe(VI) → Fe(III) is limiting the process.

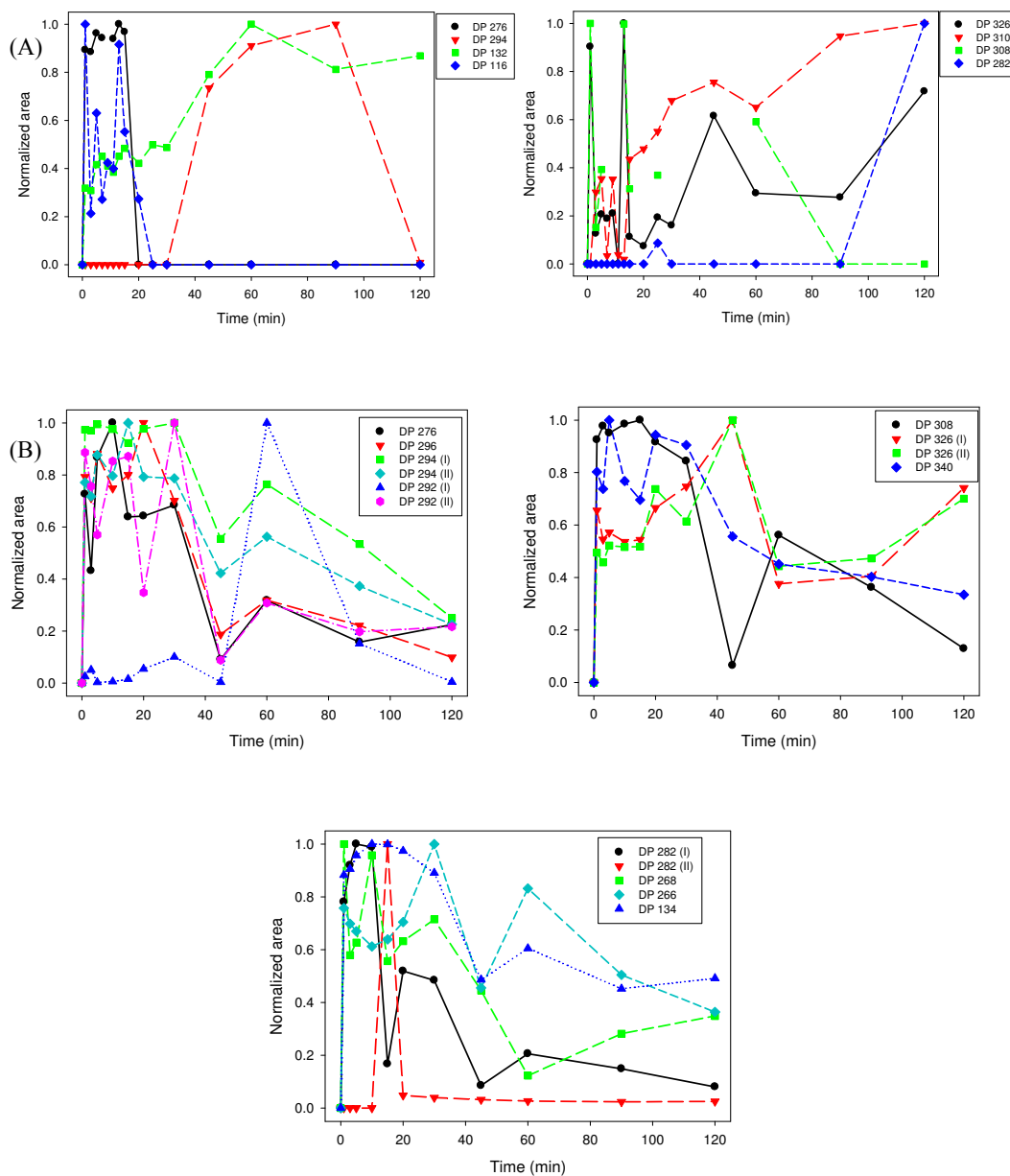


Figure S43. Time course of the normalized peak area of extracted degradation products during the oxidation coagulation of Propranolol by Fe(VI). (A) [PRO]:[Fe(VI)] 1:1 mol L⁻¹:mol L⁻¹, (B) [PRO]:[Fe(VI)] 1:10 mol L⁻¹:mol L⁻¹.

Text S11. Evolution of the pH during the oxidation-coagulation process by Fe(VI).

The evolution of the pH can be seen in Figure S44. The increase in the pH might be due to the aqueous decomposition of Fe(VI) → Fe(III) (Jiang and Lloyd, 2002). The

pH decrease after the initial evolution and during the process 1:1 $[\beta\text{-blocker}]:[\text{Fe}^{\text{VI}}]$ (Figure S41 (A)) may be due to degradation and the formation of NO_2 .

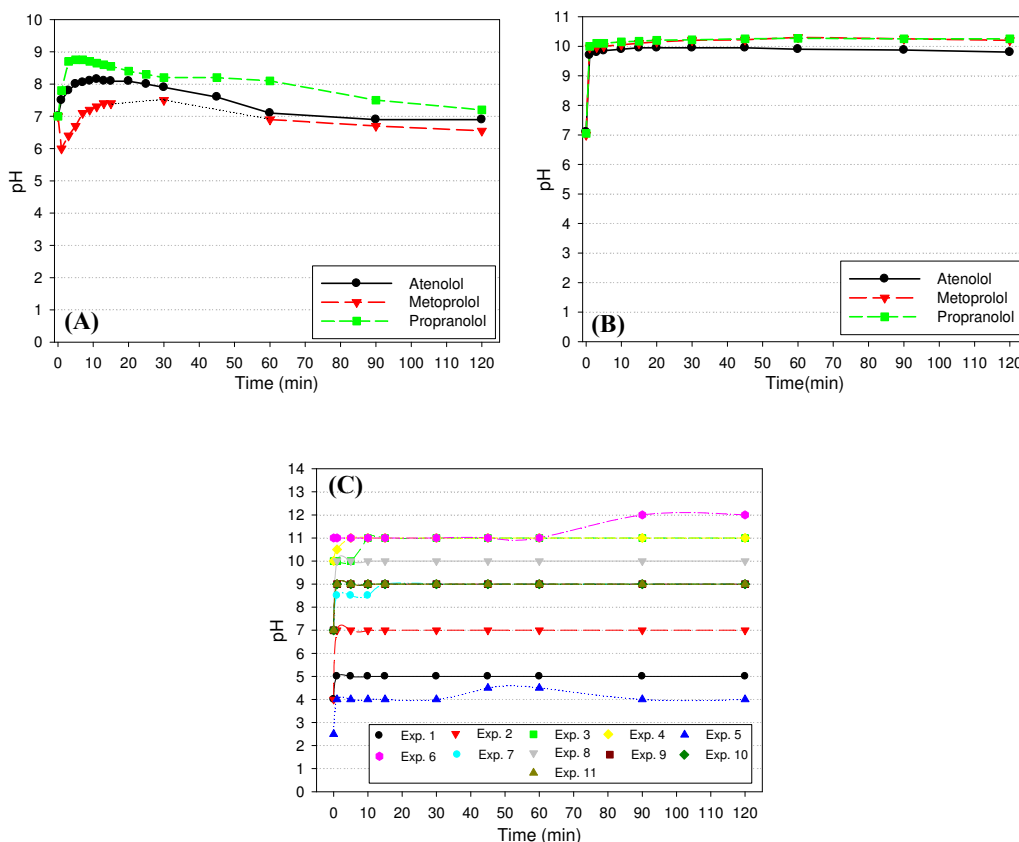


Figure S44. Evolution of the pH during the oxidation-coagulation process of Atenolol, Metoprolol and Propranolol by Fe(VI). (A) $[\beta\text{-blocker}]:[\text{Fe}(\text{VI})]$ 1:1 mol L⁻¹:mol L⁻¹; (B) $[\beta\text{-blocker}]:[\text{Fe}(\text{VI})]$ 1:10 mol L⁻¹:mol L⁻¹; (C) Hospital wastewater.

References

- Benner J, Ternes TA. Ozonation of propranolol: formation of oxidation products. Environ. Sci. Technol. 2009a;43:5086–93.
- Benner J, Ternes TA.. Ozonation of metoprolol: elucidation of oxidation pathways and major oxidation products. Environ. Sci. Technol. 2009b;43:5472–80.

- Chen Y, Liu Z, Wang Z, Xue M, Zhu X, Tao T. Photodegradation of propranolol by Fe(III)-citrate complexes: kinetics, mechanism and effect of environmental media. *J. Hazard. Mater.* 2011;194:202–8.
- Huang H, Sommerfeld D, Dunn BC, Lloyd CR, Eyring EM. Ferrate (VI) oxidation of aniline. *J. Chem. Soc. - Dalton Trans.* 2001:1301–5.
- Isarain-Chávez E, Arias C, Cabot PL, Centellas F, Rodríguez RM, Garrido JA, Brillas E. Mineralization of the drug β -blocker atenolol by electro-Fenton and photoelectro-Fenton using an air-diffusion cathode for H_2O_2 electrogeneration combined with a carbon-felt cathode for Fe^{2+} . *Appl. Catal. B: Environ.* 2010;96:361–9.
- Jiang J-Q, Lloyd B. Progress in the development and use of ferrate(VI) salt as an oxidant and coagulant for water and wastewater treatment. *Wat. Res.* 2002;36:1397–408.
- Li C, Li XZ, Graham N. A study of the preparation and reactivity of potassium ferrate. *Chemosphere* 2005;61:537–43.
- Licht S, Naschitz V, Halperin L, Halperin N, Lin L, Chen J, Ghosh S, Liu B. Analysis of ferrate(VI) compounds and super-iron Fe(VI) battery cathodes: FTIR, ICP, titrimetric, XRD, UV/VIS, and electrochemical characterization. *J. Power Sources* 2001;101:167–76.
- Marco-Urrea E, Radjenovic J, Caminal G, Petrovic M, Vicent T, Barceló D. Oxidation of atenolol, propranolol, carbamazepine and clofibric acid by a biological Fenton-like system mediated by the white-rot fungus *Trametes versicolor*. *Wat. Res.* 2009:1–12.

- Martins A F, Mayer F, Confortin EC, Frank CS. A study of photocatalytic processes involving the degradation of the organic load and amoxicillin in hospital wastewater. *Clean* 2009;37:365–71.
- Martins A. F., Arsand DR, Brenner CB, Minetto L. COD Evaluation of Hospital Effluent by Means of UV-Spectral Deconvolution. *Clean* 2008;36:875–8.
- Medana C, Calza P, Carbone F, Pelizzetti E, Hidaka H, Baiocchi C. Characterization of atenolol transformation products on light-activated TiO₂ surface by high-performance liquid chromatography/high-resolution mass spectrometry. *Rapid Commun. Mass Spectrom.* 2008;22:301–13.
- OECD. Organisation for Economic Co-operation and Development, 2006. OECD Guideline for Testing of Chemicals 301 D: Ready Biodegradability. Closed Bottle Test. OECD Publishing, Paris. Organisation for Economic Co-operation and Development OECD.; 1992.
- Radjenovic J, Escher BI, Rabaey K. Electrochemical degradation of the β -blocker metoprolol by Ti/Ru_{0.7}Ir_{0.3}O₂ and Ti/SnO₂-Sb electrodes. *Wat. Res.* 2011;45:3205–14.
- Radjenović J, Pérez S, Petrović M, Barceló D. Identification and structural characterization of biodegradation products of atenolol and glibenclamide by liquid chromatography coupled to hybrid quadrupole time-of-flight and quadrupole ion trap mass spectrometry. *J. Chromatogr. A* 2008;1210:142–53.
- Sirés I, Oturan N, Oturan MA. Electrochemical degradation of β -blockers. Studies on single and multicomponent synthetic aqueous solutions. *Wat. Res.* 2010;44:3109–20.
- Slegers C, Maquille A, Deridder V, Sonveaux E, Jiwan J-LH, Tilquin B. LC–MS analysis in the e-beam and gamma radiolysis of metoprolol tartrate in aqueous

- solution: Structure elucidation and formation mechanism of radiolytic products. *Radiat. Phys. Chem.* 2006;75:977–89.
- Song W, Cooper WJ, Mezyk SP, Greaves J, Peake BM. Free radical destruction of β -blockers in aqueous solution. *Environ. Sci. Technol.* 2008;42:1256–61.
- Tay KS, Rahman NA, Abas MRB. Characterization of atenolol transformation products in ozonation by using rapid resolution high-performance liquid chromatography/quadrupole-time-of-flight mass spectrometry. *Microchem. J.* 2011;99:312–26.
- Vasconcelos TG, Kümmerer K, Henriques DM, Martins A F. Ciprofloxacin in hospital effluent: degradation by ozone and photoprocesses. *J. Hazard. Mater.* 2009;169:1154–8.
- Wang H-L, Liu S-Q, Zhang X-Y. Preparation and application of sustained release microcapsules of potassium ferrate(VI) for dinitro butyl phenol (DNBP) wastewater treatment. *J. Hazard. Mater.* 2009;169:448–53.
- Yang H, An T, Li G, Song W, Cooper WJ, Luo H, Guo X. Photocatalytic degradation kinetics and mechanism of environmental pharmaceuticals in aqueous suspension of TiO₂: A case of β -blockers. *J. Hazard. Mater.* 2010;179:834–9.

Paper III

Simultaneous determination of 11 sulfonamides by
HPLC–UV and application for fast screening of their
aerobic elimination and biodegradation in a simple test

CLEAN – Soil, Air, Water (2013)

DOI: 10.1002/clen.201200508

Waleed M. M. Mahmoud^{1,2}
Nareman D. H. Khaleel^{1,2}
Ghada M. Hadad²
Randa A. Abdel-Salam²
Annette Haiß¹
Klaus Kümmerer¹

¹Sustainable Chemistry and Material Resources, Institute of Sustainable and Environmental Chemistry, Leuphana University Lüneburg, Lüneburg, Germany

²Pharmaceutical Analytical Chemistry Department, Faculty of Pharmacy, Suez Canal University, Ismailia, Egypt

Research Article

Simultaneous Determination of 11 Sulfonamides by HPLC–UV and Application for Fast Screening of Their Aerobic Elimination and Biodegradation in a Simple Test

Sulfonamides (SAs) are one of the most frequently used antibiotics. SAs have been found in various environmental compartments. If SAs are not degraded in the environment, they can affect bacteria by their antibiotic properties and contribute to bacterial antibiotic resistance. Therefore, the biodegradability of 11 SAs (sulfanilamide, sulfaguanidine monohydrate, sulfadiazine, sulfathiazole, sulfapyridine, sulfamerazine, sulfamethoxy-pyridazine, sulfachloropyridazine, sulfamethazine, sulfamethoxazole, and sulfadimethoxine) was studied. For this purpose, the Closed Bottle Test (CBT, OECD 301D) was performed, which includes a toxicity control. In order to monitor the environmental fate of the parent compound and to check for transformation products, a simple, efficient, and reliable HPLC–UV method for the simultaneous determination of these SAs has been developed. Acetonitrile and water (with 0.1% formic acid) were used as mobile phase solvents for gradient elution. The method was validated in terms of precision, detection and quantitation limits, selectivity, and analytical solution stability. In the CBT, none of these SAs was readily biodegradable. The HPLC–UV analysis confirmed that no degradation of any SA took place. In the toxicity control, these SAs showed no toxic effect in the used concentration of environmental bacteria applied in the test.

Keywords: Aerobic biodegradation; Antibiotics; Aquatic environment; Closed Bottle Test; HPLC

Received: September 25, 2012; *revised:* January 9, 2013; *accepted:* February 12, 2013

DOI: 10.1002/clean.201200508



Additional supporting information may be found in the online version of this article at the publisher's web-site

1 Introduction

Sulfonamides (SAs) are synthetic derivatives of sulfanilamide (SAM). Their general structure contain 4-aminobenzene sulfonamide core and differ between each other in the N-substituent of the sulfonamide linkage. Because of their effects, they are used in aquaculture and agriculture as herbicides, in animal husbandry, and also as human medicines for the prevention and treatment of infectious diseases. In humans, they are used in treatment of diseases such as urinary tract infections, ear infections, bronchitis, bacterial meningitis, certain eye infections, *Pneumocystis carinii* associated pneumo-

nia, and traveler's diarrhea. In veterinary medicine they are also used at sub-therapeutic levels as feed additives in livestock production to promote growth in animals. Their mechanism of action is based on inhibiting folic acid synthesis in bacteria by acting as competitive inhibitors of *p*-aminobenzoic acid. Thereby they interrupt bacterial utilization of this compound in the synthesis of essential folic acid and ultimately of purine and DNA. The final result is inhibition of protein synthesis, metabolism and growth of bacteria [1–3].

In the USA at the beginning of the 21st century 16 000 tons of antibiotics were consumed each year. Thereof were SAs 2.3% of the total amount of antibiotics used in veterinary medicine. This value ranged from 11 to 23% in European countries. In 2000, 21% of the sales in UK were SAs. In Kenya, which represents a model example of an African country, SAs account for 22% of active antimicrobials used in animal food production [4, 5]. In most developing countries there is a lack of garbage and effluent treatment as showed in a study for Ghana [6].

Many pharmaceuticals used in human and veterinary medicines are excreted unchanged or together with their metabolites. In humans, SAs are typically excreted via urine 1–2 days after administration. They reach effluent and, if available, sewage treatment

Correspondence: Professor K. Kümmerer, Nachhaltige Chemie und Stoffliche Ressourcen, Institut für Nachhaltige Chemie und Umweltchemie, Leuphana Universität Lüneburg, C.13, Scharnhorststraße 1, D-21335 Lüneburg, Germany
E-mail: klaus.kuemmerer@uni.leuphana.de

Abbreviations: CBT, Closed Bottle Test; LOD, limit of detection; LOQ, limit of quantitation; SAs, sulfonamides; SAM, sulfanilamide; SDZ, sulfadiazine; SMP, sulfamethoxy-pyridazine; SMT, sulfamethazine; SMX, sulfamethoxazole; STPs, sewage treatment plants; STZ, sulfathiazole; ThOD, theoretical oxygen demand

plants (STPs). In husbandry most antibiotics are excreted non-metabolized via swine and cattle and end up in manure. As much as 30–90% can be excreted as parent compounds, because of their poor absorption or metabolism. In urine and therefore in manure the compounds are present as the parent compound and as a derivative (“metabolite”) carrying an acetyl group at the NH_2 group of the sulfonamide. In manure during storage and in STPs the acetyl moiety attached during metabolism to the SAs can be cleaved back by bacteria so that the active parent compound is set free again [7]. SAs possess high migration potential in the environment as they are amphoteric, polar substances that are readily soluble in water. Upon their release into the environment, they become widespread in nature [8]. Significant amounts of these pharmaceuticals are introduced to surface water and ground water through effluents from waste dumps, animal manure, and manure waste lagoons from swine farms. Furthermore, pharmaceutical compounds are released into the environment through improper disposal by private households or hospitals. Their traces are found in almost all kinds of biotopes, e.g., they are frequently detected in surface water at concentrations up to the $\mu\text{g L}^{-1}$ range [9–14]. Recently, it was found that various antibiotics used as veterinary drugs can attach to dust particles and spread through the air of pig stables. This introduces an evidence of unsuspected direct risk for human health arising from the inhalation of dust contaminated with a cocktail of antibiotics [15].

Besides chemical and photochemical degradation, biodegradation is an important aspect for the elimination of organic chemicals discharged into the environment. Biodegradation depends on the activity of microorganisms. It is necessary to assess the impact of the SAs on the bacterial populations as antibiotics exert their activity by adverse effects on microorganisms [16]. Therefore, it is essential to perform degradation tests on the chemicals reaching surface water and STPs.

There are different opinions about the susceptibility of SAs to biodegradation. Various studies have indicated that the removal of SAs during sewage treatment has been incomplete. Sulfamethoxazole (SMX) removal in the effluent of Braunschweig wastewater treatment plant effluent (WWTP) was found to be only 24% [8]. Others reported that removal rates of SMX in conventional WWTPs were between 50 and 60% due to SAs low tendency to accumulate in sludge [17]. Carballa et al. [18] observed overall removal efficiency of 60% for SMX within a Spanish WWTP. According to POSEIDON, the removal of SMX by biodegradation in batch experiments and also on laboratory and full scale plants can vary from 0 to 90% (http://undine.bafg.de/servlet/is/2888/Final-Report-POSEIDON-Jan_2005.pdf?command=downloadContent&filename=Final-Report-POSEIDON-Jan_2005.pdf) [19]. Also results found by Ingerslev and Halling-Sørensen [20] indicated that SAM, sulfadiazine (SDZ), sulfameter, and sulfabenzamide were not degraded in the respiratory screening test, which was performed according to the guidelines in ISO 9408 using lower bacterial density than present in sewage sludge. However, they found the highest biodegradation rates in activated sludge. On the other side, Peng et al. [21] have reported that the removal of SDZ and SMX from STPs in Guangzhou, China, was practically 100% effective during their biological treatment. In surface water, Perez et al. [22] found that after more than a month, sulfamethazine (SMT), sulfathiazole (STZ), and SMX were not degraded by surface-water microorganisms. In the Closed Bottle Test (CBT, OECD 301 D) [23], Alexy et al. [16] results' indicated that SMX was not readily biodegradable. CBT is a test working with low bacterial density and which can be regarded as a proxy for surface water.

Because of the different results obtained by the analysis of environmental samples and from different tests for different SAs, we focus here in a more stringent way on testing the biodegradability of 11 SAs antibiotics in one test. The widely used CBT is applied for this purpose [23]. The CBT is considered as an optimum simple test for assessing the readily biodegradability of organic substances in the environment. Compounds that pass CBT are categorized as readily biodegradable. In the aquatic environments, they are expected not to accumulate as they are considered to be rapidly and completely biodegraded under aerobic conditions [24]. To the authors' best knowledge there is no data available about the studied SAs with tests like CBT except for SMX [16] and sulfamethoxy-pyridazine (SMP) [25]. The 11 studied SAs were: sulfaguandine monohydrate (SGD-MH), SAM, SDZ, STZ, sulfapyridine (SPY), sulfamerazine (SMR), SMT, SMP, sulfachloropyridazine (SCP), SMX, and sulfadimethoxine (SDX). The biodegradation of the test compound was monitored by the biological oxygen demand (BOD).

HPLC-UV analysis was carried out in order to account for removal of the test substances and the possible formation of new degradation products. Several LC-MS methods have been reported for determination of various SAs mixtures [26–30]. Analysis using LC-MS is a favored methodology as it offers several advantages such as confirmation of compound's identity and high sensitivity. On the other hand, it is not available in all laboratories and still rather expensive. A few numbers of analytical methods are reported for the determination of SAs based on HPLC-UV, although in most laboratories HPLC-UV remains the most preferable technique for the analysis of SAs [31, 32]. For the monitoring purposes within our study classical HPLC with UV-Vis detection was sufficient because of the well-known target analytes and their concentrations in the mg L^{-1} range as demanded by the test guideline. No report of HPLC method for simultaneous determination of the studied 11 SAs mixture was found thorough literature search. Therefore, such a method was developed as a part of this study.

2 Materials and methods

2.1 Chemicals and reagents

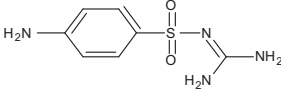
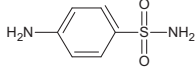
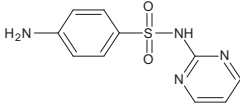
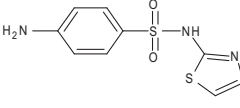
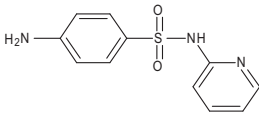
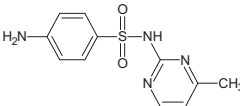
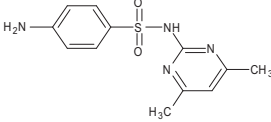
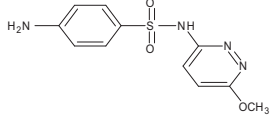
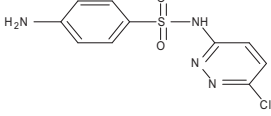
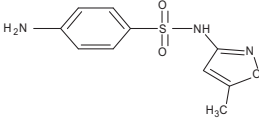
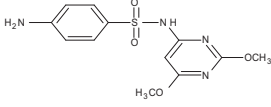
In this study, reference standards (>99% purity) of all SAs were obtained from Sigma-Aldrich (Steinheim, Germany). All the nutrients used in biodegradability testing have at least purity of 98.5%. The pK_a values and molecular structures of the studied SAs are shown in Tab. 1.

Ultrapure water was obtained from a SG Ultra Clear UV TM Water Purification System with TOC monitoring from SG Wasseraufbereitung und Regenerierstation (Barsbüttel, Germany). Acetonitrile and methanol (LiChrosolv[®], LC-MS grade) were purchased from VWR (Darmstadt, Germany).

2.2 Instrumentation

Analysis was carried out using HPLC-UV apparatus (Shimadzu, Duisburg, Germany) equipped with the HPLC system controller CBM-20A, two pumps LC-20 AT, a column oven CTO-20 AC VP, an autosampler SIL-20 AC HT, and photodiode array detector (SPD-M20). The UV wavelength detection was set at 270 nm. Collected data were analyzed using the software package LabSolutions version 5.32 SP1. A RP-C18 column (CC 125/4 NUCLEODUR 100-5 C18 ec, Macherey and

Table 1. Characteristics of the studied SAs

Analyte	Abbreviation	Chemical structures	Test concentration (mg L ⁻¹)	pK _a (most acidic)	pK _a (most basic)	Refs.
Sulfaguanidine monohydrate	SGD-MH		5.18	11.22 ± 0.70	2.22 ± 0.70	Scifinder ^{a)}
Sulfanilamide	SAM		3.84	10.10 ± 0.10	1.85 ± 0.10	[1]
Sulfadiazine	SDZ		3.91	6.50 ± 0.30	1.57 ± 0.10	[1]
Sulfathiazole	STZ		3.63	7.24 ± 0.10	2.19 ± 0.10	Scifinder ^{a)}
Sulfapyridine	SPY		3.25	8.54 ± 0.30	2.90 ± 0.19	[1]
Sulfamerazine	SMR		3.59	6.98 ± 0.30	1.58 ± 0.10	[1]
Sulfamethazine	SMT		3.35	7.45 ± 0.50	2.79 ± 0.24	[1]
Sulfamethoxy pyridazine	SMP		3.98	7.19 ± 0.30	2.18 ± 0.50	[1]
Sulfachloropyridazine	SCP		4.68	5.90 ± 0.30	1.88 ± 0.10	Scifinder ^{a)}
Sulfamethoxazole	SMX		3.77	8.81 ± 0.50	1.39 ± 0.10	[1]
Sulfadimethoxine	SDX		4.04	6.21 ± 0.50	2.44 ± 0.48	[1]

^{a)}Calculated using Advanced Chemistry Development (ACD/Labs) Software V11.02.

Nagel, Düren, Germany) preceded by a guard column (CC 8/4 HYPERSIL 100-3 (ODS) C18 ec) was used.

The chromatographic separations were performed by: (i) gradient method 1 using a binary gradient mode consisted of mobile phase A contained water (with 0.1% formic acid) and mobile phase B contained acetonitrile. The chromatographic separation was obtained by applying a gradient elution composed of 0 min 1% B, 4 min 10% B, 11.50 min 20% B, 13 min 30% B, 15 min 45% B, 18 min 50% B, 20 min 50% B, 23 min 1% B, 28 min 1% B. The mobile phase flow rate was pumped at 0.7 mL min^{-1} , column oven temperature maintained at 25°C and the injection volume was $20 \mu\text{L}$. (ii) Gradient method 2 using the same conditions of the first one but differ only in the flow rate which was set at 0.5 mL min^{-1} and the column oven temperature which was set to 40°C . (iii) Isocratic elution method with a mobile phase composed of water (with 0.1% formic acid) and acetonitrile (85:15 v/v). The mobile phase flow rate was pumped at 0.35 mL min^{-1} , column oven temperature maintained at 50°C , and the injection volume was $10 \mu\text{L}$. Total run time was 50 min. In the CBT, the 11 SAs were measured separately by applying the first gradient method which runs at 25°C .

2.3 Standard solution and sample preparation

Stock solutions were prepared by separately dissolving each standard (10 mg) in 100 mL methanol to obtain a concentration of 100 mg L^{-1} for each compound, and then were stored in dark at 4°C . The stock solutions were diluted with ultrapure water in order to prepare the working standard solutions. The resulting standards of seven concentrations were from 0.25 to 5 mg L^{-1} . Triplicate injections of each concentration were analyzed by applying the specified HPLC conditions described here.

2.4 Biodegradation testing: Closed Bottle Test (CBT, OECD 301 D)

CBT was conducted according to the test guideline [23] and the routine established in our laboratory [33–37]. This test can be performed even if the substance has very limited solubility in water, also elimination by sorption is negligible because of the absence of other organic materials. In addition to that there is no interference of other materials present with the testing substance [38, 39].

The test system consisted of four different series. Each of them was run in parallel. All test vessels contained the same mineral salt solution prepared according to the test guideline. The “blank” series contained only inoculum and mineral medium, whereas the “quality control” series contained in addition to mineral medium and inoculum, the sodium acetate (the readily biodegradable substance) in a concentration equivalent to 5 mg L^{-1} theoretical oxygen demand (ThOD). The “test” series contained inoculum and the test compound. Whereas “toxicity control” series contained in addition to the inoculum, the test compound and the sodium acetate also in a concentration corresponding to 5 mg L^{-1} ThOD. The concentration of SAs in the “test vessel” series and the “toxicity control” series were corresponding to a ThOD of 5 mg L^{-1} . The effluent of a local municipal STP (13,000 inhabitant equivalents, Kenzingen, Germany) was used as inoculum. One liter of medium is inoculated with two drops of inoculum which results in low bacterial density about 500–1000 colony forming units/mL (CFU mL^{-1}). All series vessels were run as duplicates and the test was performed two times ($n = 4$).

The toxicity control allows for the recognition of false negative results caused by the toxicity of the test compound against the degrading bacteria. Toxicity was monitored by comparing the expected level calculated from the oxygen consumption in the test vessel and in the quality control with the measured oxygen consumption in the toxicity controls. A substance is assumed to be toxic if the measured amount of oxygen consumption differs from the predicted one by $>25\%$ [23]. The standard CBT period is 28 days. In a valid test, the reference substance has to have degraded by at least 60% after 14 days of testing.

In all test vessels series, the aerobic biodegradation process was monitored by measuring oxygen concentration with the Fibox 3 system (fiber-optic oxygen meter connected with temperature sensor PT 1000) (PreSens, Precision Sensing, Regensburg, Germany) using sensor spots in the vessels [40, 41]. Fibox 3 system allows monitoring the oxygen concentration without opening the test bottles. Therefore, Fibox 3 system gives more reliable results than the conventional measurement with an oxygen electrode in accordance with international standard methods [42]. During the course of the test, pH and temperature were also monitored. Samples were taken at test beginning and test end and stored at -20°C for later HPLC–UV analysis.

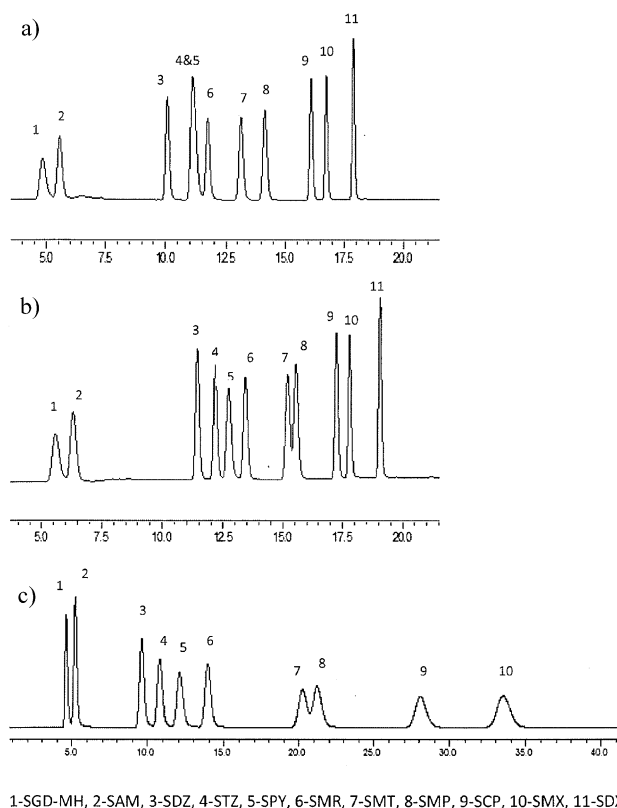


Figure 1. Chromatograms of the studied sulfonamides (SAs) with UV detection at 270 nm: (a) 1 mg L^{-1} of 11 SAs, gradient elution with water (with 0.1% formic acid) and acetonitrile at 25°C and a flow rate of 0.7 mL min^{-1} , (b) 1 mg L^{-1} of 11 SAs, gradient elution with water (with 0.1% formic acid) and acetonitrile at 40°C and a flow rate of 0.5 mL min^{-1} , (c) 4 mg L^{-1} of 11 SAs, isocratic elution with water (with 0.1% formic acid) and acetonitrile (15–85% v/v) at 50°C and a flow rate of 0.35 mL min^{-1} .

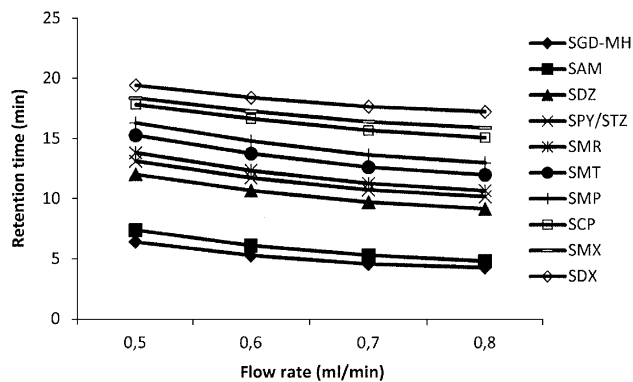


Figure 2. Influence of mobile phase flow rate on the retention time of the investigated 11 sulfonamides (SAs) at 25 °C.

The pass level for ready biodegradability of the test compound is 60% consumption of ThOD within a 10 days window after the oxygen consumption reached 10% of ThOD [23].

3 Results and discussion

3.1 Development of the HPLC operating method

The essential factors for developing liquid chromatographic separation are achieving sufficient resolution of all studied analytes, good sensitivity and acceptable analysis time. These aspects were optimized by adjusting different chromatographic factors mainly stationary-phase composition (column type and size), column oven temperature, flow rate, and optimum mobile phase compositions.

In this work, RP-C18 column (12.5 cm long, 4 mm id and 5 μm particle size) was chosen for the chromatographic separation of the investigated SAs as it achieved the best separation in term of resolution, symmetrical peaks, and good sensitivity with reasonable retention time for each SA (Fig. 1). During the optimization of the method, three columns (RP-C18 column (CC 125/4 NUCLEODUR 100-5 C18 ec, Macherey and Nagel, Düren, Germany), RP-C18 column (CC 70/3 NUCLEODUR 100-3 C18 ec, Macherey and Nagel, Düren, Germany), and RP-C8 column (CC 125/2 NUCLEODUR 100-3 C8 ec, Macherey and Nagel, Düren, Germany)) were tried with the procedures described in the experimental section except with C8 where the flow rate reduced to 0.4 mL min⁻¹ to overcome the high backpressure produced by this column. The RP-C18 column (7 cm long, 3 mm id, and 3 μm particle size) with smaller particle size and diameter gave bad and insufficient separations for all 11 studied SAs, shown in Supporting Information Fig. S1a. Also, the RP-C8 column (12.5 cm long, 2 mm id, and 3 μm particle size) gave insufficient separations for most of the 11 studied SAs, shown in Supporting Information Fig. S1b.

Mobile-phase consists of water (with 0.1% formic acid) and acetonitrile in gradient mode was chosen for the separation. Isocratic elution method was first tried, but it gave bad separation results due to different polarities and the amphoteric nature of SAs which makes their separation difficult. Therefore, gradient elution was used to improve the separation of the analytes in shorter period. Buffered mobile phase was not used, as avoiding the use of buffer may prolong the lifetime of the HPLC column. Also column separation capacity can be reduced because of crystallization of the remaining buffer salt traces on the column [25]. Methanol was tried instead of acetonitrile

Table 2. Chromatographic parameters (retention time ± standard deviation, retention factor, resolution, selectivity, and tailing) for the gradient method 1

Analyte	$t_R \pm SD$	K'	R_s	α	Tailing factor
SGD-MH	4.85 ± 0.052	1.20	1.63	1.31	1.14
SAM	5.66 ± 0.020	1.57	5.89	2.32	1.14
SDZ	10.22 ± 0.006	3.65	3.16	1.13	1.15
STZ	11.25 ± 0.006	4.11	0.00	1.00	1.18
SPY	11.25 ± 0.008	4.11	1.57	1.08	1.35
SMR	11.93 ± 0.007	4.42	4.01	1.15	1.12
SMT	13.35 ± 0.007	5.07	3.00	1.09	1.12
SMP	14.38 ± 0.006	5.54	6.67	1.16	1.10
SCP	16.27 ± 0.003	6.40	2.88	1.04	1.22
SMX	16.87 ± 0.002	6.67	5.77	1.07	1.26
SDX	17.94 ± 0.005	7.15			1.31

$t_R \pm SD$ (retention time ± standard deviation); K' , retention factor; R_s , resolution; α , selectivity.

but it gave bad results and higher column backpressure. Ammonium acetate was also tried instead of 0.1% formic acid as aqueous solvent and it gave nearly similar results. Several mobile-phase compositions were tried to achieve best chromatographic separation of the tested SAs in acceptable time. Different mobile phase gradient program were tried but they require longer time. Mobile-phase composition described in experimental section allowed the studied SAs to be baseline separated with good resolution in acceptable time.

The flow rate effect on the resolution and the retention times of the studied SAs was studied at gradient elution 1 conditions. By decreasing the flow rate, the retention times were increased and the resolutions decreased (Fig. 2). The studied SAs could be separated at a flow rate of 0.7 mL min⁻¹ with high resolution (>1.5). More decrease in the analysis time could be achieved by using higher flow rates, such as 0.8 mL min⁻¹, but at this flow rate SGD-MH and SAM showed bad resolution. A flow rate of 0.7 mL min⁻¹ was chosen for the separation as it provides better resolution of the investigated SAs from each other. For gradient method 2 and isocratic method flow rates of 0.5 and 0.35 mL min⁻¹ were optimal for good separation in a reasonable time.

The influence of temperature on resolution and retention times of the SAs was studied at 25, 30, 35, and 40 °C under gradient method 1 conditions. When the temperature increased, slight decrease in retention times occurs (Fig. 3). At higher temperature SGD-MH/SAM, SMR/

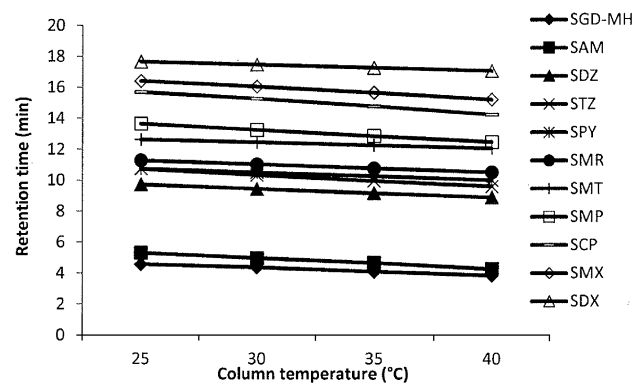


Figure 3. Influence of temperature on the retention time of the investigated 11 sulfonamides (SAs) at flow rate 0.7 mL min⁻¹.

SMT and SMP/SCP are not completely separated, while at 25°C the six SAs can be well separated. The selectivity, resolution, capacity factor, and retention time of the studied SAs at 4 mg L⁻¹ under gradient method 1 and gradient method 2 conditions at 25 and 40°C are presented in Tabs. 2 and 3, respectively. They were calculated according to United States Pharmacopeia (USP) prescriptions [43].

In the selected methods, gradient method 1, showed good resolution except for STZ and SPY which were co-eluted (Fig. 1a). Gradient method 2 with the same gradient system as in method 1 but raising the column temperature to 40°C and decreasing flow rate to 0.5 mL min⁻¹, STZ and SPY are well resolved, but SMT and SMP are partially separated (Fig. 1b). In the isocratic elution method which was developed mainly for STZ and SPY separation, good results take place but SMT and SMP are partially separated and SDX peak can not be detected until 50 min (Fig. 1c).

3.2 Validation of the method

The HPLC-UV method performance was validated with respect to the range, linearity, precision, detection and quantitation limits, selectivity, specificity, robustness, and analytical solution stability.

3.2.1 Linearity and range

The responses of the studied SAs HPLC area were linear with seven calibrators over a concentration range of 0.25–5 mg L⁻¹. Each concentration was measured three times. Peak areas and concentrations of each compound were treated by least square linear regression analysis to calculate the linearity plot equations and correlation coefficients. The linearity plots for SAs analysis were linear over the calibration range of 0.25–5 mg L⁻¹. The linearity plots were validated by the high value of correlation coefficient of the regression (Tab. 4).

The high values of regression coefficient can not ensure the absolute linearity. Therefore, the test for lack of fit was checked in order to ensure a good linearity (e.g., www.rsc.org/Membership/Networking/InterestGroups/Analytical/AMC/TechnicalBriefs.asp) [44, 45] (Tab. 5). This test assessed the variance of the residual values. The calculated lack of fit test results were less than the tabulated ones ($\alpha = 0.05$). This result allows us to prove the existence of linearity for our calibration graphs.

Table 3. Chromatographic parameters (retention time \pm standard deviation, retention factor, resolution, selectivity, and tailing) for the gradient method 2

Analyte	$t_R \pm SD$	K'	R_s	α	Tailing factor
SGD-MH	5.57 \pm 0.035	0.90	1.47	1.28	1.28
SAM	6.31 \pm 0.033	1.15	9.71	2.51	1.11
SDZ	11.42 \pm 0.006	2.89	2.46	1.09	1.12
STZ	12.16 \pm 0.006	3.15	1.59	1.06	1.12
SPY	12.71 \pm 0.007	3.33	1.95	1.07	1.19
SMR	13.41 \pm 0.005	3.57	5.08	1.17	1.10
SMT	15.18 \pm 0.006	4.18	0.97	1.03	1.12
SMP	15.53 \pm 0.006	4.30	5.50	1.13	1.12
SCP	17.23 \pm 0.004	4.88	2.18	1.04	1.13
SMX	17.78 \pm 0.005	5.06	5.34	1.09	1.14
SDX	19.05 \pm 0.005	5.50			1.15

$t_R \pm SD$ (retention time \pm standard deviation); K' , retention factor; R_s , resolution; α , selectivity.

Table 4. Characteristic parameters of the calibration curve equations

Analyte	R^2	Slope	Intercept	LOD	LOQ
SGD-MH	1	85 542	-2548.3	0.1	0.25
SAM	0.9998	65 801	-2907.3	0.1	0.25
SDZ	0.9999	120 266	700.4	0.05	0.1
STZ	0.9999	97 229	-202.97	0.05	0.1
SPY	0.9995	88 139	-78.66	0.05	0.1
SMR	0.9984	81 333	-51.92	0.05	0.1
SMT	0.9999	97 569	-1178.7	0.05	0.1
SMP	0.9999	99 526	-4986.2	0.05	0.1
SCP	0.9998	99 818	9133.1	0.05	0.1
SMX	0.9997	100 946	10 963	0.02	0.05
SDX	0.9999	99 632	-1885.9	0.02	0.05

LOD, limit of detection; LOQ, limit of quantitation.

3.2.2 Precision

Precision of the method was assessed depending on the analysis of intra-day and inter-day repeatability. The repeatability was assessed by three replicates of ultrapure water samples fortified with SAs standard at three different concentrations (low: 0.5 mg L⁻¹, medium: 2 mg L⁻¹, and high: 5 mg L⁻¹) on a single assay day and on three consecutive days. The precision was expressed as relative standard deviation (RSD) and satisfactory results were achieved. The intra-day repeatability ranged between 0.05 and 7.21% RSD, and the inter-day repeatability ranged between 0.1 and 4.6% RSD (Tab. 6).

3.2.3 Limit of detection (LOD) and quantitation (LOQ)

According to International Conference on Harmonization (ICH) recommendations [46], LOD and LOQ were determined. LODs and LOQs were calculated experimentally from the injection of serially diluted standard solutions till the signal-to-noise ratio is ≥ 3 for LOD and 10 for LOQ. The values of the LODs and LOQs are given in Tab. 4. The low LOD showed an acceptable sensitivity for the method.

3.2.4 Selectivity

Method selectivity was assessed by comparing the retention times of the studied SAs obtained from the chromatograms of ultrapure water fortified with the 11 SAs to the chromatograms of the unfortified ones (blank samples). The positive results from samples containing the analytes coupled with negative results from samples which do not contain the analytes and good separation ensures that the peak measured is not influenced by other compounds.

3.2.5 Specificity

Method specificity was evaluated by its ability to be used for analysis of a certain analyte in a mixture or matrix without interference from other components. In this study, the method specificity was evaluated by analysis of the 11 SAs in STP effluent matrix and then determining peak homogeneity or purity. The results showed well-resolved peaks which indicate good specificity.

3.2.6 Robustness

It was done to study the effects of deliberate variations in the operational factors on the system suitability parameters of the studied SAs. These factors were the mobile phase composition ($\pm 2\%$ of gradient composition), flow rate ($\pm 5\%$), column batch (two different column batches), and column temperature ($\pm 2^\circ\text{C}$). These parameters were studied using one-variable-at-a-time procedure. The samples were ana-

Table 5. ANOVA (showing lack of fit calculation) for SGD-MH, SAM, SDZ, STZ, SPY, SMR, SMT, SMP, SCP, SMX, and SDX

Compound	Source of variation	Sum of squares	Degree of freedom	Mean sum of squares	F-ratio ^{a)}
SGD-MH	Total	9.23×10^{10}	24	3.85×10^9	0.82
	Regression	9.23×10^{10}	2	4.62×10^{10}	
	Residual	4.26×10^6	22	1.94×10^5	
	Replicate	1.75×10^6	8	2.19×10^5	
SAM	Lack of fit	2.51×10^6	14	1.79×10^5	0.81
	Total	1.58×10^{11}	24	6.58×10^9	
	Regression	1.58×10^{11}	2	7.89×10^{10}	
	Residual	2.04×10^7	22	9.27×10^5	
SDZ	Replicate	2.54×10^8	8	1.05×10^6	0.37
	Lack of fit	1.20×10^7	14	8.54×10^5	
	Total	3.19×10^{11}	24	1.33×10^{10}	
	Regression	3.19×10^{11}	2	1.59×10^{11}	
STZ	Residual	1.49×10^7	22	6.78×10^5	1.15
	Replicate	9.08×10^6	8	1.14×10^6	
	Lack of fit	5.83×10^6	14	4.16×10^5	
	Total	2.10×10^{11}	24	8.77×10^9	
SPY	Regression	2.10×10^{11}	2	1.05×10^{11}	1.60
	Residual	8.09×10^6	22	3.68×10^5	
	Replicate	2.69×10^6	8	3.36×10^5	
	Lack of fit	5407165	14	3.86×10^5	
SMR	Total	1.69×10^{11}	24	7.04×10^9	0.77
	Regression	1.69×10^{11}	2	8.45×10^{10}	
	Residual	6.23×10^6	22	2.83×10^5	
	Replicate	1.64×10^6	8	2.05×10^5	
SMT	Lack of fit	4.59×10^6	14	3.28×10^5	1.07
	Total	1.47×10^{10}	24	6.12×10^8	
	Regression	1.47×10^{10}	2	7.33×10^9	
	Residual	1.37×10^7	22	6.22×10^5	
SMP	Replicate	5.85×10^6	8	7.31×10^5	1.21
	Lack of fit	7.84×10^6	14	5.60×10^5	
	Total	2.08×10^{11}	24	8.65×10^9	
	Regression	2.08×10^{11}	2	1.04×10^{11}	
SCP	Residual	2.18×10^7	22	9.92×10^5	0.47
	Replicate	7.59×10^6	8	9.49×10^5	
	Lack of fit	1.42×10^7	14	1.02×10^6	
	Total	2.14×10^{11}	24	8.93×10^9	
SMX	Regression	2.14×10^{11}	2	1.07×10^{11}	2.38
	Residual	4.74×10^7	22	2.16×10^6	
	Replicate	1.52×10^7	8	1.90×10^6	
	Lack of fit	3.22×10^7	14	2.30×10^6	
SDX	Total	2.25×10^{11}	24	1.23×10^{11}	1.58
	Regression	2.25×10^{11}	2	9.38×10^9	
	Residual	4.41×10^7	22	2.01×10^6	
	Replicate	2.42×10^7	8	3.03×10^6	
SGD-MH	Lack of fit	1.99×10^7	14	1.42×10^6	1.58
	Total	2.29×10^{11}	24	9.55×10^9	
	Regression	2.29×10^{11}	2	1.14×10^{11}	
	Residual	1.17×10^8	22	5.33×10^6	
SAM	Replicate	2.27×10^7	8	2.84×10^6	1.58
	Lack of fit	9.46×10^7	14	6.76×10^6	
	Total	1.68×10^{11}	24	6.01×10^9	
	Regression	1.68×10^{11}	2	8.41×10^{10}	
SDZ	Residual	1.17×10^7	22	5.30×10^5	1.58
	Replicate	3.10×10^6	8	3.87×10^5	
	Lack of fit	8.57×10^6	14	6.11×10^5	

^{a)}The critical value of F-ratio is 3.24 at $\alpha = 0.05$.

lyzed under original and varied conditions. The robustness of the method was judged by RSD% of system suitability parameters (three replicates) for each SA; which were $\leq 2\%$.

3.2.7 Analytical solution stability

The analytical solution stability of the studied SAs in methanol/water solvent exhibited no chromatographic changes after 24 h

when kept at room temperature, and for 3 days when stored refrigerated at 4°C. Samples stored at –20°C stable for at least 2 months.

3.3 Biodegradation

According to test guidelines, the CBT was performed for the 11 SAs [23]. The OECD test guidelines criteria were met and the test was

Table 6. Intra- and inter-day precision of the determination of the analytes studied

Analyte	Intra-day precision (RSD)			Inter-day precision (RSD)		
	Low conc. ^{a)}	Medium conc. ^{b)}	High conc. ^{c)}	Low conc. ^{a)}	Medium conc. ^{b)}	High conc. ^{c)}
SGD-MH	4.46	1.35	0.49	1.6	0.7	1.2
SAM	0.35	0.31	0.22	2.6	0.8	0.4
SDZ	0.30	0.45	0.19	1.0	0.5	0.1
STZ	0.24	0.63	0.15	0.9	0.3	0.1
SPY	0.74	3.29	0.18	3.9	1.8	0.4
SMR	2.36	1.99	0.35	4.6	1.0	0.4
SMT	2.12	0.80	0.23	0.9	0.2	0.1
SMP	0.92	0.27	0.45	0.4	0.3	0.3
SCP	7.21	0.27	0.44	3.6	1.2	0.5
SMX	3.48	1.52	0.61	3.2	1.3	0.8
SDX	1.17	0.05	0.22	1.2	0.2	0.5

RSD, relative standard deviation (%).

^{a)}The concentration for all analytes was 0.25 mg L⁻¹ except SPY & SGD-MH (0.5 mg L⁻¹).

^{b)}The concentration for all analytes was 2 mg L⁻¹ except SPY & SGD-MH (1 mg L⁻¹).

^{c)}The concentration for all analytes was 5 mg L⁻¹ except SPY & SGD-MH (4 mg L⁻¹).

valid, as the sodium acetate (quality control substrate) was biodegraded more than 60% ThOD within 14 days.

In the CBT, the biodegradation values for the studied 11 SAs determined by monitoring the BOD for the two test bottles are characterizing those substances as being not readily biodegradable. No toxic effects were seen in both toxicity control bottles of all studied SAs. CBT and LC chromatogram for SDZ as an example of one of the studied 11 SAs are shown in Figs. 4 and 5. The results of test and toxicity series of the other 10 SAs are shown in Supporting Information Figs. S2-S11.

According to the test guideline, all the investigated SAs were not toxic against bacteria since sodium acetate was biodegraded in the toxicity control by >25%. None of the tested SAs showed any antibacterial effect against the bacterial growth.

Under the Japanese Chemical Substances Control Law (CSCL), the Japanese National Institute of Technology and Evaluation (NITE) database (www.safe.nite.go.jp/english/sougou/)

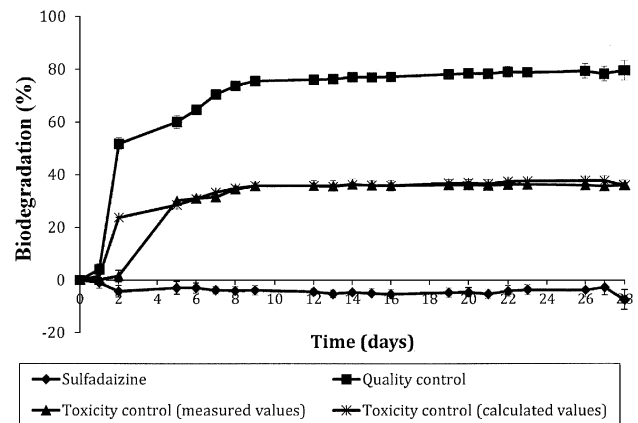


Figure 4. Closed Bottle Test of sulfadiazine (SDZ) ($n = 2$).

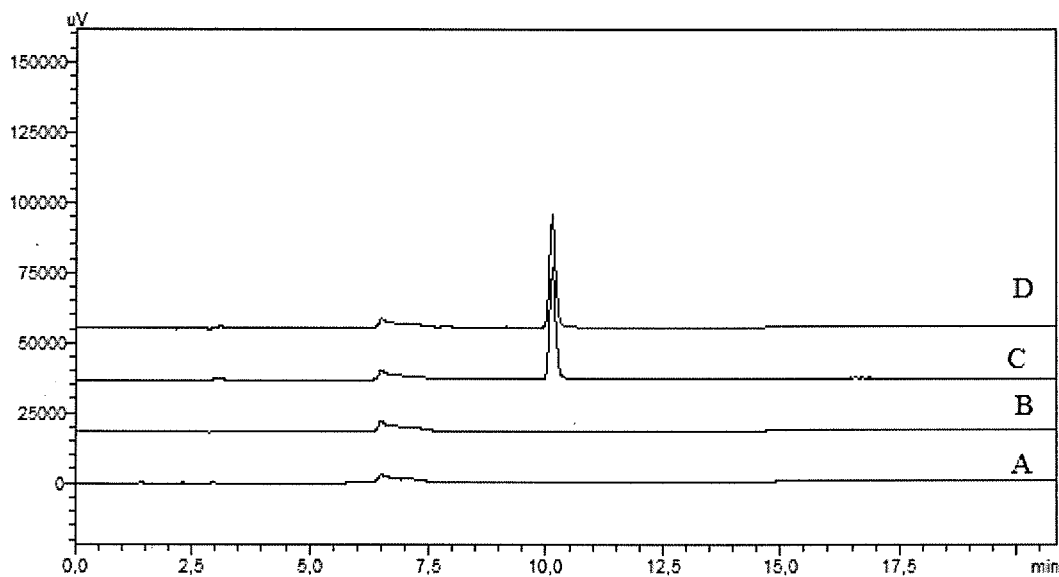


Figure 5. Liquid chromatography (LC) chromatograms of Closed Bottle Test (CBT): (a) Blank Day 0, (b) Blank Day 28, (c) sulfadiazine (SDZ) Day 0, and (d) SDZ Day 28.

view/ComprehensiveInfoDisplay_en.faces) which allows access to biodegradation and other data on a lot of compounds. In NITE, The benzene sulfonic acid (CAS-No.: 98-11-3) is readily biodegradable but the 4-aminobenzenesulfonic acid (CAS-No.: 121-57-3) is not biodegradable. Therefore, the presence of 4-aminobenzenesulfone in the skeleton of these SAs makes the biodegradation problematic.

HPLC–UV measurements confirmed that no primary elimination of any SAs took place. From these results, studied SAs are assumed to be not readily biodegradable and not eliminated by sorption in surface water. Therefore, SAs are expected to reach or accumulate in the aquatic environment. So, the development of bacterial resistance cannot be ruled out due to the presence of these antibiotics in aquatic environment.

4 Concluding remarks

The studied SAs were not readily biodegraded in the CBT whose conditions (low bacterial density and low concentration of the test substance) is comparable to the situation in surface water. A simple and sensitive method for the determination of SAs has been developed using HPLC with photodiode array detection. The simplified and effective procedure enables quantitative determination of 11 of the most extensively used SAs. The HPLC method can be applied for the quantitative determination of SAs in CBT. Our results underline the need for further investigation of the fate and effects on SAs in the aquatic environment. As a next step additional aerobic and anaerobic biodegradation tests of different bacteria density for the SAs will be performed.

Acknowledgments

Waleed M. M. Mahmoud Ahmed thanks the Ministry of Higher Education and Scientific Research of the Arab Republic of Egypt (MHESR) and the German Academic Exchange Service (DAAD) for the scholarship (Egyptian-German Research Long Term Scholarship (GERLS)). Part of this work was carried out within the Project (Reduction of the introduction of animal medicinal products in the environment by better degradable sulfonamides, Grant No 26852-31) for which financial support by the German environmental foundation (DBU) is acknowledged. The authors wish to thank Natalie Hoehn and Evgenia Logunova (Sustainable Chemistry and Material Resources, Institute of Sustainable and Environmental Chemistry, Leuphana University Lüneburg, Germany) for their help with the biodegradation experiments.

The authors have declared no conflict of interest.

References

- [1] P. Sukul, M. Spittler, Sulfonamides in the Environment as Veterinary Drugs, *Rev. Environ. Contam. Toxicol.* **2006**, *187*, 67–101.
- [2] E. Tolika, V. Samanidou, I. Papadoyannis, Development and Validation of an HPLC Method for the Determination of Ten Sulfonamide Residues in Milk According to 2002/657/EC, *J. Sep. Sci.* **2011**, *34* (14), 1627–1635.
- [3] L. Hu, P. M. Flanders, P. L. Miller, T. J. Strathmann, Oxidation of Sulfamethoxazole and Related Antimicrobial Agents by TiO₂ Photocatalysis, *Water Res.* **2007**, *41* (12), 2612–2626.
- [4] A. K. Sarmah, M. T. Meyer, A. B. A. Boxall, A Global Perspective on the Use, Sales, Exposure Pathways, Occurrence, Fate and Effects of Veterinary Antibiotics (VAs) in the Environment, *Chemosphere* **2006**, *65* (5), 725–759.
- [5] M. J. García-Galán, M. S. Díaz-Cruz, D. Barceló, Identification and Determination of Metabolites and Degradation Products of Sulfonamide Antibiotics: Advanced MS Analysis of Metabolites and Degradation Products – II, *TrAC, Trends Anal. Chem.* **2008**, *27* (11), 1008–1022.
- [6] S. Sasu, K. Kümmerer, M. Kranert, Assessment of Pharmaceutical Waste Management at Selected Hospitals and Homes in Ghana, *Waste Manage. Res.* **2012**, *30* (6), 625.
- [7] S. A. I. Mohring, I. Strzysch, M. R. Fernandes, T. K. Kiffmeyer, J. Tuerk, G. Hamscher, Degradation and Elimination of Various Sulfonamides during Anaerobic Fermentation: A Promising Step on the Way to Sustainable Pharmacy? *Environ. Sci. Technol.* **2009**, *43* (7), 2569–2574.
- [8] T. A. Ternes, M. Bonerz, N. Herrmann, B. Teiser, H. R. Andersen, Irrigation of Treated Wastewater in Braunschweig, Germany: An Option to Remove Pharmaceuticals and Musk Fragrances, *Chemosphere* **2007**, *66* (5), 894–904.
- [9] J. H. Al-Rifai, C. L. Gabelish, A. I. Schäfer, Occurrence of Pharmaceutically Active and Non-Steroidal Estrogenic Compounds in Three Different Wastewater Recycling Schemes in Australia, *Chemosphere* **2007**, *69* (5), 803–815.
- [10] K. Kümmerer, *Pharmaceuticals in the Environment: Sources, Fate, Effects and Risks*, Springer, Berlin **2001**.
- [11] E. Zuccato, D. Calamari, M. Natangelo, R. Fanelli, Presence of Therapeutic Drugs in the Environment, *Lancet* **2000**, *355* (9217), 1789–1790.
- [12] W. Baran, E. Adamek, J. Ziemianska, A. Sobczak, Effects of the Presence of Sulfonamides in the Environment and Their Influence on Human Health, *J. Hazard. Mater.* **2011**, *196*, 1–15.
- [13] M. J. García-Galán, M. S. Díaz-Cruz, D. Barceló, Occurrence of Sulfonamide Residues along the Ebro River Basin: Removal in Wastewater Treatment Plants and Environmental Impact Assessment, *Environ. Int.* **2011**, *37* (2), 462–473.
- [14] M. J. García-Galán, T. Garrido, J. Fraile, A. Ginebreda, M. S. Díaz-Cruz, D. Barceló, Application of Fully Automated Online Solid Phase Extraction-Liquid Chromatography-Electrospray-Tandem Mass Spectrometry for the Determination of Sulfonamides and Their Acetylated Metabolites in Groundwater, *Anal. Bioanal. Chem.* **2011**, *399* (2), 795–806.
- [15] G. Hamscher, H. T. Pawelzick, S. Sczesny, H. Nau, J. Hartung, Antibiotics in Dust Originating from a Pig-Fattening Farm: A New Source of Health Hazard for Farmers? *Environ. Health Perspect.* **2003**, *111* (13), 1590–1594.
- [16] R. Alexy, T. Kümpel, K. Kümmerer, Assessment of Degradation of 18 Antibiotics in the Closed Bottle Test, *Chemosphere* **2004**, *57* (6), 505–512.
- [17] M. Clara, B. Strenn, O. Gans, E. Martinez, N. Kreuzinger, H. Kroiss, Removal of Selected Pharmaceuticals, Fragrances and Endocrine Disrupting Compounds in a Membrane Bioreactor and Conventional Wastewater Treatment Plants, *Water Res.* **2005**, *39* (19), 4797–4807.
- [18] M. Carballa, F. Omil, J. M. Lema, M. Llopart, C. García-Jares, I. Rodríguez, M. Gómez, et al., Behavior of Pharmaceuticals, Cosmetics and Hormones in a Sewage Treatment Plant, *Water Res.* **2004**, *38* (12), 2918–2926.
- [19] T. A. Ternes, M. Laure, J.-H. Thomas, N. Kreuzinger, H. Siegrist, *Project acronym POSEIDON Contract No. EVK1-CT-2000-0004 7: Assessment of technologies for the removal of pharmaceuticals and personal care products in sewage and drinking water facilities to improve the indirect potable water reuse*, Bundesanstalt für Gewässerkunde, Koblenz **2004**.
- [20] F. Ingerslev, B. Halling-Sørensen, Biodegradability Properties of Sulfonamides in Activated Sludge, *Environ. Toxicol. Chem.* **2000**, *19* (10), 2467–2473.
- [21] X. Peng, Z. Wang, W. Kuang, J. Tan, K. Li, A Preliminary Study on the Occurrence and Behavior of Sulfonamides, Ofloxacin and Chloramphenicol Antimicrobials in Wastewaters of Two Sewage Treatment Plants in Guangzhou, China, *Sci. Total Environ.* **2006**, *371* (1–3), 314–322.

- [22] S. Perez, P. Eichhorn, D. S. Aga, Evaluating the Biodegradability of Sulfamethazine, Sulfamethoxazole, Sulfathiazole, and Trimethoprim at Different Stages of Sewage Treatment, *Environ. Toxicol. Chem.* **2005**, *24* (6), 1361–1367.
- [23] OECD, *Organisation for Economic Co-Operation and Development Guideline for Testing of Chemicals 301 D: Ready Biodegradability. Closed Bottle Test*, OECD Publishing, Paris **1992**.
- [24] N. Nyholm, The European System of Standardized Legal Tests for Assessing the Biodegradability of Chemicals, *Environ. Toxicol. Chem.* **1991**, *10* (10), 1237–1246.
- [25] N. D. H. Khaleel, W. M. M. Mahmoud, G. M. Hadad, R. A. A. Salam, K. Kümmerer, Photolysis of Sulfamethoxypyridazine in Various Aqueous Media: Aerobic Biodegradation and Identification of Photoproducts by LC-UV-MS/MS, *J. Hazard. Mater.* **2013**, *244–245*, 654–661.
- [26] V. Balakrishnan, K. Terry, J. Toito, Determination of Sulfonamide Antibiotics in Wastewater: A Comparison of Solid Phase Micro-extraction and Solid Phase Extraction Methods, *J. Chromatogr. A* **2006**, *1131* (1–2), 1–10.
- [27] M. E. Lindsey, T. M. Meyer, E. M. Thurman, Analysis of Trace Levels of Sulfonamide and Tetracycline Antimicrobials in Groundwater and Surface Water Using Solid-Phase Extraction and Liquid Chromatography/Mass Spectrometry, *Anal. Chem.* **2001**, *73* (19), 4640–4646.
- [28] J. E. Renew, C.-H. Huang, Simultaneous Determination of Fluoroquinolone, Sulfonamide, and Trimethoprim Antibiotics in Wastewater using Tandem Solid Phase Extraction and Liquid Chromatography–Electrospray Mass Spectrometry, *J. Chromatogr. A* **2004**, *1042* (1–2), 113–121.
- [29] M. Rodriguez, D. B. Orescan, Confirmation and Quantitation of Selected Sulfonamide, Imidazolinone, and Sulfonamide Herbicides in Surface Water Using Electrospray LC/MS, *Anal. Chem.* **1998**, *70* (13), 2710–2717.
- [30] S. Yang, J. Cha, K. Carlson, Quantitative Determination of Trace Concentrations of Tetracycline and Sulfonamide Antibiotics in Surface Water Using Solid-Phase Extraction and Liquid Chromatography/Ion Trap Tandem Mass Spectrometry, *Rapid Commun. Mass Spectrom.* **2004**, *18* (18), 2131–2145.
- [31] J.-F. Jen, H.-L. Lee, B.-N. Lee, Simultaneous Determination of Seven Sulfonamide Residues in Swine Wastewater by High-Performance Liquid Chromatography, *J. Chromatogr. A* **1998**, *793* (2), 378–382.
- [32] H. Shaaban, T. Górecki, High Temperature–High Efficiency Liquid Chromatography Using Sub-2 μ m Coupled Columns for the Analysis of Selected Non-Steroidal Anti-Inflammatory Drugs and Veterinary Antibiotics in Environmental Samples, *Anal. Chim. Acta* **2011**, *702* (1), 136–143.
- [33] M. Bergheim, R. Gieré, K. Kümmerer, Biodegradability and Ecotoxicity of Tramadol, Ranitidine, and Their Photoderivatives in the Aquatic Environment, *Environ. Sci. Pollut. Res.* **2012**, *19* (1), 72–85.
- [34] K. Kümmerer, J. Menz, T. Schubert, W. Thielemans, Biodegradability of Organic Nanoparticles in the Aqueous Environment, *Chemosphere* **2011**, *82* (10), 1387–1392.
- [35] A. Längin, R. Alexy, A. König, K. Kümmerer, Deactivation and Transformation Products in Biodegradability Testing of β -Lactams Amoxicillin and Piperacillin, *Chemosphere* **2009**, *75* (3), 347–354.
- [36] W. M. M. Mahmoud, K. Kümmerer, Captopril and Its Dimer Captopril Disulfide: Photodegradation, Aerobic Biodegradation and Identification of Transformation Products by HPLC-UV and LC-Ion trap-MSⁿ, *Chemosphere* **2012**, *88* (10), 1170–1177.
- [37] C. Trautwein, K. Kümmerer, Incomplete Aerobic Degradation of the Antidiabetic Drug Metformin and Identification of the Bacterial Dead-End Transformation Product Guanylurea, *Chemosphere* **2011**, *85* (5), 765–773.
- [38] F. H. Frimmel, R. Niessner, *Nanoparticles in the Water Cycle: Properties, Analysis and Environmental Relevance*, Springer-Verlag, Berlin/Heidelberg **2010**.
- [39] K. Tiede, M. Hasselov, E. Breitbarth, Q. Chaudhry, A. Boxall, Considerations for Environmental Fate and Ecotoxicity Testing to Support Environmental Risk Assessments for Engineered Nanoparticles, *J. Chromatogr. A* **2009**, *1216* (3), 503–509.
- [40] J. Friedrich, A. Längin, K. Kümmerer, Comparison of an Electrochemical and Luminescence-Based Oxygen Measuring System for Use in the Closed Bottle Test, *Clean – Soil Air Water* **2013**, *41* (3), 251–257.
- [41] O. S. Wolfbeis, Fiber-Optic Chemical Sensors and Biosensors, *Anal. Chem.* **2004**, *76* (12), 3269–3284.
- [42] International Standards Organization (ISO), Water quality – determination of dissolved oxygen, in *German Standard Methods for the Examination of Water, Wastewater and Sludge*, WILEY-VCH Verlag, Weinheim **1990**.
- [43] United States Pharmacopeial Convention, *The United States Pharmacopeia 30: The National Formulary 25*, United States Pharmacopeial Convention, Rockville, MD **2006**.
- [44] M. Thompson, *Analytical Methods Committee Technical Briefs*, AMCTB No 3, The Royal Society of Chemistry, London **2005**.
- [45] G. M. Hadad, S. Emara, W. M. M. Mahmoud, Development and Validation of a Stability-Indicating RP-HPLC Method for the Determination of Paracetamol with Dantrolene or/and Cetirizine and Pseudoephedrine in Two Pharmaceutical Dosage Forms, *Talanta* **2009**, *79* (5), 1360–1367.
- [46] International Conference on Harmonization, *ICH topic Q2B note for Guidance on Validation of Analytical Procedures: Methodology GPMP/ICH/281/95*, ICH, London **1996**.

Supplementary materials

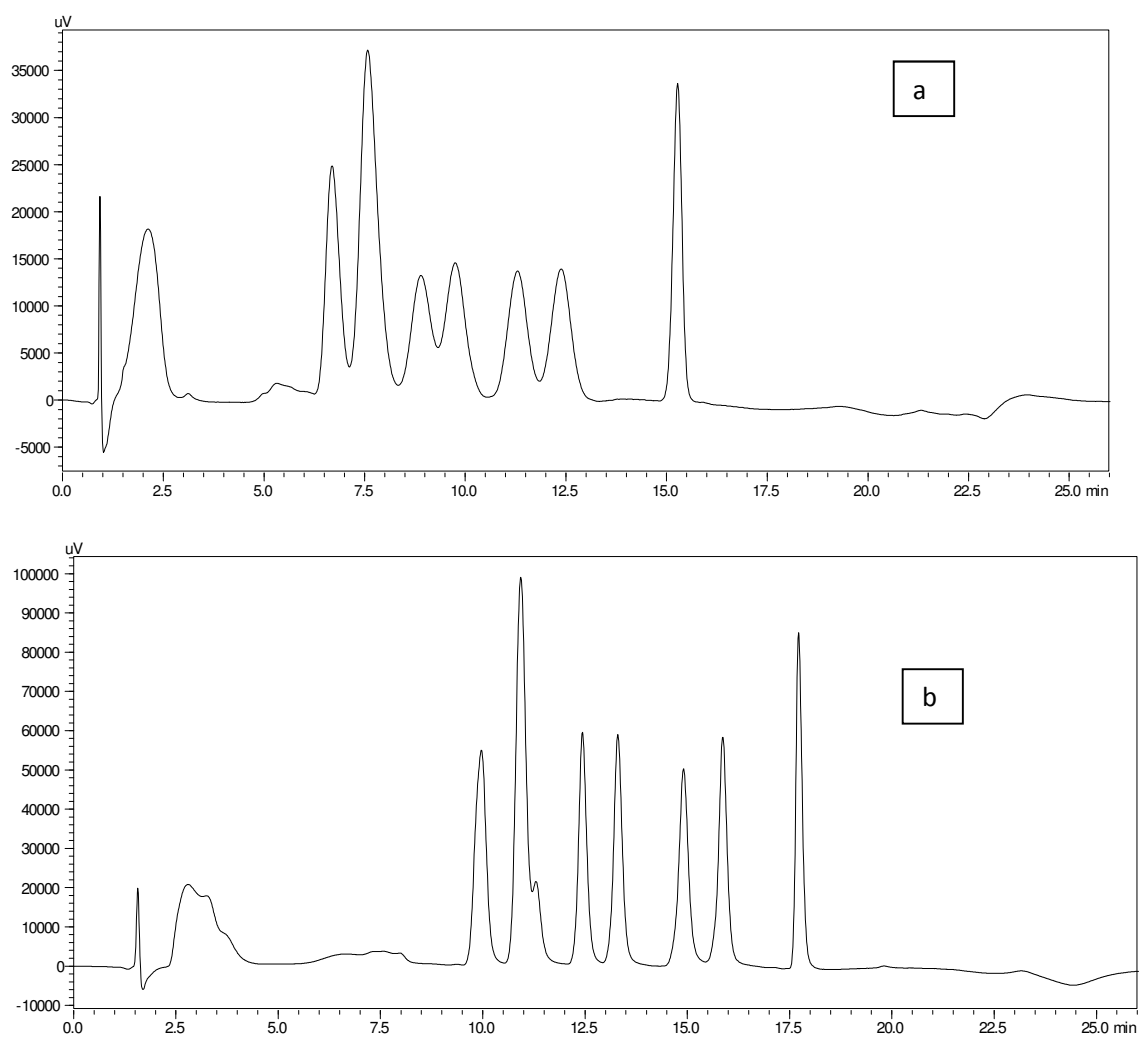


Fig.S1: HPLC chromtaograms for the separation of the 11 SAs using (a) RP-C18 column (CC 70/3 NUCLEODUR 100-3 C18) and (b) RP-C8 column (CC 125/2 NUCLEODUR 100-3 C8 ec).

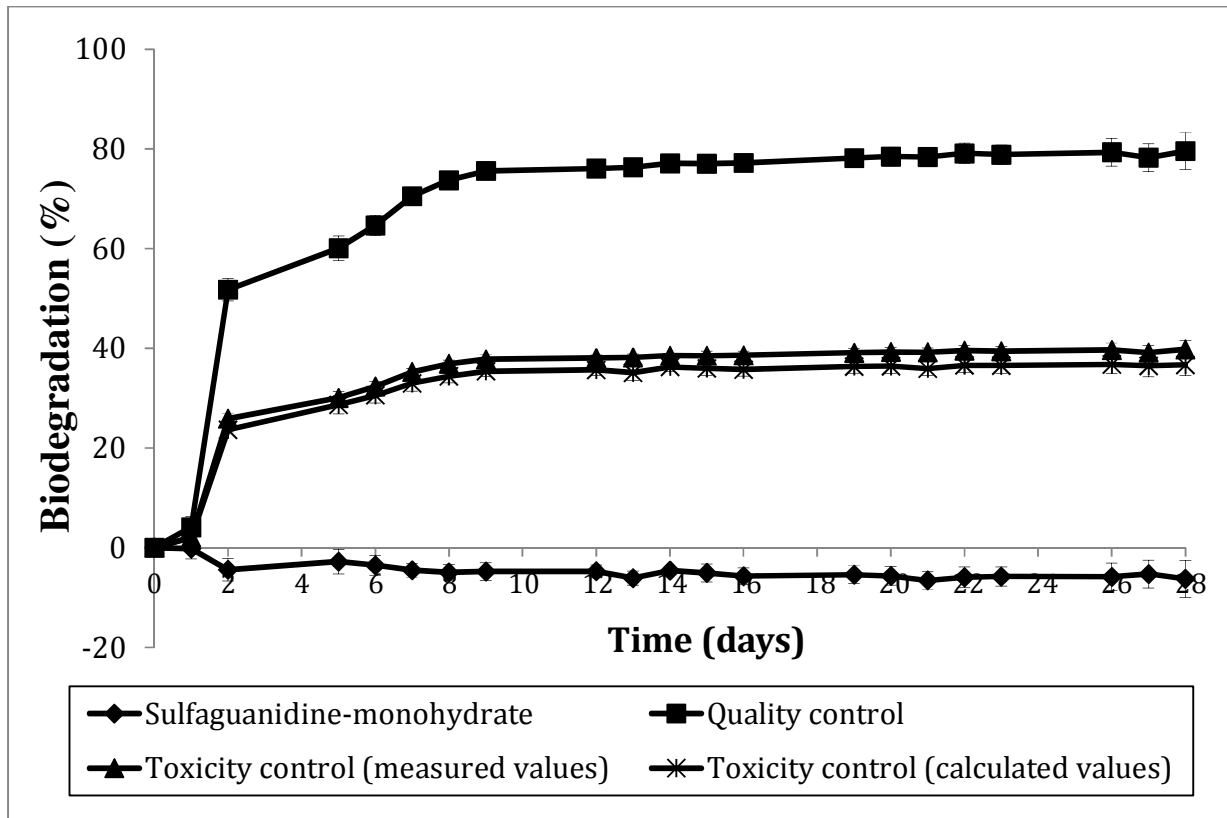


Figure S2. Closed Bottle test of SGM (n = 2).

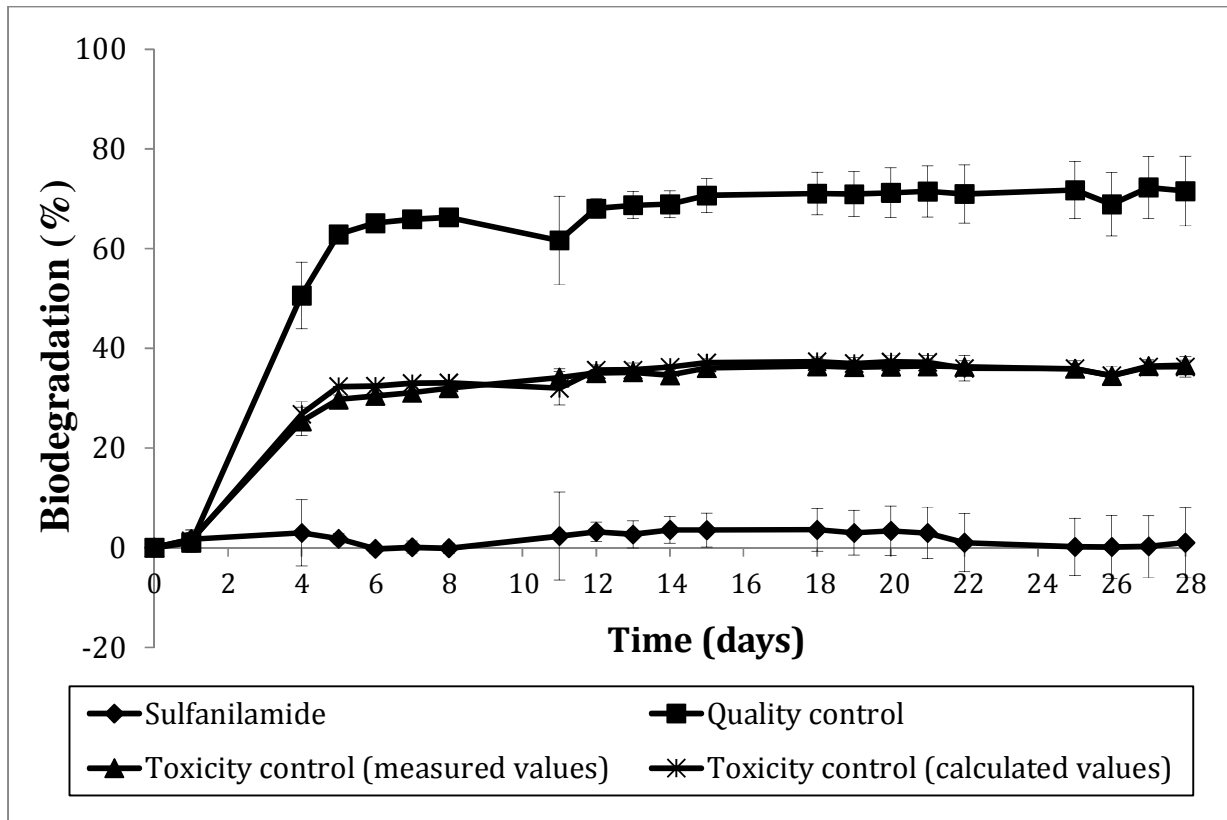


Figure S3. Closed Bottle test of SAM (n = 2).

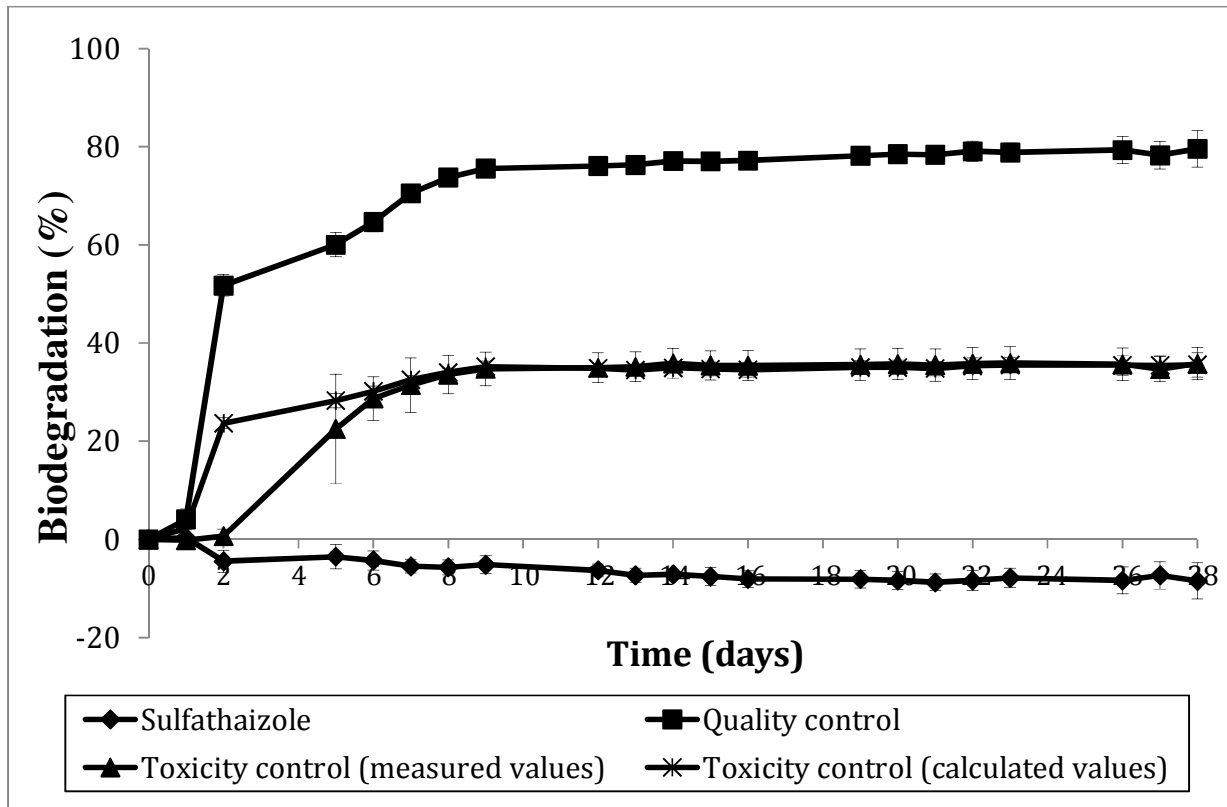


Figure S4. Closed Bottle test of STZ (n = 2).

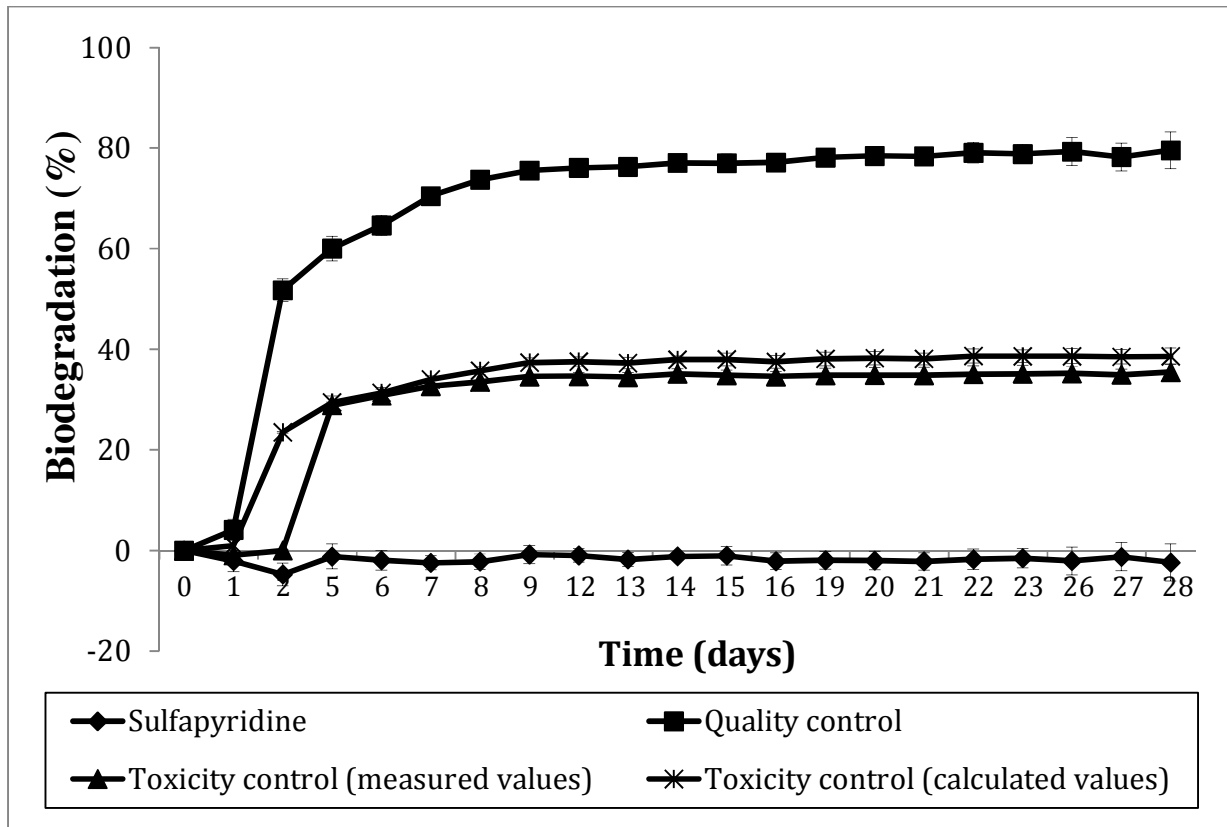


Figure S5. Closed Bottle test of SPY (n = 2).

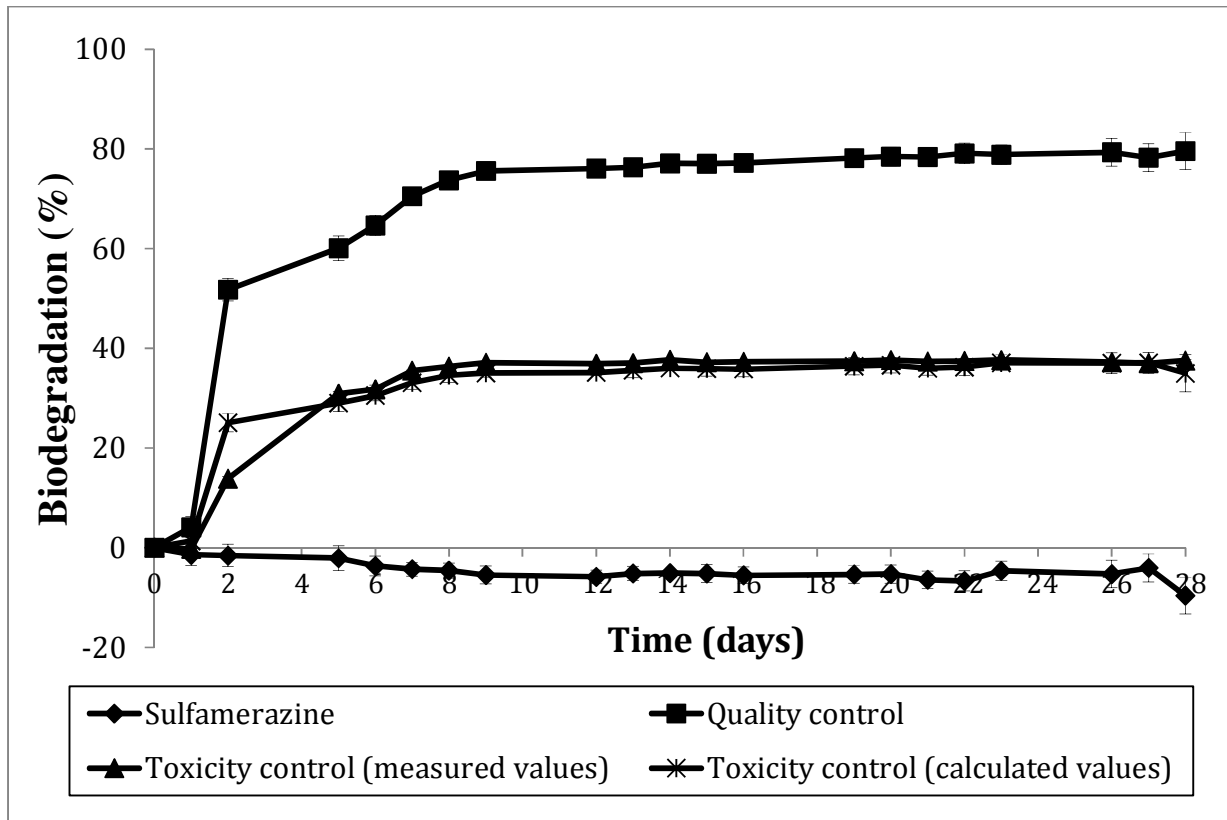


Figure S6. Closed Bottle test of SMR (n = 2).

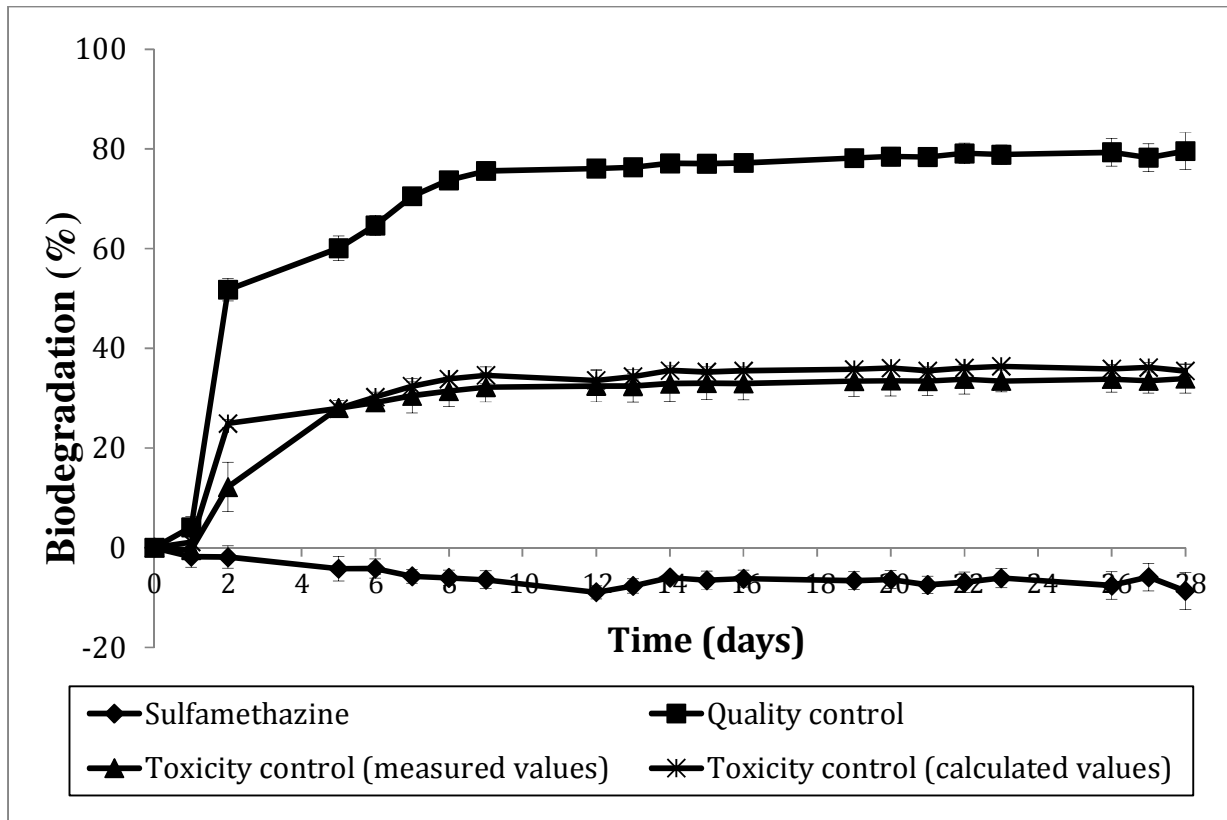


Figure S7. Closed Bottle test of SMT (n = 2).

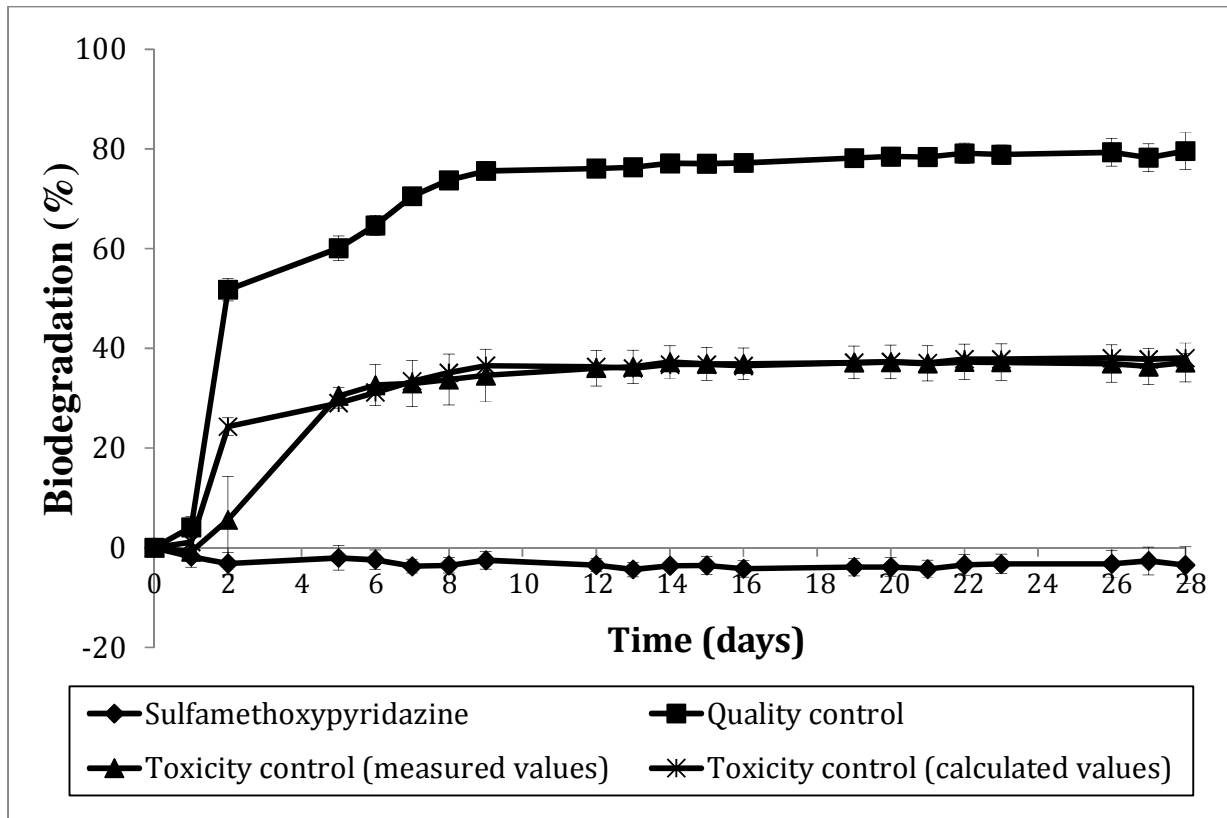


Figure S8. Closed Bottle test of SMP (n = 2).

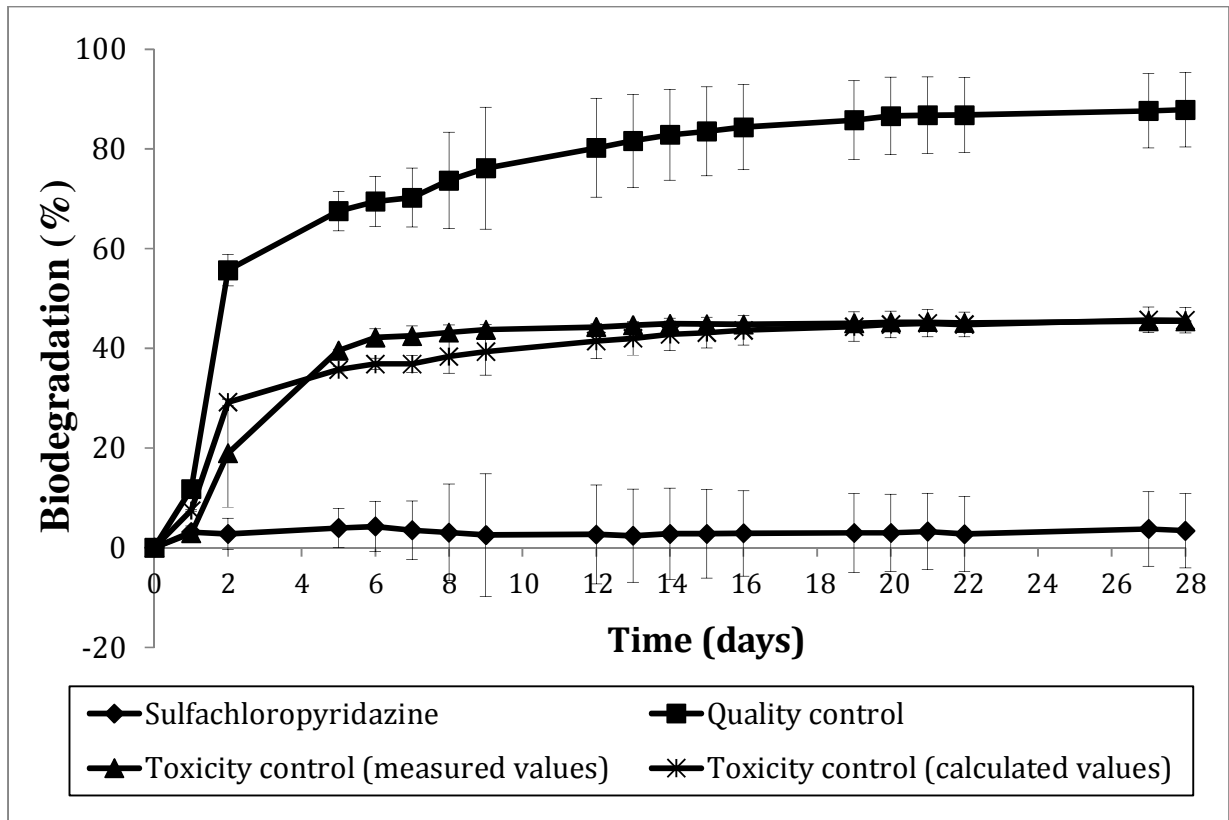


Figure S9. Closed Bottle test of SCP (n = 2).

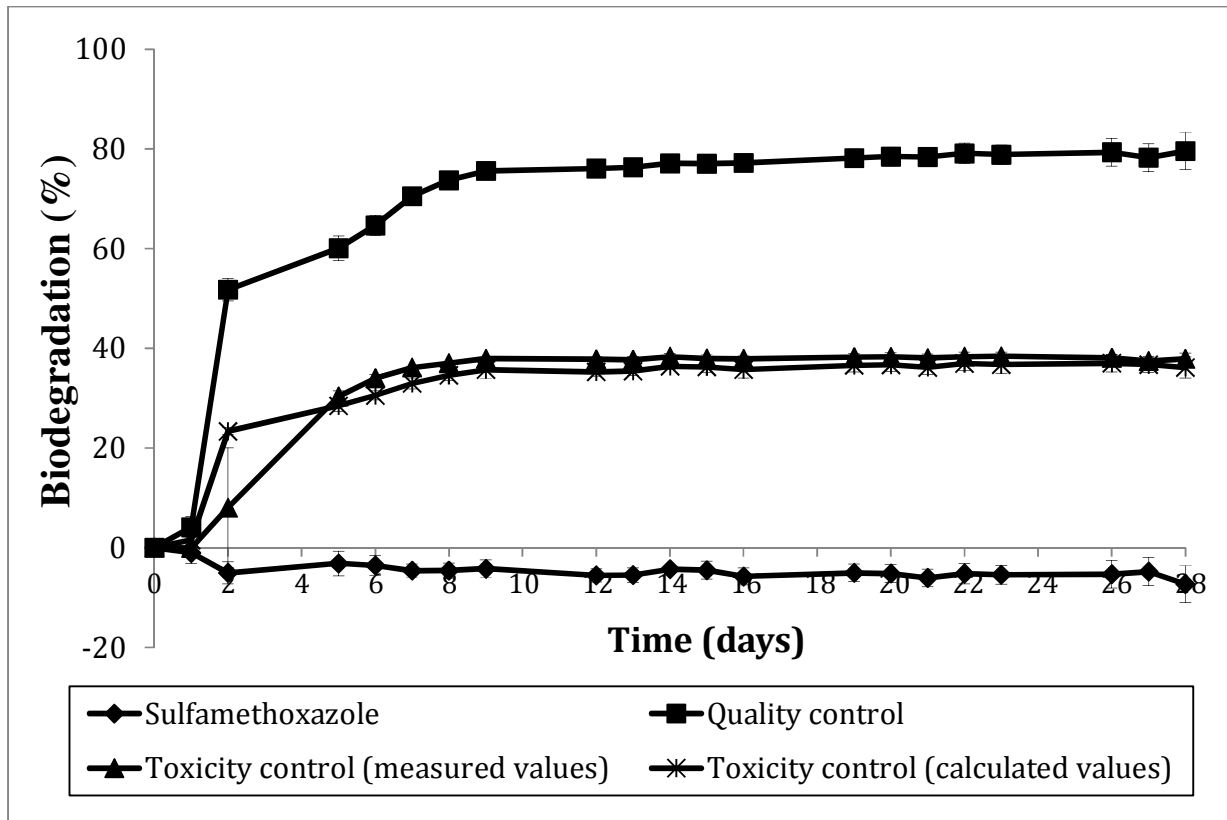


Figure S10. Closed Bottle test of SMX (n = 2).

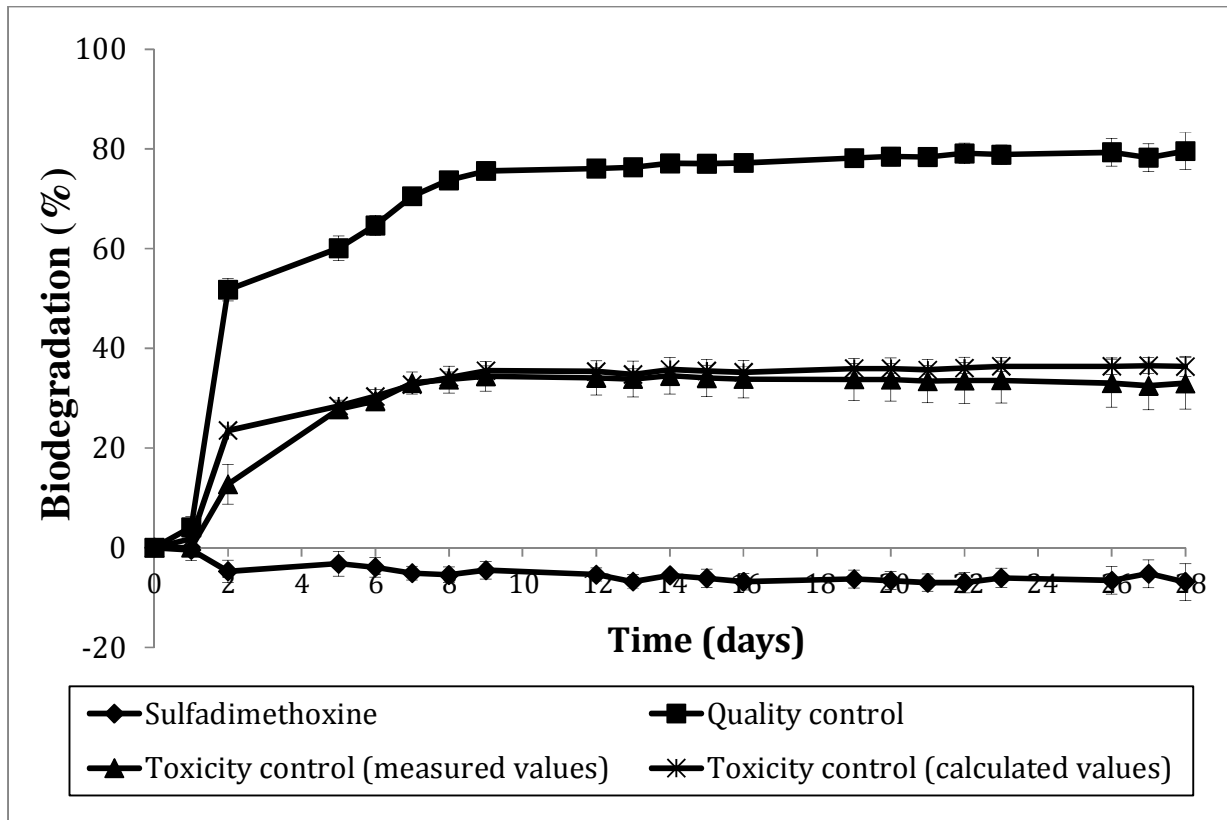


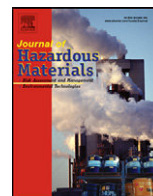
Figure S11. Closed Bottle test of SDX (n = 2).

Paper IV

Photolysis of sulfamethoxypyridazine in various aqueous media: aerobic biodegradation and photoproducts identification by LC-UV-MS/MS

Journal of Hazardous Materials 244-245: 654–661(2013)

doi:10.1016/j.jhazmat.2012.10.059



Photolysis of sulfamethoxy pyridazine in various aqueous media: Aerobic biodegradation and identification of photoproducts by LC-UV-MS/MS

Nareman D.H. Khaleel^{a,b}, Waleed M.M. Mahmoud^{a,b}, Ghada M. Hadad^b, Randa A. Abdel-Salam^b, Klaus Kümmerer^{a,*}

^a Sustainable Chemistry and Material Resources, Institute of Sustainable and Environmental Chemistry, Leuphana University Lüneburg, C13, DE-21335 Lüneburg, Germany

^b Pharmaceutical Analytical Chemistry Department, Faculty of Pharmacy, Suez Canal University, Ismailia 41522, Egypt

HIGHLIGHTS

- ▶ Sulfonamides are one of the most extensively used antibiotics in human and veterinary medicine.
- ▶ Sulfamethoxy pyridazine (SMP) underwent photodegradation in three different media.
- ▶ SMP was not readily biodegradable.
- ▶ SMP and some of its degradation products were identified by LC-UV-MS/MS.

ARTICLE INFO

Article history:

Received 27 July 2012

Received in revised form 5 October 2012

Accepted 28 October 2012

Available online 3 November 2012

Keywords:

Sulfonamides
Photodegradation
Biodegradation
Transformation products
Aquatic environment

ABSTRACT

Sulfonamides are one of the most frequently used antibiotics worldwide. Therefore, mitigation processes such as abiotic or biotic degradation are of interest. Photodegradation and biodegradation are the potentially significant removal mechanisms for pharmaceuticals in aquatic environments. The photolysis of sulfamethoxy pyridazine (SMP) using a medium pressure Hg-lamp was evaluated in three different media: Millipore water pH 6.1 (MW), effluent from sewage treatment plant pH 7.6 (STP), and buffered demineralized water pH 7.4 (BDW). Identification of transformation products (TPs) was performed by LC-UV-MS/MS. The biodegradation of SMP using two tests from the OECD series was studied: Closed Bottle test (OECD 301 D), and Manometric Respirometry test (OECD 301 F). In biodegradation tests, it was found that SMP was not readily biodegradable so it may pose a risk to the environment. The results showed that SMP was removed completely within 128 min of irradiation in the three media, and the degradation rate was different for each investigated type of water. However, dissolved organic carbon (DOC) was not removed in BDW and only little DOC removal was observed in MW and STP, thus indicating the formation of TPs. Analysis by LC-UV-MS/MS revealed new TPs formed. The hydroxylation of SMP represents the main photodegradation pathway.

© 2012 Elsevier B.V. All rights reserved.

1. Introduction

In the recent years, there has been a great effort to study the sources, occurrence, fate, and possible effects of human and veterinary pharmaceuticals in the environment [1]. Pharmaceuticals can reach the aquatic environment in a variety of ways: via wastewater effluent as a result of incomplete metabolism in the body after use in human or animal therapy, or through improper disposal by private households, hospitals and industrial units. Most of them are

insufficiently removed by wastewater treatment plants because of their polarity and high stability. So these pharmaceuticals can enter ground and drinking water at concentrations ranging from ng L^{-1} to $\mu\text{g L}^{-1}$ [2,3].

There is a high consumption of antibiotics in Asia and Africa, due to the lack of proper guidelines for their uses. The most frequently used antibiotics are the tetracyclines, penicillins and sulfonamides [4]. In the USA, 2.3% of the total antibiotics used are SNs (mainly sulfamethoxy pyridazine, sulfachloropyridazine, sulfamethazine and sulfathiazole). In the European Union, sulfonamides are the second most widely used veterinary antibiotics. In Kenya, as an example of African country, SNs account for 22% of active antimicrobials used in animal food production [5,6].

Sulfonamides are sulfanilamide derivatives that belong to an important class of synthetic antibacterial agents. They are used in human and veterinary medicine for the prevention and treatment

* Corresponding author at: Nachhaltige Chemie und Stoffliche Ressourcen, Institut für Nachhaltige Chemie und Umweltchemie, Leuphana Universität Lüneburg, C.13, Scharnhorststraße 1, D-21335 Lüneburg, Germany. Tel.: +49 4131 677 2893.

E-mail addresses: drndahshan@yahoo.com (N.D.H. Khaleel), Klaus.Kuemmerer@uni.leuphana.de (K. Kümmerer).

of diseases and infections, as well as feed additives in livestock production to promote growth in animals [7]. In bacteria, they inhibit folic acid synthesis by competitive inhibition of the enzyme dihydropteroate synthetase [8]. Sulfonamides are excreted from the human body and animal organisms partially unmetabolized but also as the biotransformation products. The metabolites glucuronide and N-4-acetylated sulfonamides are converted back to the parent form in liquid manure [9] and biological sewage treatment.

Sulfonamides are amphoteric, polar substances that are readily soluble in water. So, they possess high migration ability in the environment. Their traces are found in almost all kinds of biotopes, for example they are frequently detected in surface water at concentrations up to the $\mu\text{g L}^{-1}$ range [10–13]. Furthermore, it has been shown very recently that various antibiotics used as veterinary drugs can attach to dust particles and spread through the air of pig confinement buildings. That retrospective study provided the first evidence of a heretofore unsuspected direct risk for human health arising from the inhalation of dust contaminated with a cocktail of antibiotics [14].

Although the use of this group of pharmaceuticals has positive effects on treating many diseases, their release into the environment may induce the development of resistant bacterial strains. Continuous input of these pharmaceuticals into the environment can lead to a life-long consumption of low doses of potentially toxic antibiotics through drinking water resulting in adverse effects on humans and wildlife. As a result, there is growing interest in the development of innovative technologies to efficiently transform these compounds to non-toxic and pharmaceutically inactive byproducts [15].

Biotic degradation is the first line in the pharmaceuticals' degradation effluent treatment. Abiotic elimination processes such as photolysis, hydrolysis, and sorption are also of great importance for the aquatic fate of pharmaceutical compounds. Photolysis is among the important abiotic degradation mechanisms for many pharmaceutical pollutants' degradation. Therefore knowledge of the photodegradation pathways and kinetics are essential to predict the environmental fate of these pollutants in natural water [16].

Incomplete biotic or abiotic degradation occurring in the environment or within treatment can result in transformation products (TPs) with significantly different physical, chemical and toxic properties. They may even be more toxic than the parent compound [17–19]. Therefore, complete mineralization is desirable.

There are different results for biodegradation of sulfonamides [20]. Some articles claim that sulfonamides are resistant to biodegradation: Ingerslev and Hallig-Sorensen results indicated that sulfanilamide, sulfadiazine, sulfameter, and sulfabenzamide were not degraded in the respiratory screening test, which was performed according to the guidelines in ISO 9408 [21] and Alexy et al. results indicated that sulfamethoxazole was not readily biodegradable in the Closed Bottle Test (CBT) which simulate surface water [22]. Other authors reported that removal of sulfamethoxazole in a wastewater treatment plant was only 24% by biodegradation [23]. It was also reported that removal rates of sulfamethoxazole was between 50% and 60% [24]. However, an article has reported that the removal of sulfadiazine and sulfamethoxazole from wastewater during their biological treatment was practically 100% effective [25]. Also POSEJDON report reported that the removal efficiency of sulfonamides during routine wastewater treatment can vary from 0% to 90% [15]. Direct photolysis of many sulfonamides as sulfamethoxazole in different water compartments were studied [26,27]. No reported data about photolysis of SMP.

In order to obtain information on the biodegradation of SMP, two tests of the OECD series were used: the widely used CBT (OECD

301 D) working with low bacterial density, and the Manometric Respirometry Test (MRT, OECD 301 F) working with medium bacterial density were used. CBT is an aerobic biodegradation test with low nutrient and low bacterial density in order to simulate the conditions of surface water. It is recommended as a screening test of the first tier for the assessment of biodegradability of organic chemicals. Substances that pass the test are classified as readily biodegradable. They are also assumed to be readily biodegradable in sewage treatment plants and are therefore not expected to reach or accumulate in the aquatic environment [28].

Many analytical techniques can be used for the detection of TPs. Mass spectrometry combined with liquid chromatography (LC–MS) or gas chromatography (GC–MS) provides high sensitivity and ability to provide structural information of the compound. LC–MS has resulted in a robust and effective technique, which overcomes the drawbacks for polar compounds such as SNs associated to the use of GC–MS techniques. LC–MS is a technique suitable for analytes with a wider range of polarity, and has been shown to be a powerful tool for the identification of intermediates and unknown compounds in environmental samples [29,30].

The aim of our work was: (i) the comparison of the course of photolysis of SMP in various aqueous media, (ii) the comparison of the degree of mineralization of SMP in various aqueous media during photolysis, (iii) the identification of TPs of SMP in photolysis, and (iv) the studying of aerobic biodegradability of SMP.

2. Materials and methods

2.1. Reagents

All chemicals used in this study were of analytical grade and were used without further purification. SMP (CAS Number: 80-35-3) was purchased from Sigma–Aldrich (Steinheim, Germany). Acetonitrile and methanol (LiChrosolv[®], LC–MS grade) were purchased from VWR (Darmstadt, Germany). Ultrapure water was obtained from a SG Ultra Clear UV TM Water Purification System with TOC monitoring from SG Wasseraufbereitung und Regenerierstation GmbH (Barsbüttel, Germany). All the chemicals used as nutrients in biodegradability testing in this study were at least of >98.5% purity.

Samples of final effluent from sewage treatment plants (AGL Lüneburg, Germany, final effluent, 73 000 inhabitant, DOC = 11.28 mg L^{-1} , pH = 7.6) were collected in 1 L glass bottles, filtered, and freshly used in the photolysis experiment. Just before photolysis experiments, weighed amount of SMP was added to MW and STP effluent. In buffered demineralized water (BDW), certain volume from stock solution of SMP (100 g L^{-1}) in dimethylsulfoxide (DMSO) was added and samples were intensively mixed. The theoretical initial concentration of SMP was 10 mg L^{-1} in the resulting solutions. In case of MW and STP effluent, no buffer was added to SMP solutions and samples at natural pH (without correction) were used. In case of BDW pH 7.4, SMP stock solution was dissolved in phosphate buffer pH 7.4. Before illumination, the samples were sonicated for 5 min by means of sonication bath.

2.2. Analytical methods

SMP concentrations were quantified using HPLC–UV apparatus (Shimadzu, Duisburg, Germany) consisting of the software package Class LC10, the communication interface CBM-10 A, two LC-10 AT VP-pumps, auto sampler SIL-10, column oven CTO-10 AS VP, and diode array detector (SPD-M10). Chromatographic separation was performed on a RP-18 column (CC 125/4 NUCLEODUR 100-5 C18 ec, Macherey and Nagel, Düren, Germany) protected by a CC 8/4

HYPERSIL 100-3 (ODS) C18 ec, guard column. 0.1% formic acid in water (CH₂O₂: solution A) and 100% acetonitrile (CH₃CN: solution B) gradient method was used, by applying the following linear gradient: 0 min 1% B, 4 min 10% B, 11.50 min 20% B, 13 min 30% B, 15 min 45% B, 18 min 50% B, 23 min 1% B, 28 min 1% B, with 0.7 mL min⁻¹ flow rate. The injection volume was 20 µL, and the oven temperature was set to 25 °C. Detection wavelength was set to 270 nm.

In order to get information about the degree of mineralization, dissolved organic carbon (DOC) was determined with a Total Organic Carbon (TOC) Analyzer Shimadzu 5000A (TOC 5000, Shimadzu GmbH, Duisburg, Germany) in three replicates. The pH of the samples was measured by (WTW pH/ION 735P inoLab® Laboratory Ion Meters).

In order to make identification of the photolysis TPs, the irradiated samples were analyzed by LC-UV-MS/MS using a Bruker Daltonic Esquire 6000 plus ion-trap mass spectrometer equipped with a Bruker data analysis system and atmospheric pressure electrospray ionization interface (Bruker Daltonic GmbH, Bremen, Germany). The MS was connected to Agilent Technologies HPLC system (Agilent Technologies, Böblingen, Germany, HPLC 1100 series) consisting of two G1312A binary pumps, an ALS G1329A+ ALS Therm G1330B auto sampler, a G1316A column oven and a G1322A degasser (Agilent, Germany). Chromatographic separation was performed with the same gradient method used in HPLC-UV apparatus. The Esquire 6000 plus mass spectrometer was operated in positive polarity (S1, Supplementary material).

As a first step in the strategy of the TP identification in the LC-UV-MS/MS, chromatograms of the samples obtained at different irradiation times were compared with the chromatogram of 0 min sample (i.e. of the parent compound). The development of new peaks in the chromatograms of the samples obtained at different irradiation times is indicative of TP formation.

2.3. Photolysis

The photolysis experiments were conducted in a 1 L batch photoreactor, filled with about 800 mL of SMP solution, provided with a cooling system (WKL230, LAUDA, Berlin) and magnetic stirring. For the photolysis, a medium-pressure mercury lamp (TQ150, UV Consulting Peschl, Mainz, Germany) with ilmasil quartz immersion tube was used. The lamp emits polychromatic radiation in the range from 200 to 600 nm. The maximal intensities were at 254, 265, 302, 313, 366, 405/408, 436, 546, and 577/579 nm. Radiation flux Φ from 200 to 600 nm is 47 W.

During the entire experiment, mixtures were magnetically stirred, in order to ensure a constant mixing of the solutions. The temperature was maintained between 20 ± 2 °C by a circulating cooler (WKL230, LAUDA, Berlin) and pH was also monitored. Samples at different time intervals (0, 2, 4, 8, 16, 32, 64, and 128 min), during the irradiation were collected for the analysis of SMP concentration by HPLC-UV, LC-UV-MS/MS and TOC. Before analysis, all samples were filtered by 0.45 µm filter membranes (CHROMAFIL® Xtra. Typ: PES 45/25, Macherey-Nagel, Germany). Samples were analyzed directly or stored in the dark at -20 °C until analysis.

In order to estimate the kinetics of degradation processes in the three media, the following relationship was applied:

$$\ln \frac{C}{C_0} = -kt$$

where k is the reaction rate constant and t is irradiation time.

Half-lives were calculated by the following equation:

$$t_{1/2} = \ln \frac{2}{k}$$

2.4. Biodegradation testing

2.4.1. Closed Bottle Test (OECD 301 D, CBT)

The CBT is recommended as a first, simple test for the assessment of the biodegradability of organic compounds in the environment. This test can be applied even if the tested substance possesses very limited water solubility, no other organic matter is present and therefore interference and elimination by sorption is minor [31,32]. The standard test period for the CBT is 28 days, it was performed with a low bacterial density (10²–10⁵ colony forming units per mL (CFU mL⁻¹), low nutrient content, and at room temperature (20 ± 1 °C) in the dark as described elsewhere in detail [33,34].

The test system consisted of four different series. Each series was run in parallel (Table 1). The readily biodegradable sodium acetate and the test substance (SMP) were adjusted to a concentration corresponding to 5 mg L⁻¹ theoretical oxygen demand (ThOD). All test vessels were inoculated with an aliquot from the effluent of the municipal STP in AGL Lüneburg, Germany (73 000 inhabitant equivalents). Two drops of inoculum were added to 1 L of medium, which results in about 500–1000 CFU mL⁻¹. The influence of two different inocula source on the degradation pattern of SMP was investigated. The test was repeated with an aliquot from the municipal STP in Kenzingen, Germany (13 000 inhabitant equivalents).

The progress of aerobic biodegradation was monitored by measuring the oxygen concentration in the test vessels with an optical oxygen sensor system (Fibox 3 PreSens, Regensburg, Germany) using sensor spots in the bottles. It allows detection of the oxygen concentration without opening the test vessels. During the course of the test, temperature and pH were also monitored.

The toxicity control can be used to check if there is any possible inhibitory effect. This allows for the recognition of false negative results caused by the toxicity of the test compound against the degrading bacteria. Toxicity was assessed by comparing oxygen consumption as measured in the toxicity controls with the predicted level computed from the oxygen consumption in the quality control and in the test vessel, respectively. A compound is labeled toxic if the difference between the predicted amount of oxygen consumption and the measured one exceeds 25% [35].

Biodegradability is expressed as the percentage of oxygen consumption based on ThOD. A test compound is classified as “readily biodegradable” if biodegradation, expressed as a percentage of oxygen consumed in the test vessel, exceeds 60% within a period of 10 days after the oxygen consumption reached 10% ThOD [35]. After 14 days of testing at least 60% of the reference substance sodium acetate has to have decomposed. Samples at day 0 and day 28 were taken and stored at -20 °C for later HPLC-UV, and LC-UV-MS/MS analysis.

2.4.2. Manometric Respiratory Test (OECD 301 F, MRT)

MRT is another method for assessing the degradability of chemicals. It used higher bacterial concentration and higher concentration of the test substance. It was performed in accordance to the test guidelines in the dark at room temperature (20 ± 1 °C) under gentle stirring [36]. The testing scheme for the MRT is equivalent to that of the CBT, but it was performed with a higher bacterial density of approximately (5–10) × 10⁶ CFU mL⁻¹ and a higher sodium acetate and test compound concentration (Table 1). Sodium acetate and test compound concentration corresponded to a ThOD of 30 mg L⁻¹.

The test consisted of five different series; (test substance, toxicity control, sterile control, blank, and quality control bottles). The sterile control contained sodium azide in order to account

Table 1
Composition of biodegradation test series in the CBT (1–4), MRT (1–5).

Test series	1 Blank	2 Quality control	3 Test compound	4 Toxicity control	5 Sterile/negative control
SMP ^a	–	–	+	+	+
Mineral medium	+	+	+	+	+
Inoculum	+	+	+	+	–
Reference substance (sodium acetate)	–	+	–	+	–
Sodium azide	–	–	–	–	+

^a SMP concentration in CBT: 4.3 mg L⁻¹, and in MRT: 17.9 mg L⁻¹.

for abiotic degradation. All test bottles were inoculated with an aliquot from the effluent of the STP AGL Lüneburg, Germany. 80 mL of inoculum were added to 1 L of medium. The influence of two different inocula source on the degradation pattern of SMP was investigated. The test was repeated with an aliquot from the effluent of the municipal STP in Kenzingen, Germany. The OxiTop OC110-system (WTW GmbH, Weilheim, Germany) was used as measuring system. The bottles of the OxiTop OC110-system were firmly closed with measuring heads which cover an exactly defined gas volume.

The process of aerobic biodegradation was monitored by the measurement of carbon dioxide (CO₂) production. The measuring heads contained sodium hydroxide which reacted with the generated CO₂ and converted it to sodium carbonate so remove the CO₂ from the gas phase. The resulting pressure decrease shows the corresponding oxygen consumption. At the end of the test all values were transmitted to the computer for further processing. The measurement of the pressure and the following biological oxygen demand (BOD) calculation were automatically performed by the system. Measurements were made in duplicate, i.e. two individual bottles were used in parallel, respectively. Blank values were subtracted from the quality, toxicity control and test compound values, respectively, and final biodegradation in percentage was calculated. The validity criterion is a removal of 60% ThOD within a 14 days window for the quality control. Samples at test begin and end were taken and stored at –20 °C for later HPLC-UV, and LC-UV-MS/MS analysis.

2.5. STP effluent sample preparation and extraction

Solid-phase extraction (SPE) was performed for STP effluent photolysis sample preparation and cleanup. A manual 10-opened vacuum manifold system connected to diaphragm vacuum pump MZ 2 C (Vacuuband, GMBH, Germany) was used for the extraction. ISOLUTE ENV+ SPE cartridge was used with 200 mg packing material and 6 mL reservoir purchased from Biotage (Sweden). The cartridge sorbent is a hyper cross-linked hydroxylated polystyrene-divinyl benzene copolymer based solid-phase material. Before extraction, the cartridge was conditioned with 10 mL methanol pH 2.5 (adjusted with acetic acid), followed by 5 mL methanol, and then equilibrated with 12 mL 0.5 M citric acid buffer (pH 5). A photolysis sample volume of 3 mL was acidified with 4 mL of 1 M citric acid buffer (pH 5), sonicated for 2 min by using sonication bath before it was applied to the cartridge at a flow rate not exceeding 2 mL min⁻¹. The loaded cartridge was washed with 10 mL MW. Finally, the loaded cartridge was eluted with 10 mL methanol. Following the elution, the filtrate was evaporated to dryness under gentle nitrogen stream. The dried extract was dissolved in 1 mL of 0.1% formic acid in water (CH₂O₂: solution A) and 100% acetonitrile (CH₃CN: solution B) (90:10, v/v). Non-spiked STP effluent samples were also extracted in all experiments, using the same procedure, in order to detect any possible contribution of the water matrix to the SMP and its photolysis TPs signals. The sorbent was never allowed to dryness during the whole procedure.

3. Results and discussion

The performance of the HPLC-UV used method was evaluated according to International Conference on Harmonization (ICH) recommendations [37]. Calibration curves for seven concentrations ranging between 0.5 mg L⁻¹ and 5 mg L⁻¹ showed good linearity with coefficient of determination (*R*²) of 0.9998. Intra-day repeatability for three concentration levels were 0.06, 0.34, and 1.65% RSD, respectively, while the inter-day ones were 0.23, 0.34, and 0.43% RSD, respectively. The detection and quantification limits were 0.05, and 0.1 mg L⁻¹, respectively. The low limits of detection confirmed an acceptable sensitivity for the method. The method can be used for the analysis of SMP and its photolysis TPs in MW and in STP effluent matrix which indicates good specificity.

3.1. Biodegradation of SMP

The CBT was performed according to test guidelines for SMP. Criteria of the OECD test guideline were met, as more than 60% ThOD of the quality control substrate (sodium acetate) was biodegraded within 14 days, classifying this test valid according to the OECD. The biodegradation value for SMP determined in the CBT by monitoring the oxygen concentration was –3.48% as an average for the two test bottles. This value is characterizing this substance as being not readily and not at all biodegradable. In both toxicity control bottles, no toxic effects were seen. For a better overview, results of test and toxicity series were averaged, respectively (Fig. 1). HPLC-UV measurements confirmed that no elimination of SMP took place.

The MRT was performed according to test guidelines for SMP. The test was valid since 60% ThOD of the quality control substrate was biodegraded within 10 days (Fig. 2). The biodegradation value for SMP determined in the MRT was 6% as an average for the four test bottles. In the toxicity control, biodegradation of 36.33% belongs to the degradation of sodium acetate, which indicates no toxicity against the bacteria present. No degradation was found in the sterile control bottle. These values are characterizing this substance as being not biodegradable. HPLC-UV measurements confirmed that no elimination of SMP took place.

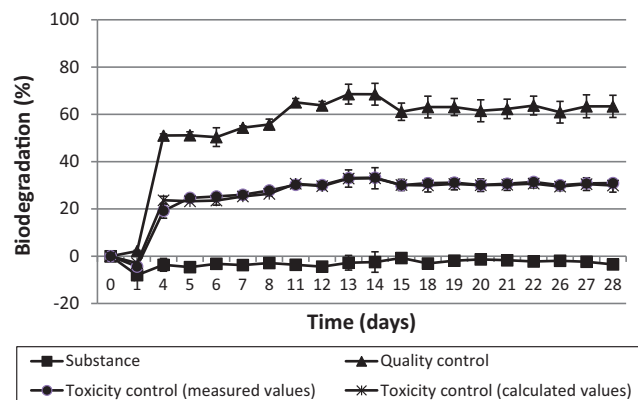


Fig. 1. Closed Bottle test of SMP (*n* = 2).

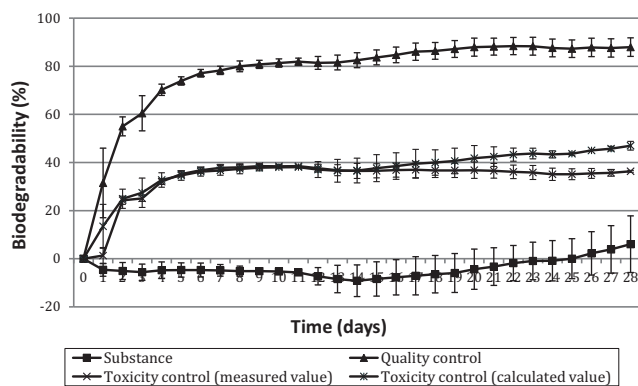


Fig. 2. Manometric Respiratory test of SMP ($n = 4$).

The results of using other inocula were nearly the same in both CBT and MRT as it showed biodegradation resistance with little differences in biodegradation values. Thus indicating that, the type of inoculum has no effect on the overall results of SMP degradation pattern.

3.2. Photolysis

SMP solutions prepared in MW (pH=6.1), STP (pH=7.6), and BDW pH 7.4 were irradiated under the conditions described in Section 2. The dynamic of the photolytic degradation of SMP in the three media are presented in Fig. 3. It was proved that SMP underwent photolysis degradation under the used UV-Lamp.

In the MW experiment, HPLC analysis showed a degradation of about 80% of the initial concentration of SMP (10 mg L^{-1}) was observed during the first 32 min of irradiation. Afterwards the degradation rate slowed down relatively until 128 min where 98.8% of the initial concentration was removed. An explanation for this slowdown can be the presence of newly formed TPs, which may absorb the radiation, and thus, screen the remaining parental analyte from the irradiation source [38]. In the BDW experiment, a slight difference in kinetics was observed; where it showed the slowest degradation rate. Perhaps this is because sulfonamide photolysis is strongly affected by the pH or buffer salts [39,40]. At pH 7.4 (BDW), SMP is in its anionic form ($\text{pK}_{a1} = 7.19 \pm 0.3$ and $\text{pK}_{a2} = 2.18 \pm 0.50$) which can be less accessible to photolysis.

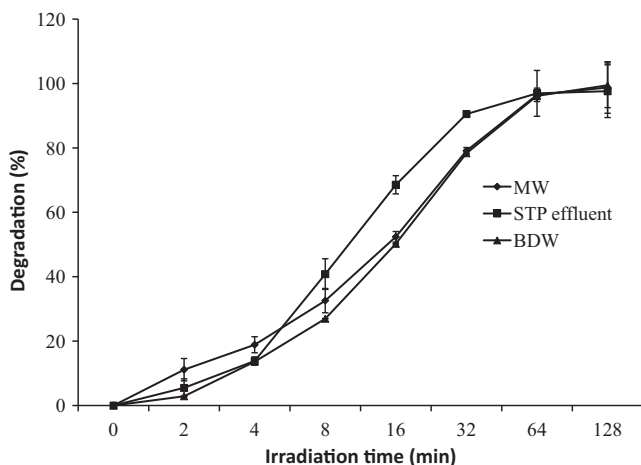


Fig. 3. Degradation of SMP (10 mg L^{-1}) during UV-irradiation in the studied three different media ($n = 3$, error bars include analysis).

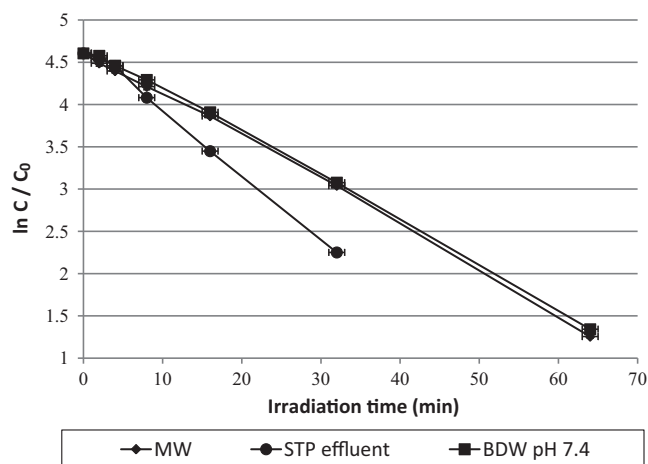


Fig. 4. Kinetics of the photolytic degradation of SMP (10 mg L^{-1}) in the three investigated media ($n = 3$, error bars include analysis).

In the STP effluent experiment, also a slight difference in the kinetics from MW was observed; where until 4 min of irradiation, the photolysis rate in STP effluent is a little lower than in the MW, then from 4 to 64 min, the photolysis rate increased slightly and was a little faster than in the MW, but finally at 128 min in both cases nearly 99% of the initial concentration was removed. The observed differences may be due to the presence of photosensitizers in STP effluent which may enhance photolysis rates [26]. This means that the influence of pH and salinity in STP effluent is over compensated by the photosensitizers present such as humic acids, nitrates which results in a higher degradation rate.

The degree of DOC removal in samples was monitored as a measure of mineralization of SMP during irradiation. The results indicate that, after 128 min irradiation in the experiments in MW and STP effluent, mineralization observed was about 24% and 13% respectively. In BDW, no DOC variation was observed, thus demonstrating the formation of intermediates more persistent to photolysis.

Based on data in the literature, it was assumed that photolysis of sulfonamides was pseudo-first-order [27,41]. For MW and BDW pH 7.4, a linear relationship of $\ln C/C_0$ versus t (from 0 min to 64 min), but for STP effluent, a linear relationship of $\ln C/C_0$ versus t (from 0 min to 32 min) was established based on the results obtained for reactions conducted in the three media. After these times the degradation rate slowed down as described in Section 3 and did not obey first order kinetics model. Continuous lines illustrate first-order processes (Fig. 4). From the results, it can be concluded that SMP photolysis in the three media fitted the pseudo-first-order kinetic model until 64 min (for MW and BDW pH 7.4) and 32 min (for STP effluent). The rate constants were 0.052 , 0.076 , and 0.052 min^{-1} and half-life times were 13.34, 9.12, and 13.45 min in MW, STP effluent, and BDW pH 7.4, respectively.

3.3. Identification of intermediates and SMP degradation pathway

The TPs generated during photolysis studies are considered as potential environmental pollutants. Thus, identification of the most relevant TPs is important to predict the environmental impact of original compound. For this reason, LC-UV-MS/MS analyses based on accurate mass measures was performed during the photolysis assays. Sample pre-treatment (SPE) was performed only in case of STP effluent photolysis samples, but it did not lead to any losses of intermediates which could give false

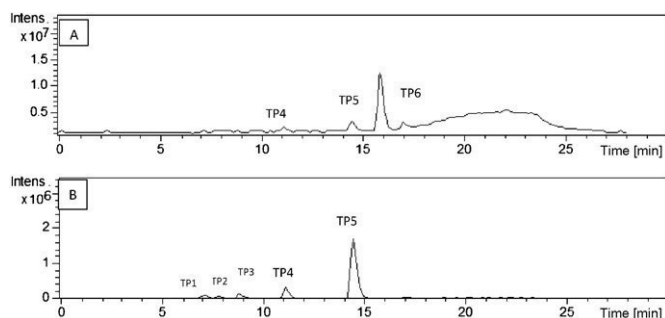


Fig. 5. Mass spectra of SMP sample after 32 min UV-irradiation in MW showing (A) total ion chromatogram (TIC), (B) extracted ion chromatogram (EIC) at 297 m/z .

results. This was confirmed by comparing LC-UV-MS/MS chromatograms of one sample with and without SPE. No differences were observed.

The development of new peaks in the chromatograms of the samples obtained at different irradiation times is indicative of possible TPs formation. For example, Fig. 5A shows the total ion chromatogram obtained after 32 min of SMP photolysis in MW, where some new peaks (TP4, TP5, and TP6), not present in 0 min sample, were detected.

As the low response of some TPs in the chromatographic system can hamper their detection in the total ion chromatograms, the obtaining of extracted ion chromatograms of ions suspected to be present is useful. Thus, since hydroxylation reactions are typical of photolytic processes, extracted ion chromatograms at m/z 297 $[M+H+16]^+$ and 315 $[M+H+32]^+$, corresponding to the possible formation of mono- and di-hydroxyl derivatives of SMP, were checked. Only in case of mono-hydroxylation at m/z 297, the presence of five peaks, at different retention times (7.2, 7.8, 8.8, 11.1, and 14.5 min) were observed. These compounds are labeled as TP1, TP2, TP3, TP4 and TP5 in Fig. 5B. From these results it can be concluded

that hydroxylation of SMP represents the main photolysis pathway. One can assume that the photolysis TPs generated could still have part of their structure common with the parent compound, and thus present similar fragments. The extracted ion chromatograms at different smaller m/z were also checked, but no signal were seen. Six TPs were detected. TP5 was the main TP detected during the photolysis assays. TP5 was reported previously as a photocatalytic product of SMP [42]. In case of STP effluent and BDW, only one TP appears which labeled as TP4.

For the six formed TP peaks, depending on the peak intensity of each TP, up to MS^3 spectra were generated using the Auto MS^n mode in order to have structural information on the photolysis TPs and make structural elucidation (Table 2). The most intense precursor ion peak (TP5) at 297.1 m/z gave several product ions, which were fragmented again so that a complex fragmentation pattern of mass spectra emerged. A MS^2 fragment with 172 m/z indicates hydroxylation at the benzene ring. This position was determined based on the observation of the fragmentation pattern of SMP, which yielded a characteristic fragment at m/z 156 $[C_6H_6NO_2S]$. This fragment arises from the cleavage of the bond between the aminophenylsulfone and the methoxypyridazineamine moieties. The absence of the fragment at m/z 156 and the appearance of a new fragment at m/z 172 $[C_6H_6NO_3S]$ suggested the addition of the (OH) radical in the benzene ring [16]. Fig. 6 gives a proposal for the structure of TP5, $m/z=297.1$ according to the acquired MS^{1-3} data. The 2nd most intense peak (TP6), $m/z=295.1$ eluted at $t_r=16.9$ min with $M+14$ can indicate N-oxidation of SMP fragmentation pattern confirmed this TP as SMP N-oxide. The product ion (MS^2 214 m/z) indicates extrusion of a SO_2 moiety with dehydroxylation. Fig. 7 shows the possible fragmentation pattern for TP6 at $m/z=295.1$ according to the acquired MS^{1-3} data. The fragmentation patterns for the TPs 1, 2, 3, and 4 confirmed that these are hydroxylation products but it is difficult to know the exact position of the hydroxylation (Table 2).

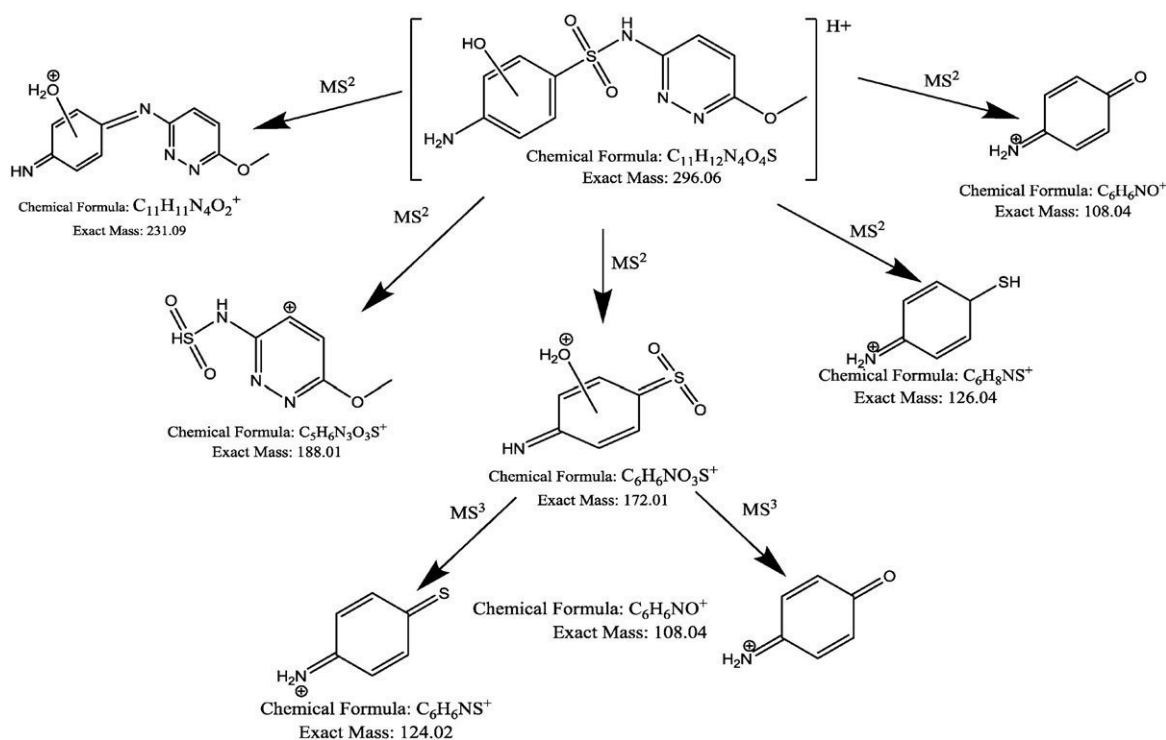


Fig. 6. Fragmentation scheme for the 1st main photolysis TP of SMP, TP5; 297.1 m/z according to the acquired MS^{1-3} spectra.

Table 2
Chromatographic and mass spectrometer parameters for SMP and its photolysis TPs in LC-UV-MS/MS using gradient method (positive mode; RT, retention time; *m/z*, mass to charge ratio; relative abundance in brackets).

Compound	RT (min)	Precursor ions (<i>m/z</i>)	Product ions (<i>m/z</i>)
SMP standard	15.8	281.1 (100).	281.1 → 156 (100), 188 (39.46), 126.2 (33.9), 215 (22.79), 108.2 (16.19), 92.2 (10.03).
TP 1	7.2	297.1 (44.36).	297.1 → 215.1 (100), 231 (29.65), 203 (28.3), 158 (11.06), 279 (5.93)
TP 2	7.8	297.1 (39.31).	297.1 → 215.1 (100), 203 (36.29), 279 (22.13), 231 (20.89), 186 (9.32).
TP 3	8.8	297.1 (78.48).	297.1 → 215.1 (100), 231 (16.3), 200 (14.87).
TP 4	11.1	297.1 (100).	297.1 → 217 (100).
TP 5	14.5	297.1 (100).	297.1 → 126.1 (100), 172 (22.7), 188 (18.9), 108.2 (5.15), 231 (5.27).
TP 6	16.9	295.1 (100).	295.1 → 214 (100), 186 (94.96), 231 (47.93), 174 (12.2), 202 (6.3), 278 (4.27).

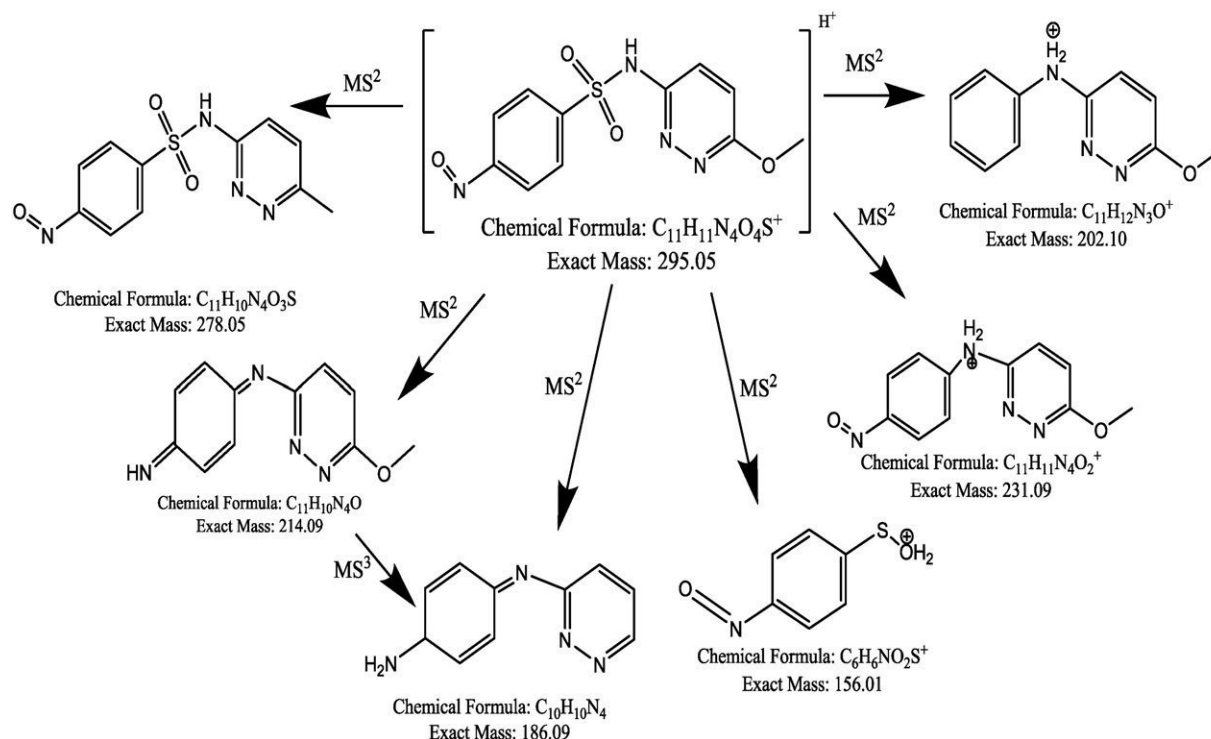


Fig. 7. Fragmentation scheme for TP6 of SMP 295.1 *m/z* according to the acquired MS^{1–3} spectra.

4. Conclusion

The results obtained in the present study showed that SMP was UV-photolysed in MW, STP effluent, and BDW. The three different aqueous media spiked with 10 mg L⁻¹ of SMP were tested, showing that SMP was completely removed after 128 min of irradiation. Although almost total disappearance of SMP was reached, little or no removal of DOC was obtained, which indicates the presence of stable intermediates. LC-UV-MS/MS analysis permitted the identification of six TPs during SMP photolysis. In parallel, the results of biodegradation tests indicate that SMP is not readily biodegradable under conditions of low bacterial density (CBT) and medium bacterial density (MRT). From these results, the application of other combined treatments is necessary to guarantee the total degradation and mineralization of SMP. Also further research on SMP and its TPs, including their biodegradability, analysis of environmental samples, as well as toxicity tests are strongly recommended in order to know its environmental impact.

Acknowledgments

The authors wish to thank Evgenia Logunova and Janin Westphal (Sustainable Chemistry and Material Resources, Leuphana University Lüneburg) for their help with the experiments. Waleed M.M.

Mahmoud Ahmed thanks the Ministry of Higher Education and Scientific Research of the Arab Republic of Egypt (MHESR) and the German Academic Exchange Service (DAAD) for their scholarship.

Appendix A. Supplementary data

Supplementary data associated with this article can be found, in the online version, at <http://dx.doi.org/10.1016/j.jhazmat.2012.10.059>.

References

- [1] K. Kümmerer (Ed.), *Pharmaceuticals in the Environment: Sources, Fate, Effects and Risks*, third ed., Springer, Berlin, Heidelberg, 2008, pp. 3–21.
- [2] G. Hamscher, H.T. Pawelzick, H. Höper, H. Nau, Different behavior of tetracyclines and sulfonamides in sandy soils after repeated fertilization with liquid manure, *Environ. Toxicol. Chem.* 24 (2005) 861–868.
- [3] H. Shaaban, T. Górecki, Optimization and validation of a fast ultrahigh-pressure liquid chromatographic method for simultaneous determination of selected sulphonamides in water samples using a fully porous sub-2 μm column at elevated temperature, *J. Sep. Sci.* 35 (2012) 216–224.
- [4] I. Ali, H.Y. Aboul-Enein, K. Kümmerer, Analyses of drugs and pharmaceuticals in the environment, in: B. Xing, N. Senesi, P.M. Huang (Eds.), *Biophysico-Chemical Processes of Anthropogenic Organic Compounds in Environmental Systems*, John Wiley & Sons, Inc, 2011, pp. 439–462.
- [5] A.K. Sarmah, M.T. Meyer, A.B.A. Boxall, A global perspective on the use sales, exposure pathways, occurrence, fate and effects of veterinary antibiotics (VAs) in the environment, *Chemosphere* 65 (2006) 725–759.

- [6] M.J. García-Galán, M. Silvia Díaz-Cruz, D. Barceló, Identification and determination of metabolites and degradation products of sulfonamide antibiotics, *Trends Anal. Chem.* 27 (2008) 1008–1022.
- [7] E. Tolika, V. Samanidou, I. Papadoyannis, Development and validation of an HPLC method for the determination of ten sulfonamide residues in milk according to 2002/657/EC, *J. Sep. Sci.* 34 (2011) 1627–1635.
- [8] L. Hu, P.M. Flanders, P.L. Miller, T.J. Strathmann, Oxidation of sulfamethoxazole and related antimicrobial agents by TiO₂ photocatalysis, *Water Res.* 41 (2007) 2612–2626.
- [9] S.A.I. Mohring, I. Strzysch, M.R. Fernandes, T.K. Kiffmeyer, J. Tuerk, G. Hamscher, Degradation and elimination of various sulfonamides during anaerobic fermentation: a promising step on the way to sustainable pharmacy? *Environ. Sci. Technol.* 43 (2009) 2569–2574.
- [10] E. Zuccato, D. Calamari, M. Natangelo, R. Fanelli, Presence of therapeutic drugs in the environment, *Lancet* 355 (2000) 1789–1790.
- [11] W. Baran, E. Adamek, J. Ziemińska, A. Sobczak, Effects of the presence of sulfonamides in the environment and their influence on human health, *J. Hazard. Mater.* 196 (2011) 1–15.
- [12] M.J. García-Galán, M.S. Díaz-Cruz, D. Barceló, Occurrence of sulfonamide residues along the Ebro River basin: removal in wastewater treatment plants and environmental impact assessment, *Environ. Int.* 37 (2011) 462–473.
- [13] M.J. García-Galán, T. Garrido, J. Fraile, A. Ginebreda, M.S. Díaz-Cruz, D. Barceló, Application of fully automated online solid phase extraction–liquid chromatography–electrospray–tandem mass spectrometry for the determination of sulfonamides and their acetylated metabolites in groundwater, *Anal. Bioanal. Chem.* 399 (2011) 795–806.
- [14] G. Hamscher, H.T. Pawelzick, S. Sczesny, H. Nau, J. Hartung, Antibiotics in dust originating from a pig-fattening farm: a new source of health hazard for farmers? *Environ. Health Perspect.* 111 (2003) 1590–1594.
- [15] T.A. Ternes, M. Laure, J.-H. Thomas, N. Kreuzinger, H. Siegrist, Project acronym POSEIDON Contract No. EVK1-CT-2000-00047: assessment of technologies for the removal of pharmaceuticals and personal care products in sewage and drinking water facilities to improve the indirect potable water reuse, 2004.
- [16] A.G. Trovó, R.F.P. Nogueira, A. Agüera, C. Sirtori, A.R. Fernández-Alba, Photodegradation of sulfamethoxazole in various aqueous media: persistence, toxicity and photoproducts assessment, *Chemosphere* 77 (2009) 1292–1298.
- [17] M. Petrovic, D. Barceló, LC–MS for identifying photodegradation products of pharmaceuticals in the environment: pharmaceutical-residue analysis, *Trends Anal. Chem.* 26 (2007) 486–493.
- [18] M. Bergheim, R. Gieré, K. Kümmerer, Biodegradability and ecotoxicity of tramadol ranitidine, and their photoderivatives in the aquatic environment, *Environ. Sci. Pollut. Res.* 19 (2012) 72–85.
- [19] M. Garcia-Käufer, T. Haddad, M. Bergheim, R. Gminski, P. Gupta, N. Mathur, K. Kümmerer, V. Mersch-Sundermann, Genotoxic effect of ciprofloxacin during photolytic decomposition monitored by the in vitro micronucleus test (MNvit) in HepG2 cells, *Environ. Sci. Pollut. Res.* 19 (2012) 1719–1727.
- [20] W. Baran, E. Adamek, A. Sobczak, A. Makowski, Photocatalytic degradation of sulfa drugs with TiO₂, Fe salts and TiO₂/FeCl₃ in aquatic environment—kinetics and degradation pathway, *Appl. Catal. B* 90 (2009) 516–525.
- [21] F. Ingerslev, B. Halling-Sørensen, Biodegradability properties of sulfonamides in activated sludge, *Environ. Toxicol. Chem.* 19 (2000) 2467–2473.
- [22] R. Alexy, T. Kümpel, K. Kümmerer, Assessment of degradation of 18 antibiotics in the Closed Bottle Test, *Chemosphere* 57 (2004) 505–512.
- [23] T.A. Ternes, M. Bonerz, N. Herrmann, B. Teiser, H.R. Andersen, Irrigation of treated wastewater in Braunschweig, Germany: an option to remove pharmaceuticals and musk fragrances, *Chemosphere* 66 (2007) 894–904.
- [24] M. Clara, B. Strenn, O. Gans, E. Martinez, N. Kreuzinger, H. Kroiss, Removal of selected pharmaceuticals, fragrances and endocrine disrupting compounds in a membrane bioreactor and conventional wastewater treatment plants, *Water Res.* 39 (2005) 4797–4807.
- [25] X. Peng, Z. Wang, W. Kuang, J. Tan, K. Li, A preliminary study on the occurrence and behavior of sulfonamides, ofloxacin and chloramphenicol antimicrobials in wastewaters of two sewage treatment plants in Guangzhou, China, *Sci. Total Environ.* 371 (2006) 314–322.
- [26] C.C. Ryan, D.T. Tan, W.A. Arnold, Direct and indirect photolysis of sulfamethoxazole and trimethoprim in wastewater treatment plant effluent, *Water Res.* 45 (2011) 1280–1286.
- [27] M.V.N. Mouamfon, W. Li, S. Lu, Z. Qiu, N. Chen, K. Lin, Photodegradation of sulfamethoxazole under UV-light irradiation at 254 nm, *Environ. Technol.* 31 (2010) 489–494.
- [28] N. Nyholm, The European system of standardized legal tests for assessing the biodegradability of chemicals, *Environ. Toxicol. Chem.* 10 (1991) 1237–1246.
- [29] Z.L. Cardeal, A.G. Souza, L.C. Amorim, Analytical methods for performing pesticide degradation studies in environmental samples, in: M. Stoytcheva (Ed.), *Pesticides—Formulations, Effects, Fate, InTech*, Rijeka, 2011, pp. 595–617.
- [30] A. Längin, R. Alexy, A. König, K. Kümmerer, Deactivation and transformation products in biodegradability testing of β -lactams amoxicillin and piperacillin, *Chemosphere* 75 (2009) 347–354.
- [31] K. Tiede, M. Hasselöf, E. Breitbarth, Q. Chaudhry, A. Boxall, Considerations for environmental fate and ecotoxicity testing to support environmental risk assessments for engineered nanoparticles, *J. Chromatogr. A* 1216 (2009) 503–509.
- [32] F.H. Frimmel, R. Niessner, Nanoparticles in the water cycle: properties, in: *Analysis and Environmental Relevance*, Springer-Verlag, Berlin, Heidelberg, 2010.
- [33] K. Kümmerer, J. Menz, T. Schubert, W. Thielemans, Biodegradability of organic nanoparticles in the aqueous environment, *Chemosphere* 82 (2011) 1387–1392.
- [34] W.M.M. Mahmoud, K. Kümmerer, Captopril and its dimer captopril disulfide: photodegradation, aerobic biodegradation and identification of transformation products by HPLC–UV and LC–ion trap–MSⁿ, *Chemosphere* 88 (2012) 1170–1177.
- [35] OECD, Organisation for Economic Co-operation and Development Guideline for Testing of Chemicals 301 D: Ready Biodegradability. Closed Bottle Test, OECD Publishing, Paris, 1992.
- [36] OECD, Organisation for Economic Co-operation and Development Guideline for Testing of Chemicals 301 F: Ready Biodegradability. Manometric Respiratory Test, OECD Publishing, Paris, 1992.
- [37] International Conference on Harmonization, Validation of Analytical Procedures: Text and Methodology Q2 (R1), 2005.
- [38] E.A. Gad Kariem, M.A. Abounassif, M.E. Hagga, H.A. Al-Khamees, Photodegradation kinetic study and stability-indicating assay of danazol using high-performance liquid chromatography, *J. Pharm. Biomed. Anal.* 23 (2000) 413–420.
- [39] A.L. Boreen, W.A. Arnold, K. McNeill, Photochemical fate of sulfa drugs in the aquatic environment: sulfa drugs containing five-membered heterocyclic groups, *Environ. Sci. Technol.* 38 (2004) 3933–3940.
- [40] P. Sukul, M. Spittler, Sulfonamides in the environment as veterinary drugs, *Rev Environ. Contam. Toxicol.* 187 (2006) 67–101.
- [41] M.J. García-Galán, Kinetic studies and characterization of photolytic products of sulfamethazine, sulfapyridine and their acetylated metabolites in water under simulated solar irradiation, *Water Res.* 46 (2012) 711–722.
- [42] L.-C. Chuang, C.-H. Luo, C.-J. Lin, Degradation characteristics of sulfamethoxy-pyridazine in water by ozonation and photocatalysis, *Procedia Eng.* 15 (2011) 5133–5137.

***Supplementary material S1**

The operating conditions of the source were: -500 V end plate, +4500 V capillary voltage, 30.00 Psi (206 kPa) nebulizer pressure, 12 L min⁻¹ dry gas flow at a dry temperature of 350 °C. The selected lens and block voltages were: +112.5 V capillary exit, +10.38 V octopole 1, +1.74 V octopole 2, 300 Vpp octopole reference amplitude, 30.6 V skimmer, 33.6 trap drive, -6.0 V lens one and -73.0 V lens two. The scan range was determined from m/z 40 to 1000 and the scan time was 200 ms.

Paper V

Photodegradation, photocatalytic and aerobic
biodegradation of sulfisomidine and identification of
transformation products By LC–UV-MS/MS

CLEAN – Soil, Air, Water 40 (11) 1244-1249 (2012)

DOI: 10.1002/clen.201100485

Faten Sleman¹
Waleed M. M. Mahmoud^{2,3}
Rolf Schubert⁴
Klaus Kümmerer²

Research Article

Photodegradation, Photocatalytic, and Aerobic Biodegradation of Sulfisomidine and Identification of Transformation Products by LC–UV-MS/MS

¹Department of Environmental Health Sciences, University Medical Center Freiburg, Freiburg, Germany

²Sustainable Chemistry and Material Resources, Institute of Sustainable and Environmental Chemistry, Leuphana University Lüneburg, Lüneburg, Germany

³Faculty of Pharmacy, Pharmaceutical Analytical Chemistry Department, Suez Canal University, Ismailia, Egypt

⁴Department of Pharmaceutical Technology and Biopharmacy, Albert-Ludwigs University, Freiburg, Germany

Much attention has recently been devoted to the fate and effects of pharmaceuticals in the water cycle. Removal of antibiotics in effluents by photo-treatment or biodegradation is a topic currently under discussion. Degradation and removal efficiencies of sulfisomidine (SUI) by photodegradation and aerobic biodegradability were studied. SUI behavior was monitored during photolysis and photocatalysis (catalyst titanium dioxide) using 150-W medium-pressure Hg lamp. Also an aerobic bacterial degradation test from the OECD series (closed bottle test (CBT, OECD 301 D)) was performed. The primary elimination of SUI was monitored. Structures of photo-degradation products were assessed by chromatographic separation on a C18 column with ultraviolet detection at 270 nm and ion trap MS. The results demonstrate that SUI is not readily biodegradable in CBT. Photo catalysis was more effective than photolysis. SUI underwent photodegradation and several SUI photoproducts were identified. Accordingly, the photodegradation pathway of SUI was postulated. When reaching the aquatic environment, SUI and its photo products can constitute a risk to the environment.

Keywords: Antibiotic; Biodegradation; Closed bottle test; Pharmaceutical; Photo-treatment; Titanium dioxide

Received: September 2, 2011; *revised:* December 17, 2011; *accepted:* December 27, 2011

DOI: 10.1002/cle.201100485

1 Introduction

Pharmaceuticals have received much attention as organic pollutants in aquatic environments as they have been continuously discharged into the aquatic environment for decades without any restrictions [1–8].

In recent years an increasing number of studies focusing on pharmaceuticals, illustrate their persistency and unwanted effects on the aquatic environment. Antibiotics are among the most important groups of pharmaceuticals used to control the undesirable effects of microbial infection in human and veterinary medicine as well as aquaculture [9–11]. Antibiotics have attracted special attention from researchers around the world due to the possibility of increased bacterial resistance and other adverse effects, e.g., in waste water and sewage system by affecting the microbial community that may appear because of their presence in the aquatic environment [3, 12–15].

Antibiotics and their metabolites enter the wastewater treatment and can then reach surface water, groundwater and even drinking water [16–20]. Sulfa drugs are one class of antibiotics that are usually used as human and veterinary medicines, and they are frequently

detected in surface water at concentrations up to the $\mu\text{g L}^{-1}$ range [7, 8, 21, 22]. The widespread occurrence of sulfa compounds as contaminants in the aquatic environment has increased attention in this group of pharmaceuticals within the last years. Like the other types of antibiotics, the release of sulfa drugs into the environment is related primarily to the potential for the development of antimicrobial resistance in microorganisms.

An example of a sulfa drug that is frequently used for veterinary purposes is sulfisomidine (SUI). However, there are no experimental data for the environmental fate of SUI such as degradation by light and bacteria. SUI is a short-acting sulfonamide with properties similar to those of sulfamethoxazole. It has been used topically for skin or vaginal infections and has also been given orally. This pharmaceutical preparation for humans is not used nowadays [23]. SUI has been detected in sewage water treatment plants [7]. Biodegradation in sewage treatment plants, water bodies, photodegradation in effluent treatment, surface water, and potable water treatment are the most essential processes that may play a role in controlling the fate of sulfa drugs in the water cycle. Photocatalysis is one of these light-related technical treatment processes for advanced effluent treatment processes. Its potential has been demonstrated to degrade and mineralize a variety of organic and inorganic pollutants [24, 25]. Titanium dioxide (TiO_2) has emerged as a powerful photocatalyst due to several properties such as its high photoactivity, stability, chemical inertness, and relatively low cost [26, 27].

In this work, in order to obtain information about the biodegradation of SUI, the closed bottle test (CBT) was used according to OECD 301D [28]. This is an aerobic biodegradation test with low nutrient and bacterial density in order to simulate the conditions of surface

Correspondence: Professor K. Kümmerer, Nachhaltige Chemie und Stoffliche Ressourcen, Institut für Nachhaltige Chemie und Umweltchemie, Leuphana Universität Lüneburg, C.13, Scharnhorststraße 1, D-21335 Lüneburg, Germany
E-mail: klaus.kuemmerer@leuphana.de

Abbreviations: CBT, closed bottle test; LOD, limits of detection; LOQ, limits of quantification; NPOC, non-purgeable organic carbon; SUI, sulfisomidine; ThOD, theoretical oxygen demand

waters. According to the OECD, it is recommended as a screening test of the first tier for the assessment of biodegradability of organic chemicals. Substances that pass the test are classified as readily biodegradable. They are also assumed to be readily biodegradable in sewage treatment plants and are therefore not expected to reach or accumulate in the aquatic environment [29]. In order to get information on dead-end transformation products formed, the primary elimination of SUI was monitored with a complete study of the structural elucidation of the photodegradation products by LC-UV and LC ion trap MS (LC-MS/MS). Because of low biodegradability found the photodegradation of SUI by UV radiation was studied. The focus of these experiments was the identification and characterization of the degradation products formed during the photolysis. Moreover, the photocatalytic degradation of SUI with TiO₂ suspensions was investigated in order to compare the photodegradation process efficiency between photolysis and photocatalysis.

2 Experimental

2.1 Chemicals

All the chemicals used as nutrients in biodegradability testing in this study were at least of >98.5% purity. Acetonitrile (LiChrosolv[®], gradient grade), and formic acid (analytical grade) were purchased from Merck (Darmstadt, Germany). HPLC-grade water was generated using a Milli-Q water-purification system from Millipore (Molsheim, France). Titanium dioxide, TiO₂ (Degussa P25, Frankfurt/Main, Germany). SUI was obtained from Sigma-Aldrich (Sigma-Aldrich, Steinheim, Germany).

2.2 Photo-degradation

In the present study, both the photolysis and photocatalysis (with TiO₂) were studied. The experiment was conducted in a 1L batch photo-reactor provided with a cooling system (WKL230, LAUDA, Berlin) and magnetic stirring. For the photolysis, a medium-pressure mercury lamp (TQ150, UV Consulting Peschl, Mainz) with a quartz immersion tube was used which has a UV Transmission of 92%. The lamp emits polychromatic radiation in the range from 200 to 436 nm. The maximal intensities were at 254, 265, 302, 313, and 366 nm. During the photo-reaction is necessary to ensure a constant mixing of the solution. Prior to each experiment, the lamp was warmed up for 2 min. SUI samples were taken at different time intervals from 0 to 256 min for the analysis of the SUI concentration and the degree of mineralization by non-purgeable organic carbon (NPOC), LC-UV-Vis, and LC-MS/MS. NPOC was determined with a TOC (total organic carbon) analyzer (TOC 5000, Shimadzu GmbH, Duisburg, Germany) in three replicates. SUI concentration was 10 mg L⁻¹ in Milli-Q purified water. The pH of the solution was neutral. The experiment was performed at 18–20°C and Milli-Q purified water was used to prepare all of the solutions.

For photocatalytic degradation studies, a TiO₂ concentration of 100 mg L⁻¹ was used. Before indirect photolysis, 10 mg L⁻¹ SUI

solution with 100 mg L⁻¹ TiO₂ was kept in the dark for 30 min under stirring to reach adsorption equilibrium on the TiO₂ surface. Samples at different time intervals during the irradiation were collected, centrifuged at 4000 rpm for 5 min and then filtered through 0.2-μm filter membranes (CHROMAFIL[®] Xtra.Type: PES 20/25, Macherey-Nagel, Germany). Samples were stored in the dark at 5°C until analysis.

2.3 Biodegradation testing: Closed bottle test (OECD 301 D, CBT)

The CBT was performed according to test guidelines [28] with a low bacterial density (10²–10⁵ colony forming units (CFU) mL⁻¹) and low nutrient content at room temperature (20 ± 1°C) in the dark [30, 31]. The standard test period for the CBT is 28 days. According to the guidelines, after 14 days of testing at least 60% of the reference substance sodium acetate has to have decomposed. The test consisted of four different series and each series were run as duplicates. Each test bottle contained the same amount of mineral salt solution. An aliquot from the effluent of a local municipal sewage treatment plant (Kenzingen, Germany, 13 000 inhabitant equivalents) was used to inoculate all test bottles. The “blank” series contained only mineral medium and inoculum, while the “quality control” series contained readily biodegradable sodium acetate as the only carbon source. The “actual test” and the “toxicity control” series contained the test substance (SUI). Besides SUI the “toxicity control” series also contained sodium acetate. The amount of SUI and sodium acetate corresponded to a theoretical oxygen demand (ThOD) of 5 mg L⁻¹ (Tab. 1). The toxicity control shows a possible inhibitory effect. This allows for the recognition of false negative results caused by the toxicity of the test compound against the degrading bacteria. Toxicity was assessed by comparing oxygen consumption measured in the toxicity control bottles with the predicted level computed from the oxygen consumption in the quality control and in the test bottle containing only the test compound, respectively. A compound is defined as toxic if the difference greater than 25% between the predicted oxygen consumption and the measured one [28]. A test compound is classified as “readily biodegradable” if biodegradation, expressed as a percentage of oxygen consumed in the test vessel (ThOD), exceeds 60% within a period of 10 days after the oxygen consumption reaches 10% ThOD. The process of aerobic biodegradation was monitored for 28 days by measuring oxygen concentration in the test vessels with Fibox 3 (Fiberoptic oxygen meter connected with Temperature sensor PT 1000) (PreSens, Precision Sensing GmbH, Regensburg, Germany). pH values were measured at day 0 and 28 for qualitative reasons. Monitoring of primary elimination by LC-UV-Vis, and LC-MS/MS.

The samples were measured for their primary elimination using HPLC-UV-Vis (with ultraviolet detection at 270 nm) and ESI-LC-MS/MS (ion trap) in order to get more knowledge about the elimination process in the NPOC measurement, i.e., about the substructures of the molecule containing the main chromophore (aromatic ring).

Table 1. Test system of the closed bottle test

	Blank	Quality control	Test	Toxicity control
Mineral medium	x	x	x	x
Inoculum (2 drops L ⁻¹)	x	x	x	x
SUI (3.35 mg L ⁻¹) (ThOD = 5 mg L ⁻¹)	–	–	x	x
Sodium acetate (6.4 mg L ⁻¹) (ThOD = 5 mg L ⁻¹)	–	x	–	x

“x” = addition, “–” = no addition.

Table 2. HPLC-Gradient system for SUI analysis

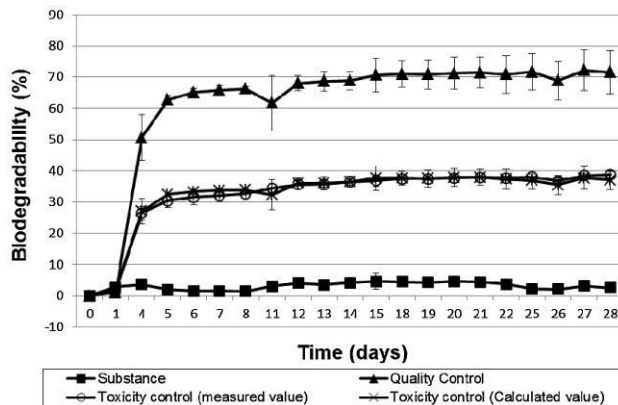
Time (min)	Solvent A %	Solvent B %
0	1	99
3	1	99
3.5	5	95
5	5	95
7	20	80
13	20	80
15	50	50
21	50	50
23	20	80
27	5	95
30	1	99

A Shimadzu HPLC apparatus (Duisburg, Germany) consisting of the software package Class LC10, the communication interface CBM-10 A, two LC-10 AT VP-pumps, column oven CTO-10 AS VP, auto sampler SIL-10, and diode array detector (SPD-M10) was used. Chromatographic separation was carried out on a NUCLEODUR C18 ec column (70×3 mm, $3 \mu\text{m}$, Macherey and Nagel, Düren, Germany) in combination with a HYPERSIL C18 ec guard cartridge (8×4 mm, $5 \mu\text{m}$). The gradient system consisting of 0.1% formic acid in water (solution A) and 100% acetonitrile (solution B) were used by applying the following linear gradient (Tab. 2). The flow rate was set at 0.6 mL min^{-1} with UV detection at 270 nm, and the column heater was set to 20°C . Total run time was 30 min. The sample injection volume was $50 \mu\text{L}$.

LC-MS/MS detection and quantification was carried out on a Bruker Daltonic Esquire 6000 plus ion-trap mass spectrometer equipped with a Bruker data analysis system and atmospheric pressure electrospray ionization (API-ESI) interface (Bruker Daltonic GmbH, Bremen, Germany). It was operated in the positive mode. The MS was connected to an Agilent HPLC 1100 series system (Agilent Technologies, Böblingen, Germany). Prior to analysis of the samples, a standard solution of SUI (10 mg L^{-1}) was infused via a syringe pump (Cole-Parmer 74900 series) at a flow rate of $4 \mu\text{L min}^{-1}$ in order to tune the mass spectrometer for SUI, optimizing the ionization source parameters, lens voltages and trap conditions in the Smart Tune mode of the Esquire software. The source operating conditions were: 30.00 psi nebulizer pressure, 12 L min^{-1} dry gas flow at a dry temperature of 350°C , -500 V end plate, and -3950 V capillary voltage. The selected lens and block voltages were: $+62.5 \text{ V}$ capillary exit, $+7.19 \text{ V}$ octopole 1, $+1.68 \text{ V}$ octopole 2, 266.7 Vpp octopole reference amplitude, 15 V skimmer, 33.7 trap drive, -1.2 V lens one, and -46.0 V lens two. The scan range was determined from m/z 40 to 1000 and the scan time was 200 ms. For further investigation of possible degradation products, the samples of interest were analyzed by auto MSⁿ mode, where product ions of interest were isolated and fragmented again in order to identify degradation products of SUI. Quantification and detection was performed with the Bruker data analysis system. A stock solution of SUI ($100 \mu\text{g mL}^{-1}$) was prepared in water. Standard solutions were prepared from the stock solutions by serial dilutions. Triplicate $50\text{-}\mu\text{L}$ SUI injections for LC-UV-Vis and LC-MS/MS were made for each concentration and chromatographed under the specified chromatographic conditions described below.

3 Results and discussion

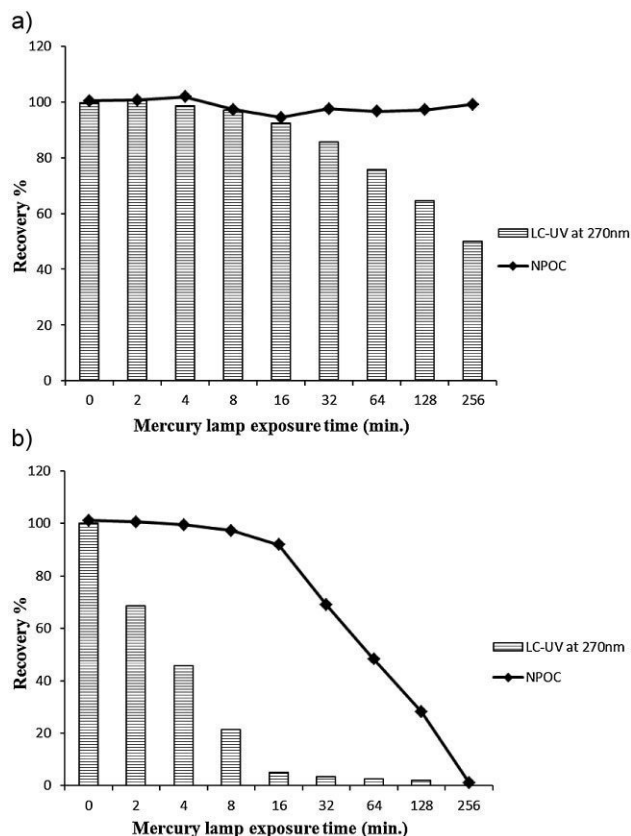
The aim of this research was to assess biodegradability and photodegradability of SUI in aqueous solution.

**Figure 1.** Closed bottle test of SUI ($n=2$).

3.1 Degradation of SUI

In accordance with the test guidelines, the CBT experiment was valid. SUI was not readily biodegradable in the CBT. SUI was not toxic for the biocenosis presented in the test according to the results of the measured toxicity control series (Fig. 1).

SUI photolysis (UV light) was not accompanied by any decrease in NPOC concentration (Fig. 2). So SUI photodegradation did not

**Figure 2.** Time course of recovery % of SUI concentration by NPOC and LC-UV at 270 nm during photodegradation (a) without TiO_2 , and (b) photocatalysis in the presence of 100 mg L^{-1} TiO_2 as catalyst; SUI concentration 10 mg L^{-1} in each case.

result in any mineralization. Therefore, it was checked by LC if any primary elimination occurred: The primary elimination of SUI was monitored and structures of photo-products were assessed by combined with LC-UV-Vis-MS/MS. SUI photocatalytic degradation was accompanied by a decrease of NPOC concentration, leading to complete mineralization of the SUI sample after 256 min of treatment.

3.2 LC-UV-Vis and LC-ion trap-MS/MS analysis

SUI standards were used to establish a calibration curve. Calibration curve was prepared by plotting the peak area versus the concentration. Linear relationships were obtained. The limits of detection (LOD) and quantification (LOQ) were determined based on signal to noise ratio. LOD ($S/N=3$) and LOQ ($S/N=10$) were derived from the injections of standard solutions serially diluted until the analyte signal at least three and ten times the noise of the blank response for LOD and LOQ, respectively. The LOD and LOQ were about 0.05 and 0.1 $\mu\text{g mL}^{-1}$, respectively.

The concentration of SUI ($t_r=10$ min) was monitored during photodegradation. The LC-UV-Vis chromatographic analysis revealed that many degradation products were formed during the irradiation. After 256 min of irradiation (treatment without catalyst) about 50% of SUI was eliminated, thereby increasing the number and concentration of degradation products with the duration of irradiation (Fig. 2a). These photo-transformation products already began to appear after 4 min of photolysis. The total ion chromatograms (TICs) of ($t_r=10.3$ min) the samples showed four photodegradation products at t_r 1.1, 2, 3,

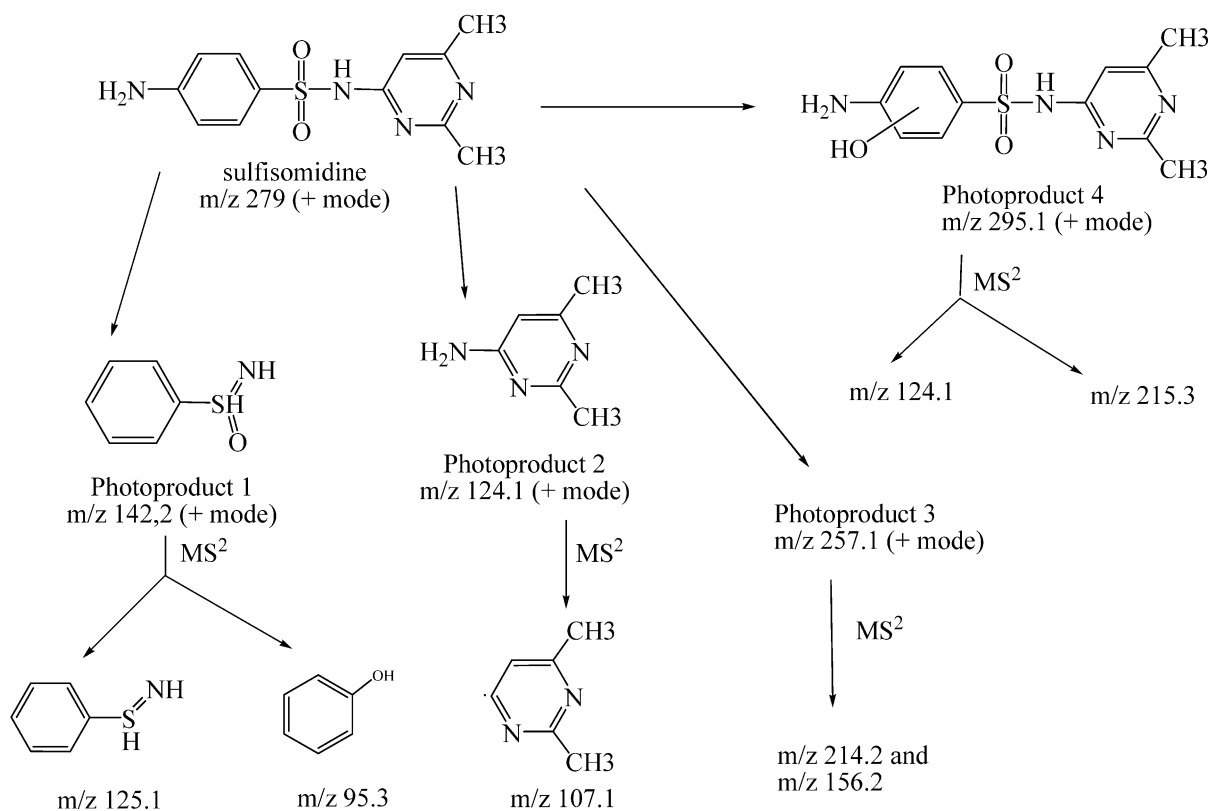
and 9.2 min for photodegradation products I, II, III, and IV, respectively.

In order to get more information about these transformation products, the sample taken after 128 min of photolysis was selected, as the peak areas of SUI and its transformation products were high. So the MS^1 mode of the mass spectrometer was used in order to investigate and perform MS^2 and MS^3 fragmentation of the isolated photoproduct ions (Scheme 1). The found transformation products show that the degradation can occur by separation of a pyrimidine ring, or cleavage of the sulfonamide functional group, and by the addition of hydroxyl groups (stemming from hydroxyl radicals). Other studies of structurally related sulfa drugs containing six-membered heterocyclic substituents have shown that the photolytic degradation leads to formation of another transformation product $m/z=214$, which is produced by loss of SO_2 [32]. In the case of SUI, the product $m/z=214$ was not found as a transformation product.

In photocatalysis, SUI was completely mineralized (Fig. 2b). The transformation products that are found in the photolysis are the same formed in the photocatalysis but in photocatalysis the transformation products are more rapidly formed. However, within the course of the treatment the concentration of these products increased until 16 min of photocatalysis after that it began to decrease until complete mineralization.

4 Conclusion

Under conditions of low bacterial density (CBT which simulate the situation in surface water) SUI was not readily biodegraded.



Scheme 1. Suggested photodegradation pathway of SUI during the photolysis.

Photodegradation can be an important loss process in limiting SUI persistence in the aquatic environment. SUI was completely mineralized by photocatalysis but no mineralization occurred during photolysis. Therefore, photocatalysis is the better method to remove these substances fully from water [33] without residual transformation products if treatment time is long enough. In contrast, photolysis, e.g., within effluent treatment, in surface water by sunlight, and drinking water treatment will lead to stable photo-products of unknown fate and toxicity. In this respect, photocatalysis is the better technical method to remove these substances from the wastewater and drinking water. However, if nanoparticles are used as a photocatalyst, these may cause unwanted effects if they are not removed properly.

Furthermore, it was demonstrated that for structure elucidation of formed unknown transformation products a combination of LC–UV and MS is necessary. HPLC–UV, LC–MS/MS, and DOC monitoring gave valuable knowledge about the resulting transformations products and the degree of mineralization. Further research on SUI and its transformation product, including analysis of environmental samples (e.g., surface waters), as well as toxicity tests are therefore strongly recommended in order to know its environmental impact.

Acknowledgments

Faten Sleman thanks Damaskus University (Syria) for a scholarship. Waleed M. M. Mahmoud Ahmed thanks the Ministry of Higher Education and Scientific Research of the Arab Republic of Egypt (MHESR) and the German Academic Exchange Service (DAAD) for their scholarship (GERLS program).

The authors have declared no conflict of interest.

References

- [1] E. R. Cooper, T. C. Siewicki, K. Phillips, Preliminary Risk Assessment Database and Risk Ranking of Pharmaceuticals in the Environment, *Sci. Total Environ.* **2008**, 398 (1-3), 26.
- [2] C. G. Daughton, T. A. Ternes, Pharmaceuticals and Personal Care Products in the Environment: Agents of Subtle Change?, *Environ. Health Perspect.* **1999**, 107 (6), 907.
- [3] K. Kümmerer, Antibiotics in the Aquatic Environment – a Review, Part I, *Chemosphere* **2009**, 75 (4), 417.
- [4] K. Kümmerer, Antibiotics in the Aquatic Environment – a Review, Part II, *Chemosphere* **2009**, 75 (4), 435.
- [5] K. Kümmerer, The Presence of Pharmaceuticals in the Environment due to Human Use – Present Knowledge and Future Challenges, *J. Environ. Manage.* **2009**, 90 (8), 2354.
- [6] M. Huerta-Fontela, M. T. Galceran, F. Ventura, Occurrence and Removal of Pharmaceuticals and Hormones through Drinking Water Treatment, *Water Res.* **2011**, 45 (3), 1432.
- [7] M. J. García-Galán, M. S. Díaz-Cruza, D. Barceló, Occurrence of Sulfonamide Residues along the Ebro River Basin: Removal in Wastewater Treatment Plants and Environmental Impact Assessment, *Environ. Int.* **2011**, 37 (2), 462.
- [8] M. García-Galán, T. Garrido, J. Fraile, A. Ginebreda, M. Díaz-Cruz, D. Barceló, Application of Fully Automated Online Solid Phase Extraction–Liquid Chromatography–Electrospray–Tandem Mass Spectrometry for the Determination of Sulfonamides and Their Acetylated Metabolites in Groundwater, *Anal. Bioanal. Chem.* **2011**, 399 (2), 795.
- [9] C. Cháfer-Pericás, Á. Maquieira, R. Puchades, B. Company, J. Miralles, A. Moreno, Multiresidue Determination of Antibiotics in Aquaculture Fish Samples by HPLC–MS/MS, *Aquacult. Res.* **2010**, 41 (9), e217.
- [10] T. Bergan, Antibiotic Usage in Nordic Countries, *Int. J. Antimicrob. Agents* **2001**, 18 (3), 279.
- [11] K. Kümmerer (Ed.), *Pharmaceuticals in the Environment: Sources, Fate, Effects and Risks*, 3rd Ed., Springer, Berlin, Heidelberg **2008**.
- [12] C. G. Daughton, I. S. Ruhoy, Environmental Footprint of Pharmaceuticals: The Significance of Factors beyond Direct Excretion to Sewers, *Environ. Toxicol. Chem.* **2009**, 28 (12), 2495.
- [13] K. Kümmerer, A. Henninger, Promoting Resistance by the Emission of Antibiotics from Hospitals and Households into Effluent, *Clin. Microbiol. Infect.* **2003**, 9 (12), 1203.
- [14] I. M. Gould, A Review of the Role of Antibiotic Policies in the Control of Antibiotic Resistance, *J. Antimicrob. Chemother.* **1999**, 43 (4), 459.
- [15] M. A. Gilliver, M. Bennett, M. Begon, S. M. Hazel, C. A. Hart, Enterobacteria: Antibiotic Resistance Found in Wild Rodents, *Nature* **1999**, 401 (6750), 233.
- [16] J.-Y. Pailler, A. Krein, L. Pfister, L. Hoffmann, C. Guignard, Solid Phase Extraction Coupled to Liquid Chromatography–Tandem Mass Spectrometry Analysis of Sulfonamides, Tetracyclines, Analgesics and Hormones in Surface Water and Wastewater in Luxembourg, *Sci. Total Environ.* **2009**, 407 (16), 4736.
- [17] U. Schulte-Oehlmann, J. Oehlmann, W. Püttmann, Pharmaceutical Agents in the Environment, Their Entries, Occurrence, and an Inventory of Them, *Umweltwiss. Schadst. Forsch.* **2007**, 19 (3), 168.
- [18] K. Kümmerer, A. Eitel, U. Braun, P. Hubner, F. Daschner, G. Mascart, M. Milandri, et al., Analysis of Benzalkonium Chloride in the Effluent from European Hospitals by Solid-phase Extraction and High-performance Liquid Chromatography with Post-column Ion-pairing and Fluorescence Detection, *J. Chromatogr. A* **1997**, 774 (1-2), 281.
- [19] K. Kümmerer, *Habilitation Treatise*, Universität Freiburg, Freiburg **1998**.
- [20] K. Kümmerer, E. Schramm, Röntgenkontrastmittel in der Umwelt – eine genauere Betrachtung, *Krankenhauspharmazie* **1998**, 19, 481.
- [21] E. Zuccato, D. Calamari, M. Natangelo, R. Fanelli, Presence of Therapeutic Drugs in the Environment, *Lancet* **2000**, 355 (9217), 1789.
- [22] D. W. Kolpin, E. T. Furlong, M. T. Meyer, E. M. Thurman, S. D. Zaugg, L. B. Barber, H. T. Buxton, Pharmaceuticals, Hormones, and Other Organic Wastewater Contaminants in U.S. Streams, 1999–2000: A National Reconnaissance, *Environ. Sci. Technol.* **2002**, 36 (6), 1202.
- [23] S. C. Sweetman, *Martindale: The Complete Drug Reference*, 36th Ed., Pharmaceutical Press, London, Chicago **2009**.
- [24] M. Klavarioti, D. Mantzavinou, D. Kassinos, Removal of Residual Pharmaceuticals from Aqueous Systems by Advanced Oxidation Processes, *Environ. Int.* **2009**, 35 (2), 402.
- [25] S. Esplugas, D. M. Bila, L. G. T. Krause, M. Dezotti, Ozonation Advanced Oxidation Technologies to Remove Endocrine Disrupting Chemicals (EDCs) and Pharmaceuticals and Personal Care Products (PPCPs) in Water Effluents, *J. Hazard. Mater.* **2007**, 149 (3), 631.
- [26] A. Fujishima, T. N. Rao, D. A. Tryk, Titanium Dioxide Photocatalysis, *J. Photochem. Photobiol.* **2000**, 1 (1), 1.
- [27] D. Keane, S. Basha, K. Nolan, A. Morrissey, M. Oelgemöller, J. M. Tobin, Photodegradation of Famotidine by Integrated Photocatalytic Adsorbent (IPCA) and Kinetic Study, *Catal. Lett.* **2011**, 141 (2), 300.
- [28] Organisation for Economic Co-operation and Development, *OECD Guideline for Testing of Chemicals 301 D: Ready Biodegradability. Closed Bottle Test*, OECD Publishing, Paris **1992**.
- [29] N. Nyholm, The European System of Standardized Legal Tests for Assessing the Biodegradability of Chemicals, *Environ. Toxicol. Chem.* **1991**, 10 (10), 1237.

- [30] K. Kümmerer, A. Al-Ahmad, T. Steger-Hartmann, Epirubicin Hydrochloride in the Aquatic Environment – Biodegradation and Bacterial Toxicity, *Umweltmed. Forsch. Prax.* **1996**, 1 (3), 133.
- [31] C. Trautwein, K. Kümmerer, J. W. Metzger, Aerobic Biodegradability of the Calcium Channel Antagonist Verapamil and Identification of a Microbial Dead-end Transformation Product Studied by LC-MS/MS, *Chemosphere* **2008**, 72 (3), 442.
- [32] A. L. Boreen, W. A. Arnold, K. McNeill, Triplet-sensitized Photodegradation of Sulfa Drugs Containing Six-membered Heterocyclic Groups: Identification of an SO₂, *Environ. Sci. Technol.* **2005**, 39 (10), 3630.
- [33] L. Hu, P. M. Flanders, P. L. Miller, T. J. Strathmann, Oxidation of Sulfamethoxazole and Related Antimicrobial Agents by TiO₂ Photocatalysis, *Water Res.* **2007**, 41 (12), 2612.

Paper VI

Aquatic photochemistry, abiotic and aerobic
biodegradability of thalidomide: identification of stable
transformation products by LC-UV-MSⁿ

Science of the Total Environment 463–464: 140–150 (2013)

DOI: [10.1016/j.scitotenv.2013.05.082](https://doi.org/10.1016/j.scitotenv.2013.05.082)



Aquatic photochemistry, abiotic and aerobic biodegradability of thalidomide: Identification of stable transformation products by LC–UV–MSⁿ



Waleed M.M. Mahmoud ^{a,b}, Christoph Trautwein ^a, Christoph Leder ^a, Klaus Kümmerer ^{a,*}

^a Sustainable Chemistry and Material Resources, Institute of Sustainable and Environmental Chemistry, Faculty of Sustainability, Leuphana University of Lüneburg, Scharnhorststraße 1/C13, DE-21335 Lüneburg, Germany

^b Pharmaceutical Analytical Chemistry Department, Faculty of Pharmacy, Suez Canal University, Ismailia 41522, Egypt

HIGHLIGHTS

- Thalidomide (TD) undergoes photolysis with mercury and xenon lamp.
- New photoproducts were identified by HPLC–MSⁿ and QSAR.
- Partial mineralization by UV-photolysis was obtained.
- TD and its photoproducts were not readily biodegradable experimentally and by QSAR.

ARTICLE INFO

Article history:

Received 5 March 2013

Received in revised form 3 May 2013

Accepted 26 May 2013

Available online xxxx

Editor: Damia Barcelo

Keywords:

Aquatic environment

Biodegradation

Dead-end transformation product

Pharmaceuticals

Photodegradation

QSAR

ABSTRACT

Thalidomide (TD), besides being notorious for its teratogenicity, was shown to have immunomodulating and anti-inflammatory activities. This is why recently TD became a promising drug for the treatment of different cancers and inflammatory diseases. Yet nothing is known about the environmental fate of TD, which therefore was assessed experimentally and by *in silico* prediction programs (quantitative structure activity relationship (QSAR) models) within this study. Photolytic degradation was tested with two different light sources (medium-pressure mercury lamp; xenon lamp) and aerobic biodegradability was investigated with two OECD tests (Closed Bottle test (CBT), Manometric Respirometry test (MRT)). An additional CBT was performed for TD samples after 16 min of UV-photolysis. The primary elimination of TD was monitored and the structures of its photo-, abiotic and biodegradation products were elucidated by HPLC–UV–Fluorescence–MSⁿ. Furthermore, elimination of dissolved organic carbon was monitored in the photolysis experiment. LC–MS revealed that new photolytic transformation products (TPs) were identified, among them two isomers of TD with the same molecular mass. These TPs were different to the products formed by biodegradation. The experimental findings were compared with the results obtained from the *in silico* prediction programs where e.g. a good correlation for TD biodegradation in the CBT was confirmed. Moreover, some of the identified TPs were also structurally predicted by the MetaPC software. These results demonstrate that TD and its TPs are not readily biodegradable and not fully mineralized by photochemical treatment. They may therefore pose a risk to the aquatic environment due to the pharmacological activity of TD and unknown properties of its TPs. The applied techniques within this study emphasize the importance of QSAR models as a tool for estimating environmental risk assessments.

© 2013 Elsevier B.V. All rights reserved.

1. Introduction

Public and scientific concerns about the occurrence of pharmaceutical compounds in the environment have become an important issue in the last decade. Pharmaceuticals and their metabolites are continuously released into the environment in a variety of ways. A variety of different pharmaceuticals have been found in several environmental compartments (Halling-Sørensen et al., 1998; Heberer, 2002; Kümmerer, 2008, 2009; Nikolaou et al., 2007), some of them even in ground and drinking

* Corresponding author at: Nachhaltige Chemie und Stoffliche Ressourcen, Institut für Nachhaltige Chemie und Umweltchemie, Fakultät für Nachhaltigkeit, Leuphana Universität Lüneburg, Scharnhorststraße 1/C13, D-21335 Lüneburg, Germany. Tel.: +49 4131 677 2893.

E-mail addresses: waleed.ahmed@uni.leuphana.de, welfishawy@yahoo.com (W.M.M. Mahmoud), christoph.trautwein@leuphana.de (C. Trautwein), clleder@leuphana.de (C. Leder), klaus.kuemmerer@uni.leuphana.de (K. Kümmerer).

waters (Carballa et al., 2004; Oosterhuis et al., 2013; Ternes, 1998). However, little is known about the risk to humans from pharmaceuticals and their metabolites in surface and drinking water (Kosjek and Heath, 2011; Kümmerer, 2008; Kümmerer and Al-Ahmad, 2010). Special attention has to be attributed to the fact that some metabolites can be more harmful than their parent compound (Gros et al., 2006). Once pharmaceuticals and their metabolites are released into the environment, they are subject to many physico-chemical processes (e.g., dilution, hydrolysis, biodegradation, photolysis and sorption to bed sediments and sewage sludge) that contribute to their removal (Gartiser et al., 2007; Petrovic and Barceló, 2007) or the formation of new transformation products (TPs) which have not been identified so far (Trautwein and Kümmerer, 2011).

Phototreatment for the removal of organic pollutants such as drugs e.g. from potable water, surface water or treated sewage is a topic currently under discussion (Lam and Mabury, 2005; Tixier et al., 2003). Phototreatment with ultraviolet (UV) light irradiation is an established method for sterilization and water disinfection (Canonica et al., 2008), and a growing technology for wastewater purification (Kang et al., 2004; Liberti and Notarnicola, 1999; Meneses et al., 2010; U.S. EPA, 1998). However, photodegradation does not necessarily end up with the complete mineralization of a chemical. Photolytic reactions are often complex, involving various competing or parallel pathways, leading to multiple reaction products which can have physical, chemical and toxicological properties that differ from the parent compound (Fatta-Kassinos et al., 2011; Petrovic and Barceló, 2007). Although developers and manufacturers rigorously test the stability of pharmaceutical compounds, photoinduced degradation under environmental conditions is not widely investigated. Elucidation of photolytic reaction pathways and identification of TPs are therefore of crucial importance in understanding the fate of emerging organic pollutants in the aquatic environment.

Many antineoplastic drugs used in cancer therapy have a high mutagenic and cancerogenic potential, which is also expected for exposed aquatic organisms (Kümmerer, 2008). Due to the mode of action of cytotoxic drugs, practically all eukaryotic organisms are vulnerable to damage, with teratogenicity being the greatest concern at such levels. The exposure of the pregnant mother, or more specifically her fetus, to these drugs via drinking water should be minimized (Johnson et al., 2008).

Thalidomide (TD), 2-(2,6-dioxo-3-piperidinyl)-1*H*-isoindole-1,3(2*H*)-dione, is a sedative, hypnotic, immunomodulating and anti-inflammatory pharmaceutical compound. TD has many adverse effects and it can develop teratogenic effects after a single dose. As a consequence, TD should not be ingested by women with a child-bearing potential. As TD distributes into the semen, male patients receiving TD should use barrier methods of contraception if their sexual partner is of child-bearing potential. Patients should not donate blood or sperm during TD therapy (Sweetman, 2009). TD was withdrawn from its use as a hypnotic in the early 1960s after it was discovered that it produced teratogenic effects, when given in early pregnancy. Therefore, TD is listed in the Hazardous Substances Data Bank (HSDB) due to its teratogenicity (U.S. National Library of Medicine, 8600 Rockville Pike, Bethesda, MD 20894). Its use is being revived since TD was approved by the FDA in July 1998 for the treatment of erythema nodosum leprosum associated with leprosy. Recently, TD is expected to be a promising drug in the treatment of a number of cancers and inflammatory diseases, such as multiple myeloma and inflammatory bowel disease (Crohn's disease), HIV and cancer associated cachexia (Bosch et al., 2008; Meyring et al., 1999; Sweetman, 2009). Consequently, a potential increased influx of TD into the aquatic environment has to be expected.

The exact metabolic fate of TD is unknown. TD is sensitive to hydrolytic decomposition and it has been found to be eliminated mainly by spontaneous hydrolysis at pH higher than 6 in blood. The hydrolysis

rate of TD accelerates with increasing pH. Consequently, hydrolysis will play an important role in the sewage treatment plant (STP) where pH is above 7. The number of possible metabolites of TD is very large; exceeding more than 100 different compounds (Schumacher et al., 1965a). Some twelve substances are derived from the parent drug by simple hydrolysis (Schumacher et al., 1965a, 1965b). Hydrolysis is thought to occur by nucleophilic substitution involving specific and general base as well as nucleophilic catalysis (Reist et al., 1998). The main urinary metabolites in humans are 2-phthalimidoglutaramic acid (about 50%) and R-(*o*-carboxybenzamido)glutarimide (about 30%) (Reist et al., 1998). Only those three of the hydrolysis products which contain the intact phthalimide moiety showed teratogenic activity (Meise et al., 1973). Because of the well documented teratogenic potential of TD and its expected increase of use in the future, it is desirable to have at least some knowledge of its environmental fate. Therefore, we investigated the environmental fate of TD and its TPs.

The general objective of this study was to assess the photo- and biodegradability of TD with the identification of stable dead-end TPs formed in both degradation pathways. The primary elimination of TD was monitored and structures of its photo- and biodegradation products were assessed by high performance liquid chromatography with ultraviolet detection at 220 nm, fluorescence detection (λ_{ex} : 225 nm, λ_{em} : 398 nm) and mass spectrometry (ion trap LC-UV-FL-MS/MS). Furthermore, dissolved organic carbon (DOC) elimination was monitored during irradiation.

Moreover, TD and the observed TPs were assessed by a set of *in silico* predictions for biodegradation. A set of programs for predicting biodegradation was applied in order to take into account that the available programs might have individual strengths because of different algorithms and training sets. Programs based on quantitative structure activity relationship (QSAR) are gaining importance especially for analyzing environmental TPs because these TPs are usually only formed in low concentrations within complex matrices so that isolation and purification is very difficult. Further, many of these TPs are not available commercially, which makes the individual analysis of their environmental fate impossible. Therefore, it can be helpful to apply QSAR models that estimate the potential for biodegradation in the environment (European Commission, 2003).

2. Experimental

2.1. Chemicals

All the chemicals used in this study were of analytical grade and were used without further purification. Acetonitrile and methanol (HiPerSolv CHROMANORM, LC-MS grade, BDH Prolabo), and formic acid (analytical grade) were purchased from VWR International GmbH (Darmstadt, Germany). TD (CAS number 50-35-1) was obtained from Sigma-Aldrich (Steinheim, Germany) and chemical point (Deisenhofer, Germany).

2.2. Photodegradation

The experiment was conducted in a 1 L batch photo-reactor. For the photolysis of TD, xenon lamp (TXE 150 W, UV Consulting Peschl, Mainz) and a medium-pressure mercury lamp (TQ150, UV Consulting Peschl, Mainz) with ilmasil quartz immersion tube were used. The cooling jacket used was made of ilmasil quartz. The mercury and xenon lamps emit polychromatic radiation in the range from 200–600 nm and 200–800 nm, respectively. The maximal intensities of mercury lamp were at 254, 265, 302, 313, 366, 405/408, 436, 546, and 577/579 nm. The maximal intensities of xenon lamp were at 460, 466, 480, 494, 617, 630, 649, 688, 710, 728, 740, 757 and 763 nm. 800 mL of the test solution was transferred into the reactor and the test started by switching on the lamp. The mixture was stirred with a magnetic stirrer during the photoreaction to ensure a constant mixing of the solution. The

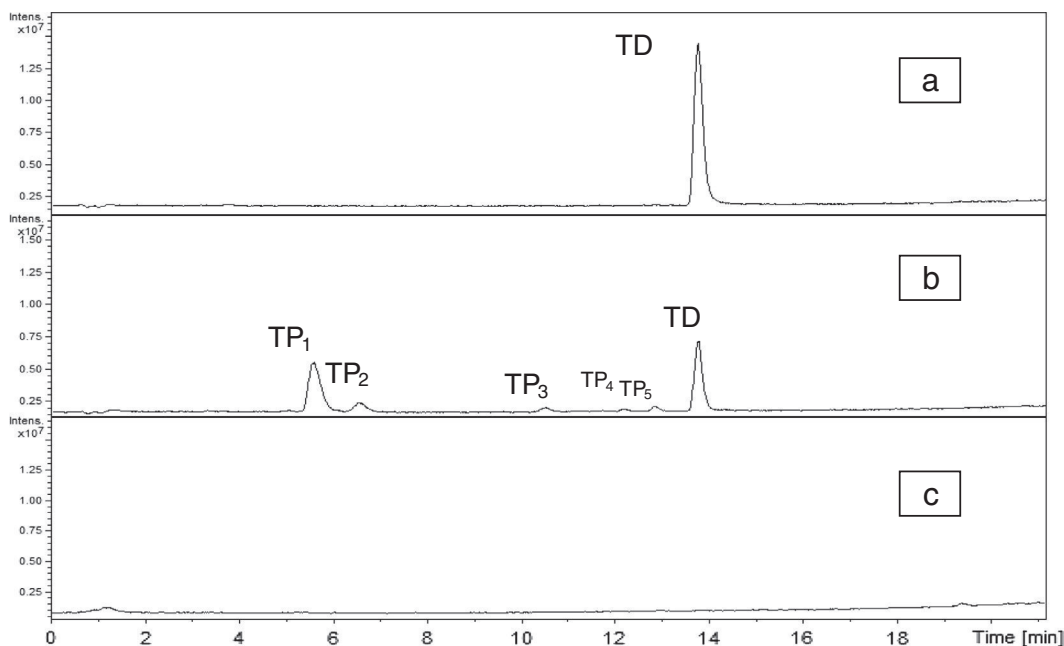


Fig. 1. Total ion chromatograms (TICs) of TD photolysis samples using mercury lamp: a) 0 min, b) after 16 min photolysis, and c) after 128 min photolysis.

temperature was maintained by a circulating cooler (WKL230, LAUDA, Berlin) between 18 and 20 °C. 20 ml of each reaction solution was withdrawn from the photo-reactor in a geometrical (2^n) time sampling interval (2, 4, 8, 16, 32, 64 and 128 min) for the analysis of the TD concentration by DOC, LC–UV–VIS/FL and LC–UV–FL–MS/MS. DOC was determined according to European standard procedure EN 1484 with a total organic carbon analyzer (TOC 5000, Shimadzu GmbH, Duisburg, Germany) in three replicates. TD initial concentration was 10 mg L^{-1} . Ultrapure water was used to prepare all test solutions to avoid the scavenger effect of any absorbing or photosensitizing chemical or other species during degradation and to assess the photoproducts that arise from the photolysis of TD only.

2.3. Biodegradation testing

To assess the biodegradability of TD and the possible formation of potential microbial degradation products, two tests from the OECD series were used in the present study: the widely used Closed Bottle test (CBT) (OECD 301D), and the Manometric Respirometry test (MRT) (OECD 301F) which work with different bacterial density and diversity. In addition to that, another CBT was performed for a TD sample received after 16 min of UV-photolysis in order to assess the biodegradability of photoproducts in the environment.

2.3.1. Closed Bottle test (OECD 301D) (CBT)

The CBT was performed according to test guidelines (Organisation for Economic Co-operation and Development, 1992a) with a low nutrient content, low bacterial density (10^2 – 10^5 colony forming units (CFU) ml^{-1}) and at room temperature (20 ± 1 °C) in the dark as described elsewhere in detail (Kümmerer et al., 1996; Mahmoud and Kümmerer, 2012; Trautwein and Kümmerer, 2011). According to the guidelines, at least 60% decomposition of the reference substance sodium acetate is required within 14 days.

The test consisted of four different series (Supplementary material Table S1). All series were run as duplicates. All test vessels were inoculated with an aliquot from the effluent of a local municipal sewage treatment plant. The test was repeated with two different inocula in order to investigate the influence of inocula sources on the degradation pattern of TD. The inocula were taken from the municipal STP in Abwasser, Grün & Lüneburger Service

GmbH (AGL) Lüneburg, Germany (144,000 inhabitant equivalents) and from the municipal STP in Kenzingen, Germany (13,000 inhabitant equivalents). The CBT for the TD sample received after 16 min of photolysis was performed using the inoculum from the municipal STP in AGL Lüneburg, Germany (Supplementary material Table S1).

According to the test guidelines a test compound is classified as “readily biodegradable” if biodegradability, expressed as a percentage of oxygen consumed in the test vessel (ThOD), exceeds 60% within a period of ten days after the oxygen consumption reached 10% ThOD.

The process of aerobic biodegradation was monitored for 28 days. In the case of the CBT using the inoculum from Lüneburg, the oxygen concentration was measured in the test vessels with the Fibox 3 system (Fiber-optic oxygen meter connected with Temperature sensor PT 1000) (PreSens, Precision Sensing GmbH, D-93053 Regensburg, Germany) using sensor spots in the bottles (Friedrich et al., 2013; Wolfbeis, 2002). In the case of the CBT using the inoculum from Kenzingen, the oxygen concentration was measured in the test vessels using two different techniques; with an oxygen electrode (Oxi 196 with EO 196-1.5, WTW Weilheim, Germany) in accordance with international standard methods (ISO (International Standards Organization), 1990) and the Fibox 3 system. Besides oxygen demand, temperature and pH were also monitored during the course of the test. Samples at test begin and test end were taken. In the classical CBT where TD biodegradation was assessed with an oxygen electrode, samples were withdrawn at days 0, 1, 7, 14, 21 and 28. All samples were stored at -80 °C until subsequent LC–MSⁿ analysis.

2.3.2. Manometric respiratory test (OECD 301F) (MRT)

Another method for assessing the readily degradability of chemicals is the MRT (Organisation for Economic Co-operation and Development, 1992b) which can be performed by the use of the Oxitop system (WTW, Weilheim, Germany) as described elsewhere in detail (Khaleel et al., 2013).

The sample scheme is equivalent to that of the CBT, although the test is performed with higher inoculum densities (5 – 10×10^6 CFU mL^{-1}) and a higher sodium acetate and TD concentration, corresponding to a theoretical oxygen demand (ThOD) of 30 mg L^{-1} (Supplementary material Table S1). The inoculum was used in a concentration of 80 mL/L. Like in the CBT, the influence of two different inocula was investigated

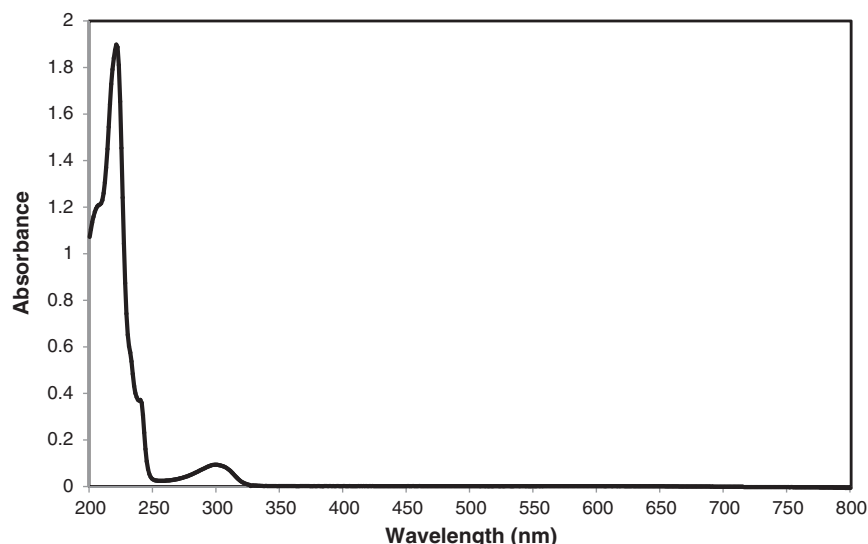


Fig. 2. UV-VIS adsorption spectra of 10 mg L^{-1} thalidomide in water.

(municipal STP Lüneburg and municipal STP Kenzingen). Measurements were made in duplicate. The OECD validity criteria are the same as for the CBT. Samples at test begin and end were taken and stored at -80°C until subsequent LC-MSⁿ analysis.

2.4. Monitoring of primary elimination by LC-UV-VIS/FL, and LC-MS/MS

In order to get more information about the observed elimination, the samples were measured for their primary elimination using HPLC-UV-VIS/FL and ESI-LC-MS/MS (ion trap). A stock solution of TD ($100 \mu\text{g mL}^{-1}$) was prepared in 100% methanol. Standard solutions were prepared by further dilution with ultrapure water to reach the concentration range of linearity. Triplicate $50 \mu\text{L}$ TD injections for LC-UV-VIS/FL and LC-MS/MS, respectively were made for each concentration and chromatographed under the specified chromatographic conditions described below. The peak area values were plotted against corresponding concentrations. Linear relationships were obtained. Prominence HPLC apparatus (Shimadzu, Duisburg, Germany) was used. Chromatographic separation was performed on an RP-18 column (CC 70/3 NUCLEODUR 100-3 C18 ec, Macherey and Nagel, Düren, Germany) protected by a CC 8/4 HYPERSIL 100-3 C18 ec, guard column. An isocratic run with a mobile phase consisting of 0.1% formic acid in water (CH_2O_2 : solution A) and 100% acetonitrile (CH_3CN : solution B) (80:20 v/v) were used for elution. The sample injection volume was $50 \mu\text{L}$. The flow rate was

set at 0.7 mL min^{-1} and the oven temperature to 30°C . Total run time was 5 min.

LC-MS/MS quantification and detection was performed on a Bruker Daltonic Esquire 6000 plus ion-trap mass spectrometer equipped with a Bruker data analysis system and atmospheric pressure electrospray ionization interface (Bruker Daltonic GmbH, Bremen, Germany). The MS was connected to the Agilent Technologies 1100 HPLC series (Agilent Technologies, Böblingen, Germany). Chromatographic separation was performed on the same RP-18 column stated above. Gradient system 0.1% formic acid in water (CH_2O_2 : solution A) and 100% acetonitrile (CH_3CN : solution B) were used by applying the following linear gradient: 0 min 5% B, 5 min 5% B, 20 min 40% B, 23 min 40% B, 26 min 5% B, and 30 min 5% B. The flow rate was set at 0.7 mL min^{-1} and the oven temperature was set to 30°C . Total run time was 30 min. For quantification, the molecule ion for TD (m/z 259.1) at a retention time of 13.8 min was used (Fig. 1a).

The mass spectrometer was operated in positive polarity. The operating conditions of the source were: -500 V end plate, -3950 V capillary voltage, 30 psi nebulizer pressure, and 12 L min^{-1} dry gas flow at a dry temperature of 350°C . The selected lens and block voltages were: $+110.4 \text{ V}$ capillary exit, 144.4 Vpp octopole reference amplitude and -60.0 V lens two. The scan range was determined from m/z 40 to 900 and the scan time was 200 ms. A typical total ion chromatogram is presented in Fig. 1.

Table 1

Chromatographic and mass spectrometric parameters for TD and its transformation products analysis in LC/MS-MS (ESI (+); (relative intensity, %)).

Compound	RT (min)	Main precursor ion (m/z)	Productions (m/z)
Photoproduct TP ₁	5.6	259.1	241.0 (100), 214.0 (16.8), 159.0 (16.4), 231.0 (14)
Photoproduct TP ₂	6.6	259.1	241.0 (100), 214.0 (23.3), 159.0 (16.6), 231.0 (18.7)
Photoproduct TP ₃	10.6	148.0	130.0 (100)
Photoproduct TP ₄	12.2	275.1	247.0 (100), 84.2 (45), 202.0 (15.2)
Photoproduct TP ₅	12.9	275.1	247.0 (100), 84.2 (50.4), 202.0 (10.6)
Thalidomide	13.8	259.1	231.1 (100), 84.2 (56.9)
Hydrolysis product MRT day 28 DP ₁	2.9	295.1	277.0 (100), 147.1 (31.2), 130.1 (20.6), 259.1 (13.7)
Hydrolysis product MRT day 28 DP ₂	3.5	278.1	102.2 (100), 250.0 (59), 130 (30.7), 84.3 (17.5), 232 (16), 214 (12)
Hydrolysis product CBT day 28 DP ₃	3.8	277.1	259.0 (100), 129.0 (28.2), 84.2 (17.2), 102.2 (11)
Hydrolysis product CBT of 16 min photolysis sample day 28 DP ₃ & DP ₄	3.8 & 4.2	277.1	259.0 (100), 214.3 (46.1)
Hydrolysis product MRT day 28 DP ₄	4.2	296.1	278.0 (100.0), 148.0 (30.2), 130.1 (32.4), 277.1 (30.1), 232.0 (22), 214.0 (18.1), 279.1 (14.8)
Hydrolysis product MRT day 0 DP ₅	8.8	277.1	232.0 (100), 214.0 (83), 260.0 (81.6), 259.1 (64.7), 231.0 (30.9), 186.0 (13.5), 84.2 (13.1)
Hydrolysis product MRT day 0 DP ₆	9.9	277.1	259.1 (100), 260.0 (17.8), 231.1 (17.3)

RT: retention time.

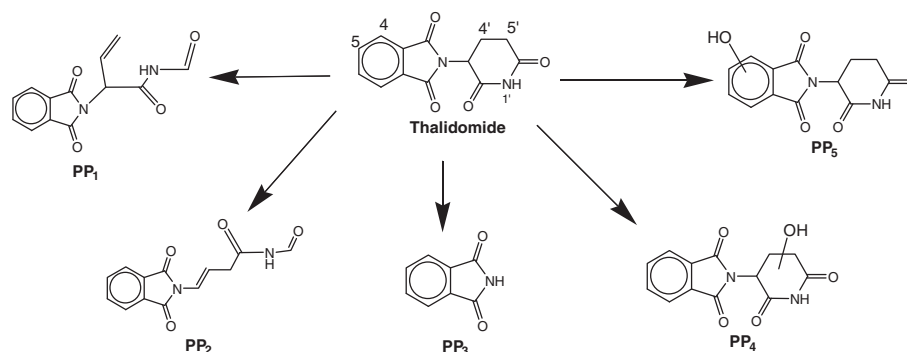


Fig. 3. Suggested photodegradation scheme of thalidomide.

2.5. In silico prediction of environmental fate

2.5.1. In silico prediction of readily biodegradability

The readily biodegradability of TD was predicted with different programs: the EPI Suite software (EPIWEB 4.1) from the U.S. Environmental Protection Agency (U.S. EPA, 2004), the Oasis Catalogic software V.5.11.6TB from the Laboratory of Mathematical Chemistry, University Bourgas, Bulgaria (Laboratory of Mathematical Chemistry U'AZBB) and Case Ultra V 1.4.5.1 (MultiCASE Inc.) (Chakravarti et al., 2012). Chemical structure illustrations were performed by using MarvinSketch 5.8.0. Simplified molecular input line entry specification (SMILES) codes from the molecular TP structures were taken as input.

The readily biodegradability values of TD and its phototransformation products were predicted according to the Ministry of International

Trade and Industry (MITI) test, which is not directly comparable to the Closed Bottle test. The MITI test is one of the officially approved tests in the OECD guidelines for ready biodegradability (Organisation for Economic Co-operation and Development, 1981). The MITI data from JNITE (Japanese National Institute of Technology and Evaluation) are a large collection of results from a single biodegradation test: the MITI-I test for ready biodegradability (OECD 301C) (Rücker and Kümmerer, 2012). OECD 301C Modified MITI-I is a 28 day respirometry test that measures oxygen demand. The data from MITI are used as training set for the informatical model generation in EpiSuite, Case Ultra and Oasis Catalogic.

The MITI test often indicates better biodegradability than the CBT because of higher bacterial density and diversity, respectively (Trautwein and Kümmerer, 2012). The obtained results were compared with

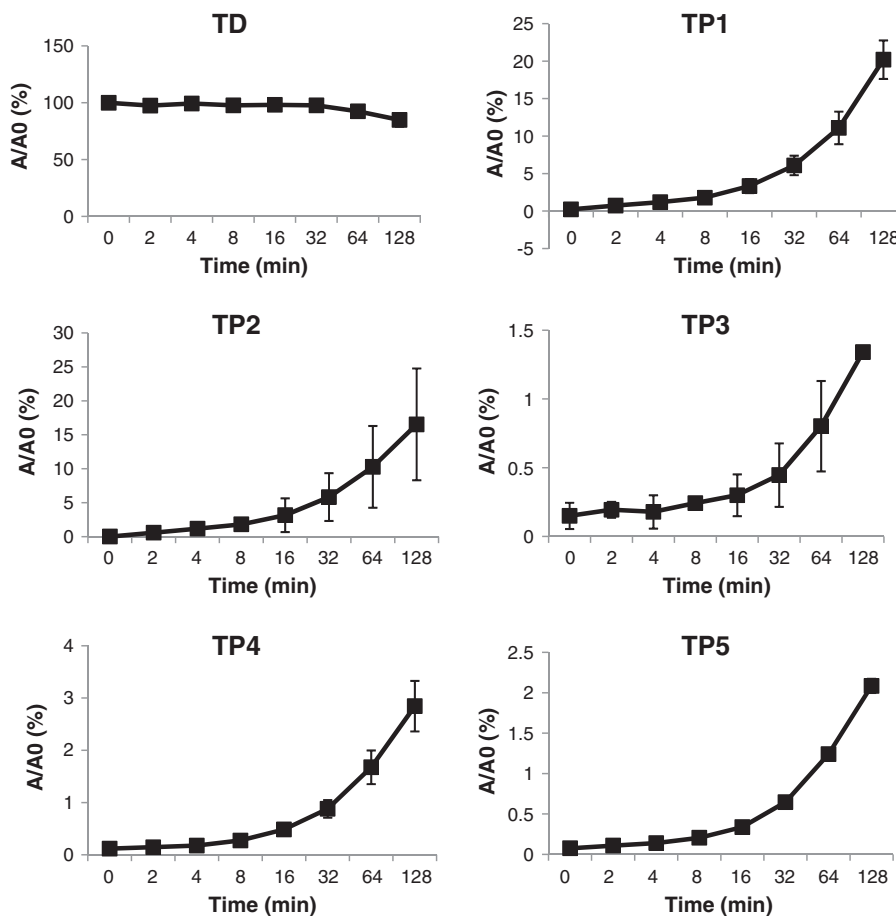


Fig. 4. Time course of the percentual recovery of area ratio (A/A_0 as A is the area of the TP and A_0 is the area of TD at 0 min) of the formed TPs during photolysis with xenon lamp ($n = 2$).

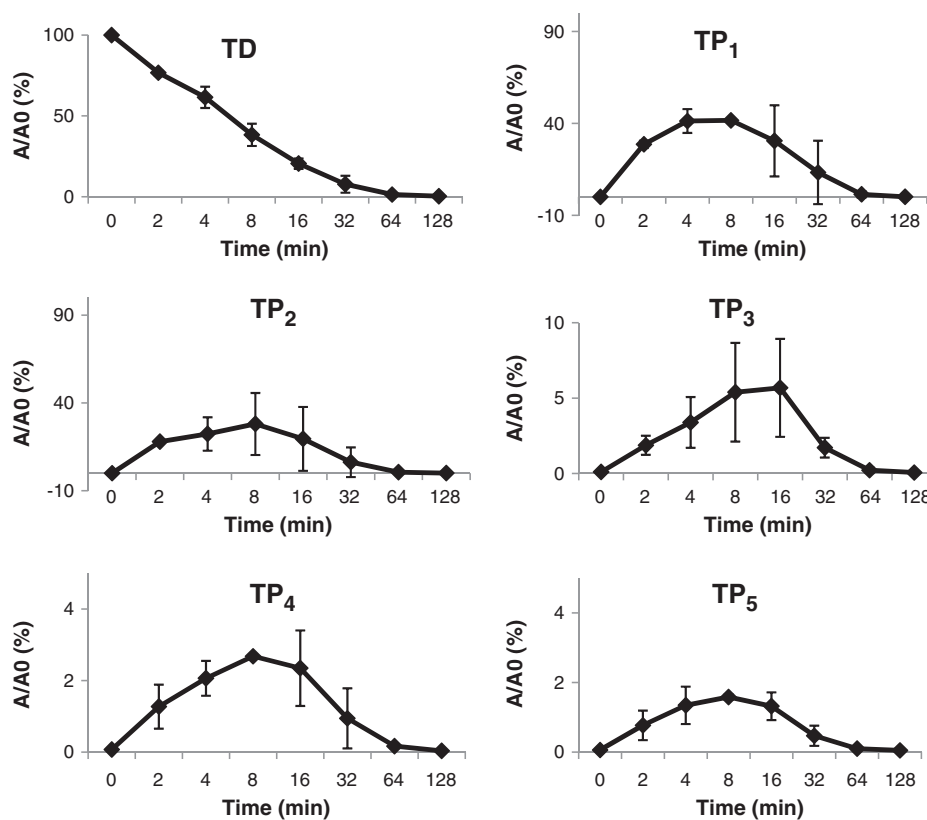


Fig. 5. Time course of the percentual recovery of area ratio (A/A_0 as A is the area of the TP and A_0 is the area of TD at 0 min) of the formed TPs during photolysis with mercury lamp ($n = 2$).

experimentally determined values and with critical limits according to EU guidelines (European Commission, 2003).

2.5.2. In silico prediction of photodegradation products

The photodegradation pathway of TD was simulated with the QSAR software MetaPC (Version 1.8.1, MultiCASE Inc., Beachwood, USA). The identified TP structures acquired from the MS data were compared with those predicted by the software.

Meta is a rule-based expert system which predicts transformation of chemicals under a set of different conditions such as mammalian metabolism, aerobic and anaerobic degradation and photodegradation (Sedykh et al., 2001). The program's workflow is based on a library of known pairs of target and transform sequences ("transforms"). Investigated molecules are scanned for their target sequences which are replaced one by one by the relevant transform sequences. This creates a set of predicted TPs. Furthermore the software monitors thermodynamic stability of the molecules and includes a spontaneous reaction module for unstable structural moieties. The output is a list of possibly generated TPs.

The photodegradation module of MetaPC software consists of approximately 1200 transformations divided into 9 large subdivisions. The module was validated with 40 known industrial chemical products and had a hit/miss ratio of 92.7%.

3. Results and discussion

3.1. Photodegradation

The fact that a compound absorbs radiation in the UV–VIS region of the electromagnetic spectrum means that it is absorbing energy sufficient to break a bond in the molecule (Tønnesen, 2004). The absorption property of TD is a first indication that it may be capable of participating in a photochemical process leading to its own decomposition. From the

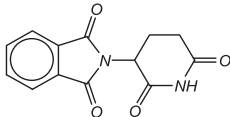
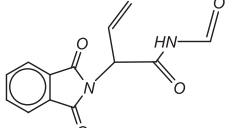
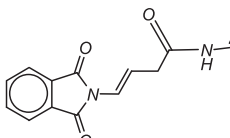
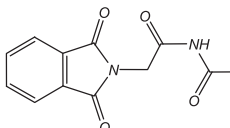
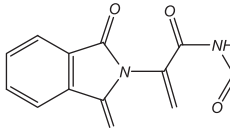
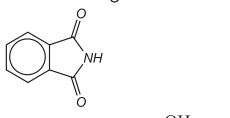
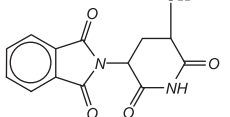
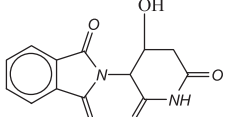
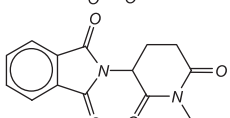
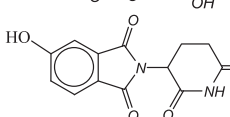
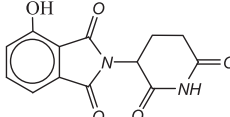
UV absorption spectra of TD (Fig. 2), TD has an extremely well UV absorption mainly until 240 nm ($\lambda_{\max} = 220$ nm). Therefore, it can be expected that the degradation rates of TD with a mercury lamp will be faster than the degradation of TD with a xenon lamp.

The LC–MS analysis of photodegradation samples showed a pseudo-first order kinetics. Further, the polychromatic mercury lamp appears to be more effective than the polychromatic xenon lamp for the degradation of TD, as indicated by the degradation rates. The pseudo-first order rate constants of the degradation of TD increased by fifty five fold using the mercury lamp as compared to the xenon lamp, 8.88×10^{-2} and 1.6×10^{-3} , respectively.

The concentration of TD declined during the irradiation process using the xenon lamp and Hg lamp. No significant variation of the DOC values was observed during the irradiation process using the xenon lamp after 128 min. On the other hand, the photodegradation process using the Hg lamp was accompanied by a DOC loss of 77.8% after 128 min. The pH at the beginning of the experiment was 5.8 and the pH decreased to 5.4 and 4.6 after 128 min of photolysis using the xenon and Hg lamp, respectively. This pH indicates that the hydrolysis reaction doesn't play an important role in photolysis.

The development of new peaks in the chromatograms of the samples obtained at different irradiation times is an indication of possible TP formation. The predictions of the TP were depending on a non-target approach (comparing samples at initial time with other samples at increasing time period). The same photolytical TPs are formed either using the xenon and the Hg lamp, but the degradation rate using the xenon lamp was slower than with the Hg lamp. The chromatographic behavior demonstrated that TPs formed by photolysis were of higher polarity than TD itself (Fig. 1b). Structural identification of the photoproducts was based on the analysis of the total ion chromatogram (TIC) and the corresponding mass spectrum. For TP peaks – depending on the peak intensity of each TP – up to MS³ spectra were generated using the Auto MSⁿ mode in order to have structural

Table 2
 Predicted environmental parameters of TD and its phototransformation products calculated with 1: Catabol MITI (OECD 301C), BOD, 28 days, 2: Catalogic BOD 28 days MITI (OECD 301C), 3: Case Ultra, MITI Ready biodegradation, 4: MITI Biodegradation probability Biowin 5 (linear model), 5: MITI Biodegradation probability Biowin 6 (MITI non-linear model).

Compound	Structures	QSAR model				
		1 ^a	2 ^a	3	4 ^b	5 ^b
TD		0.07	0.17	Inconclusive (orange)	0.029	0.016
TP ₁		0.17	0.30	Inconclusive (black)	0.055	0.011
TP ₂		0.39	0.40	Inconclusive (black)	0.039	0.019
TP _{2,2}		0.23	0.33	Marginally positive	0.045	0.019
TP _{2,3}		0.15	0.27	Inconclusive (orange)	0.010	0.013
TP ₃		0.26	0.42	Negative	0.307	0.224
TP _{4,1}		0.07	0.16	Inconclusive (orange)	0.135	0.019
TP _{4,2}		0.18	0.29	Inconclusive (black)	0.135	0.019
TP _{4,3}		0.07	0.17	Inconclusive (black)	0.019	0.01
TP _{5,1}		0.07	0.15	Inconclusive (orange)	0.037	0.015
TP _{5,2}		0.07	0.17	Inconclusive (orange)	0.037	0.015

^a "100% biodegradation" was assigned a numeric value of 1 and "0% biodegradation" was assigned a numeric value of 0.

^b "Readily biodegradable" was assigned a numeric value of 1 and "not readily biodegradable" was assigned a numeric value of 0. (0 to 1 is the probability range to undergo biodegradation).

information on the photolysis TPs and make structural elucidation (Table 1). Therefore, the precursor ion was fragmented first. The two most abundant product ions were then selected and fragmented again if peak intensity was high enough.

The major TPs (accounting for $\geq 2\%$ of the TD area in an individual sample at any sampling time) are labeled as TP₁ (m/z 259.1, t_r = 5.7 min), TP₂ (m/z 259.1, t_r = 6.7 min), TP₃ (m/z 148.1, t_r = 10.6 min), TP₄ (m/z 275.1, t_r = 12.2 min) and TP₅ (m/z 275.1, t_r =

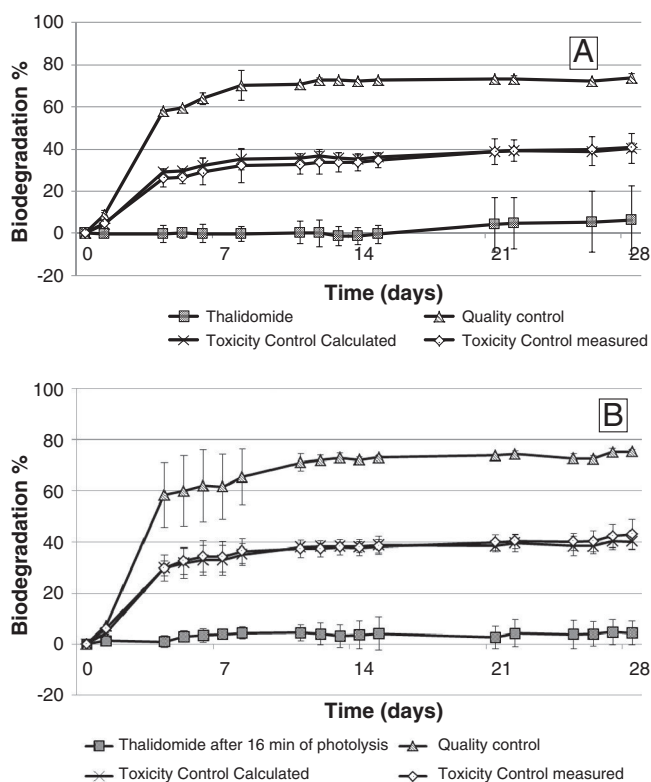


Fig. 6. Closed Bottle test of a) pure TD ($n = 4$) and b) TD sample after 16 min of photolysis ($n = 2$).

12.9 min) (Figs. 3, 4, 5 and Table 1). With regard to the photodegradation peaks it should be pointed out that the major TPs were TP₁ and TP₂ which are isomers of TD with the same molecular mass (Figs. 1b, 4 and 5). The TPs' $[M + H]^+$ molecular ions with m/z 259 presumably are due to homolytic cleavage of the α -bond (α -cleavage; Norrish type I reaction), which can be accompanied by competing processes such as the Norrish type II reaction (Klán and Wirz, 2009). MS² results point to the products being those of Norrish type I reaction (Supplementary material Fig. S1 and S2). MetaPC software proposed all four possible products by Norrish types I and II reaction. TP₁ and TP₂ can be formed due to Norrish-type I and TP₂₋₂ and TP₂₋₃ can be formed due to Norrish-type II reaction (Table 2). According to the Log P values predicted with the MetaPC software, the TPs formed due to Norrish-type I will be more polar than TD whereas TPs formed due to Norrish-type II are less polar. Furthermore, the identified TP with m/z 148 is also predicted by the MetaPC software and is formed due to fragmentation between the phthalimide and the glutamiride ring.

Finally, an additional 16 Da was observed for the TPs with the molecular ion m/z 275 compared to m/z 259 of TD. This is likely due to hydroxylation of TD which renders the molecules more polar. The MetaPC software also predicted three hydroxylation products labeled as 4'-OH thalidomide (TP₄₋₂), 4-OH thalidomide (TP₅₋₂) and 5-OH thalidomide (TP₅₋₁) (Table 2).

Also, hydroxylation of TD occurs during biological metabolism (Eriksson et al., 1998; Meyring et al., 1999). The mass fragmentation results don't provide information about the exact hydroxylation position. Price et al. have shown that at least one of the hydroxylated metabolites (5'-OH thalidomide, hydroxylation on glutarimide moiety) has moderate anti-angiogenic activity at high concentrations (Price et al., 2002). The postulated MS² fragmentation pattern of photolytic TPs can be found in the Supplementary material (Figs. S1–S5). In the case of photodegradation with xenon lamp, all TP peaks increased with irradiation time until 128 min of photolysis with no change in

the observed DOC (Fig. 4). In the case of photodegradation with Hg lamp, all TP peaks increased with irradiation time until 16 min of photolysis and then began to decrease which is in accordance with the observed DOC loss (Fig. 5). So this can be an indication that TD and its photoproducts can be degraded and mineralized by prolonged photolysis.

3.2. Biodegradability of TD and its photoproducts

Criteria of the OECD test guideline were met, since more than 60% ThOD of the quality control substrate (sodium acetate) was biodegraded within 14 days, classifying this test as valid. The average biodegradation values for TD determined in the CBT by monitoring the dissolved oxygen concentration were 9.05% (three repetitions, six test bottles) and 6.21% (two repetitions, four test bottles) using the inoculum from Kenzingen and Lüneburg, respectively (Fig. 6a). The average biodegradation values for TD after 16 min of photolysis determined in the CBT were 4.43% ($n = 2$) (Fig. 6b). These biodegradation values are characterizing TD and its photo-transformation products after 16 min of photolysis as being resistant against biodegradation. There was no impact by the source of the inoculum and by using two different measuring techniques. In the toxicity control bottles, no toxic effects were observed (Fig. 6a, b).

Similarly to the CBT, TD was not readily biodegradable in the MRT. The average biodegradation values for TD determined in the MRT by monitoring the oxygen partial pressure were 30.4% (two test bottles) and 20.7% (three repetitions, six test bottles) using the inoculum from Kenzingen and Lüneburg, respectively (data not shown). In the toxicity control bottles, no toxic effects for this high concentration of TD were observed for both inocula sources (data not shown).

These biodegradation results are in accordance with QSAR data from the EPI Suite, Case Ultra (MultiCASE) and Oasis Catalogic softwares. Two applied models from Oasis Catalogic (module Catabol MITI, BOD, 28 days and module Catalogic BOD 28 days MITI) confirmed the experimental evidence that TD and its phototransformation products are most likely not readily biodegraded (Table 2). The program provides values between 0 (no biodegradation) and 1 (complete biodegradation). Case Ultra (MITI Ready biodegradation module) strengthened these predictions because it also didn't provide positive estimations for the biodegradation of TD and its TPs (Table 2) with the exception of TP₂₋₂ with a marginally positive alert. "Inconclusive (orange)" means in this context that the program identified both positive alerts and negative alerts, which conflicts a firm conclusion. Instead, "inconclusive (black)" means that the molecule contained too many unknown fragments. "Out of domain" means that the molecule is not covered by the underlying training set. Biowin 5 and 6 from EPI Suite confirmed these results by providing biodegradation probability predictions of well below 0.1 for TD and its TPs with the exception of TP₃ and TP₄₋₁ as well as TP₄₋₂ (Table 2). Howard et al. have classified TD as one of the high production volume pharmaceuticals that has not been detected in the environment. They assumed TD to be persistent and/or bioaccumulative due to this Biowin 5 result (Howard and Muir, 2011). This classification might be wrong since the model doesn't take into consideration that TD may undergo spontaneous hydrolysis in the aquatic environment giving rise to abiotic TPs.

LC-MS analysis of samples taken at the end of the biodegradation tests revealed that even though no biodegradation was observed according to oxygen consumption and CO₂ evolution in the CBTs and MRT, respectively, no TD was present anymore (Fig. 7 and Supplementary material Fig. S6). LC-MS data showed six main TPs different to those formed in photolysis but identical to the ones in all biodegradation tests (Figs. 1 and 7). Probably they are the result of hydrolysis as the pH in the biodegradation tests ranges between pH 7 and 8. They were labeled as degradation products DP₁ (m/z 295.1, $t_r = 2.9$ min), DP₂ (m/z 278.1, $t_r = 3.5$ min), DP₃ (m/z 277.1, $t_r = 3.8$ min), DP₄ (m/z 296.1, $t_r = 4.2$ min), DP₅ (m/z 277.1, $t_r = 8.8$ min), and DP₆ (m/z

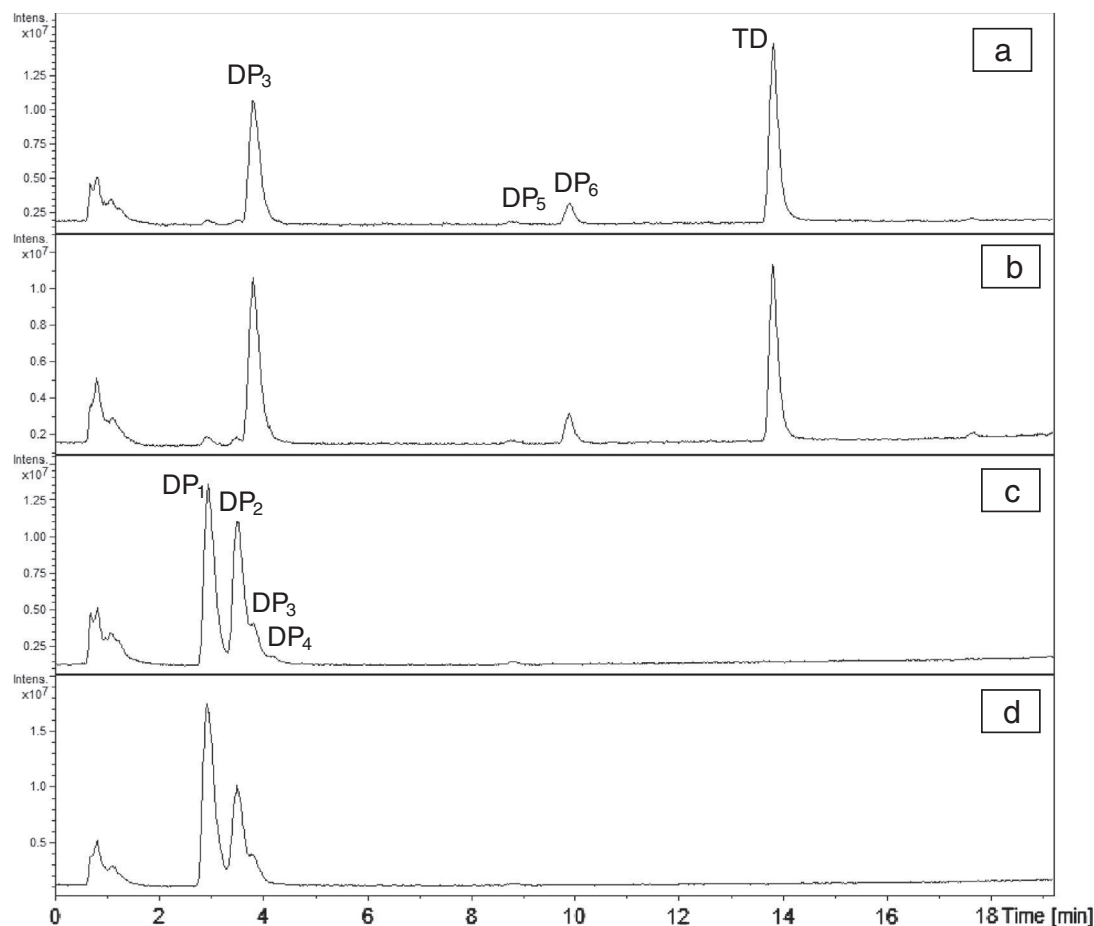


Fig. 7. Total ion chromatograms (TICs) of TD samples in MRT test: a) day 0, b) day 0 sterile, c) day 28, and d) day 28 sterile. TD = thalidomide, DP = degradation product.

277.1, $t_r = 9.8$ min) in Fig. 8 (Table 1). The hydrolysis begins by splitting one of the amide bonds of the phthalimide ring or of glutarimide ring, resulting in DP₃, DP₅ and DP₆. The main primary hydrolysis product is DP₃ and this is in accordance with the previous finding by Schumacher et al. (1965b). In order to interpret the acquired MSⁿ data correctly, previous hydrolysis studies upon TD and its hydrolysis products were evaluated and compared (Schumacher et al., 1965a, 1965b).

In the TIC of the CBT one can observe that primary elimination of TD occurred immediately from the beginning of the test. TD, DP₅ and DP₆ completely disappeared after 7 days. The peak intensities of DP₂ & DP₃ increased until days 21 and 7, respectively and then decreased. The intensity of peak DP₄ increased from day 21 until the end of the test. The intensity of peak DP₁ also increased until test end (Supplementary material Fig. S7). In the TIC on day 28 of the TD sample after 16 min of photolysis in the CBT, DP₁ and DP₃ are the most intensive peaks which were found and DP₂ can still be detected but in a lower intensity (supplementary material Fig. S6). DP₄ in the CBT of the TD sample after 16 min of photolysis has a different mass spectrum than the one from TD in the CBT (Table 1). The photoproducts of the 16 min irradiation sample (TP₁–TP₅) were completely degraded in the CBT after 28 days (Supplementary material Fig. S6).

In the MRT, a partial biodegradation was observed for “TD” which in fact can be directed to the formation of hydrolysis products. Nevertheless, the same degradation products (identical precursor and products ions at the same retention time) were formed in the test, toxicity control and sterile bottle (Supplementary material Fig. S8). Therefore, it has to be concluded that the formed degradation products are not of bacterial origin but a result of abiotic hydrolysis. Thus, we conclude that a high environmental concentration of the hydrolysis products of TD can be expected.

Hydrolysis products of TD in aqueous solution were reported previously (Schumacher et al., 1965b) and the stability of some of them was examined spectrophotometrically and by paper chromatography, showing that the primary hydrolysis products are also unstable and can undergo further secondary, tertiary and quaternary hydrolyses (Schumacher et al., 1965b). This is in agreement with our results (Fig. 7). Many of these hydrolysis products of TD have also been found in the MRT day 0 sample, as the pH value 7.4 was sufficiently high to allow spontaneous hydrolysis. In the TIC on day 0 of the MRT, the peaks DP₃, DP₅ and DP₆ can be detected and this finding is in accordance with the previous published paper by Schumacher et al. (1965b). In the TIC on day 28 of the MRT, neither TD nor DP₆ but DP₃ and DP₅ can be still detected, accompanied by the formation of new degradation products DP₁, DP₂, & DP₄ (Fig. 7). Fig. 8 suggests a pathway for the degradation scheme. The postulated MS² fragmentation pattern of degradation products can be found in the Supplementary material (Figs. S9–S14).

As the low response of some hydrolysis products of TD in the chromatographic system can hamper their detection in the total ion chromatograms, obtaining of extracted ion chromatograms of suspected ions is useful. Thus, ion chromatograms of the other hydrolysis products of TD reported by Schumacher et al. (1965b) at m/z 167, m/z 147, m/z 148, and m/z 129 were extracted with the data analysis software. All of them except m/z 167 were detected. The extracted ion chromatograms of m/z 147, m/z 148, and m/z 129 were detected at early retention times: 2.9, 2.9 and 3.8 min, respectively.

This indicates that the dead-end degradation products are more polar than spontaneously formed abiotic degradation products of TD (Fig. 6). They are more soluble than TD, possibly providing a higher risk to organisms of the aquatic environment. Our results have proven that not only TD, but also its TPs can exhibit environmental risks.

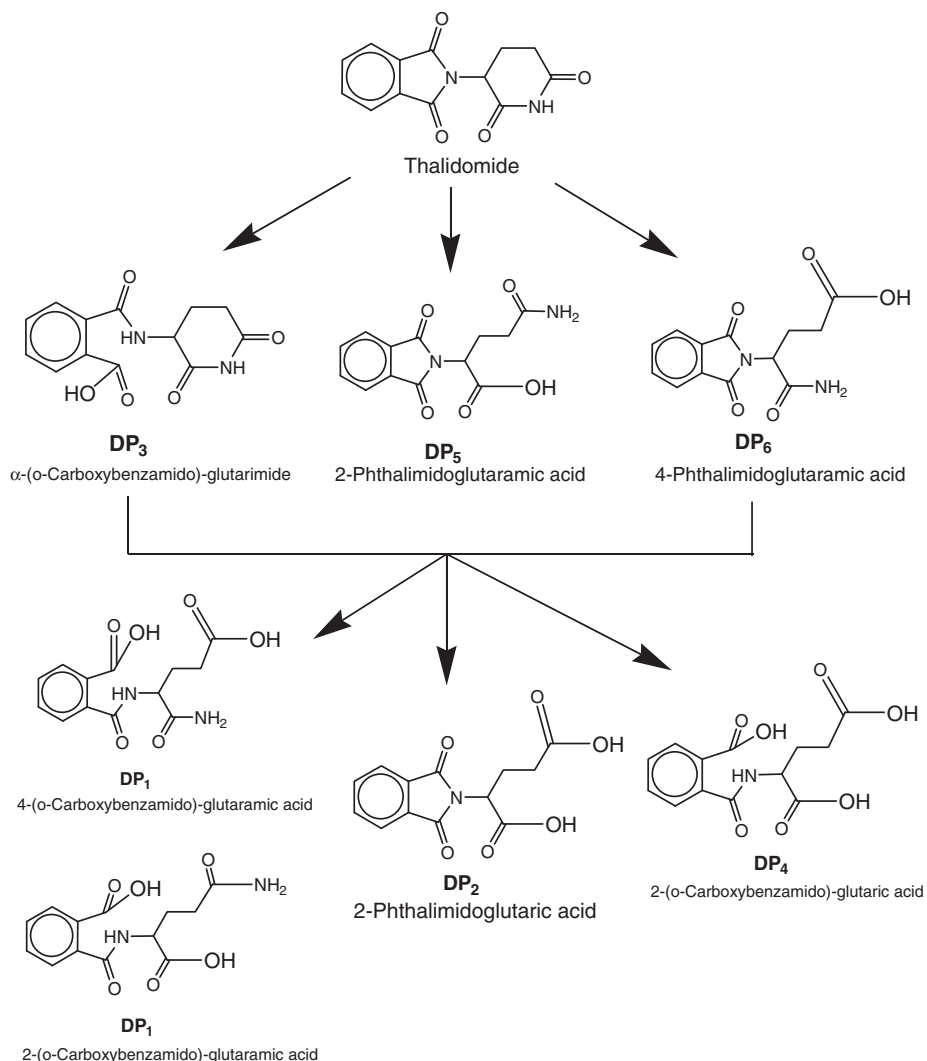


Fig. 8. Proposed degradation pathway for TD in biodegradation tests.

Moreover, its TPs might be persistent. This is of particular interest, since the findings of Meise et al. indicate that three of the identified hydrolysis products (DP₂, DP₅ and DP₆) which contain the intact phthalimide moiety showed teratogenic activity (Meise et al., 1973).

In summary, our study shows that once TD is released into the aquatic environment, it will be completely transformed by biological and photochemical processes, resulting in expected high environmental concentration of not yet fully characterized TPs. Therefore, TD is probably not detectable in the environment because of its instability in aqueous solution.

4. Conclusion

TD was not readily biodegraded in the CBT and MRT. However, TD undergoes primary elimination to form new degradation products. Photodegradation can be an important transformation process in limiting TD persistence in the aquatic environment. The data obtained from these photodegradation assays show clearly the positive effect of irradiation on the removal of TD. UV-photodegradation leads to complete transformation of TD after 64 min of photolysis and around 77.8% mineralization after 128 min of photolysis occur.

The combination of LC–UV–MS/MS and DOC monitoring gave valuable insights into the degree of mineralization and the resulting TPs. The data presented here demonstrate that TPs of TD are more important in the environmental monitoring than TD itself. Therefore, the authors strongly recommend further research on parent compounds as well as especially on their TPs, including additional toxicity and teratogenicity tests.

Acknowledgments

Waleed Mohamed Mamdouh Mahmoud Ahmed thanks the Ministry of Higher Education and Scientific Research of the Arab Republic of Egypt (MHESR) and the German Academic Exchange Service (DAAD) for the scholarship (Egyptian–German Research Long Term Scholarship (GERLS)). The authors wish to thank MultiCASE Inc. for providing CASE Ultra and MetaPC softwares.

Appendix A. Supplementary data

Supplementary data to this article can be found online at <http://dx.doi.org/10.1016/j.scitotenv.2013.05.082>.

References

- Bosch ME, Sánchez AR, Rojas FS, Ojeda CB. Recent advances in analytical determination of thalidomide and its metabolites. *J Pharm Biomed* 2008;46:9–17.
- Canonica S, Meunier L, von Gunten U. Phototransformation of selected pharmaceuticals during UV treatment of drinking water. *Water Res* 2008;42:121–8.
- Carballa M, Omil F, Lema JM, Llopart M, García-Jares C, Rodríguez I, et al. Behavior of pharmaceuticals, cosmetics and hormones in a sewage treatment plant. *Water Res* 2004;38:2918–26.
- Chakravarti SK, Saiakhov RD, Klopman G. Optimizing predictive performance of CASE Ultra expert system models using the applicability domains of individual toxicity alerts. *J Chem Inf Model* 2012;52:2609–18.
- Eriksson T, Björkman S, Roth B, Björk H, Höglund P. Drug metabolism: hydroxylated metabolites of thalidomide: formation in-vitro and in-vivo in man. *J Pharm Pharmacol* 1998;50:1409–16.
- European Commission. Technical guidance document on risk assessment part II. http://ec.europa.eu/environment/chemicals/exist_subst/pdf/tgdpart2_2ed.pdf, 2003.
- Fatta-Kassinos D, Vasquez MI, Kümmerer K. Transformation products of pharmaceuticals in surface waters and wastewater formed during photolysis and advanced oxidation processes – degradation, elucidation of byproducts and assessment of their biological potency. *Chemosphere* 2011;85:693–709.
- Friedrich J, Längin A, Kümmerer K. Comparison of an electrochemical and luminescence-based oxygen measuring system for use in the Closed Bottle test. *Clean – Soil Air Water* 2013;41:251–7.
- Gartiser S, Ulrich E, Alexy R, Kümmerer K. Ultimate biodegradation and elimination of antibiotics in inherent tests. *Chemosphere* 2007;67:604–13.
- Gros M, Petrović M, Barceló D. Multi-residue analytical methods using LC–tandem MS for the determination of pharmaceuticals in environmental and wastewater samples: a review. *Anal Bioanal Chem* 2006;386:941–52.
- Halling-Sørensen B, Nors Nielsen S, Lanzky PF, Ingerslev F, Holten Lützhøft HC, Jørgensen SE. Occurrence, fate and effects of pharmaceutical substances in the environment – a review. *Chemosphere* 1998;36:357–93.
- Heberer T. Occurrence, fate, and removal of pharmaceutical residues in the aquatic environment: a review of recent research data. *Toxicol Lett* 2002;131:5–17.
- Howard PH, Muir DCG. Identifying new persistent and bioaccumulative organics among chemicals in commerce II: pharmaceuticals. *Environ Sci Technol* 2011;45:6938–46.
- ISO (International Standards Organization). Water quality – determination of dissolved oxygen. German standard methods for the examination of water, wastewater and sludge. Berlin: WILEY-VCH Verlag GmbH & Co. KGaA; Weinheim, and Beuth Verlag GmbH; 1990.
- Johnson AC, Jürgens MD, Williams RJ, Kümmerer K, Kortenkamp A, Sumpter JP. Do cytotoxic chemotherapy drugs discharged into rivers pose a risk to the environment and human health? An overview and UK case study. *J Hydrol* 2008;348:167–75.
- Kang SJ, Allbaugh TA, Reynhout JW, Erickson TL, Olmstead KP, Thomas L, et al. Selection of an ultraviolet disinfection system for a municipal wastewater treatment plant. *Water Sci Technol* 2004;50:163–9.
- Khaleel NDH, Mahmoud WMM, Hadad GM, Abdel-Salam RA, Kümmerer K. Photolysis of sulfamethoxy-pyridazine in various aqueous media: aerobic biodegradation and identification of photoproducts by LC–UV–MS/MS. *J Hazard Mater* 2013;244–245:654–61.
- Klán P, Wirz J. Photochemistry of organic compounds: from concepts to practice. Chichester, U.K: Wiley; 2009.
- Kosjek T, Heath E. Occurrence, fate and determination of cytostatic pharmaceuticals in the environment: biogenic volatile organic compounds S.I. *TrAC Trends Anal Chem* 2011;30:1065–87.
- Kümmerer K, editor. *Pharmaceuticals in the environment: sources, fate, effects and risks*. 3rd ed. Berlin, Heidelberg: Springer; 2008.
- Kümmerer K. The presence of pharmaceuticals in the environment due to human use – present knowledge and future challenges. *J Environ Manage* 2009;90:2354–66.
- Kümmerer K, Al-Ahmad A. Estimation of the cancer risk to humans resulting from the presence of cyclophosphamide and ifosfamide in surface water. *Environ Sci Pollut Res* 2010;17:486–96.
- Kümmerer K, Al-Ahmad A, Steger-Hartmann Thomas. Epirubicin hydrochloride in the aquatic environment – biodegradation and bacterial toxicity. *Umweltmed Forsch Prax* 1996;1:133–7.
- Laboratory of Mathematical Chemistry. “Prof. Dr. Assen Zlatarov” University, Bourgas, Bulgaria. Oasis Catalogic software V.5.11.6TB; 2012.
- Lam MW, Mabury SA. Photodegradation of the pharmaceuticals atorvastatin, carbamazepine, levofloxacin, and sulfamethoxazole in natural waters. *Aquat Sci* 2005;67:177–88.
- Liberti L, Notarnicola M. Advanced treatment and disinfection for municipal wastewater reuse in agriculture. *Water Sci Technol* 1999;40:235–45.
- Mahmoud WMM, Kümmerer K. Captopril and its dimer captopril disulfide: Photodegradation, aerobic biodegradation and identification of transformation products by HPLC–UV and LC–ion trap–MSⁿ. *Chemosphere* 2012;88:1170–7.
- Meise W, Ockenfels H, Köhler F. Teratologische Prüfung der Hydrolysenprodukte des Thalidomids. *Experientia* 1973;29:423–4.
- Meneses M, Pasqualino JC, Castells F. Environmental assessment of urban wastewater reuse: treatment alternatives and applications. *Chemosphere* 2010;81:266–72.
- Meyring M, Strickmann D, Chankvetadze B, Blaschke G, Desiderio C, Fanali S. Investigation of the in vitro biotransformation of R-(+)-thalidomide by HPLC, nano-HPLC, CEC and HPLC–APCI–MS. *J Chromatogr B* 1999;723:255–64.
- Nikolaou A, Meric S, Fatta D. Occurrence patterns of pharmaceuticals in water and wastewater environments. *Anal Bioanal Chem* 2007;387:1225–34.
- Oosterhuis M, Sacher F, ter Laak TL. Prediction of concentration levels of metformin and other high consumption pharmaceuticals in wastewater and regional surface water based on sales data. *Sci Total Environ* 2013;442:380–8.
- Organisation for Economic Co-operation and Development. OECD guidelines for the testing of chemicals degradation and accumulation test no. 302C: inherent biodegradability: modified MITI test (II). Paris: OECD Publishing; 1981.
- Organisation for Economic Co-operation and Development. OECD guideline for testing of chemicals 301D: ready biodegradability. Closed Bottle test. Paris: OECD Publishing; 1992a.
- Organisation for Economic Co-operation and Development. OECD guideline for testing of chemicals 301F: ready biodegradability. manometric respiratory test. Paris: OECD Publishing; 1992b.
- Petrovic M, Barceló D. LC–MS for identifying photodegradation products of pharmaceuticals in the environment: pharmaceutical-residue analysis. *TrAC Trends Anal Chem* 2007;26:486–93.
- Price DK, Ando Y, Kruger EA, Weiss M, Figg WD. 5'-OH-thalidomide, a metabolite of thalidomide, inhibits angiogenesis. *Ther Drug Monit* 2002;24:104–10.
- Reist M, Carrupt P, Francotte E, Testa B. Chiral inversion and hydrolysis of thalidomide: mechanisms and catalysis by bases and serum albumin, and chiral stability of teratogenic metabolites. *Chem Res Toxicol* 1998;11:1521–8.
- Rücker C, Kümmerer K. Modeling and predicting aquatic aerobic biodegradation – a review from a user's perspective. *Green Chem* 2012;14:875.
- Schumacher H, Smith RL, Williams RT. The metabolism of thalidomide: the fate of thalidomide and some of its hydrolysis products in various species. *Br J Pharmacol Chemother* 1965a;25:338–51.
- Schumacher H, Smith RL, Williams RT. The metabolism of thalidomide: the spontaneous hydrolysis of thalidomide in solution. *Br J Pharmacol Chemother* 1965b;25:324–37.
- Sedykh A, Saiakhov R, Klopman GMETAV. A model of photodegradation for the prediction of photoproducts of chemicals under natural-like conditions. *Chemosphere* 2001;45:971–81.
- Sweetman SC. Martindale: the complete drug reference. 36th ed. London, Chicago: Pharmaceutical Press; 2009.
- Termes TA. Occurrence of drugs in German sewage treatment plants and rivers. *Water Res* 1998;32:3245–60.
- Tixier C, Singer HP, Oellers S, Müller SR. Occurrence and fate of carbamazepine, clofibrac acid, diclofenac, ibuprofen, ketoprofen, and naproxen in surface waters. *Environ Sci Technol* 2003;37:1061–8.
- Tønnesen HH. Photostability of drugs and drug formulations. 2nd ed. Boca Raton, New York: CRC Press; 2004.
- Trautwein C, Kümmerer K. Incomplete aerobic degradation of the antidiabetic drug metformin and identification of the bacterial dead-end transformation product guanlylurea. *Chemosphere* 2011;85:765–73.
- Trautwein C, Kümmerer K. Ready biodegradability of trifluoromethylated phenothiazine drugs, structural elucidation of their aquatic transformation products, and identification of environmental risks studied by LC–MSⁿ and QSAR. *Environ Sci Pollut Res* 2012;19(8):3162–77.
- U.S. EPA. United States Environmental Protection Agency, wastewater technology fact sheet ultraviolet disinfection. http://water.epa.gov/scitech/wastetech/upload/2002_06_28_mtb_uv.pdf, 1998. [832-F99-064].
- U.S. National Library of Medicine, 8600 Rockville Pike, Bethesda, MD 20894. THALIDOMIDE – National Library of Medicine HSDB database. <http://toxnet.nlm.nih.gov/cgi-bin/sis/search/a?dbs+hsdb:@term+@DOCNO+3586>. [accessed September 21, 2011].
- US EPA United States Environmental Protection Agency. EPA/OPPT/Exposure Assessment Tools and Models/Estimation Program Interface (EPI) suite version 3.12 (August 17, 2004). <http://www.epa.gov/oppt/exposure/pubs/episuite.htm>, 2004. [accessed November 28, 2012].
- Wolfbeis OS. Fiber-optic chemical sensors and biosensors. *Anal Chem* 2002;74:2663–78.

Supplementary Material

Aquatic photochemistry, abiotic and aerobic biodegradability of thalidomide: identification of stable transformation products by LC–UV-MSⁿ

Waleed M. M. Mahmoud^{1,2}, Christoph Trautwein¹, Christoph Leder¹, Klaus Kümmerer^{1*}

- 1- Sustainable Chemistry and Material Resources, Institute of Sustainable and Environmental Chemistry, Faculty of Sustainability, Leuphana University of Lüneburg, Scharnhorststraße 1/C13, DE-21335 Lüneburg, Germany.
- 2- Pharmaceutical Analytical Chemistry Department, Faculty of Pharmacy, Suez Canal University, Ismailia 41522, Egypt

Table S1. Composition of biodegradation test series in the Closed Bottle test (1–4), Manometric Respiratory test (1–5).

Test series	1	2	3	4	5
	Blank	Quality control	Test compound	Toxicity control	Sterile/Negative control
Test substance*	-	-	+	+	+
Mineral medium	+	+	+	+	+
Inoculum	+	+	+	+	-
Reference substance (Sodium acetate)**	-	+	-	+	-
Sodium azide ***	-	-	-	-	+

* TD concentration in CBT: 3.4 mg L⁻¹, and in MRT: 20.2 mg L⁻¹; Sample volume of 10mg L⁻¹ of TD after 16min of photolysis used in CBT: 340 ml L⁻¹.

** Sodium acetate in CBT: 6.4 mg L⁻¹, and in MRT: 38.5 mg L⁻¹.

*** Sodium azide in MRT: 160 mg L⁻¹.

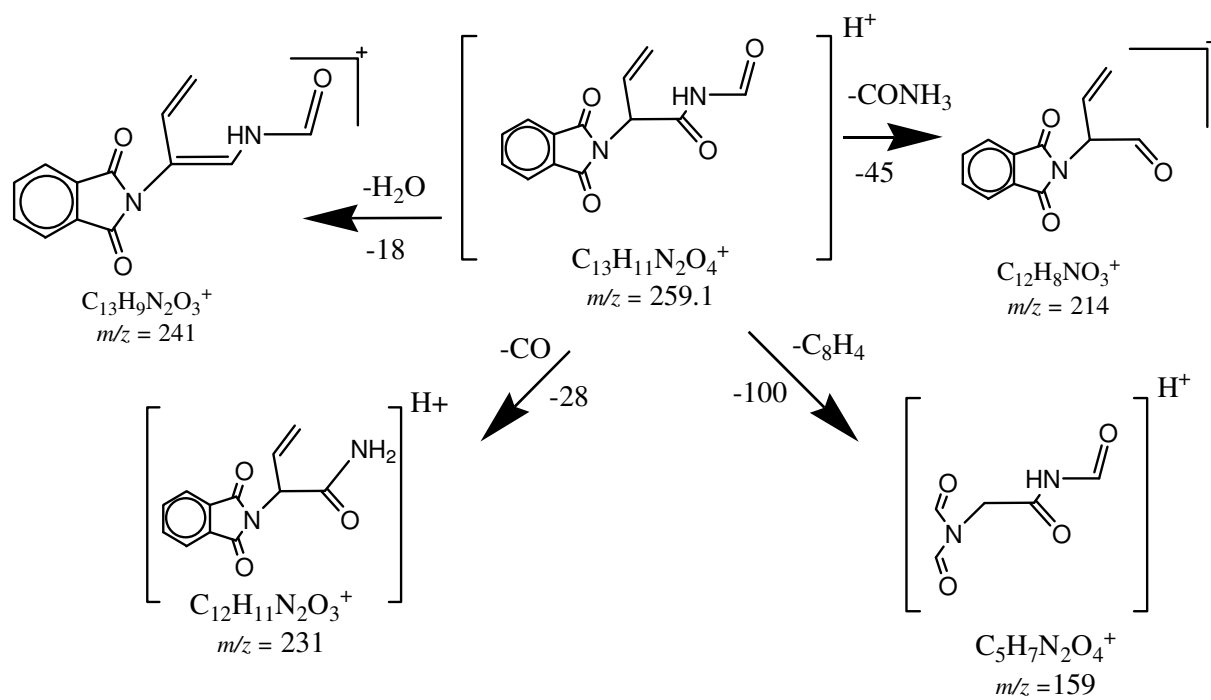


Figure S1: MS² fragmentation pattern for the transformation photoproduct 1 (TP1).

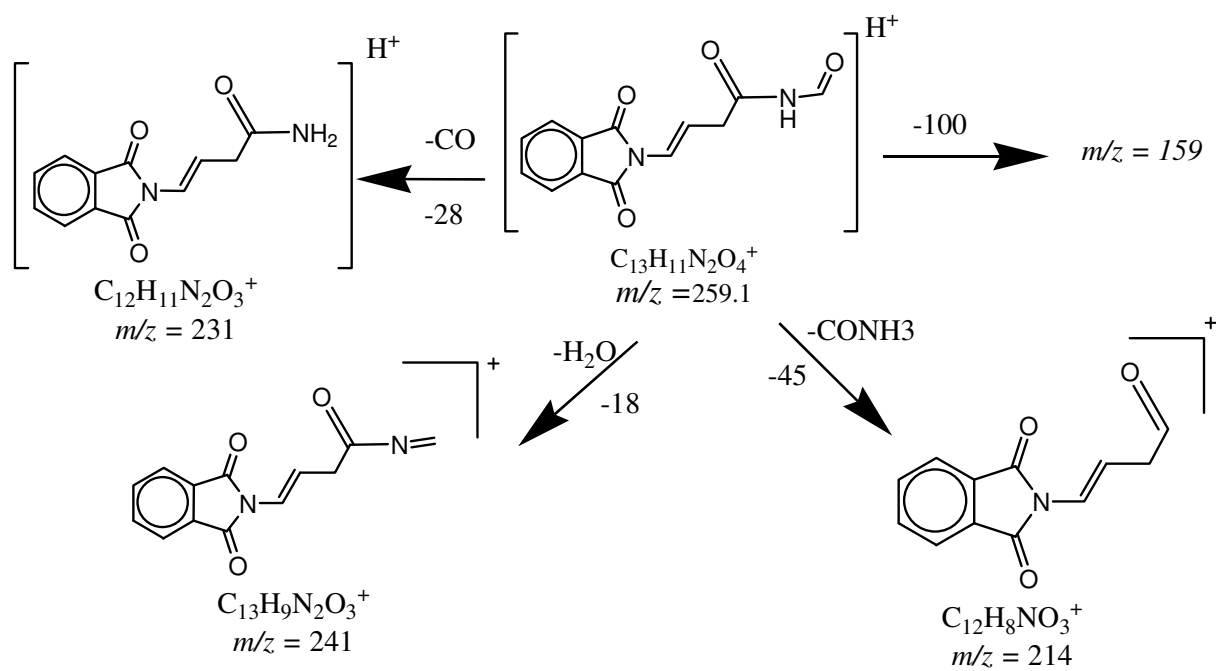


Figure S2: MS² fragmentation pattern for the transformation photoproduct 2 (TP2).

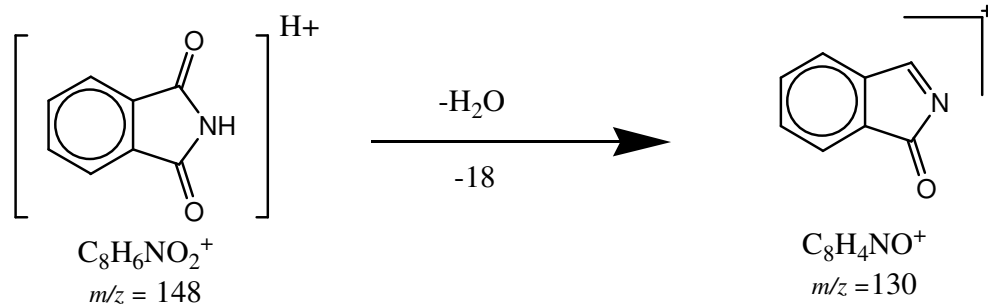


Figure S3: MS² fragmentation pattern for the transformation photoproduct 3 (TP3).

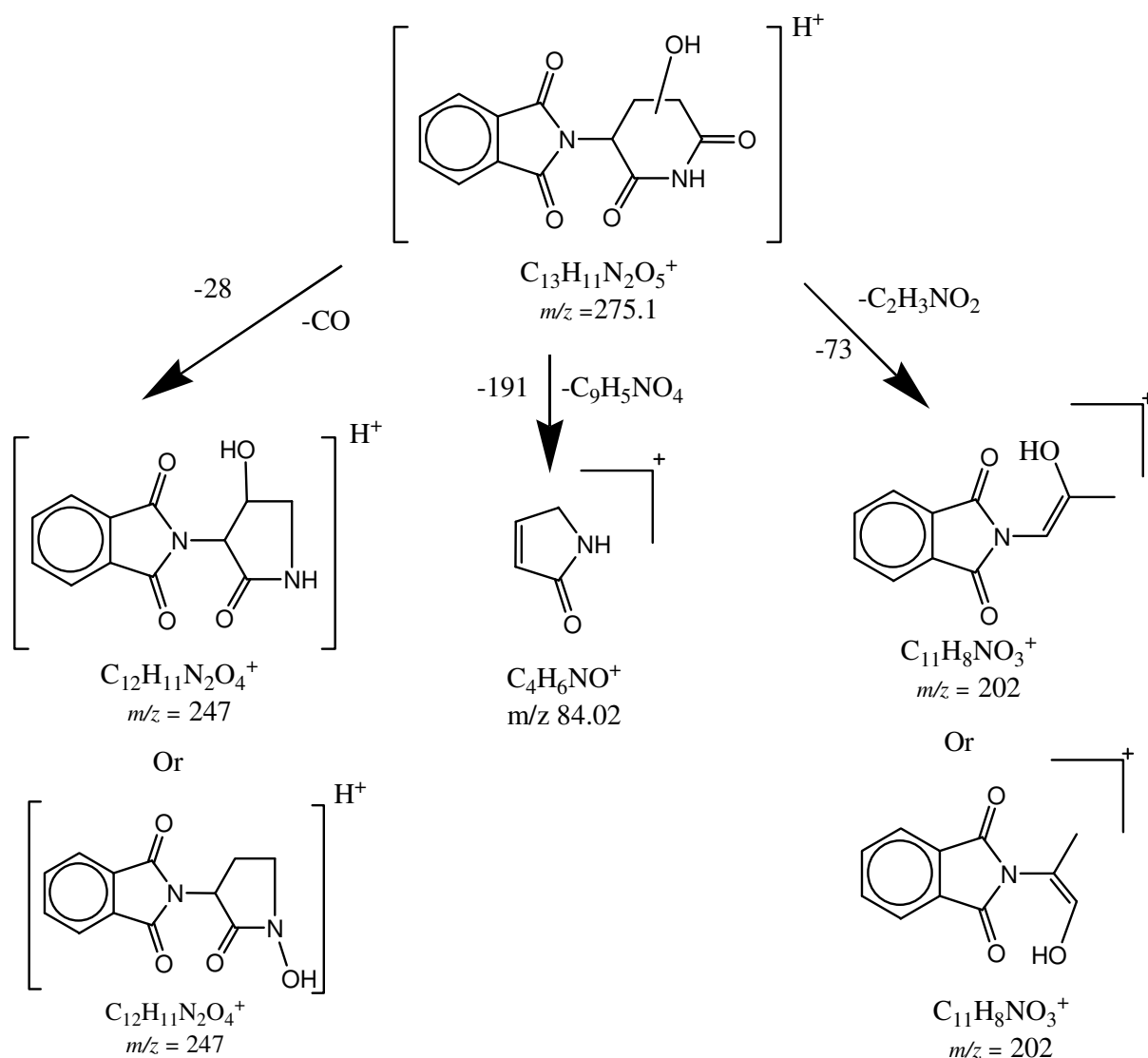


Figure S4: Proposed MS² fragmentation pattern for the transformation photoproduct 4(TP4)

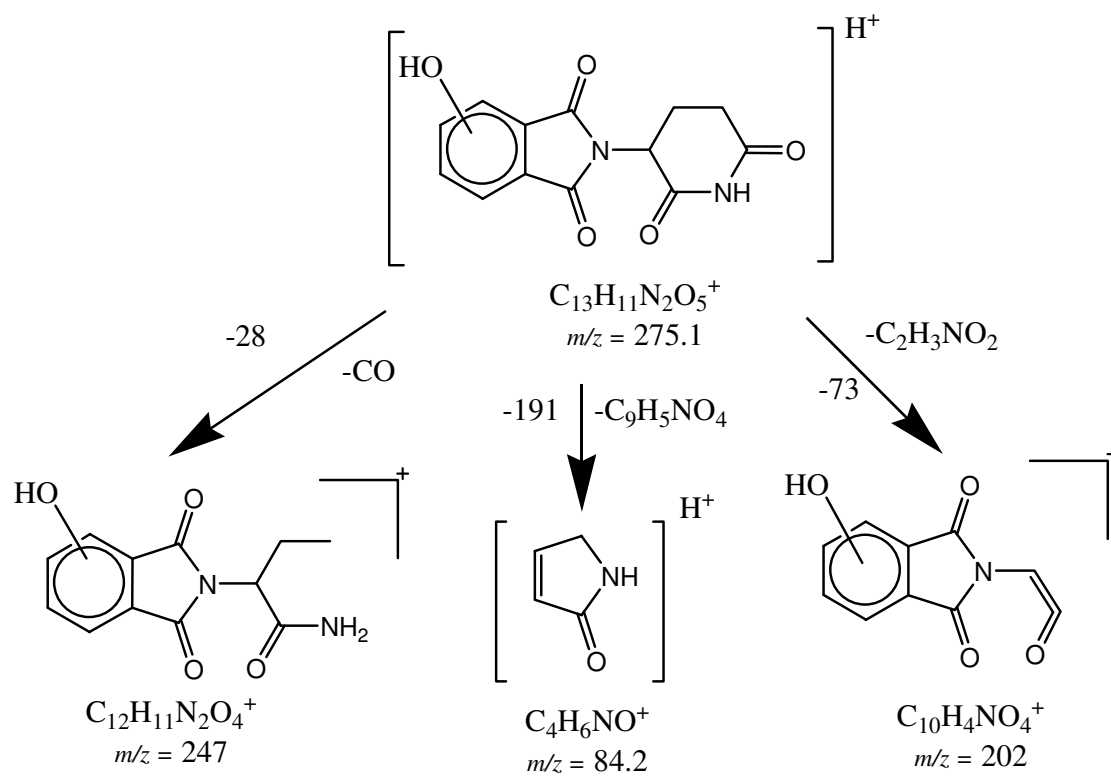


Figure S5: Proposed MS² fragmentation pattern for the transformation photoproduct 5(TP5).

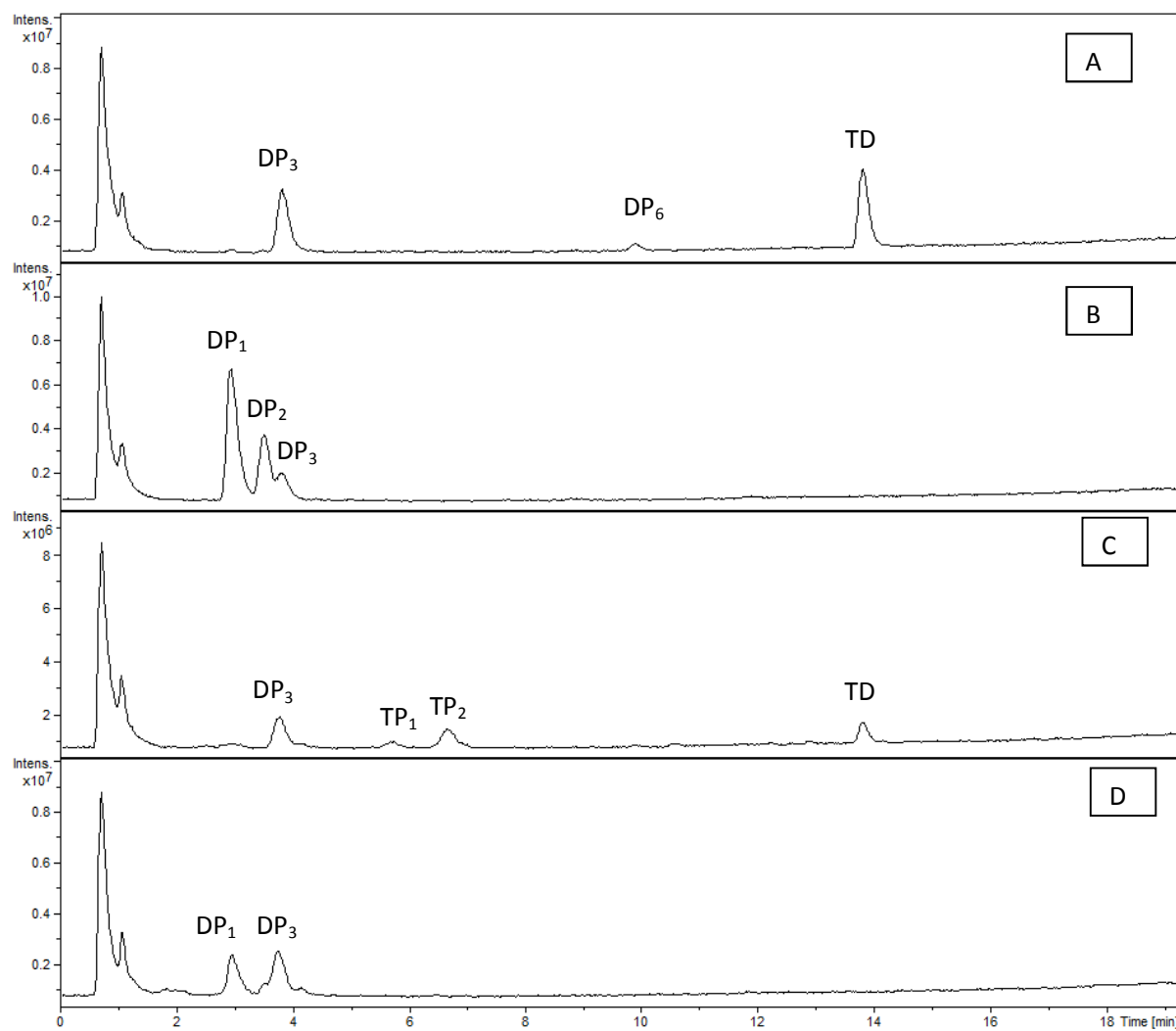


Figure S6. Total ion chromatograms (TICs) of TD samples in CBT test: a) day 0, b) day 28, c) after 16 min of photolysis of CBT day 0, d) after 16 min of photolysis of CBT day 28.

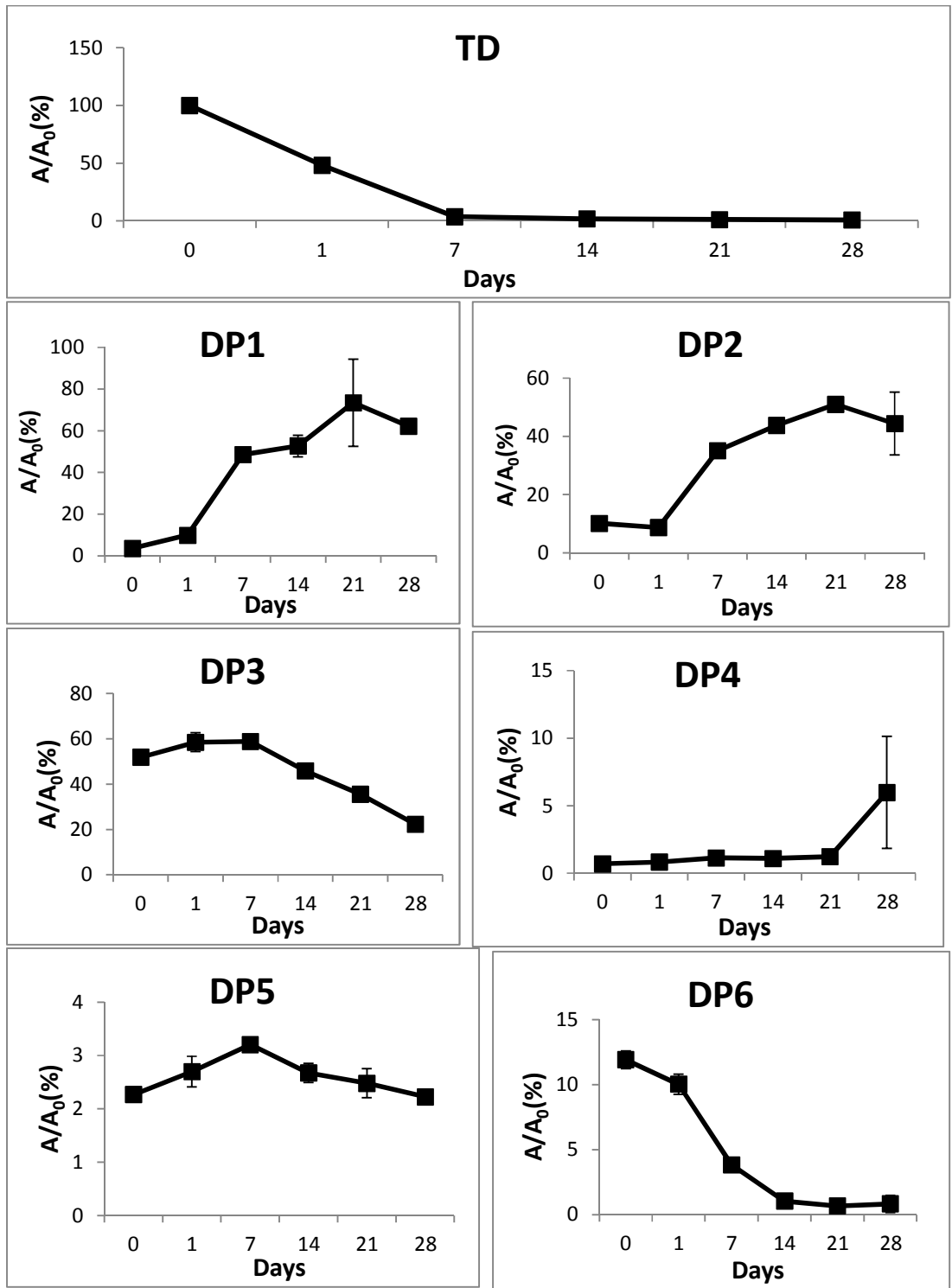


Fig. S7 Time course of the percentual recovery of area ratio (A/A_0 as A is the area of the DP and A_0 is the area of TD at day 0) of the formed DPs during CBT ($n=2$).

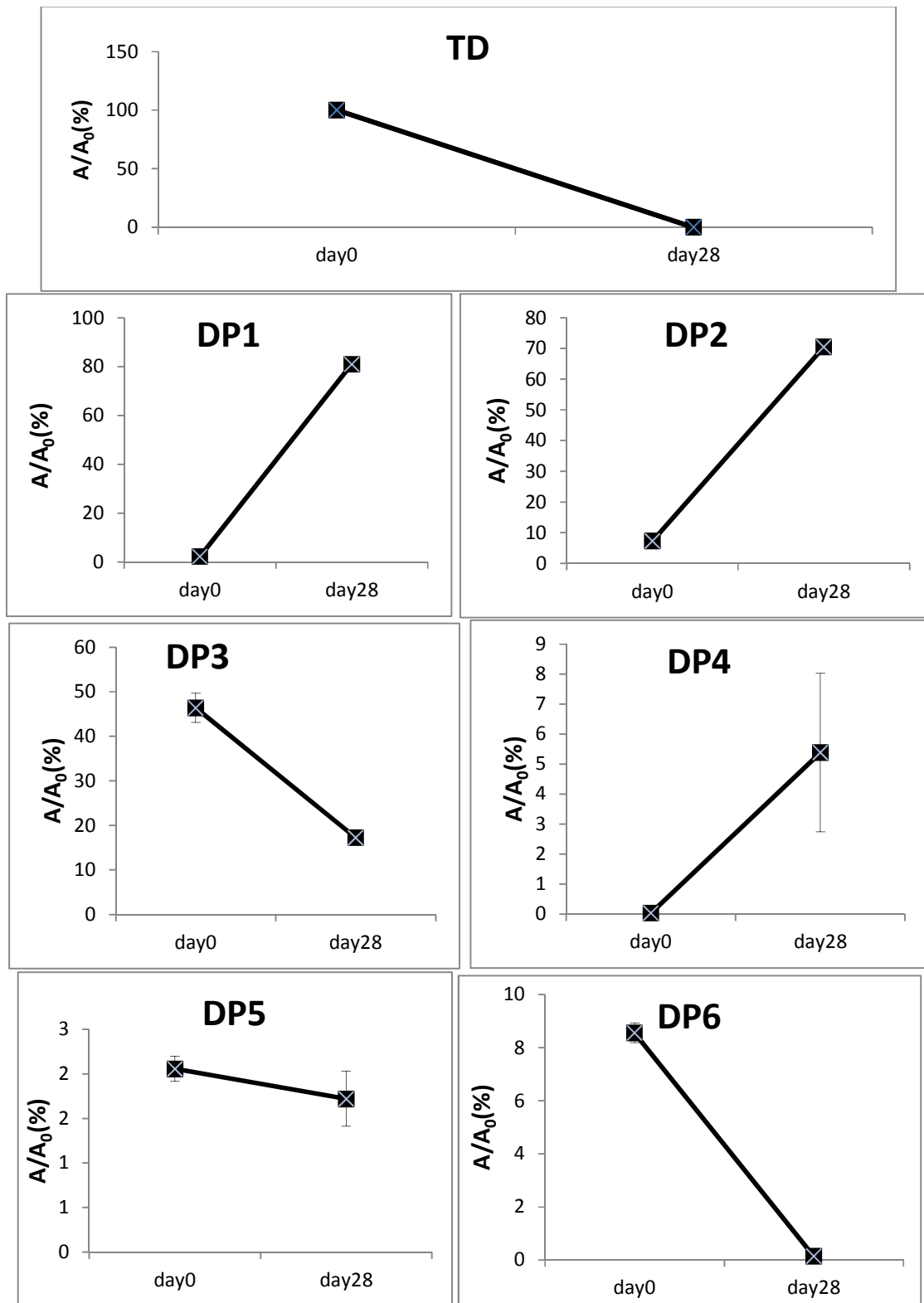
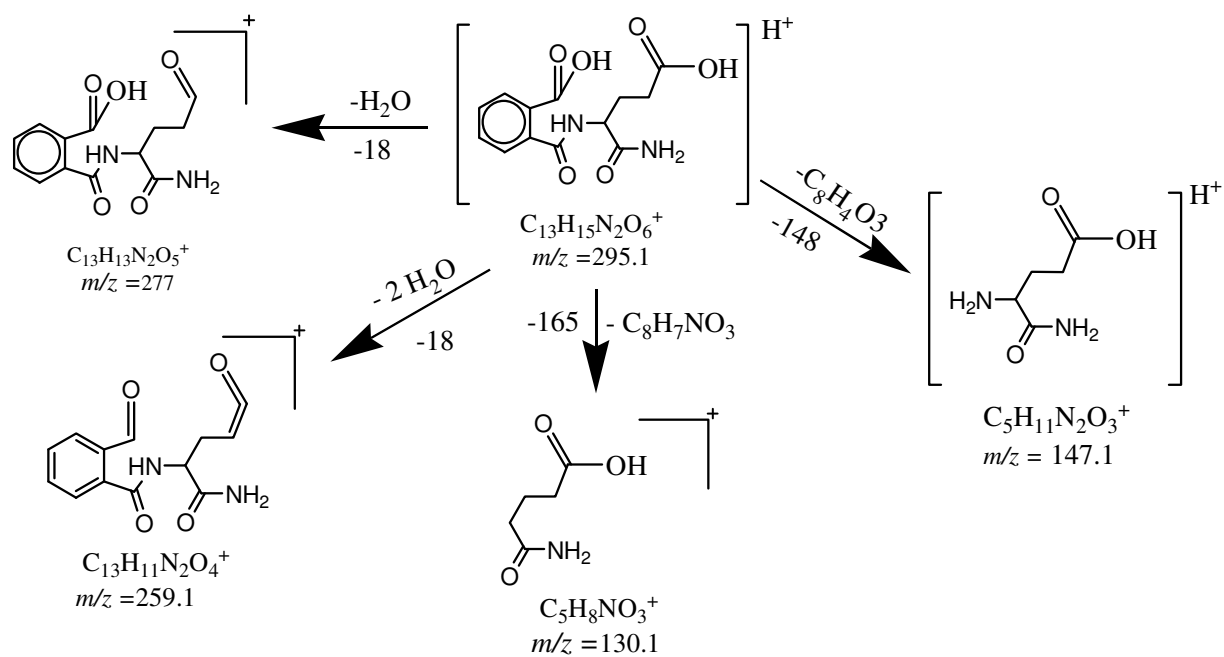


Fig. S8 Time course of the percentual recovery of area ratio (A/A_0 as A is the area of the DP and A_0 is the area of TD at day 0) of the formed DPs during MRT ($n=2$).



or

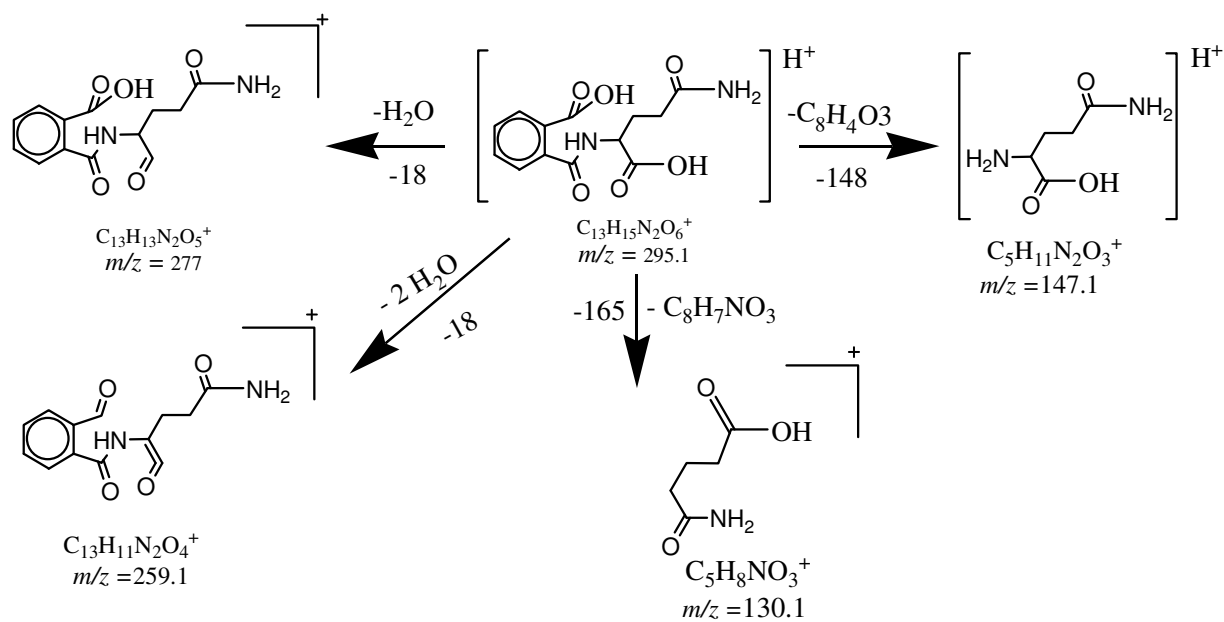


Figure S9: MS² fragmentation pattern for the degradation product 1 (DP1).

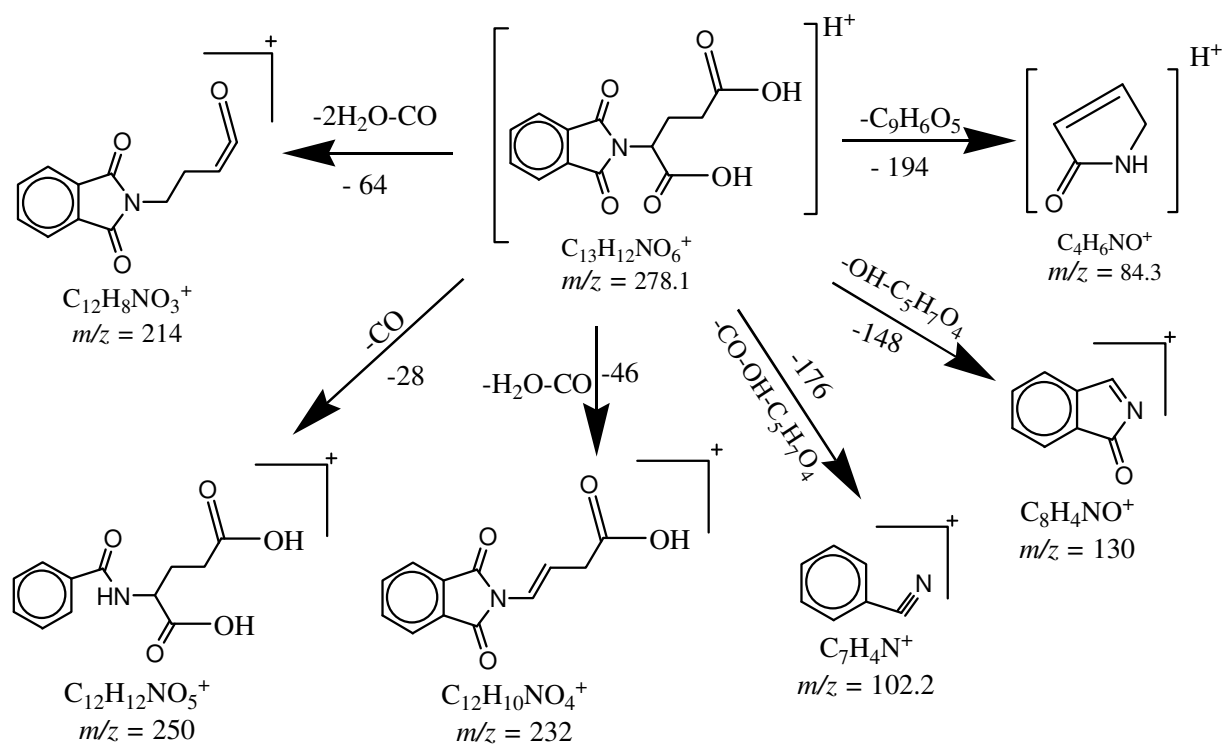


Figure S10: MS² fragmentation pattern for the degradation product 2 (DP2).

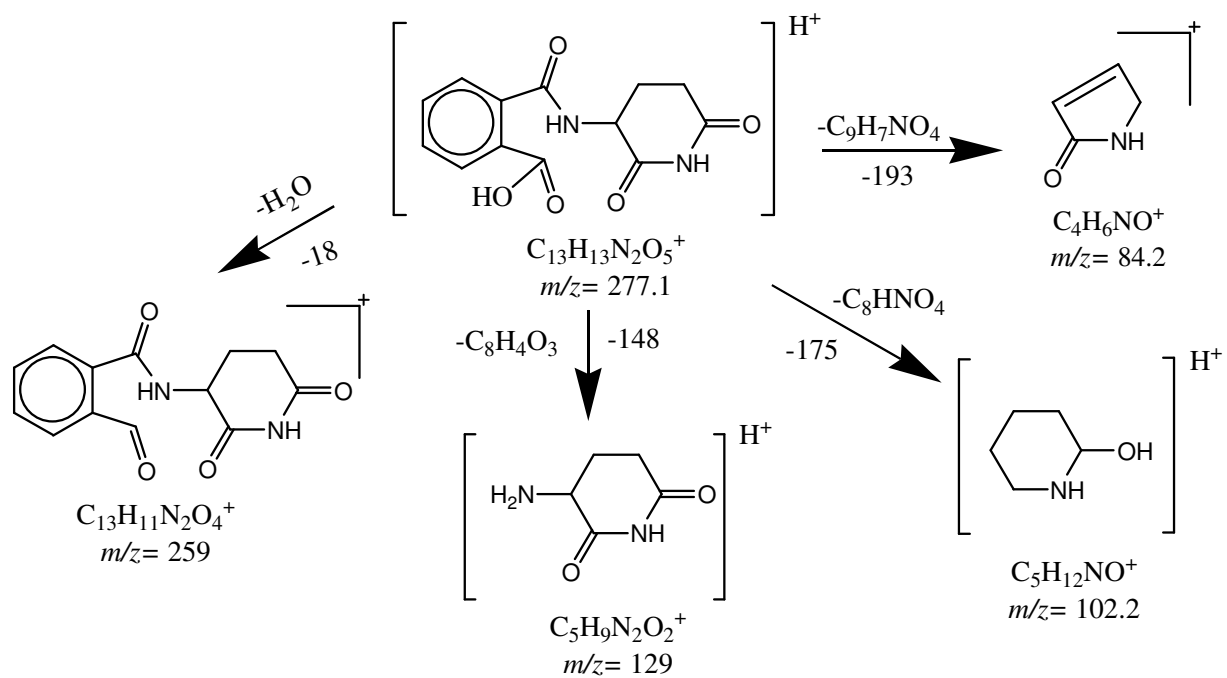


Figure S11: MS² fragmentation pattern for the degradation product 3 (DP3).

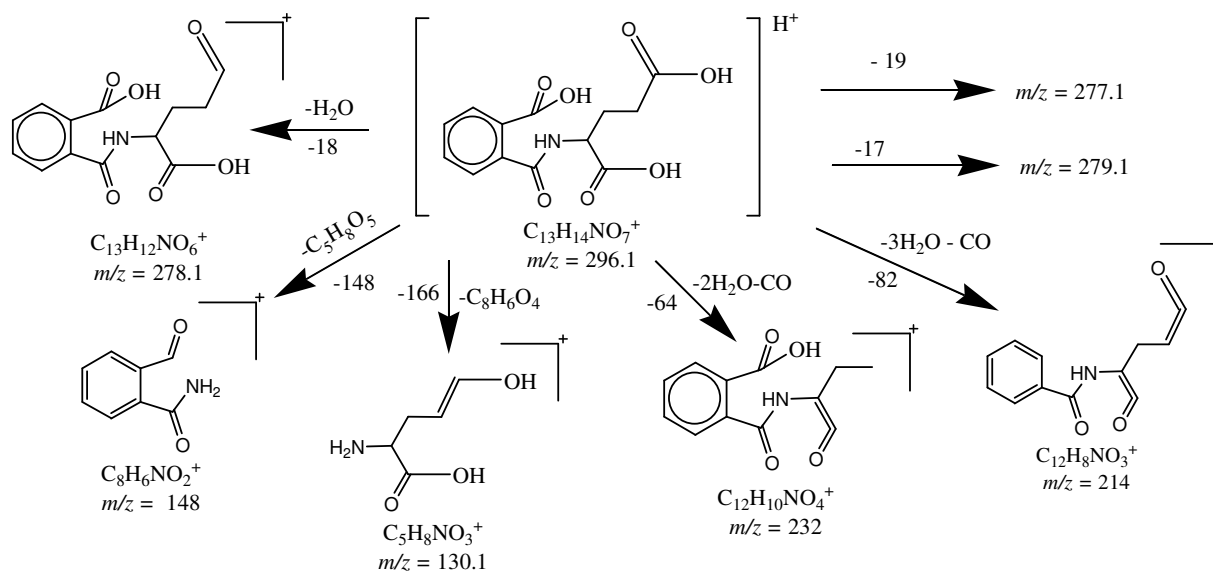


Figure S12: MS² fragmentation pattern for the degradation product 4 (DP4).

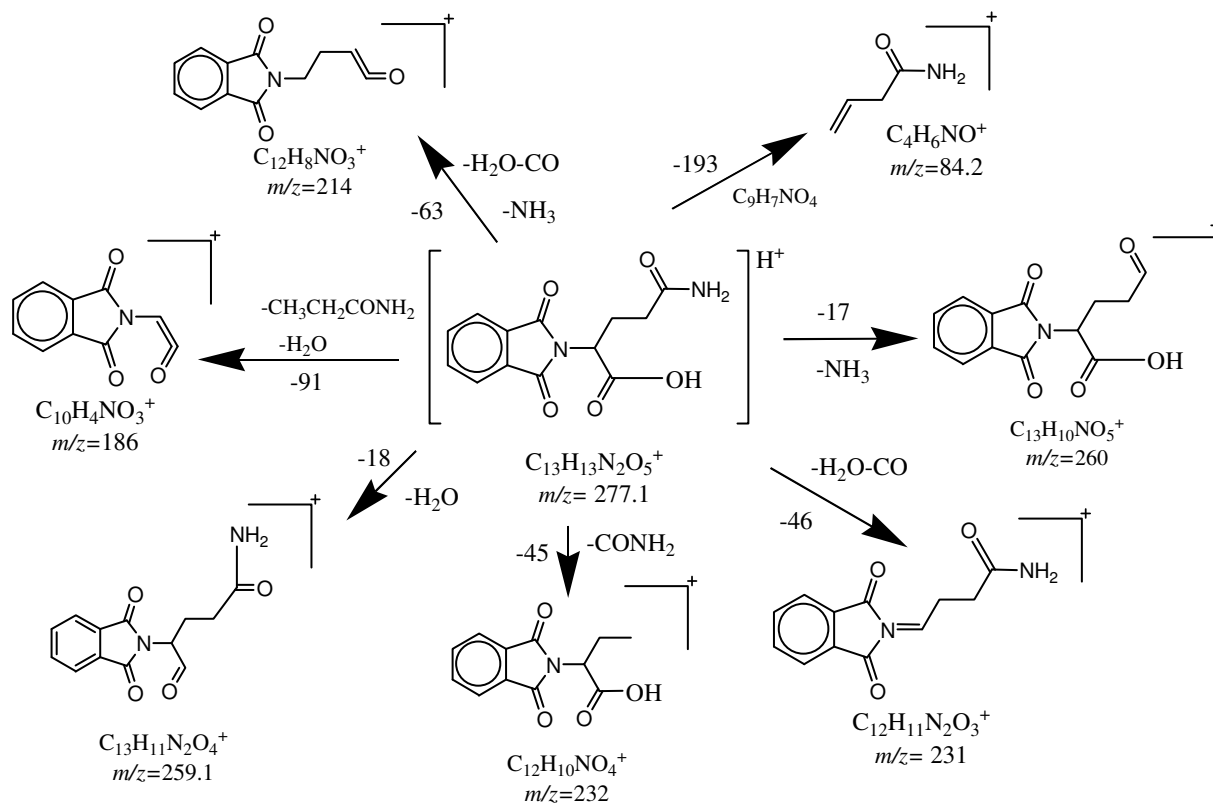


Figure S13: MS² fragmentation pattern for the degradation product 5 (DP5).

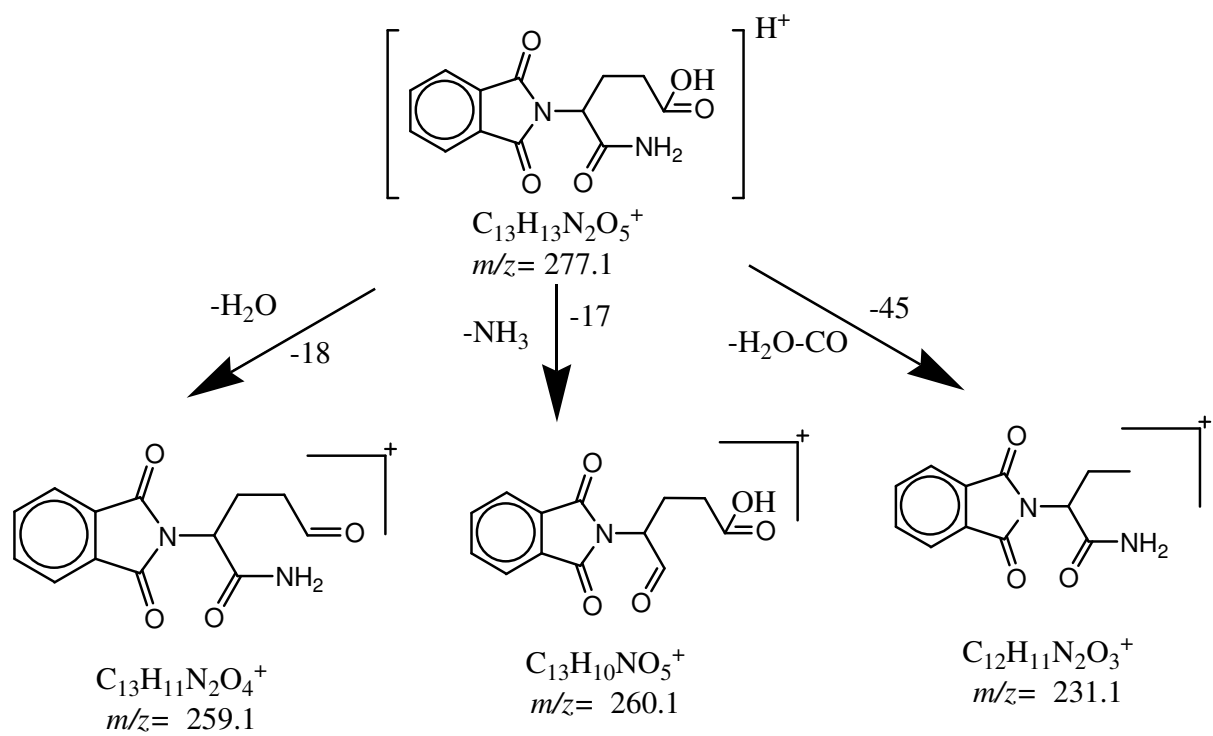


Figure S14: MS² fragmentation pattern for the degradation product 6 (DP6).

Paper VII

Identification of phototransformation products of
Thalidomide and mixture toxicity assessment: an
experimental and quantitative structural activity
relationships (QSAR) approach

Water Research (2013)
DOI: 10.1016/j.watres.2013.11.014.

Accepted Manuscript

Identification of phototransformation products of Thalidomide and mixture toxicity assessment: an experimental and quantitative structural activity relationships (QSAR) approach

Waleed M.M. Mahmoud, Anju P. Toolaram, Jakob Menz, Christoph Leder, Mandy Schneider, Klaus Kümmerer

PII: S0043-1354(13)00925-1

DOI: [10.1016/j.watres.2013.11.014](https://doi.org/10.1016/j.watres.2013.11.014)

Reference: WR 10324

To appear in: *Water Research*

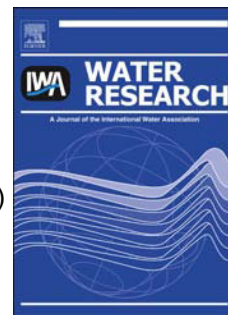
Received Date: 29 July 2013

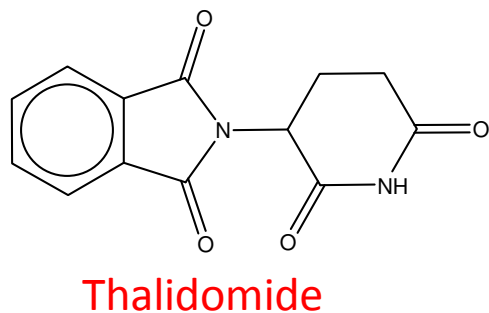
Revised Date: 8 November 2013

Accepted Date: 9 November 2013

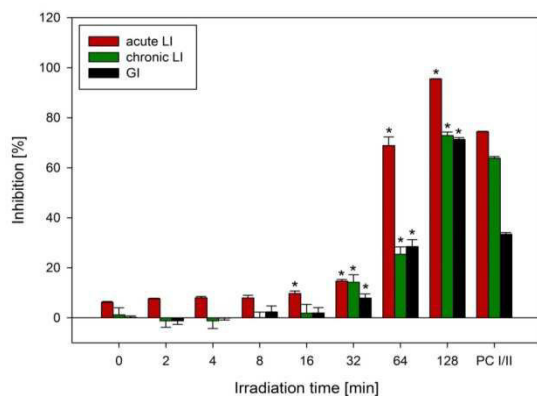
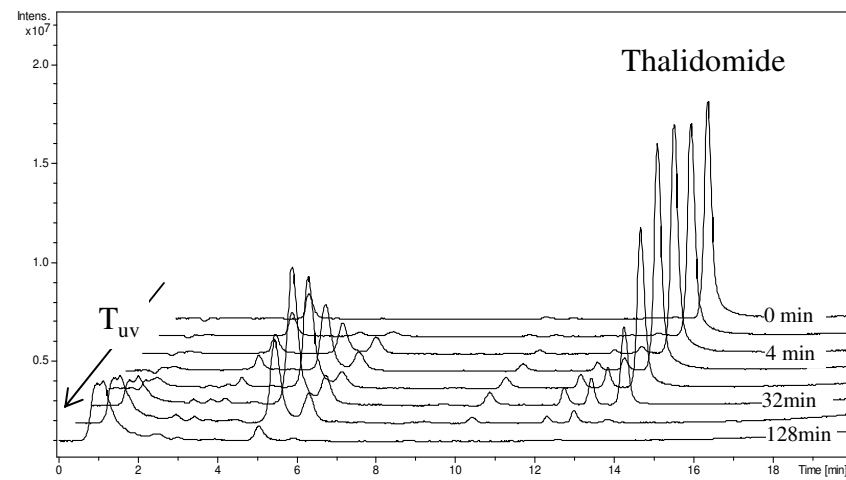
Please cite this article as: Mahmoud, W.M.M., Toolaram, A.P., Menz, J., Leder, C., Schneider, M., Kümmerer, K., Identification of phototransformation products of Thalidomide and mixture toxicity assessment: an experimental and quantitative structural activity relationships (QSAR) approach, *Water Research* (2013), doi: 10.1016/j.watres.2013.11.014.

This is a PDF file of an unedited manuscript that has been accepted for publication. As a service to our customers we are providing this early version of the manuscript. The manuscript will undergo copyediting, typesetting, and review of the resulting proof before it is published in its final form. Please note that during the production process errors may be discovered which could affect the content, and all legal disclaimers that apply to the journal pertain.





UV irradiation →



Experimental toxicity assesment

Identification and structure elucidation of transformation products by LC-MSⁿ

Time (min)	Number of revertants			
	TA98		TA100	
	-S9	+S9	-S9	+S9
NC	1±1	2±1	7±3	3±2
0	1±1	1±1	7±3	4±2
2	1±1	1±1	5±3	3±2
4	1±1	2±1	9±4	5±1
8	1±1	2±1	8±3	4±2
16	1±1	2±1	6±3	3±1
32	2±1	1±1	9±5	5±3
64	2±1	2±1	7±3	5±3
128	3±2	2±1	8±2	4±1
PC	42±3*	48±0*	47±2*	48±0*

Correlation between experimental toxicity and QSAR results

In silico predictions (QSAR)

- Case Ultra software
- Oasis Catalogic software
- Leadscope software

1 **Identification of phototransformation products of Thalidomide and mixture**
2 **toxicity assessment: an experimental and quantitative structural activity**
3 **relationships (QSAR) approach**
4

5 Waleed M. M. Mahmoud^{1,2}, Anju P. Toolaram¹, Jakob Menz¹, Christoph Leder¹,
6 Mandy Schneider¹, Klaus Kümmerer¹

7 1- Sustainable Chemistry and Material Resources, Institute of Sustainable and
8 Environmental Chemistry, Faculty of Sustainability, Leuphana University of Lüneburg,
9 Scharnhorststraße 1/C13, DE-21335 Lüneburg, Germany.

10 2- Pharmaceutical Analytical Chemistry Department, Faculty of Pharmacy, Suez Canal
11 University, Ismailia 41522, Egypt

12
13 * Corresponding author. Address: Nachhaltige Chemie und Stoffliche Ressourcen, Institut für
14 Nachhaltige Chemie und Umweltchemie, Fakultät für Nachhaltigkeit, Leuphana Universität
15 Lüneburg, Scharnhorststraße 1/C13, D-21335 Lüneburg, Germany.

16 Tel.: +49 4131 677-2893

17
18 E-mail address:

19 waleed.ahmed@uni.leuphana.de (W. M.M. Mahmoud Ahmed), toolaram@leuphana.de (A.P.
20 Toolaram), jakob.menz@uni.leuphana.de (J. Menz), cleder@leuphana.de (C. Leder),
21 mandy.schneider@leuphana.de (M. Schneider), klaus.kuemmerer@uni.leuphana.de (K.
22 Kümmerer).

23 Abstract:

24 The fate of thalidomide (TD) was investigated after irradiation with a medium-pressure Hg-
25 lamp. The primary elimination of TD was monitored and structures of phototransformation
26 products (PTPs) were assessed by LC-UV-FL-MS/MS. Environmentally relevant properties of
27 TD and its PTPs as well as hydrolysis products (HTPs) were predicted using *in silico* QSAR
28 models. Mutagenicity of TD and its PTPs was investigated in the Ames microplate format (MPF)
29 aqua assay (Xenometrix, AG). Furthermore, a modified luminescent bacteria test (kinetic
30 luminescent bacteria test (kinetic LBT)), using the luminescent bacteria species *Vibrio fischeri*,
31 was applied for the initial screening of environmental toxicity. Additionally, toxicity of
32 phthalimide, one of the identified PTPs, was investigated separately in the kinetic LBT.

33 The UV irradiation eliminated TD itself without complete mineralization and led to the
34 formation of several PTPs. TD and its PTPs did not exhibit mutagenic response in the
35 *Salmonella typhimurium* strains TA 98, and TA 100 with and without metabolic activation. In
36 contrast, QSAR analysis of PTPs and HTPs provided evidence for mutagenicity, genotoxicity
37 and carcinogenicity using additional endpoints *in silico* software. QSAR analysis of different
38 ecotoxicological endpoints, such as acute toxicity towards *V. fischeri*, provided positive alerts for
39 several identified PTPs and HTPs. This was partially confirmed by the results of the kinetic
40 LBT, in which a steady increase of acute and chronic toxicity during the UV-treatment procedure
41 was observed for the photolytic mixtures at the highest tested concentration. Moreover, the
42 number of PTPs within the reaction mixture that might be responsible for the toxification of TD
43 during UV-treatment was successfully narrowed down by correlating the formation kinetics of
44 PTPs with QSAR predictions and experimental toxicity data. Beyond that, further analysis of the

45 commercially available PTP phthalimide indicated that transformation of TD into phthalimide
46 was not the cause for the toxification of TD during UV-treatment.

47 These results provide a path for toxicological assessment of complex chemical mixtures and
48 in detail show the toxic potential of TD and its PTPs as well as its HTPs. This deserves further
49 attention as UV irradiation might not always be a green technology, because it might pose a
50 toxicological risk for the environment in general and specifically for water compartments.

51

52 **Keywords:** pharmaceuticals; UV irradiation; QSAR; phthalimide, mutagenicity, bacterial
53 toxicity

54

55 **1. Introduction**

56 When pharmaceuticals are released into the environment, they can be transformed
57 through many abiotic and biotic processes that can contribute to their degradation and
58 elimination or lead to the formation of transformation products (TPs) (Fatta-Kassinos et al.,
59 2011; Khaleel et al., 2013). Therefore, the removal of pharmaceuticals and their TPs provides a
60 new challenge to treatment systems for drinking water, wastewater and water reuse. Ultraviolet
61 (UV) light treatment is an established method for water disinfection and sterilization (Canonica
62 et al., 2008), It is also in discussion as a technology for wastewater purification (Liberti and
63 Notarnicola, 1999; Meneses et al., 2010). However, photodegradation can lead to
64 phototransformation products (PTPs) which can have more toxic effects than the parent
65 compound investigated for different toxicological endpoints (Vasquez et al., 2013; Wang and
66 Lin, 2012). Therefore, it is important to gather more information about environmental properties
67 of pharmaceuticals and their TPs and to consider this information in environmental risk
68 assessment.

69 In the early 1960s, Thalidomide (TD) was withdrawn from the market due to its
70 teratogenic effects when given in early pregnancy. In 1998, its use is being revived since the
71 FDA approved TD for the treatment of erythema nodosum leprosum associated with leprosy
72 (Sweetman, 2009). Recently, TD is expected to be a promising drug in the treatment of a number
73 of inflammatory and cancers diseases (Bosch et al., 2008; Sweetman, 2009). Consequently, a
74 potential increased influx of TD into the aquatic environment has to be expected. According to
75 our best knowledge, no study until now has detected TD in the aquatic environment. For sure as
76 a human pharmaceutical the toxic nature of TD has been well investigated, but studies of the

77 toxic effects of TPs are limited in general and even more for TD. In 1994, McBride proposed
78 that TD also may be a human germ cell mutagen based on clinical observations (McBride and
79 Read, 1994). However, Ashby et al. had provided evidence that TD neither exhibited mutagenic
80 responses in different *Salmonella typhimurium* strains (with and without metabolic activation),
81 nor induced chromosome aberration or micronucleus formation *in vivo* and *in vitro* (Ashby et al.,
82 1997). The non-genotoxic properties of the compound were confirmed further by studies from
83 Teo et al. (Teo et al., 2000). According to the best knowledge of the authors, there is no
84 information available in published literature regarding the toxicity of TD towards environmental
85 bacteria. The same applies to most of the previously known hydrolytic products (HTPs) and
86 PTPs.

87 TD is sensitive to hydrolytic decomposition leading to formation of twelve HTPs
88 (Schumacher et al., 1965) (Supplementary material Table S1). The exact metabolic route and fate
89 of thalidomide is unknown, although it appears to undergo non-enzymatic hydrolysis in plasma
90 (Sweetman, 2009). Only the three HTPs which contain the intact phthalimide moiety showed
91 teratogenic activity (Meise et al., 1973).

92 TD undergoes photolysis using xenon lamp and UV lamp without complete mineralization. New
93 PTPs are formed during photolytic process, including phthalimide (Mahmoud et al., 2013).
94 Phthalimide is classified as a high production volume chemical and it is a degradation
95 intermediate formed from many products. Although phthalimide is readily biodegradable, it was
96 detected in concentrations less than 5 µg/L in the effluent of the wastewater treatment plant of a
97 production site in Japan (OECD, 2005). Phthalimide undergoes hydrolysis in water to ammonia
98 and phthalic acid which is readily biodegradable and also one of the HTPs of TD (Lu, G. H. et
99 al., 2002).

100 Generally, experimental toxicity testing of TPs is difficult as many of them are not
101 available commercially. Computer models based on quantitative structure activity relationship
102 (QSAR) are important tools to solve and overcome this problem (European Commission, 2003).
103 Once structure elucidation of any TPs is performed, these structures can be investigated in
104 QSAR programs in order to predict the toxic potential of TPs at different toxicological endpoints
105 and other environmental parameters (Escher et al., 2009).

106 The aim of this work was to characterize TD and its PTPs after photolysis and monitor
107 their toxicity experimentally in combination with *in silico* QSAR models. The mutagenicity was
108 investigated using the Ames Microplate format (MPF) assay. Moreover, a modified luminescent
109 bacteria test with *Vibrio fischeri* (kinetic luminescent bacteria test, kinetic LBT) was used for an
110 initial screening of microbial toxicity of TD and its PTPs (Menz et al., 2013). Furthermore,
111 phthalimide, one of the identified PTPs of TD, was assessed separately in the kinetic LBT due to
112 the contradiction between different *in silico* software regarding the predicted phthalimide
113 toxicity against *V. Fischeri*.

114 **2. Experimental**

115 **2.1. Chemicals**

116 All the chemicals used in this study were of analytical grade. Acetonitrile and Methanol
117 (HiPerSolv CHROMANORM, LC-MS grade, BDH Prolabo), and formic acid were purchased
118 from VWR International GmbH (Darmstadt, Germany). TD (CAS number 50-35-1, 98.7%
119 purity) was obtained from chemical point (Deisenhofen, Germany). Phthalimide (CAS Number
120 85-41-6, PESTANAL[®] analytical standard 99.9% purity), 3,5-Dichlorophenol (CAS Number

121 591-35-5, 97% purity) and Chloramphenicol (CAS Number 56-75-7, 98% purity) were obtained
122 from Sigma-Aldrich GmbH (Steinheim, Germany).

123 **2.2. Photodegradation**

124 Photodegradation experiments were performed with a TQ 150 W medium-pressure
125 mercury lamp (UV Consulting Peschl, Mainz). The irradiation experiments of 10 mg/L of TD
126 were conducted in four different reactor sizes: 800ml (PR1), 110ml (PR2), 1.4 ml Hellma®
127 suprasil quartz cuvette (type 104 B-QS) (PR3) and 3 ml Brand® UV-cuvette Macro (PR4). The
128 irradiation experiments of 47 mg/L of TD were conducted in PR1 and PR2. The specified test
129 solution volumes 800ml, 110ml, 1.4 ml, and 3 ml were transferred into the PR1, PR2, PR3 and
130 PR4, respectively.

131 Ultrapure water was used to prepare all test solutions. In PR1 and PR2, the
132 photodegradation mixture was stirred with a magnetic stirrer during the photoreaction and the
133 temperature was maintained by a circulating cooler (WKL230, LAUDA, Berlin) between 18-20
134 °C. TD samples were taken at different reaction times from the photoreactor at defined times (2,
135 4, 8, 16, 32, 64 and 128 min) for the analysis of the TD concentration by LC-UV-FL-ion trap-
136 MS/MS. Dissolved organic carbon (DOC) was monitored during irradiation experiments of 47
137 mg/L of TD according to European standard procedure DIN EN 1484 with a total organic carbon
138 analyzer (TOC-Vcpn, Shimadzu GmbH, Duisburg, Germany). Toxicity tests performed for
139 photolysis samples of 47 mg/L of TD withdrawn from PR1.

140 A saturated aqueous solution of TD was freshly prepared before the photodegradation
141 experiments by stirring 50 mg of TD in 1L of water following by sonication and filtration
142 through 0.2 µm membrane filter. The final concentration of this solution (determined by LC-UV
143 and DOC) was approximately 47- 47.4 mg/L (pH was 5.6).

144 **2.3. Monitoring of primary elimination and structure elucidation of PTPs by**
145 **LC–UV–VIS/FL and LC–ion-trap MS/ MS**

146 In order to monitor the changes of TD in the samples, HPLC–UV–VIS/ FL and LC–ESI-
147 MS/MS (ion trap) was used to measure the primary elimination of TD. A stock solution of TD
148 (100 mg/L) was prepared in methanol. Standard solutions were prepared by further dilution with
149 ultrapure water to reach the concentration range of linearity. Triplicate TD injections were made
150 for each concentration and chromatographed under the specified conditions described below. The
151 peak area values were plotted against corresponding concentrations.

152 LC–UV quantification was performed on Prominence HPLC apparatus (Shimadzu,
153 Duisburg, Germany). Further, ion-trap LC–MS/MS quantification, detection and identification of
154 the TD and PTPs was performed on Agilent Technologies 1100 HPLC series (Agilent
155 Technologies, Böblingen, Germany) tandem mass spectrometer Bruker Daltonic Esquire 6000
156 plus ion-trap mass spectrometer equipped with atmospheric pressure electrospray ionization
157 interface (Bruker Daltonic GmbH, Bremen, Germany) (Supplementary material (Text S1)).
158 Chromatographic separation was performed on an RP-18 column (CC 70/3 NUCLEODUR 100-
159 3 C18 ec, Macherey and Nagel, Düren, Germany) protected by a CC 8/4 HYPERSIL 100-3 C18
160 ec, guard column. Gradient system 0.1% formic acid in water (solution A) and 100% acetonitrile
161 (solution B) were used by applying the following linear gradient: 0 min 5% B, 5 min 5% B, 20
162 min 40% B, 23 min 40% B, 26 min 5% B, 30 min 5% B. The flow rate was set at 0.7 mL min⁻¹
163 and the oven temperature was set to 30°C. Total run time was 30 min.

164 The mass spectrometer was operated in positive polarity. A more detailed description of
165 the mass spectrometer parameter can be found elsewhere (Mahmoud et al., 2013).

166 **2.4. *In silico prediction of toxicity***

167 TD, its PTPs and its HTPs were assessed by a set of *in silico* predictions for toxicity. A
168 set of different programs for predicting toxicity was applied in order to take into account that the
169 available programs might have individual strengths because of different algorithms and training
170 sets. The set of available programs used were the Case Ultra V.1.4.5.1 (MultiCASE Inc.)
171 (Saiakhov et al., 2013), the Oasis Catalogic software V.5.11.6TB from Laboratory of
172 Mathematical Chemistry, University Bourgas, Bulgaria (Laboratory of Mathematical Chemistry,
173 2012) and Leadscope software V.3.0.11-1 with training sets from 2012 SAR Genetox Database
174 provided by Leadscope (Roberts et al., 2000). Structure illustrations were performed by using
175 MarvinSketch 5.8.0. Simplified molecular input line entry specification (SMILES) codes from
176 the molecular TP structures were used for input of molecular structures.

177 The ecotoxicity, genotoxicity and mutagenicity of TD, the identified PTPs and the
178 previously identified 12 HTPs were evaluated using the set of programs specified
179 (Supplementary material (Text S2)).

180 **2.5. *Mutagenicity and initial microbial toxicity testing of single substances and*** 181 ***photolytic mixtures***

182 The mutagenicity of TD and its photolytic mixtures were determined by experimental
183 testing using the Ames microplate format (MPF) aqua assay (Xenometrix, AG, Switzerland). In
184 addition, the kinetic LBT was used to evaluate the acute and chronic toxicity to the
185 environmental bacteria species *V. fischeri*. Samples from photodegradation experiments were
186 sterile filtered, and stored at -150 °C for a maximum timespan of 7 days. Every toxicity

187 experiment was conducted in two independent repetitions, including the UV-treatment
188 procedure. The pH was adjusted to 7.0 ± 0.2 before testing.

189 **2.5.1. Ames MPF 98/100 Aqua Assay**

190 Materials: Ames MPF 98/100 Aqua test kit containing Exposure medium, Reversion
191 indicator medium, Growth medium, Aroclor 1254-induced rat liver homogenate (S9), positive
192 controls: 4-nitroquinoline-N-oxide (4-NQO) and 2-nitrofluorene (2-NF) and 2-aminoanthracene
193 (2-AA) as well as bacterial strains *Salmonella typhimurium* TA 98 and TA 100 were supplied by
194 Xenomatrix AG.

195 Method: In brief an overnight culture was grown until the OD600 reached ≥ 2.0 . In a 24-
196 well plate, the bacteria were exposed the photolytic mixtures, collected at 0, 2, 4, 8, 16, 32, 64
197 and 128 min of UV exposure, in the presence or absence of metabolic activation (+/- S9).The
198 final test concentration of TD at time point 0 min was 35 mg/L. After exposure for 90 min (at
199 37°C) while shaking (250 rpm) the exposure mixture was diluted with reversion indicator
200 medium, transferred into 384-well plates and incubate at 37°C for 48 h. During this time, the pH
201 dependent reversion indicator dye would change from purple to yellow in the presence of
202 bacterial growth. The result was colorimetrically scored by eye to give the number of revertants
203 (yellow colored wells). As positive controls a mixture of 4-NQO and 2-NF (+S9) and 2-AA (-
204 S9) were used like described in the test kit. Before the testing of mutagenicity, the cytotoxicity of
205 TD and its PTPs were assessed to dismiss the possibility of false 'negative' mutagenicity results.

206 Analysis: The results were considered positive when the response was ≥ 2 fold increase
207 in the number of revertants over that of the baseline number of revertants (the mean revertants of
208 the negative control plus 1 SD). The statistical significance determined by ANOVA (Holm-Sidak

209 method, overall significance level $p \leq 0.01$) was also used to assist in the determination of positive
210 results.

211 **2.5.2. Kinetic luminescent bacteria test (kinetic LBT)**

212 The kinetic LBT allows for the combined analysis of acute and chronic toxicity towards
213 the luminescent bacteria species *V. fischeri*. A more detailed description and assessment of the
214 kinetic LBT can be found elsewhere (Menz et al., 2013).

215 Materials: The freeze-dried luminescent bacteria (*V. fischeri* NRRL-B-11177) for the
216 LBT were purchased from Hach-Lange GmbH, Düsseldorf.

217 Method: For the testing of single substances, saturated stock solutions of TD and
218 phthalimide were prepared freshly and the final concentration was determined by DOC-Analysis.
219 Subsequently, serial dilutions were prepared for the analysis of concentration-response
220 relationship. Prior to testing, samples were supplemented with NaCl [2% (w/v)].

221 An overnight culture of *V. fischeri* was prepared in SSWC media (supplemented seawater
222 complete media, DIN, 2009) and grown at 20 °C for 22-24 h. Turbidity of the bacteria
223 suspension was measured according to DIN EN ISO 7027:2000-04 and the overnight culture was
224 diluted with SSWC media to an initial turbidity of 20 formazin turbidity units (FTU). The
225 luminescent bacteria suspension was transferred to the wells of a 96-well plate and an initial
226 measurement of luminescence and optical density ($\lambda=578$ nm) was conducted. Subsequently, the
227 samples were added and a kinetic measurement of luminescence as well as optical density was
228 carried out for 24 h at 15 °C.

229 In each experiment, 4.5 mg/L 3,5-Dichloropenol and 4.5 mg/L Chloramphenicol were
230 used as positive controls for acute toxicity and chronic inhibition, respectively.

231 Analysis: The raw data was normalized to percent inhibition in relation to the negative controls.
232 This was conducted for three different endpoints that are: acute luminescence inhibition after 30
233 min (acute LI), chronic luminescence inhibition after 24 h (chronic LI) and growth inhibition
234 after 14 h (GI). The acute luminescence inhibition (acute LI) was calculated according to EN ISO
235 11348 (DIN, 2009). A more detailed description of data analysis and the calculations done is
236 available in the supplementary material (Text S3).

237 **3. Results and discussion**

238 **3.1. Photodegradation**

239 The concentration of TD decreased during the irradiation process using the Hg lamp. The
240 elimination of 10 mg/L TD in PR3 and PR4 was faster than PR1 and PR2. TD was completely
241 degraded after 8 min in PR3 and PR4 and after 64 min in PR1 and PR2. The increase in
242 elimination of TD in PR3 and PR4 might be due to the elevation in temperature of the cuvette
243 within the photodegradation process, as no cooling and stirring is done for this cuvette (Neamțu
244 and Frimmel, 2006). Therefore, further photodegradation experiment of 47mg/L TD was
245 performed in PR1 and PR2 as the photodegradation solution is stirred, under controlled
246 temperature, and larger photodegradation sample volume can be provided.

247 The photodegradation process of 47mg/L TD was accompanied by a DOC loss of 15%
248 and 18.4% after 128 min in PR1 and PR2, respectively (Supplementary material, Figure S1). The
249 pH was decreased from 5.6 (0 min of photolysis) to 3.8 (128 min of photolysis). LC-MS revealed
250 that new PTPs were formed (Figure 1). Because no isolation of pure compounds was feasible,
251 quantification of the PTPs was impossible. Therefore, the area ratio (A/A_0 as A is the area of the
252 PTP and A_0 is the area of TD at 0min) of the PTPs was plotted against the sampling time (Figure

253 2 and Figure 3). It is apparent from figure 2 that some of the PTP peaks increased with
254 irradiation time until 32 min and then began to decrease. While others PTP peaks were formed at
255 16 min then increased until 128 min (Figure 3).

256 **3.2. Identification of phototransformation products (PTPs)**

257 The PTPs generated during photolysis studies are considered as potential environmental
258 pollutants. Thus, identification of the most relevant PTPs is important to predict the
259 environmental impact of original compound. For this reason, LC-UV-MS/MS analyses based on
260 accurate mass measures was performed during the photolysis assays. The chromatographic
261 behavior demonstrated that some of the PTPs formed by photolysis were of higher polarity than
262 TD itself. Structures of the five main observed PTPs were reported previously (Mahmoud et al.,
263 2013). The photodegradation samples of 10 mg/L and 47 mg/L TD were subjected for further
264 investigation of PTPs. These samples were analyzed by the Auto MSⁿ mode, where PTPs with
265 highest peak intensity were isolated and fragmented up to MS³ in order to gain more structural
266 information.

267 The same PTPs are formed in the photodegradation samples of 10 mg/L and 47 mg/L TD.
268 The total ion chromatogram (TIC) in LC-MS showed a peak at 1.3 min which has several very
269 polar PTPs with the following m/z 129.1, 173.1, 245, 259.1, 277.1, 297.1, 313.1, and 291.1
270 (Figure 1). The extracted ion chromatograms and the postulated structures of all these PTPs and
271 their smiles codes are listed in the supplementary material (Figure S2 and Table S2). The
272 chemical structures of m/z 259.1 ($t_R = 1.2$ min) and m/z 245 ($t_R = 1.3$ min) could not be proposed,
273 even though MS² and MS³ spectra could be obtained. These very polar PTPs can be due to
274 further photolysis of the other PTPs which were eliminated after 32 min of photolysis. The
275 compounds eluting at 1.3 min are extremely polar as demonstrated by their very short retention

276 time. Trials were performed to elute these polar compounds later by changing the gradient
277 elution to begin with 0.5% ACN instead of 5%. However, these polar compounds peak still
278 eluted early.

279 Several peaks were detected with the same nominal mass of m/z 275 (PTPs_275) but
280 different retention times (supplementary materials Figure S2). A peak with additional 16 Da was
281 observed for the PTPs_275 compared to m/z 259 of TD and its isomers. This is likely due to
282 hydroxylation of TD or its isomers. In most cases these PTPs_275 also exhibited similar MS²
283 fragmentation pathways, indicating formation of constitutional isomers (Table 1). However, on
284 the basis of the MS fragmentation, the identification of the exact position of the hydroxyl group
285 was not feasible. Hydroxylation of TD occurs during biological metabolism (Eriksson et al.,
286 1998; Meyring et al., 1999). Four of the predicted structures are also reported as human
287 metabolites (Eriksson et al., 1998; Nakamura et al., 2006). These metabolites are 5'-
288 hydroxythalidomide (PTP 275_1), N-hydroxythalidomide (PTP 275_3), 5-hydroxythalidomide
289 (PTP 275_4), and 4-hydroxythalidomide (PTP 275_5) (supplementary material (Table S2)). It
290 has been reported that at least one of the hydroxylated metabolites (PTP 275_1) has moderate
291 anti-angiogenic activity at high concentrations (Price et al., 2002).

292 Moreover, there is a peak with the nominal mass of m/z 291 which has additional 32 Da
293 compared to m/z 259 of TD and its isomers. This is likely to be due to formation of dihydroxy
294 derivatives of TD and its isomers. Also, dihydroxylation of TD occurs during biological
295 metabolism. Three of the predicted structures are also reported as human metabolites (Eriksson
296 et al., 1998; Nakamura et al., 2006). These metabolites are 5,5'-Dihydroxythalidomide (PTP
297 291_1), 4,5-Dihydroxythalidomide (PTP 291_2), and 5,6-Dihydroxythalidomide (PTP 291_4)
298 (supplementary material Table S2).

299 The PTP_277 (nominal mass 277 m/z) has an additional 18 Da compared to m/z 259 of
300 TD and its isomers. This is likely due to saturation of double bond and hydroxylation of TD
301 isomers. The PTP_297 (nominal mass 297 m/z) can be due to splitting of one of the equivalent
302 amide bonds of the phthalimide ring and glutamiride ring accompanied by reduction of the
303 ketone moiety of the phthalimide ring to hydroxyl group. The PTP 129 (nominal mass 129 m/z)
304 proposed to be α - amino glutamiride. The PTP_173 (nominal mass 173 m/z) proposed to be due
305 to cleavage in the phthalimide ring.

306 **3.3. *In silico* toxicity predicted parameters**

307 The obtained results of the predicted activity of the test chemicals from the QSAR
308 modules were expressed in different ways depending on the software.

309 For Case Ultra software, the predicted activities of tested chemicals are expressed as
310 "positive" and "marginally positive" which means that one or more positive alerts for the
311 predicted activity were found for the test chemical. "Inconclusive (orange)" means that because
312 both positive and deactivating alerts were found in the same molecule and the system cannot
313 draw a firm conclusion. "Inconclusive (Black)" means that because a significant portion of the
314 test chemical is covered by unknown structural fragments the system cannot draw a firm
315 conclusion. "Negative" means that no positive alert was detected in the molecule and "out of
316 domain" means structural fragments unknown to the model were found in the molecule and that
317 for this reason the molecule is excluded from the chemical space of the training set of the model
318 used. For Oasis Catalogic software, the predicted activity of the test chemicals in the three acute
319 *Vibrio fischeri* modules are expressed as mg/L for half maximal inhibitory concentration (IC₅₀)
320 and in Salmonella Catalogic module are expressed as "mutagenic" or "not mutagenic". For

321 Leadscope software, the predicted activity of the test chemicals is expressed as “positive”,
322 “negative” and “not in domain”.

323 3.3.1. In silico toxicity predicted parameters of hydrolysis products (HTPs)

324 The HTPs included in the analysis have been reported (Schumacher et al., 1965)
325 (supplementary material (Table S1)). For genotoxicity and mutagenicity, the results in the
326 supplementary material (Table S3) show that there is no positive predicted mutagenic effect in
327 Ames tests using Salmonella Catalogic (Oasis Catalogic), and Bacterial Mutagenesis
328 (Leadscope), Mutagenicity Ames (Case Ultra) and Salmonella t. 5-strains (Case Ultra).
329 However, an inconclusive (orange) effect was predicted for TD, HTP1, HTP2 and HTP4 in the
330 Mutagenicity in Salmonella t. 5-strains module. Some positive alerts for some HTPs were
331 predicted in Human Carcinogenicity, Aneuploidy in Yeast, Micronucleus Formation *in vivo*
332 composite, and Micronucleus Formation *in vivo* Mouse whereas TD activity was predicted as
333 negative or inconclusive. In a similar manner, TD was not in domain but some of the HTPs were
334 positive in *In vitro* chromosome aberration and *In vivo* micronucleus (supplementary material
335 (Table S4)).

336 For ecotoxicity, there are some positive alerts obtained for the TD and some of its HTPs in
337 different modules (supplementary material (Table S5 and Table S4). Data from Table S5 shows
338 there are some contradictions in the prediction of bacterial toxicity such as HTP8 in the 3 Acute
339 tox *Vibrio fischeri* models give lower IC₅₀ for HTP8 compared to TD, whereas the Microtox
340 Toxicity to Environmental Bacteria give negative results.

341 **3.3.2. In silico toxicity predicted parameters of phototransformation products**
342 **(PTPs)**

343 For genotoxicity and mutagenicity, the results in supplementary material (Table S6 and
344 Table S7) show that there is no positive predicted mutagenic effect in Ames tests using
345 Salmonella Catalogic (Oasis Catalogic), and Bacterial mutagenesis (Leadscope). On the other
346 hand, some positive alerts were predicted for some PTPs in Mutagenicity in Salmonella t. 5-
347 strains (Case Ultra) whereas TD activity predicted as inconclusive (orange), and some
348 inconclusive alerts were predicted for some PTPs in Mutagenicity Ames (Case Ultra) while TD
349 activity was predicted as negative. In Salmonella t. 5-strains (Case Ultra), there are several
350 positive alerts responsible for the predicted positive or marginally positive toxicity. These alerts
351 are Alert ID 160 (PTP275_9, PTP148, and PTP259_2), Alert ID 716, 809 and 982 (PTP275_9),
352 and Alert ID: 827 (PTP 313_4 and PTP 313_9). Moreover, PTP 313_4 and PTP 313_9 are
353 predicted as marginally active due to the presence of a deactivating alert (Alert ID 1153) (Figure
354 4). Although these structural moieties responsible for this positive alerts are present in some
355 other PTPs but these PTPs activities are predicted inconclusive due to presence of some other
356 moiety responsible for deactivation or unknown structural fragments.

357 In all genotoxicity and mutagenicity QSAR modules predicted by Case Ultra
358 (supplementary material (Table S7)), the predicted TD activity was negative or inconclusive
359 except in mouse lymphoma module TD activity was positive. On the other hand, some of the
360 PTPs have a positive alert in these genotoxicity and mutagenicity QSAR modules predicted by
361 Case Ultra. In similar manner, TD was not in domain but some of the PTPs were positive in *In*
362 *vitro* chromosome aberration and *In vivo* micronucleus (supplementary material (Table S7)).
363 From the medical point of view, one striking observation to emerge from this QSAR is the

364 predicted genotoxicity for these PTPs which are human metabolites as well as transformation
365 products such as PTP_275_1. In detail, PTP_275_1 (5-hydroxy thalidomide) is predicted to be
366 positive in Micronucleus Formation *in vivo* composite (A7S) and *In vivo* micronucleus (IVMN).
367 This 5-hydroxyl metabolite was detected in human plasma (Ando et al., 2002; Eriksson et al.,
368 1998; Lu et al., 2004; Luzzio et al., 2005) and after metabolism in human liver microsomes ,
369 though at much lower levels than in mice and rabbits by Chung and colleagues (Chung, 2004; Lu
370 et al., 2004) . Since the 5-hydroxy thalidomide was recently proposed as a possible anti-
371 angiogenic compound (Noguchi et al., 2005), this possibly increased genotoxicity of the 5-
372 hydroxy thalidomide should be taken into account, when developing this substance for the use in
373 humans.

374 For ecotoxicity, there are some positive alerts obtained for the TD and some of its PTPs in
375 different modules (supplementary material (Table S7 and Table S8)). In Microtox Toxicity to
376 Environmental Bacteria (*V. fischeri*), Bioconcentration for Cyprinus Carpio and Gold Fish
377 Toxicity modules, the predicted activities of TD and some of the PTPs were positive. In contrary,
378 in the Rainbow Trout Toxicity module, TD predicted activity was negative and some of the PTPs
379 are inconclusive.

380 In the three acute *Vibrio fischeri* modules at 5 min, 15 min and 30 min, the following
381 PTPS (PTP259_1, PTP259_2, PTP148, PTP291_3, PTP291_9, PTP291_13, PTP275_5,
382 PTP275_6, PTP275_8) have lower predicted IC₅₀ than TD (Supplementary material Table S8).

383 **3.4. Toxicity testing**

384 **3.4.1. Ames MPF 98/100 Aqua Assay**

385 Cytoxicity testing of the TD and its TP confirmed that the growth of both test strains was not
386 affected by the mixtures taken at any time point. Further, TD and its PTPs formed at different
387 time points proved negative for mutagenicity in both strains (Table 2).

388 According to the QSAR predictions for the modules pertaining to mutagenicity, there were
389 some positive and marginally positive alerts for some PTPs. However, given that the
390 experimental results were negative, it cannot be excluded that perhaps the concentration of
391 these PTPs maybe too low to express a mutagenic effect or the possibility of antagonistic
392 interactions of mixture components or that these positive alerts may be for strains other than
393 TA 98 and 100 since the QSAR modules cover more strains. One should also consider that the
394 Ames MPF 98/100 Aqua test is another variation of the standard Ames test. Though this test
395 is capable of detecting strong mutagens, it is less sensitive in the case of weak mutagens
396 (Escobar et al., 2013). Nevertheless, the experimental data should not be ignored since QSAR
397 is an estimation method and these estimations can be poor, even for well evaluated models
398 (European Commission, 2003). They can give guidance but not a final proof.

399 **3.4.2. Kinetic luminescent bacteria test**

400 **3.4.2.1. Bacterial toxicity of TD during UV-treatment**

401 Application of the undiluted photolytic mixtures, leading to a final sample dilution in the test
402 of 1:2, demonstrated a significant increase of toxicity in relation to the untreated sample for
403 the reaction mixtures obtained after 16, 32, 64 and 128 min of irradiation, regarding the
404 endpoint acute luminescence inhibition (Figure 5). The analysis of chronic luminescence

405 inhibition and growth inhibition showed a significant toxification for the samples taken after
406 32, 64, and 128 min of irradiation (Figure 5). The final sample dilution of 1:50 showed no
407 significant inhibition (data not shown).

408 **3.4.2.2. Toxicity of untreated TD and Phthalimide**

409 After DOC analysis of the saturated stock solution, a maximum concentration of TD in
410 the kinetic LBT of 23 mg/L was estimated. At this concentration, only the luminescence
411 emission after 24 h (chronic LI) was significantly inhibited (15% inhibition). The endpoints of
412 the acute LI and GI were not affected. According to measured DOC, the highest concentration
413 of phthalimide applied to the test was 230 mg/L. At this concentration, a maximum chronic LI
414 of 78 % was observed. The endpoints acute of the LI and GI showed a comparatively lower
415 inhibition than the endpoint of the chronic LI, but exhibiting maximum inhibition values of 21
416 % and 31 %, respectively. EC_{10} and EC_{50} values of TD and phthalimide, including 95%
417 confidence intervals, are presented in Table 3. Regarding the most sensitive endpoint in both
418 cases, i.e. chronic LI, there was no significant difference between the EC_{10} of phthalimide and
419 the EC_{10} of the parent compound or its HTPs, probably because hydrolysis will most likely
420 occur in the setting including bigger time, i.e. the chronic test. QSAR predictions from
421 different models give contradictory results regarding the endpoint acute LI: while Oasis
422 Catalogic predicts a lower IC_{50} for phthalimide, indicating a higher acute toxicity compared to
423 TD, Case Ultra showed a positive alert for Microtox activity for TD, but a negative alert for
424 Microtox activity in case of phthalimide (supplementary material, Table S8). Moreover, the
425 photolytic mixtures, especially those obtained after 64 and 128 min, showed a major increase
426 of acute and chronic inhibition (Figure 5). In contrast, phthalimide (PTP_148) occurrence was
427 already decreasing after 32 min of irradiation (Figure 3). In summary, it can be concluded that

428 the formation of phthalimide might not be the only cause for the drastic toxification of TD
429 during UV-treatment. This leads to the assumption that other PTPs/HTPs within the
430 photolytic mixture, possibly in combination with the parent compound and phthalimide, might
431 be responsible for the observed effects. Phthalimide toxicity is not environmentally relevant
432 as high exposure level is needed to exert toxic effects and as phthalimide and its hydrolysis
433 product 'phthalic acid' are readily biodegradable.

434 **3.5. Identification of PTPs with microbial toxicity**

435 It was stated above that the toxicity in the luminescent bacteria test was increasing during
436 the photolytic process especially after 16 min of irradiation, reaching the maximum after 128
437 min of irradiation (Figure 5). Therefore it is important to correlate the kinetic luminescent
438 bacteria test results with the QSAR prediction for these PTPs formed and that increased in
439 intensity at these time points. The acute luminescence inhibition (acute LI) of the kinetic LBT
440 was compared with the following QSAR modules: Microtox Toxicity to Environmental Bacteria
441 (Case Ultra) and Acute Toxicity *Vibrio Fischeri* 5min/15min/30min (Oasis Catalogic).

442 There is a significant increase in toxicity after 16 min of photolysis that was postulated to be
443 related to the PTPs increased after 16 min (Figure 3). When looking closely at the TIC in LC-
444 MS, it can be seen that the peak intensity at 1.3 min is increased after 16 min of photolysis
445 (Figure 1). Therefore, it can be presumed that these PTPs (Figure 3) might be responsible for the
446 observed toxicity. Surprisingly, the PTPs (accounting for $\geq 4\%$ of the initial TD area at any
447 sampling time) increased with irradiation time until 32 min and then began to decrease while
448 toxicity increased, i.e. the high intensity PTPs were not responsible for this significant increase
449 in toxicity. However, the QSAR results give a positive alert for some of them (see section 3.3.2).

450 As mentioned above the mixtures of the PTPs and the residual parent compound could be
451 another reason for the changings of the toxicity during the treatment period. Earlier studies using
452 different groups of pharmaceuticals e.g. antibiotics or beta-blockers showed different effects like
453 growth or luminescence inhibition and immobilization of *Daphnia magna* (Christensen et al.,
454 2007; Cleuvers, 2004; Escher et al., 2006). Therefore not only one PTP might be responsible for
455 the toxicity.

456 According to the kinetics of PTPs formation, PTP129, PTP173, PTP297, PTP313,
457 PTP259, PTP291 and PTP245 are possible candidates that might be responsible for the
458 toxification of TD during UV-treatment. Comparing the predicted QSAR results, it can be seen
459 that PTP291_3, PTP291_9, and PTP291_13 have lower predicted IC_{50} than TD using the three
460 acute *Vibrio fischeri* modules (Table S8). Moreover, positive alerts for PTP291_1, PTP291_4,
461 PTP291_5, PTP291_6, PTP291_7, PTP291_10, and PTP291_12 have been predicted in
462 Microtox Toxicity Environmental Bacteria module. The positive alerts responsible for the
463 predicted toxicity were alert Id 175 (present in PTP291_1, PTP291_4, PTP291_5, PTP291_6,
464 PTP291_7, PTP291_10, and PTP291_12) and alert Id 214 (present in PTP291_10, and
465 PTP291_12) (Figure 6). Therefore, it can be concluded that PTP291_1, PTP291_4, PTP291_5,
466 PTP291_6, PTP291_7, PTP291_10, and PTP291_12 might be responsible for the increase of
467 toxicity in the luminescent bacteria test.

468 Of note is that the structural moieties responsible for the positive alerts (Figure 6) are
469 present in some other PTPs but these PTPs activities are predicted inconclusive or negative.
470 These inconclusive or negative predictions from the Microtox Toxicity to Environmental
471 Bacteria module (Case Ultra) are due to many reasons (Supplementary material (Text S4)).

472 **Conclusion**

473 Although photolysis was able to remove TD within the photoreactor, numerous PTPs
474 were formed. Our study has proven that the mixture of PTPs was more toxic than the parent
475 compound as evidenced by the increasing acute and chronic toxicity towards *V. fischeri*.
476 Furthermore, the number of PTPs within the photolytic mixture that might be responsible for the
477 toxification of TD during UV-treatment was successfully narrowed down by combining *in silico*
478 methods and conventional experimental testing, including analysis of the mutagenic potential
479 and the bioluminescence and growth inhibition to *V. fischeri*.

480 No mutagenic potential of the photolytic mixtures was detected with the Ames test. In
481 contrast the QSAR predictions provided indication that various PTPs and HTPs might have
482 genotoxic potential.

483 Nevertheless an elevated risk to the environment and human health resulting from the
484 various PTPs and HTPs cannot be completely excluded regarding to our initial toxicity data.
485 Therefore, further investigations need to be carried out in the future.

486 At the moment, there is no risk for public health and the environment, when taking into
487 account that TD was not detected in the aquatic environment until now. Nevertheless, TD and its
488 PTPs may become environmentally relevant in future because of the expected increased
489 consumption. These results emphasize that not only the removal of parent pollutants is important
490 but also the elimination of the PTPs from waste water should be considered.

491 **Acknowledgements**

492 Waleed Mohamed Mamdouh Mahmoud Ahmed thanks the Ministry of Higher Education and
493 Scientific Research of the Arab Republic of Egypt and the German Academic Exchange Service

494 (DAAD) for the scholarship (GERLS). The authors wish to thank MultiCASE Inc. and
495 Leadscope Inc. for providing CASE Ultra software and Leadscope software.

ACCEPTED MANUSCRIPT

496

497 **References**

- 498 Ando, Y., Price, D.K., Dahut, W.L., Cox, M.C., Reed, E., Figg, W.D., 2002. Pharmacogenetic
499 Associations of *CYP2C19* Genotype with In Vivo Metabolisms and Pharmacological Effects of
500 Thalidomide. *Cancer Biology & Therapy* 1 (1538-4047), 669–673.
- 501 Ashby, J., Tinwell, H., Callander, R.D., Kimber, I., Clay, P., Galloway, S.M., Hill, R.B.,
502 Greenwood, S.K., Gaulden, M.E., Ferguson, M.J., Vogel, E., Nivard, M., Parry, J.M.,
503 Williamson, J., 1997. Thalidomide: lack of mutagenic activity across phyla and genetic
504 endpoints. *Mutation Research/Fundamental and Molecular Mechanisms of Mutagenesis* 396 (1–
505 2), 45–64.
- 506 Bosch, M.E., Sánchez, A.R., Rojas, F.S., Ojeda, C.B., 2008. Recent advances in analytical
507 determination of thalidomide and its metabolites. *Journal of Pharmaceutical and Biomedical*
508 *Analysis* 46 (1), 9–17.
- 509 Canonica, S., Meunier, L., Gunten, U. von, 2008. Phototransformation of selected
510 pharmaceuticals during UV treatment of drinking water. *Water Research* 42 (1–2), 121–128.
- 511 Christensen, A.M., Faaborg-Andersen, S., Flemming, I., Baun, A., 2007. Mixture and single-
512 substance toxicity of selective serotonin reuptake inhibitors toward algae and crustaceans.
513 *Environmental Toxicology and Chemistry* 26 (1), 85–91.
- 514 Chung, F., 2004. Thalidomide Pharmacokinetics and Metabolite Formation in Mice, Rabbits, and
515 Multiple Myeloma Patients. *Clinical Cancer Research* 10 (17), 5949–5956.
- 516 Cleuvers, M., 2004. Mixture toxicity of the anti-inflammatory drugs diclofenac, ibuprofen,
517 naproxen, and acetylsalicylic acid. *Ecotoxicology and Environmental Safety* 59 (3), 309–315.
- 518 DIN, 2009. DIN EN ISO 11348 – Water quality - Determination of the inhibitory effect of water

519 samples on the light emission of *Vibrio fischeri* (Luminescent bacteria test) - Part 1: Method
520 using freshly prepared bacteria (Wasserbeschaffenheit - Bestimmung der Hemmwirkung von
521 Wasserproben auf die Lichtemission von *Vibrio fischeri* – Teil1: Verfahren mit frisch
522 gezüchteten Bakterien.). WILEY-VCH Verlag GmbH & Co. KGaA; Weinheim, and Beuth
523 Verlag GmbH; Berlin.

524 Eriksson, T., Björkman, S., ROTH, B., BJÖRK, H., HöGLUND, P., 1998. Drug Metabolism:
525 Hydroxylated Metabolites of Thalidomide: Formation In-vitro and In-vivo in Man. *Journal of*
526 *Pharmacy and Pharmacology* 50 (12), 1409–1416.

527 Escher, B., Baumgartner, R., Lienert, J., Fenner, K., 2009. Predicting the Ecotoxicological
528 Effects of Transformation Products, in: Boxall, A. (Ed.), *Transformation Products of Synthetic*
529 *Chemicals in the Environment*, vol. 2. *The Handbook of Environmental Chemistry*. Springer
530 Berlin Heidelberg, pp. 205–244.

531 Escher, B.I., Bramaz, N., Richter, M., Lienert, J., 2006. Comparative Ecotoxicological Hazard
532 Assessment of Beta-Blockers and Their Human Metabolites Using a Mode-of-Action-Based Test
533 Battery and a QSAR Approach. *Environmental Science & Technology* 40 (23), 7402–7408.

534 Escobar, P.A., Kemper, R.A., Tarca, J., Nicolette, J., Kenyon, M., Glowienke, S., Sawant, S.G.,
535 Christensen, J., Johnson, T.E., McKnight, C., Ward, G., Galloway, S.M., Custer, L., Gocke, E.,
536 O'Donovan, M.R., Braun, K., Snyder, R.D., Mahadevan, B., 2013. Bacterial mutagenicity
537 screening in the pharmaceutical industry. *Mutation Research/Reviews in Mutation Research* 752
538 (2), 99–118.

539 European Commission, 2003. *Technical Guidance Document on Risk Assessment Part III:*
540 *Chapter 4: Use of (Quantitative) Structure Activity Relationships ((Q)SARs), Use Categories,*

- 541 Risk Assessment Report Format.
542 http://ec.europa.eu/environment/chemicals/exist_subst/pdf/tgdpart3_2ed.pdf.
- 543 Fatta-Kassinos, D., Vasquez, M.I., Kümmerer, K., 2011. Transformation products of
544 pharmaceuticals in surface waters and wastewater formed during photolysis and advanced
545 oxidation processes – Degradation, elucidation of byproducts and assessment of their biological
546 potency. *Chemosphere* 85 (5), 693–709.
- 547 Khaleel, N.D.H., Mahmoud, W.M.M., Hadad, G.M., Abdel-Salam, R.A., Kümmerer, K., 2013.
548 Photolysis of sulfamethoxypyridazine in various aqueous media: Aerobic biodegradation and
549 identification of photoproducts by LC-UV–MS/MS. *Journal of Hazardous Materials* 244–245,
550 654–661.
- 551 Liberti, L., Notarnicola, M., 1999. Advanced treatment and disinfection for municipal
552 wastewater reuse in agriculture. *Water Science and Technology* 40 (4–5), 235–245.
- 553 Lu, J., Helsby, N., Palmer, B.D., Tingle, M., Baguley, B.C., Kestell, P., Ching, L.-M., 2004.
554 Metabolism of Thalidomide in Liver Microsomes of Mice, Rabbits, and Humans. *Journal of*
555 *Pharmacology and Experimental Therapeutics* 310 (2), 571–577.
- 556 Lu, G. H., Zhao, Y. H., Yang, S. G., Cheng, X. J., 2002. Quantitative Structure–Biodegradability
557 Relationships of Substituted Benzenes and Their Biodegradability in River Water. *Bulletin of*
558 *Environmental Contamination and Toxicology* 69 (1), 111–116.
- 559 Luzzio, F.A., Dubeau, D.Y., Lepper, E.R., Figg, W.D., 2005. Synthesis of Racemic cis-5-
560 Hydroxy-3-phthalimidoglutaramide. A Metabolite of Thalidomide Isolated from Human Plasma.
561 *The Journal of Organic Chemistry* 70 (24), 10117–10120.

- 562 Mahmoud, W.M.M., Trautwein, C., Leder, C., Kümmerer, K., 2013. Aquatic photochemistry,
563 abiotic and aerobic biodegradability of thalidomide: Identification of stable transformation
564 products by LC–UV–MSⁿ. *Science of The Total Environment* 463–464, 140–150.
- 565 McBride, W.G., Read, A.P., 1994. Thalidomide may be a mutagen. *BMJ* 308 (6944), 1635-1636.
- 566 Meise, W., Ockenfels, H., Köhler, F., 1973. Teratologische Prüfung der Hydrolysenprodukte des
567 Thalidomids: *Experientia* 29 (4), 423-424.
- 568 Meneses, M., Pasqualino, J., Castells, F., 2010. Environmental assessment of urban wastewater
569 reuse: Treatment alternatives and applications. *Chemosphere* 81 (2), 266–272.
- 570 Menz, J., Schneider, M., Kümmerer, K., 2013. Toxicity testing with luminescent bacteria –
571 characterization of an automated method for the combined assessment of acute and chronic
572 effects. *Chemosphere*. 93 (6), 990–996.
- 573 Meyring, M., Strickmann, D., Chankvetadze, B., Blaschke, G., Desiderio, C., Fanali, S., 1999.
574 Investigation of the in vitro biotransformation of R-(+)-thalidomide by HPLC, nano-HPLC, CEC
575 and HPLC–APCI-MS. *Journal of Chromatography B: Biomedical Sciences and Applications* 723
576 (1-2), 255–264.
- 577 Nakamura, T., Noguchi, T., Kobayashi, H., Miyachi, H., Hashimoto, Y., 2006. Mono- and
578 Dihydroxylated Metabolites of Thalidomide: Synthesis and TNF- α Production-Inhibitory
579 Activity. *Chemical and Pharmaceutical Bulletin* 54 (12), 1709–1714.

- 580 Neamțu, M., Frimmel, F.H., 2006. Photodegradation of endocrine disrupting chemical
581 nonylphenol by simulated solar UV-irradiation. *Science of the Total Environment* 369 (1–3),
582 295–306.
- 583 Noguchi, T., Fujimoto, H., Sano, H., Miyajima, A., Miyachi, H., Hashimoto, Y., 2005.
584 Angiogenesis inhibitors derived from thalidomide. *Bioorganic & Medicinal Chemistry Letters* 15
585 (24), 5509–5513.
- 586 OECD, 2005. Organisation for Economic Co-operation and Development's Work on Co-
587 operating in the Investigation of High Production Volume Chemicals - Chemical Detailed
588 Results "Final Assessment Report of Phthalimide, SIDS_85416.zip ". OECD (accessed
589 11.02.2013). [http://webnet.oecd.org/HPV/UI/SIDS_Details.aspx?Key=72854468-fc25-44b3-](http://webnet.oecd.org/HPV/UI/SIDS_Details.aspx?Key=72854468-fc25-44b3-b2c7-db273634ecbd&idx=0)
590 [b2c7-db273634ecbd&idx=0](http://webnet.oecd.org/HPV/UI/SIDS_Details.aspx?Key=72854468-fc25-44b3-b2c7-db273634ecbd&idx=0).
- 591 Price, D.K., Ando, Y., Kruger, E.A., Weiss, M., Figg, W.D., 2002. 5'-OH-thalidomide, a
592 metabolite of thalidomide, inhibits angiogenesis. *Therapeutic drug monitoring* 24 (1), 104–110.
- 593 Roberts, G., Myatt, G., Johnson, W., Cross, K., Blower, P., 2000. LeadScope: Software for
594 Exploring Large Sets of Screening Data. *Journal of Chemical Information and Modeling* 40 (6),
595 1302–1314.
- 596 Saiakhov, R., Chakravarti, S., Klopman, G., 2013. Effectiveness of CASE Ultra Expert System
597 in Evaluating Adverse Effects of Drugs. *Molecular Informatics* 32 (1), 87–97.
- 598 Schumacher, H., Smith, R.L., Williams, R.T., 1965. The metabolism of thalidomide: the
599 spontaneous hydrolysis of thalidomide in solution. *British Journal of Pharmacology and*
600 *Chemotherapy* 25 (2), 324–337.
- 601 Sweetman, S.C., 2009. *Martindale: The complete drug reference*, 36th ed. Pharmaceutical Press,
602 London, Chicago.

- 603 Teo, S., Morgan, M., Stirling, D., Thomas, S., 2000. Assessment of the in vitro and in vivo
604 genotoxicity of Thalomid® (thalidomide). *Teratogenesis, Carcinogenesis, and Mutagenesis* 20
605 (5), 301–311.
- 606 Vasquez, M.I., Garcia-Käufer, M., Hapeshi, E., Menz, J., Kostarelos, K., Fatta-Kassinos, D.,
607 Kümmerer, K., 2013. Chronic ecotoxic effects to *Pseudomonas putida* and *Vibrio fischeri*, and
608 cytostatic and genotoxic effects to the hepatoma cell line (HepG2) of ofloxacin
609 photo(cata)lytically treated solutions. *Science of The Total Environment* 450–451 (0), 356–365.
- 610 Wang, X.-H., Lin, A.Y.-C., 2012. Phototransformation of Cephalosporin Antibiotics in an
611 Aqueous Environment Results in Higher Toxicity. *Environmental Science & Technology* 46
612 (22), 12417–12426.

613

614 **List of figure captions**

615 Figure 1: Total ion chromatograms (TICs) of thalidomide samples collected at different time points (0, 2,
616 4, 8, 16, 32, 64, and 128 min) of UV exposure in 800 ml photoreactor (PR1) using LC-ESI-MS in positive
617 mode (initial concentration of thalidomide = 47mg/L; T_{uv} = irradiation time with UV lamp).

618 Figure 2: Comparison of the relative peak area (%) of the phototransformation products (PTPs) formed
619 and decreased during photolytic process of 47mg/L TD in 800 ml photoreactor (PR1) using LC-ESI-MS
620 ($n=2$). (t_R = retention time; A/A_0 as A is the area of the PTP at the specified irradiation time point and A_0
621 is the area of thalidomide (TD) at 0min).

622 Figure 3: Comparison of the relative peak area (%) of the phototransformation products (PTPs) increased
623 during photolytic process of 47mg/L TD in 800 ml photoreactor (PR1) using LC-ESI-MS ($n=2$). (t_R =
624 retention time; A/A_0 as A is the area of the PTP at the specified irradiation time point and A_0 is the area
625 of thalidomide (TD) at 0min).

626 Figure 4: The predicted structural moieties responsible for the positive alerts and deactivating alert in
627 PTP275_9 and PTP313_4 in Salmonella t. 5-strains model using Case Ultra software are highlighted.

628 Figure 5: Kinetic luminescent bacteria test - Toxicity of Thalidomide reaction mixtures during UV-
629 treatment for the endpoints acute Luminescence inhibition after 30 min (acute LI), chronic
630 Luminescence inhibition after 24 h (chronic LI) and Growth inhibition after 14 h (GI) Photolysis was
631 conducted with an initial thalidomide concentration of 47 mg/L. Photolytic mixtures were applied to the
632 kinetic LBT in final dilutions of 1:2. Positive control I (PCI): 4.5 mg/L 3,5-Dichlorophenol (acute LI),
633 Positive control II (PCII): 0.05 mg/L Chloramphenicol (chronic LI, Growth Inh.). Statistically significant
634 differences (*) compared to the untreated control were identified by ANOVA following post hoc multiple
635 comparisons (Holm-Sidak method, $P < 0.050$).

636 Figure 6: The predicted structural moieties responsible for the positive alerts in the phototransformation
637 product (PTP291_10) by Microtox Toxicity to Environmental Bacteria model using Case Ultra software
638 are highlighted. Alert ID number is provided by the software database. The structural moieties
639 responsible for the alerts are presented in bold.

Table 1: Chromatographic and mass spectrometric parameters for TD and its PTPs analysis in LC/MS-MS (ESI (+); (relative intensity, %).

Compound	t_R (min)	Main Precursor ion (m/z)	Product ions (m/z)
PTP129	1	129.1	84.1(100)
PTP173	1	173.1	155(100), 127(89.4), 128(24.7), 155.9(21.2), 84.1(10.5)
PTP259	1.2	259.1	240.9(100), 212.9(83.7), 173(58.6), 230.9(30.1), 213.9(19.8), 194.9(10.6)
PTP245	1.3	245.0	198.9(100), 226.9(68.4), 155(22.9), 173 (19.3), 224.9(12.6), 128 (10.2).
PTP277	1.4	277.1	259(100), 259.9(36.2), 257(19.2), 230(14.4), 241 (13), 255(12.3), 242 (10.5), 201.9(10)
PTP297	1.4	297.1	279(100), 251 (29.6), 232.9(22.6), 172.9(14.2),
PTP313	1.4	313.1	173(100), 295(60.8), 293(19.8), 297(18.6), 141(16.2), 291(13.0), 296(11.9)
PTP291	1.7	291.1	273(100), 274(60.3), 246(56.4), 263(41.2), 190.9(30.8), 275(22.9), 149(19.5), 247(15.8), 179.9(13.6), 219(13.3), 201.9(10.5), 276(10)
PTP275	2.8	275.1	257(100), 230 (43), 174.9 (37), 257.9(22.2)
PTP275	3.1	275.1	257.9(100), 257(44.6), 230(24.9), 247(12.6), 259(12.6)
PTP275	3.7	275.1	257(100), 174.9 (43.9), 230 (42.2), 258(28.6), 247(13.3)
PTP275	4.1	275.1	257.9(100), 257(75.5), 229.9(42), 247(19.9), 258.9(18.4), 174.9(15.6), 202(10.7)
PTP259	5.1	259.0	241.0(100), 213.9(33.6), 241.9(15.4), 231.0(13.3), 159.0 (12.8).
PTP259	5.9	259.1	241.0(100), 214(24.3), 231.0(19.4), 159.0 (14.6), 241.9(11.3).
PTP275	8.9 & 9.3	275	257(100), 229.9(45.5), 174.9(43.5), 202.9(16.6), 258(16.4), 228.9(14.1), 163.9(11.8), 202(11), 247(10.8), 213.9(10.1)
PTP148	10	148.0	130 (100)
PTP275	11.9	275.1	247.0 (100), 84.2(53.6), 201.9(12.4), 248(11.8), 230(10.6)
PTP275	12.5	275.1	247.0 (100), 84.1 (58.7).
Thalidomide	13.4	259.1	231.1 (100), 84.1(63.2)

 t_R : retention time.

Table 2: Mutagenicity results of Ames MPF assay of thalidomide and its PTPs formed at different time points after photolysis with *Salmonella typhimurium* TA 98 and TA 100 in the absence and presence of S9 mix.

Time (min)	Number of revertants			
	TA98		TA100	
	-S9	+S9	-S9	+S9
NC	1±1	2±1	7±3	3±2
0	1±1	1±1	7±3	4±2
2	1±1	1±1	5±3	3±2
4	1±1	2±1	9±4	5±1
8	1±1	2±1	8±3	4±2
16	1±1	2±1	6±3	3±1
32	2±1	1±1	9±5	5±3
64	2±1	2±1	7±3	5±3
128	3±2	2±1	8±2	4±1
PC	42±3*	48±0*	47±2*	48±0*

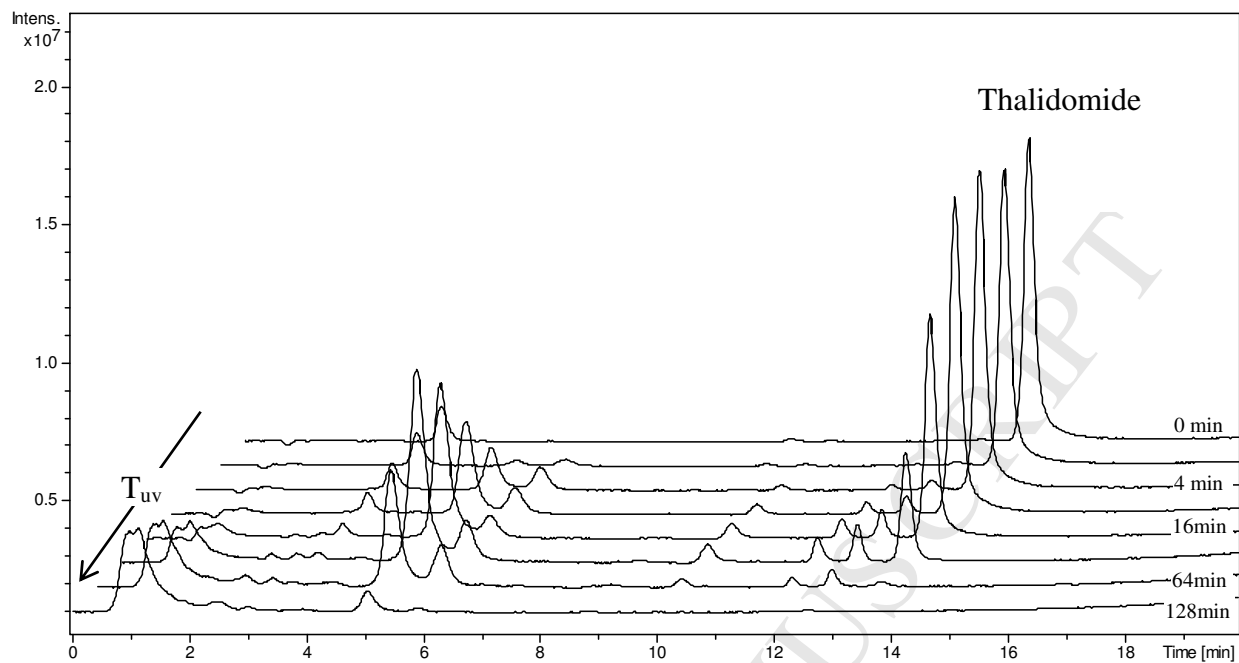
Positive results are presented in *bold italics*. PC= positive controls, NC= negative control

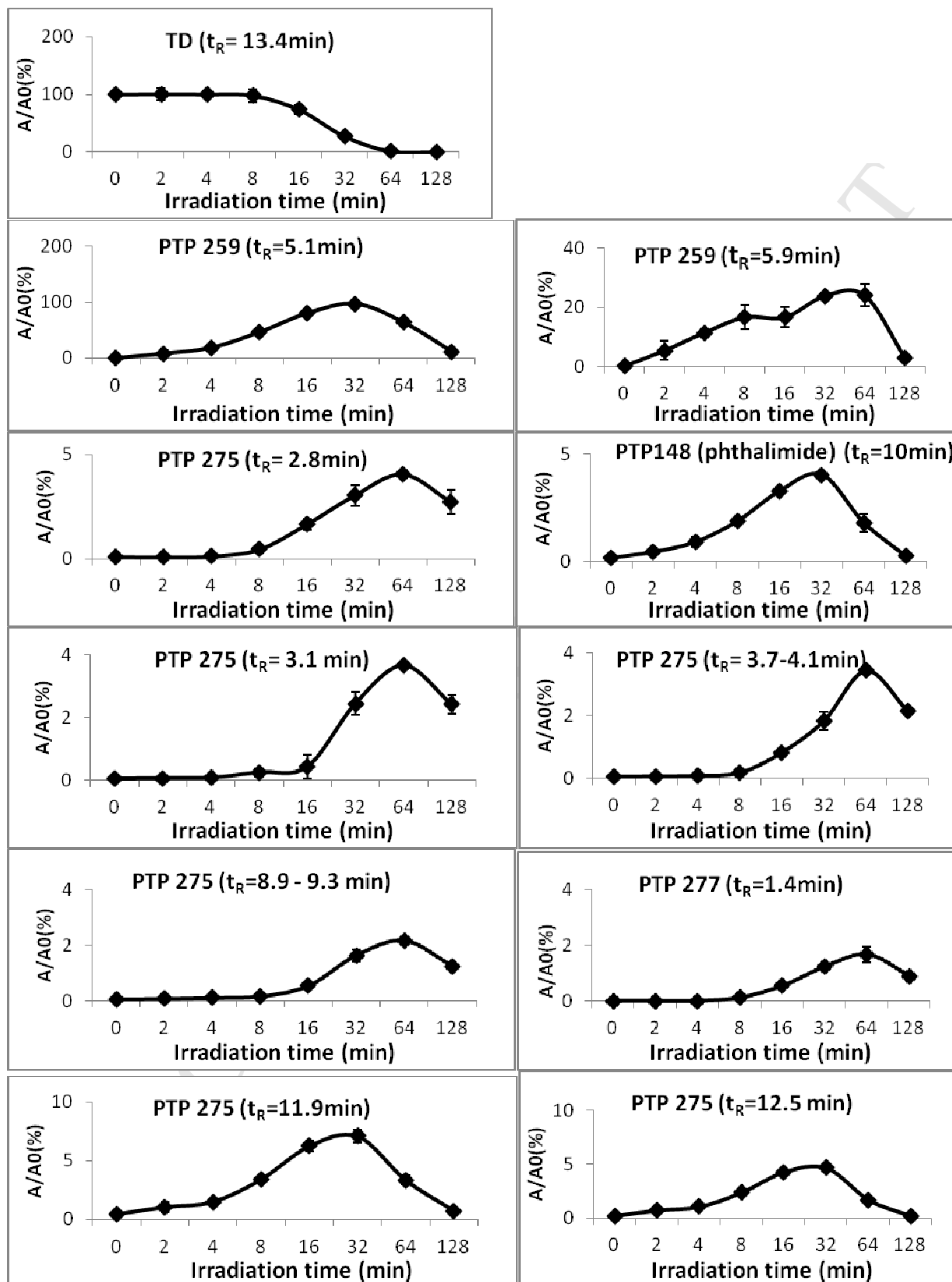
* Represents $p \leq 0.01$. Testing was done in triplicates with 2 independent repetitions.

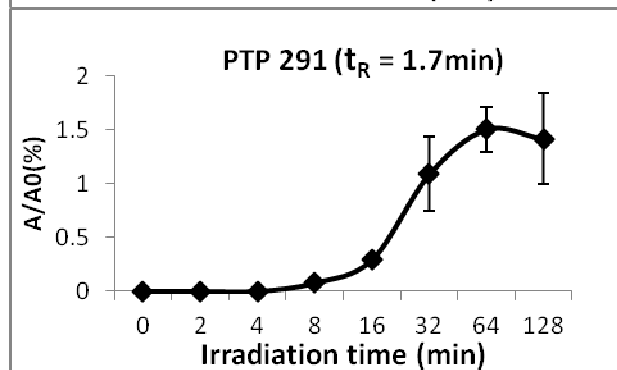
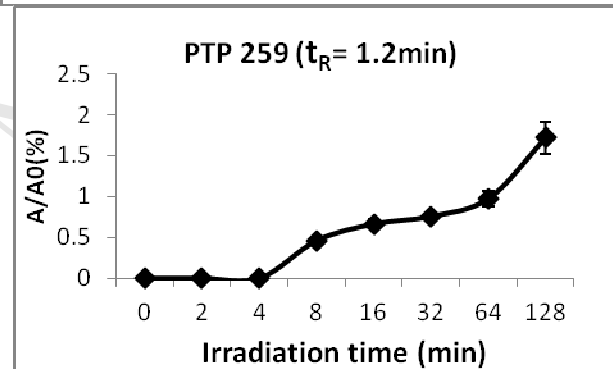
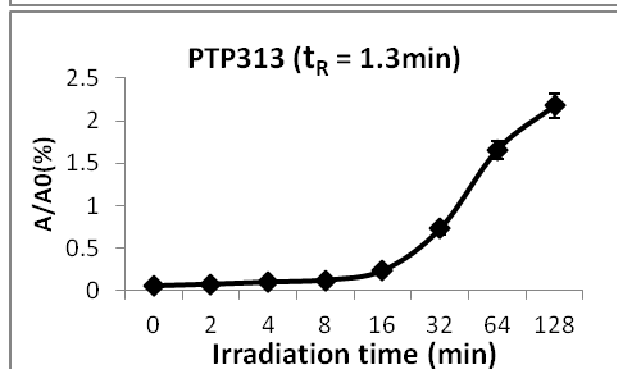
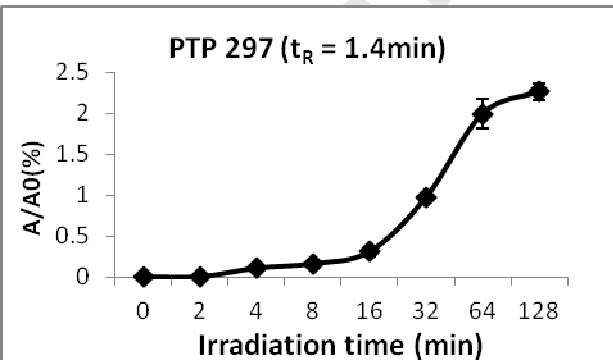
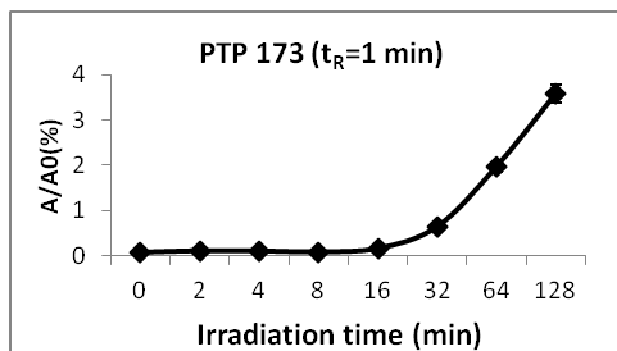
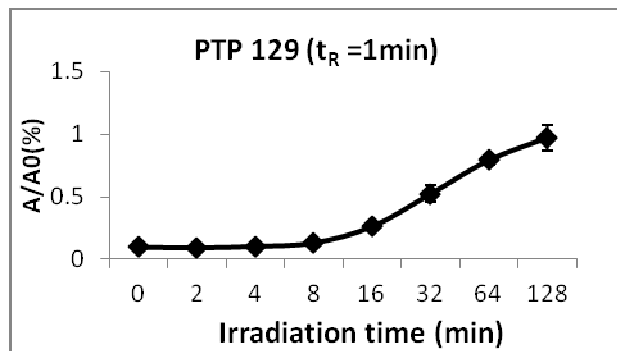
Table 3: EC₁₀ and EC₅₀ values with 95% confidence intervals (in brackets) of thalidomide and phthalimide in the kinetic LBT.

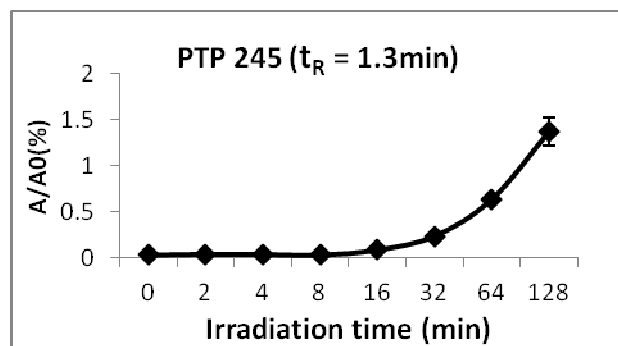
Substance	Tested Range [mg/L]	acute LI		chronic LI		GI	
		EC ₁₀ [mg/L]	EC ₅₀ [mg/L]	EC ₁₀ [mg/L]	EC ₅₀ [mg/L]	EC ₁₀ [mg/L]	EC ₅₀ [mg/L]
Thalidomide	0.2 – 23	n.d.	n.d.	16.5 (0.1-40.0)	n.d.	n.d.	n.d.
Phthalimide	2.5 - 230	70.6 (0.2-323.6)	n.d.	23.7 (14.9-33.4)	100.7 (88.2-113.2)	69.4 (21.1-136.9)	n.d.

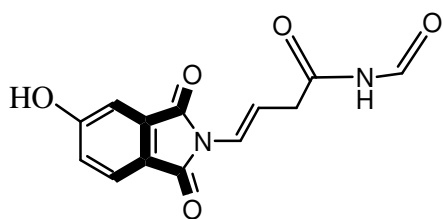
n.d.: not determinable because of low water solubility.



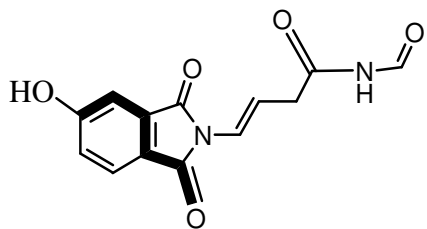




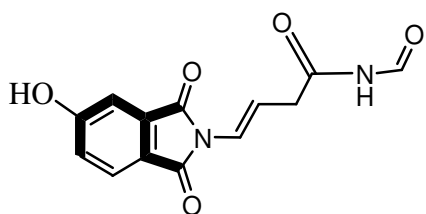




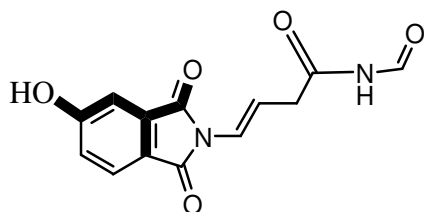
PTP275_9 (Positive alert)
Alert ID 160: C2-c(:cH):c-C2=O
Statistical significance = 100%



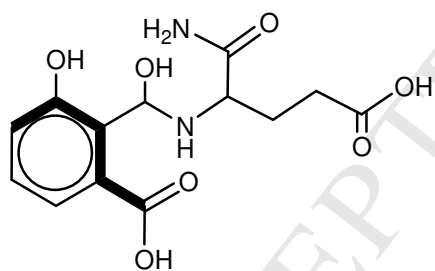
PTP275_9 (Positive alert)
Alert ID 716: c:cH:c:c-C2=O
Statistical significance = 100%



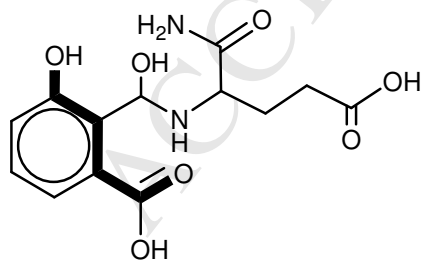
PTP275_9 (Positive alert)
Alert ID 809: C2-c:c(-C2):cH:c:cH
Statistical significance = 100%



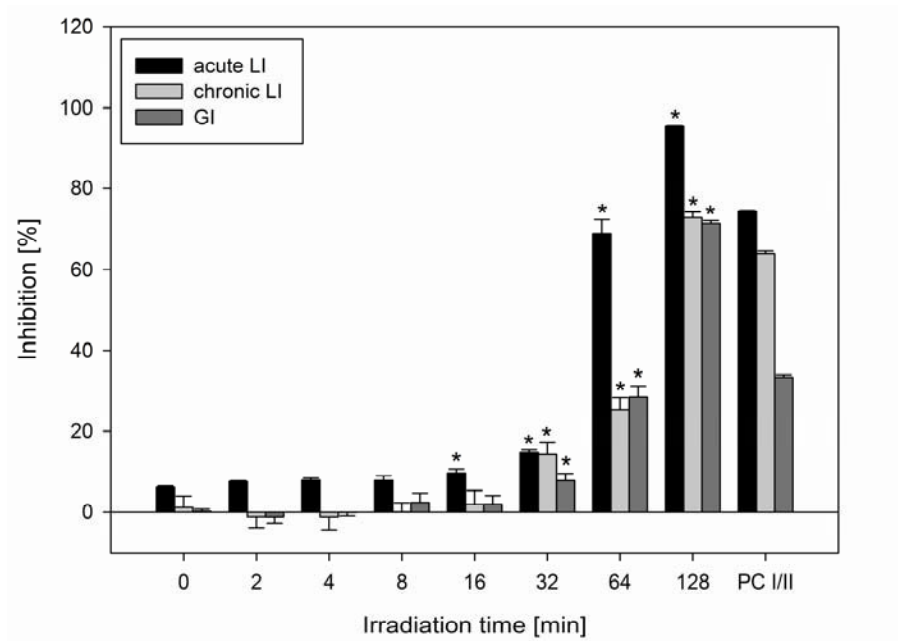
PTP275_9 (Positive alert)
Alert ID 982: C2-c(:c):cH:c-OH
Statistical significance = 99%

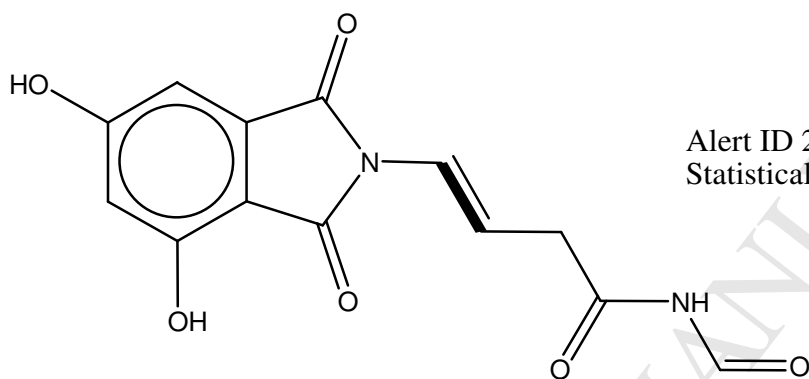
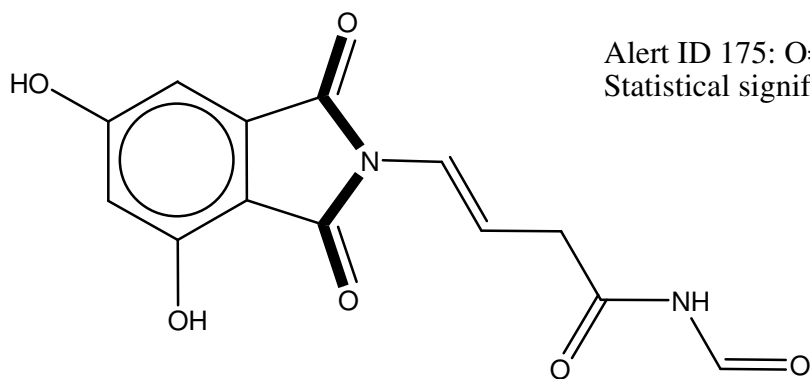


PTP 313_4 (Positive alert)
Alert ID 827: C2-c:c:c:cH
Statistical significance = 100%



PTP 313_4 (Deactivating alert)
Alert ID 1153: OH-c:c:c-C2=O
Statistical significance = 98%





Highlights:

- 1- UV irradiation eliminated thalidomide (TD) itself without complete mineralization.
- 2- Photolysis of TD led to formation of numerous phototransformation products (PTPs).
- 3- QSAR modules predicted several positive alerts from some of the identified PTPs.
- 4- TD and PTPs do not show mutagenic activity in the Ames test.
- 5- The luminescent bacteria test showed an increase in toxicity during photolysis.

Supplementary materials

Identification of phototransformation products of Thalidomide and mixture toxicity assessment: an experimental and quantitative structural activity relationships (QSAR) approach

Waleed M. M. Mahmoud^{1,2}, Anju P. Toolaram¹, Jakob Menz¹, Christoph Leder¹, Mandy Schneider¹, Klaus Kümmerer¹

1- Sustainable Chemistry and Material Resources, Institute of Sustainable and Environmental Chemistry, Faculty of Sustainability, Leuphana University of Lüneburg, Scharnhorststraße 1/C13, DE-21335 Lüneburg, Germany.

2- Pharmaceutical Analytical Chemistry Department, Faculty of Pharmacy, Suez Canal University, Ismailia 41522, Egypt

* Corresponding author. Address: Nachhaltige Chemie und Stoffliche Ressourcen, Institut für Nachhaltige Chemie und Umweltchemie, Fakultät für Nachhaltigkeit, Leuphana Universität Lüneburg, Scharnhorststraße 1/C13, D-21335 Lüneburg, Germany.

Tel.: +49 4131 677-2893

22 Text S1

23 Structural identification of the photoproducts was based on the analysis of the total ion
24 chromatogram (TIC) and the corresponding mass spectrum. For PTP peaks, depending on the
25 peak intensity of each PTP, up to MS³ spectra were generated using the Auto MSⁿ mode in order
26 to have structural information on the PTPs and to make structural elucidation. Therefore, the
27 precursor ion was fragmented first. The two most abundant product ions were then selected and
28 fragmented again if peak intensity was high enough. Furthermore, the formation kinetics of the
29 PTPs were monitored during the photodegradation of 47 mg/L TD in PR1 in order to correlate
30 them with QSAR predictions and data from toxicity experiments.

31 **Text S2**

32 The ecotoxicity, genotoxicity and mutagenicity of TD, the identified PTPs and the 12
33 HTPs were evaluated using the set of programs specified. Case Ultra was used to predict
34 ecotoxicity using the following QSAR models: Microtox Toxicity to Environmental Bacteria
35 (AUA), Bioconcentration for *Cyprinus Carpio* (BCF), Gold Fish Toxicity (AUG), and Rainbow
36 Trout Toxicity (AUE). Genotoxicity, mutagenicity and carcinogenicity was predicted with Case
37 Ultra using the following QSAR models: Human Carcinogenicity (A0J), Aneuploidy in Yeast
38 (A6A), mutagenicity in *Salmonella typhimurium* 5-strains (A7B) (including the strains TA97,
39 TA98, TA100, TA1535, TA1536, TA1537, TA1538), Micronucleus Formation *in vivo* composite
40 (A7S), Micronucleus Formation *in vivo* Mouse (A7T), Chromosome Aberrations *in vitro*
41 composite (A7U), Chromosome Aberrations *in vitro* CHO cells (A7V), Rat Carcinogenicity
42 (A0D), Mouse Lymphoma (ML), Mouse Carcinogenicity (A08), Mutagenicity Ames (A2H)
43 (Salmonella Ames mutagenicity updated from NTP, Genetox, FDA and others. It consists the *S.*
44 *typhimurium* strains TA97, TA98, TA100, TA102, TA104, TA1535, TA1536, TA1537, TA1538
45 using a different training set compared with A7B), Unscheduled DNA Synthesis (UDS) Induction
46 (A64).

47 The Oasis Catalogic software was used to predict acute toxicity towards *V. fischeri* after 5
48 min, 15 min and 30 min exposure (Acute Toxicity Vibrio Fischeri 5min/15min/30min v.01). In
49 addition to that, the Oasis Catalogic software predicts mutagenicity based on bacterial
50 mutagenicity (module mutagenicity v.04) in *S. typhimurium* (Salmonella Catalogic model (SC)).
51 The Leadscope software predicts genotoxicity and mutagenicity using the following four QSAR
52 modules: *In vitro* chromosome aberration (IVCA), Mammalian mutagenesis (MM), *In vivo*
53 micronucleus (IVMN), Bacterial mutagenesis (BM).

54 **Text S3**

55 A modified formula (1) was used for the calculation of the chronic luminescence
56 inhibition (chronic LI), which has been described before by Backhaus et al. (Backhaus et al.,
57 1997):

$$58 \quad LI_{24h} = 100 (I_{NC} - I_t) / I_{NC} \quad (1)$$

59 LI_{24h} = luminescence inhibition after 24 h (%); I_{NC} = average light intensity of the negative
60 controls after 24 h in relative luminescence units (RLU); I_t = light intensity of the test culture
61 after 24 h (RLU).

62 The measured optical density after 14 h was used for calculation of the growth inhibition
63 (GI) according to formula (2):

$$64 \quad GI_{14h} = 100 (OD_{NC} - OD_t) / (OD_{NC} - OD_0) \quad (2)$$

65 GI_{14h} = growth inhibition after 14 h (%); OD_t = optical density of the test culture after 14 h; OD_{NC}
66 = average optical density of the negative controls after 14 h; OD_0 = average optical density of the
67 negative controls after sample addition.

68 According to Menz et al. (Menz et al., 2013) the following thresholds were applied for the
69 identification of significant inhibition values: acute LI = 20% inhibition, chronic LI = 15%
70 inhibition, GI = 20% inhibition. In case of significant inhibition, analysis of concentration-
71 response relationships was performed by non-linear, logistic regression applying the function
72 “Four Parameter Logistic Curve”(3) to the normalized inhibition values.

$$73 \quad y = \min + (\max - \min) / (1 + (x / EC_{50})^{-Hillslope}) \quad (3)$$

74 y = inhibition in %; \min = bottom of the curve; \max = top of the curve; Hillslope = slope of the
75 curve at its midpoint; EC_{50} = x value for the curve point that is midway between the \max and \min
76 parameters (half-maximal effective concentration). Because of the low water solubility of TD and

77 phthalimide, only partial concentration-response curves could be obtained. Therefore, logistic
78 regression was conducted under the assumption that higher concentrations would reach a plateau
79 with a total inhibition (max = 100%). After fitting the data to the curve, EC₁₀ was derived from
80 the given plot equation using Formula (4).

$$81 \quad EC_{10} = EC_{50} (1/9)^{1/Hillslope} \quad (4)$$

82 Significant changes of inhibition during photolysis were identified by One Way ANOVA,
83 following post hoc multiple comparisons (Holm-Sidak method, overall significance level = 0.05),
84 in which the untreated sample after 0 min of irradiation was defined as the control group.

85 Non-linear regressions and analysis of variance (ANOVA) were performed with the statistical
86 software SigmaPlot 12 (Systat Software, USA).

87 **References:**

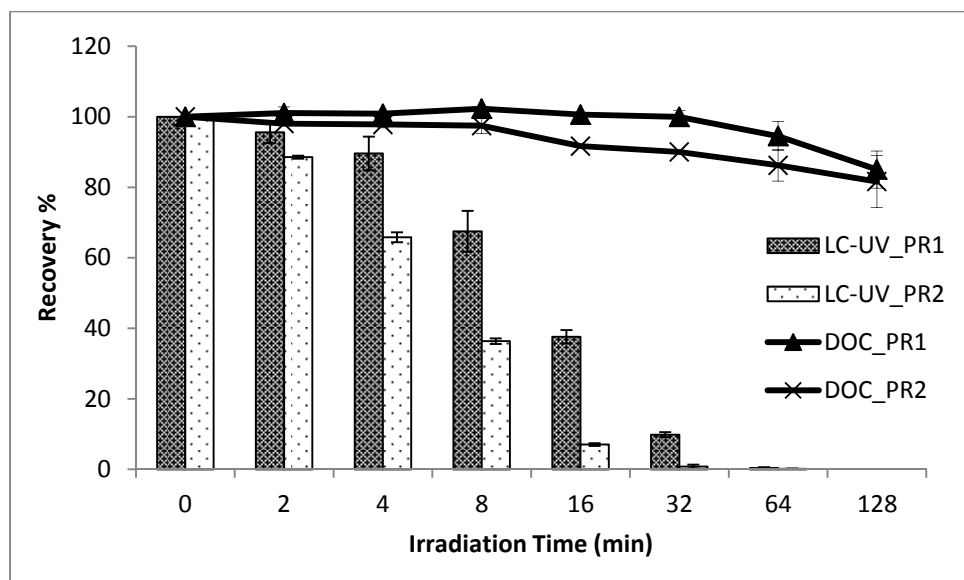
88 Backhaus, T., Froehner, K., Altenburger, R., Grimme, L.H., 1997. Toxicity testing with *Vibrio*
89 *Fischeri*: A comparison between the long term (24 h) and the short term (30 min) bioassay.
90 *Chemosphere* 35 (12), 2925–2938.

91 Menz, J., Schneider, M., Kümmerer, K., 2013. Toxicity testing with luminescent bacteria –
92 characterization of an automated method for the combined assessment of acute and chronic
93 effects. *Chemosphere* 93 (6), 990–996.

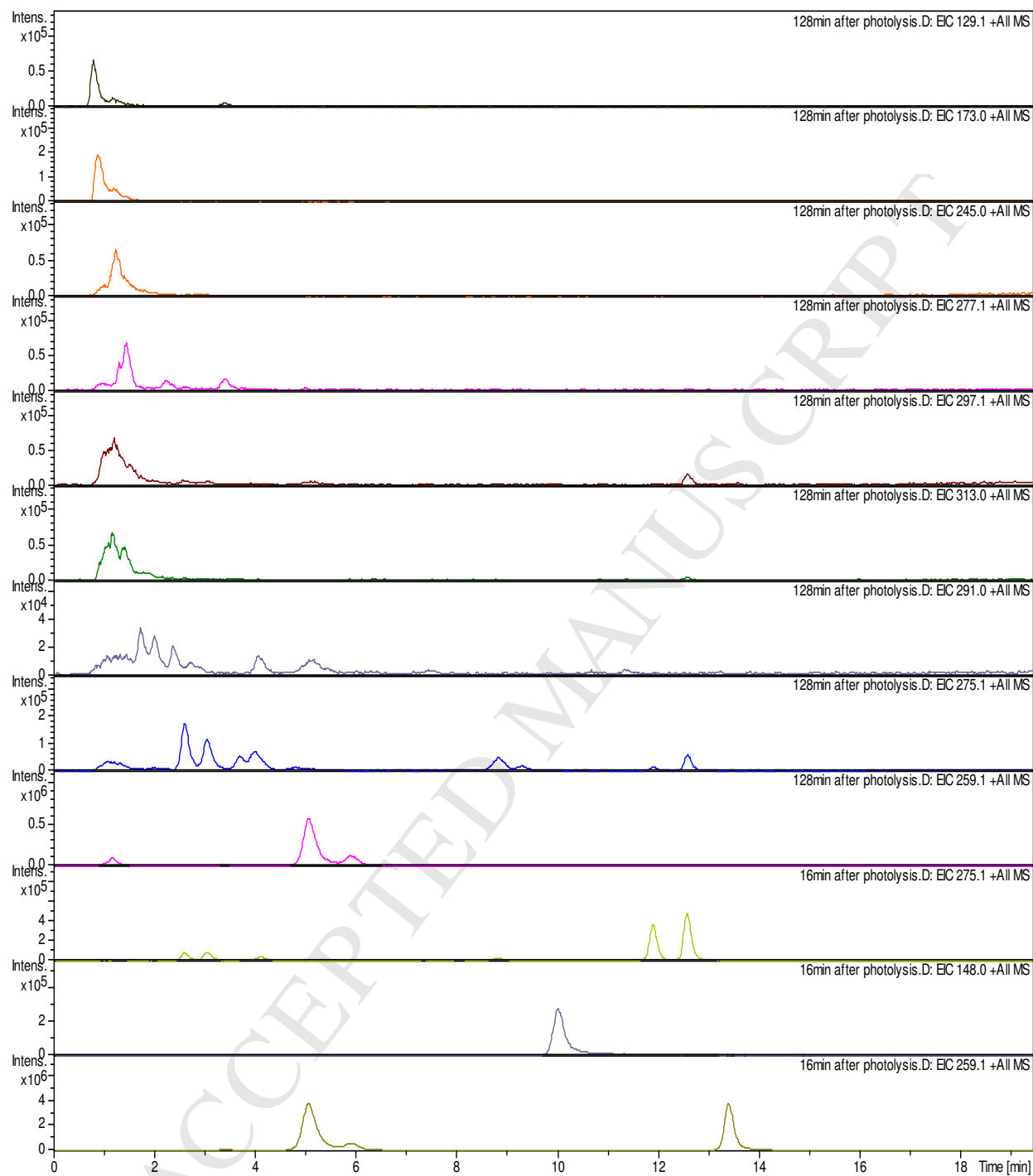
94 **Text S4**

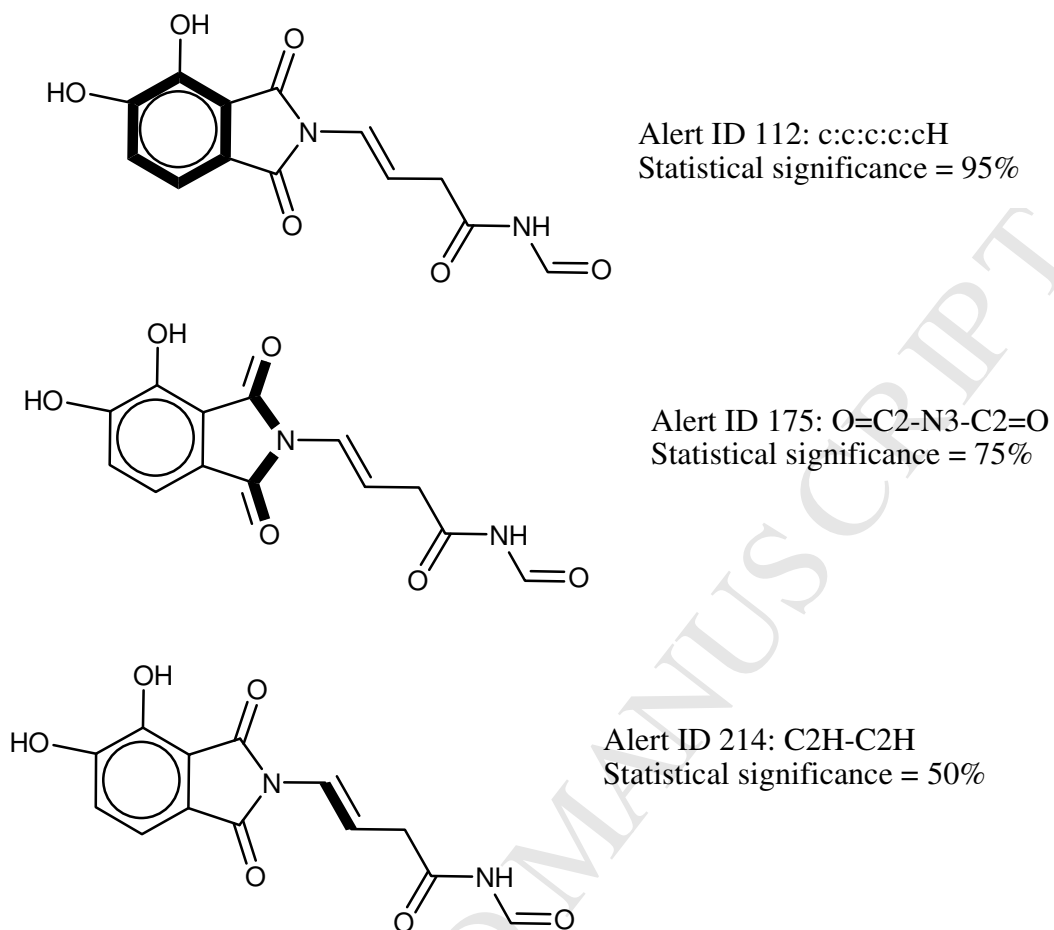
95 Of note is that the structural moieties responsible for the positive alert (Figure 6Figure 6)
96 are present in some other PTPs but these PTPs activities are predicted inconclusive or negative.
97 These inconclusive or negative predictions from the Microtox Toxicity to Environmental Bacteria
98 module (Case Ultra) are due to many reasons: 1. the presence of some other moiety responsible
99 for deactivation; 2. a significant portion of the test chemical is covered by unknown structural
100 fragments; 3. if multiple positive alerts were found then the prediction is made using the alert
101 with highest statistical significance even if the resulting activity based on the corresponding
102 compounds from the training set for this alert might be low; 4. If none of the positive alerts
103 contain any QSAR then the average activity of the alert is used as the predicted activity; 5. If a
104 positive alert contains a QSAR then the activity is calculated using the QSAR equation. For
105 example, PTP291_11 and PTP291_13 are predicted as negative in Microtox Toxicity to
106 Environmental Bacteria module although there are 3 positive alerts (alert Ids 112, 175, and 214)
107 predict in the molecule (supplementary material (Figure S 3)). Alert 112 obviously overrules
108 alerts 175 and 214, but refers to a low activity based on the training set examples containing this
109 alert.

110
111
112



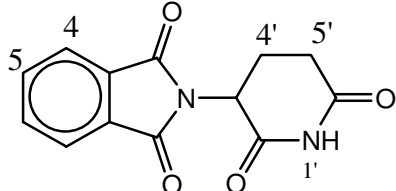
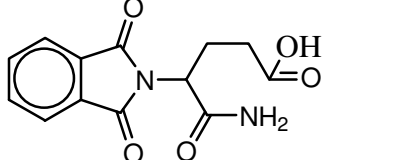
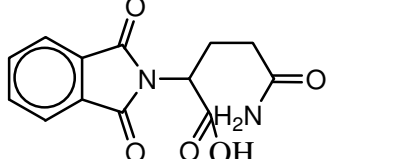
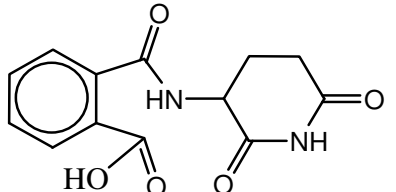
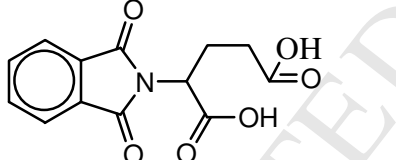
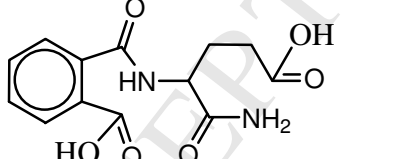
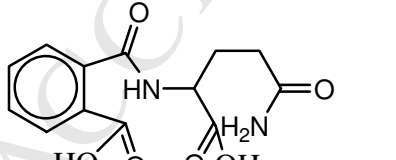
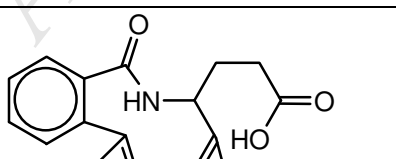
113
114 Figure S 1 Photodegradation of thalidomide (47 mg/L) in two different reactor volumes PR1
115 (800ml photoreactor) and PR2 (110 ml photoreactor) during UV-irradiation (n = 2). (DOC=
116 dissolved organic carbon)
117

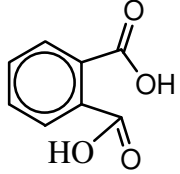
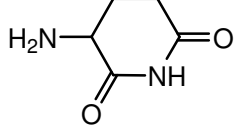
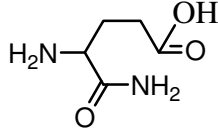
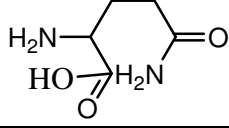
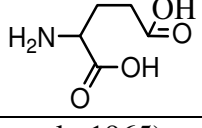




121
122
123 **Figure S 3** The structural moiety responsible for the positive alert in PTP 291_11 by Microtox
124 Toxicity to Environmental Bacteria model using Case Ultra software. Alert ID number is
125 provided by the software database. The structural moieties responsible for the alerts are presented
126 in bold.

127 **Table S 1** The structures of the previously reported HTPs*

Name	Structure	Chemical Formula	Smiles
Thalidomide		C ₁₃ H ₁₀ N ₂ O ₄	O=C(N2C3CCC(NC3=O)=O)c1cccc1C2=O
HTP_1		C ₁₃ H ₁₂ N ₂ O ₅	O=C(N2C(C(N)=O)CC(C(O)=O)c1cccc1C2=O
HTP_2		C ₁₃ H ₁₂ N ₂ O ₅	OC(C(CCC(N)=O)N2C(c1cccc1C2=O)=O)=O
HTP_3		C ₁₃ H ₁₂ N ₂ O ₅	O=C(O)c1cccc1C(NC2CCC(NC2=O)=O)=O
HTP_4		C ₁₃ H ₁₁ NO ₆	O=C(N2C(C(O)=O)CC(C(O)=O)c1cccc1C2=O
HTP_5		C ₁₃ H ₁₄ N ₂ O ₆	OC(CCC(C(N)=O)NC(c1c(C(O)=O)cccc1)=O)=O
HTP_6		C ₁₃ H ₁₄ N ₂ O ₆	OC(c1cccc1C(NC(C(O)=O)CCC(N)=O)=O)=O
HTP_7		C ₁₃ H ₁₃ NO ₇	OC(c1cccc1C(NC(C(O)=O)CCC(O)=O)=O)=O

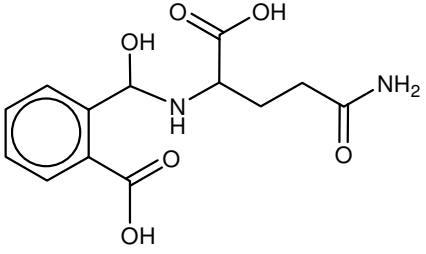
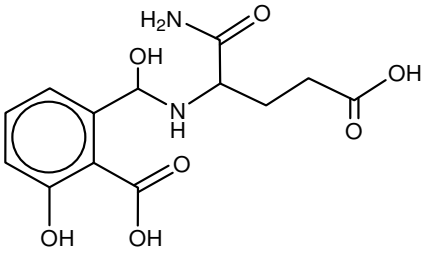
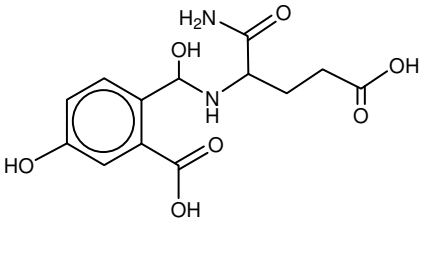
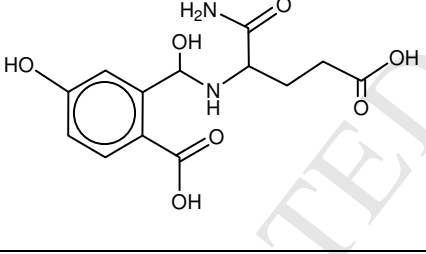
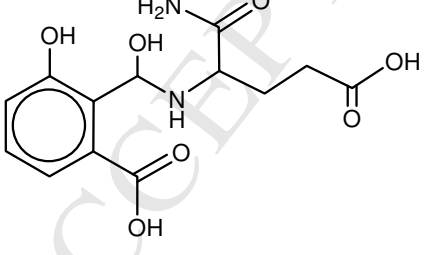
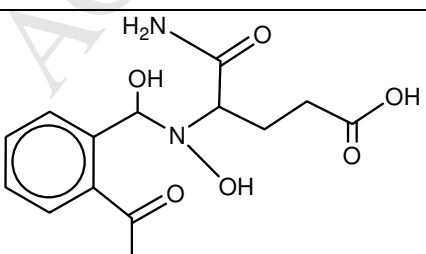
HTP_8		$C_8H_6O_4$	<chem>O=C(O)c1ccccc1C(O)=O</chem>
HTP_9		$C_5H_8N_2O_2$	<chem>NC1CCC(NC1=O)=O</chem>
HTP_10		$C_5H_{10}N_2O_3$	<chem>OC(CCC(N=O)N)=O</chem>
HTP_11		$C_5H_{10}N_2O_3$	<chem>OC(C(CCC(N=O)N)=O)N=O</chem>
HTP_12		$C_5H_9NO_4$	<chem>NC(C(O)=O)CCC(O)=O</chem>

128 *(Schumacher et al., 1965).

129

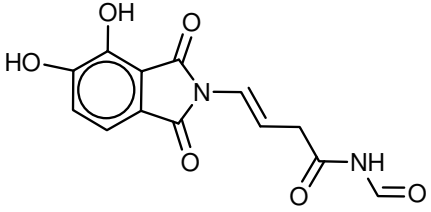
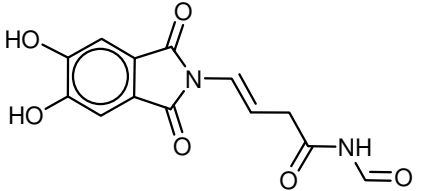
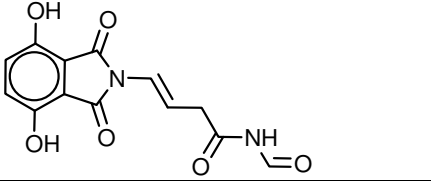
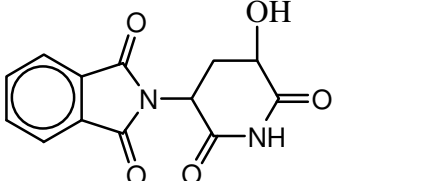
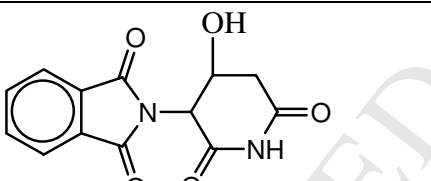
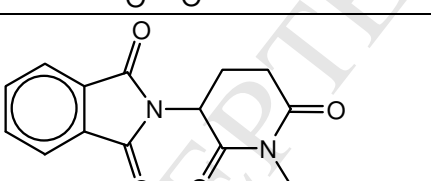
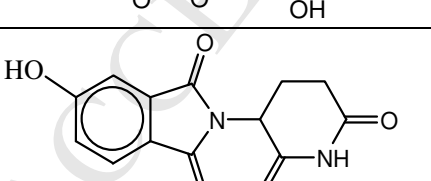
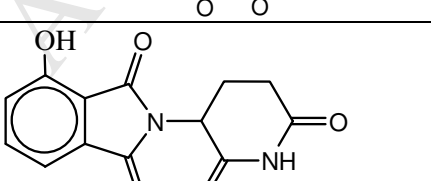
130 **Table S 2** The postulated structures of the identified PTPs

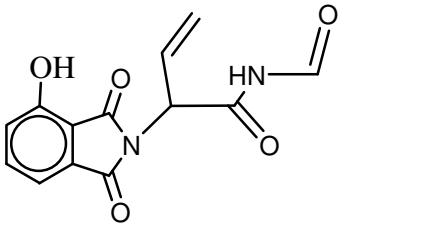
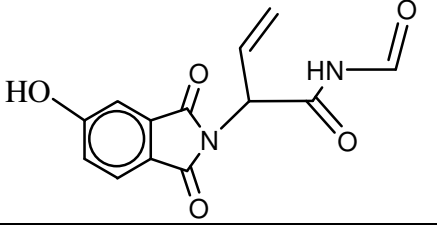
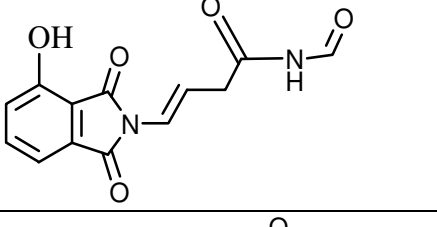
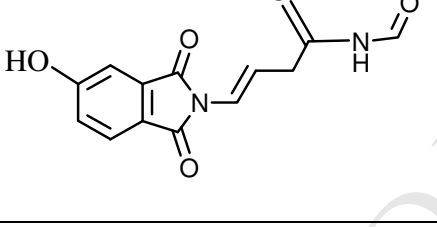
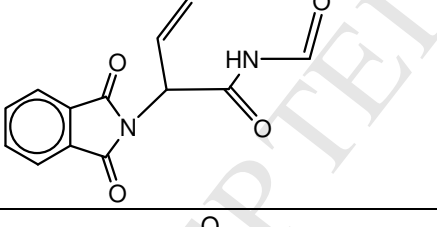
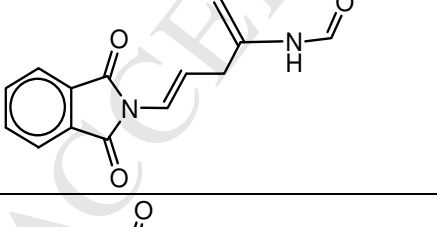
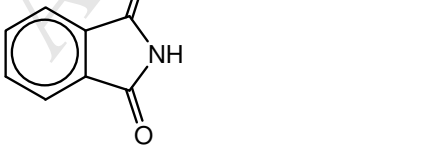
Name	Structure	Molecular Formula	Smiles
Thalidomide		C ₁₃ H ₁₀ N ₂ O ₄	O=C(N2C3CCC(NC3=O)=O)c1cccc1C2=O
PTP129_1		C ₅ H ₈ N ₂ O ₂	NC1CCC(NC1=O)=O
PTP 173_1		C ₆ H ₈ N ₂ O ₄	NC(/C(CCC(O)=O)=N/C=O)=O
PTP 173_2		C ₆ H ₈ N ₂ O ₄	OC(/C(CCC(N)=O)=N/C=O)=O
PTP 173_3		C ₆ H ₈ N ₂ O ₄	OC(NC1CCC(NC1=O)=O)=O
PTP277_1		C ₁₃ H ₁₂ N ₂ O ₅	O=CNC(C(CCO)N(C(C2=C1C=CC=C2)=O)C1=O)=O
PTP277_2		C ₁₃ H ₁₂ N ₂ O ₅	O=C(N2CC(O)CC(NC=O)=O)c1cccc1C2=O
PTP297_1		C ₁₃ H ₁₆ N ₂ O ₆	NC(C(CCC(O)=O)NC(O)C1=C(C(O)=O)C=CC=C1)=O

PTP297_2		$C_{13}H_{16}N_2O_6$	<chem>OC(C(CCC(N)=O)NC(O)C1=C(C(O)=O)C=CC=C1)=O</chem>
PTP313_1		$C_{13}H_{16}N_2O_7$	<chem>NC(C(CCC(O)=O)NC(O)C1=C(C(O)=O)C(O)=CC=C1)=O</chem>
PTP313_2		$C_{13}H_{16}N_2O_7$	<chem>NC(C(CCC(O)=O)NC(O)C1=C(C(O)=O)C=C(O)C=C1)=O</chem>
PTP313_3		$C_{13}H_{16}N_2O_7$	<chem>NC(C(CCC(O)=O)NC(O)C1=C(C(O)=O)C=CC(O)=C1)=O</chem>
PTP313_4		$C_{13}H_{16}N_2O_7$	<chem>NC(C(CCC(O)=O)NC(O)C1=C(C(O)=O)C=CC=C1O)=O</chem>
PTP313_5		$C_{13}H_{16}N_2O_7$	<chem>NC(C(CCC(O)=O)N(O)C(O)C1=C(C(O)=O)C=CC=C1)=O</chem>

PTP313_6		$C_{13}H_{16}N_2O_7$	<chem>OC(C(CCC(N)=O)NC(O)C1=C(C(O)=O)C(O)=CC=C1)=O</chem>
PTP313_7		$C_{13}H_{16}N_2O_7$	<chem>OC(C(CCC(N)=O)NC(O)C1=C(C(O)=O)C=C(O)C=C1)=O</chem>
PTP313_8		$C_{13}H_{16}N_2O_7$	<chem>OC(C(CCC(N)=O)NC(O)C1=C(C(O)=O)C=CC(O)=C1)=O</chem>
PTP313_9		$C_{13}H_{16}N_2O_7$	<chem>OC(C(CCC(N)=O)NC(O)C1=C(C(O)=O)C=CC=C1O)=O</chem>
PTP313_10		$C_{13}H_{16}N_2O_7$	<chem>OC(C(CCC(N)=O)N(O)C(O)C1=C(C(O)=O)C=CC=C1)=O</chem>
PTP291_1		$C_{13}H_{10}N_2O_6$	<chem>O=C(N2C3CC(O)C(NC3=O)=O)c1cc(O)ccc1C2=O</chem>
PTP291_2		$C_{13}H_{10}N_2O_6$	<chem>O=C(N2C3CCC(NC3=O)=O)c1c(O)c(O)ccc1C2=O</chem>

PTP291_3		C ₁₃ H ₁₀ N ₂ O ₆	O=C(N2C3CCC(NC3=O)=O)c1c(O)ccc(O)c1C2=O
PTP291_4		C ₁₃ H ₁₀ N ₂ O ₆	O=C(N2C3CCC(NC3=O)=O)c1cc(O)c(O)cc1C2=O
PTP291_5		C ₁₃ H ₁₀ N ₂ O ₆	O=C(N2C3CCC(NC3=O)=O)c1c(O)cc(O)cc1C2=O
PTP291_6		C ₁₃ H ₁₀ N ₂ O ₆	O=C(N2C(C=C)C(NC=O)=O)c1cc(O)cc(O)c1C2=O
PTP291_7		C ₁₃ H ₁₀ N ₂ O ₆	O=C(N2C(C=C)C(NC=O)=O)c1cc(O)c(O)cc1C2=O
PTP291_8		C ₁₃ H ₁₀ N ₂ O ₆	O=C(N2C(C=C)C(NC=O)=O)c1ccc(O)c(O)c1C2=O
PTP291_9		C ₁₃ H ₁₀ N ₂ O ₆	O=C(N2C(C=C)C(NC=O)=O)c1c(O)ccc(O)c1C2=O
PTP291_10		C ₁₃ H ₁₀ N ₂ O ₆	O=C(c1c(C2=O)c(O)cc(O)c1)N2/C=C/CC(NC=O)=O

PTP291_11		$C_{13}H_{10}N_2O_6$	<chem>O=C(c1c(C2=O)c(O)c(O)c1)N2/C=C/CC(NC=O)=O</chem>
PTP291_12		$C_{13}H_{10}N_2O_6$	<chem>O=C(c1c(C2=O)cc(O)c(O)c1)N2/C=C/CC(NC=O)=O</chem>
PTP291_13		$C_{13}H_{10}N_2O_6$	<chem>O=C(c1c(C2=O)c(O)ccc1O)N2/C=C/CC(NC=O)=O</chem>
PTP275_1		$C_{13}H_{10}N_2O_5$	<chem>O=C(N2C3CC(O)C(NC3=O)=O)c1cccc1C2=O</chem>
PTP275_2		$C_{13}H_{10}N_2O_5$	<chem>O=C(N2C3C(O)CC(NC3=O)=O)c1cccc1C2=O</chem>
PTP275_3		$C_{13}H_{10}N_2O_5$	<chem>O=C(N2C3CCC(N(O)C3=O)=O)c1cccc1C2=O</chem>
PTP275_4		$C_{13}H_{10}N_2O_5$	<chem>O=C(N2C3CCC(NC3=O)=O)c1ccc(O)cc1C2=O</chem>
PTP275_5		$C_{13}H_{10}N_2O_5$	<chem>O=C(N2C3CCC(NC3=O)=O)c1cccc(O)c1C2=O</chem>

PTP275_6		$C_{13}H_{10}N_2O_5$	<chem>O=C(N2C(C=C)C(NC=O)=O)c1cccc(O)c1C2=O</chem>
PTP275_7		$C_{13}H_{10}N_2O_5$	<chem>O=C(N2C(C=C)C(NC=O)=O)c1ccc(O)cc1C2=O</chem>
PTP275_8		$C_{13}H_{10}N_2O_5$	<chem>O=C(N(/C=C/CC(NC=O)=O)C2=O)C1=C2C(O)=CC=C1</chem>
PTP275_9		$C_{13}H_{10}N_2O_5$	<chem>O=C(N(/C=C/CC(NC=O)=O)C2=O)C1=C2C=C(O)C=C1</chem>
PTP259_1		$C_{13}H_{10}N_2O_4$	<chem>O=C(N2C(C=C)C(NC=O)=O)c1cccc1C2=O</chem>
PTP259_1		$C_{13}H_{10}N_2O_4$	<chem>O=C(N2/C=C/CC(NC=O)=O)c1cccc1C2=O</chem>
PTP148 (phthalimide)		$C_8H_5NO_2$	<chem>O=C(N2)c1cccc1C2=O</chem>

131
132

133 **Table S 3.** Predicted mutagenic activity of TD and its HTPs calculated with Salmonella t. 5-
 134 strains (A7B, Case Ultra), Mutagenicity Ames (A2H, Case Ultra), Salmonella Catalogic (SC,
 135 Oasis Catalogic), and Bacterial mutagenesis (BM, Leadscope).

Compounds	QSAR models*			
	A7B	A2H	SC	BM
Thalidomide	IN(O)	-	-	-
HTP1	IN(O)	-	-	-
HTP2	IN(O)	-	-	-
HTP3	-	-	-	-
HTP4	IN(O)	-	-	-
HTP5	-	-	-	-
HTP6	-	-	-	-
HTP7	-	-	-	-
HTP8	-	-	-	-
HTP9	-	-	-	-
HTP10	-	-	-	-
HTP11	-	-	-	-
HTP12	-	-	-	-

136 * negative (-), inconclusive orange (IN(O)).

137

Table S 4. Predicted QSAR toxicity of TD and its HTPs calculated with the following QSAR modules: Human Carcinogenicity (A0J), Aneuploidy in Yeast (A6A), Micronucleus Formation in vivo composite (A7S), Micronucleus Formation in vivo Mouse (A7T), Chromosome Aberrations in vitro composite (A7U), Chromosome Aberrations in vitro CHO cells (A7V), Rat Carcinogenicity (A0D), Mouse Lymphoma (ML), Mouse Carcinogenicity (A08), UDS Induction (A64), In vitro chromosome aberration (IVCA), Mammalian mutagenesis (MM), In vivo micronucleus (IVMN), Bioconcentration for Cyprinus Carpio (BCF), Gold Fish Toxicity (AUG), and Rainbow Trout Toxicity (AUE).

	QSAR genotoxicity and mutagenicity modules													QSAR ecotoxicity modules		
	AOJ	A6A	A7S	A7T	A7U	A7V	A0D	ML	A08	A64	IVCA	MM	IVMN	BCF	AUG	AUE
Thalidomide	-	IN	IN(O)	IN(O)	-	-	-	+	-	IN(O)	OD	+	OD	+	+	-
HTP1	-	IN	+	IN(O)	-	-	-	IN(O)	OD	OD	OD	-	OD	+	IN	-
HTP2	-	IN	+	IN(O)	-	-	-	IN(O)	OD	OD	-	-	+	IN	IN	-
HTP3	+	+	IN(O)	IN(O)	-	-	IN(O)	IN(O)	-	IN(O)	+	+	-	+	OD	OD
HTP4	-	+	+	IN(O)	-	-	-	IN(O)	-	OD	-	-	+	+	IN	-
HTP5	IN(O)	+	+	+	-	-	IN(O)	IN(O)	OD	-	-	-	+	+	OD	OD
HTP6	IN(O)	+	+	+	-	-	IN(O)	IN(O)	OD	-	-	-	+	+	OD	OD
HTP7	IN(O)	+	+	+	-	-	IN(O)	IN(O)	-	-	-	-	+	+	OD	OD
HTP8	-	+	-	-	-	-	-	+	-	-	-	-	-	+	OD	-
HTP9	-	+	IN(O)	IN(O)	-	-	-	+	-	IN	+	OD	+	+	OD	OD
HTP10	-	+	+	+	-	-	-	-	-	-	-	-	-	+	OD	OD
HTP11	-	+	+	+	-	-	-	-	-	-	-	-	-	IN	OD	OD
HTP12	-	+	+	+	-	-	-	-	-	-	-	-	-	+	OD	OD

*Positive (+), negative (-), inconclusive (IN), inconclusive orange (IN(O)), out of domain (OD)

Table S 5. Predicted bacterial toxicity of TD and its HTPs calculated with four acute toxicity models for *Vibrio fischeri* [Microtox Toxicity to Environmental Bacteria (AUA, Case Ultra) and three acute toxicity *Vibrio fischeri* models (Oasis Catalogic)]

Compounds	QSAR Models			
	AUA*	Acute tox 5min**	Acute tox 15min**	Acute tox 30min**
Thalidomide	+	4772	8452	22076
HTP1	IN(O)	5888	10655	28370
HTP2	+	5638	10384	27387
HTP3	-	23243	45640	149035
HTP4	IN(O)	1610	2653	5838
HTP5	-	29239	58092	194387
HTP6	-	29626	58545	196472
HTP7	-	7874	14337	39511
HTP8	-	259	366	670
HTP9	-	92675	190620	867736
HTP10	-	133202	269951	1277380
HTP11	-	14338732	42238272	3,95E+08
HTP12	-	3895611	10493339	80871480

*Positive (+), negative (-), inconclusive orange (IN(O)).

**PTPs with lower IC 50 (mg/L) than Thalidomide are presented in colored bold (orange is marginally lower and red is strongly lower).

Table S 6. Predicted mutagenic activity of TD and its PTPs calculated with Salmonella t. 5- strains (A7B, Case Ultra), Mutagenicity Ames (A2H, Case Ultra), Salmonella Catalogic (SC, Oasis Catalogic), and Bacterial mutagenesis (BM, Leadscope).

Compounds	QSAR models*			
	A7B	A2H	SC	BM
Thalidomide	IN(O)	-	-	-
PTP129_1	-	-	-	-
PTP 173_1	-	-	-	-
PTP 173_2	-	-	-	-
PTP 173_3	-	-	-	-
PTP277_1	IN(O)	-	-	-
PTP277_2	IN(O)	-	-	-
PTP297_1	-	-	-	OD
PTP297_2	-	-	-	-
PTP313_1	-	-	-	-
PTP313_2	-	-	-	-
PTP313_3	-	-	-	-
PTP313_4	+ (M)	IN(O)	-	-
PTP313_5	-	-	-	-
PTP313_6	-	-	-	-
PTP313_7	-	-	-	-
PTP313_8	-	-	-	-
PTP313_9	+ (M)	IN(O)	-	-
PTP313_10	-	-	-	-
PTP291_1	IN(O)	-	-	-
PTP291_2	-	IN(O)	-	-
PTP291_3	-	IN(O)	-	-
PTP291_4	-	-	-	-
PTP291_5	-	-	-	-
PTP291_6	-	-	-	-
PTP291_7	-	-	-	-
PTP291_8	-	IN(O)	-	-
PTP291_9	-	IN(O)	-	+
PTP291_10	-	-	-	-
PTP291_11	-	IN(O)	-	-
PTP291_12	-	-	-	-
PTP291_13	-	IN(O)	-	-
PTP275_1	IN(O)	-	-	-
PTP275_2	IN(O)	-	-	-
PTP275_3	IN(O)	-	-	-
PTP275_4	IN(O)	-	-	-
PTP275_5	-	IN(O)	-	-
PTP275_6	-	IN(O)	-	-
PTP275_7	IN(O)	-	-	-
PTP275_8	-	IN	-	-
PTP275_9	+	-	-	-
PTP148	+	-	-	-
PTP259_1	IN(O)	-	-	-
PTP259_2	+	-	-	-

*Positive (+), marginally positive (+(M)), negative (-), inconclusive (IN), inconclusive orange (IN(O)), out of domain (OD)

Table S 7. Predicted QSAR toxicity of TD and its PTPs calculated with the following QSAR modules: Human Carcinogenicity (A0J), Aneuploidy in Yeast (A6A), Micronucleus Formation in vivo composite (A7S), Micronucleus Formation in vivo Mouse (A7T), Chromosome Aberrations in vitro composite (A7U), Chromosome Aberrations in vitro CHO cells (A7V), Rat Carcinogenicity (A0D), Mouse Lymphoma (ML), Mouse Carcinogenicity (A08), UDS Induction (A64), Invitro chromosome aberration (IVCA), Mammalian mutagenesis (MM), In vivo micronucleus (IVMN), Bioconcentrationfor Cyprinus Carpio (BCF), Gold Fish Toxicity (AUG), and Rainbow Trout Toxicity (AUE).

	QSAR genotoxicity and mutagenicity													QSAR ecotoxicity models		
	AOJ	A6A	A7S	A7T	A7U	A7V	A0D	ML	A08	A64	IVCA	MM	IVMN	BCF	AUG	AUE
Thalidomide	-	IN	IN(O)	IN(O)	-	-	-	+	-	IN(O)	OD	+	OD	+	+	-
PTP129_1	-	+	IN(O)	IN(O)	-	-	-	+	-	IN(O)	+	OD	+	+	OD	OD
PTP 173_1	IN	IN	+	+	-	OD	OD	-	OD	OD	OD	-	OD	IN	OD	IN
PTP 173_2	OD	IN	IN(O)	IN(O)	-	OD	OD	-	OD	OD	OD	OD	OD	IN	OD	IN
PTP 173_3	+	+	IN(O)	IN(O)	-	-	-	IN(O)	OD	IN(O)	+	+	OD	+	OD	OD
PTP277_1	-	IN	-	-	-	-	-	+	OD	OD	+	+	+	IN	IN	OD
PTP277_2	-	IN	-	+	+(M)	-	IN	+	OD	OD	OD	-	OD	+	IN	OD
PTP297_1	OD	IN	+	IN(O)	-	-	OD	IN(O)	OD	OD	OD	OD	OD	IN	OD	IN
PTP297_2	OD	IN	+	IN(O)	-	-	-	IN	OD	OD	-	-	-	IN	OD	IN
PTP313_1	IN	IN	+	IN(O)	-	+	OD	IN(O)	OD	OD	-	-	-	IN	OD	IN
PTP313_2	OD	IN	+	IN(O)	IN(O)	IN(O)	OD	IN(O)	IN	OD	-	-	-	IN	OD	IN
PTP313_3	OD	IN	+	+	-	+(M)	OD	IN(O)	OD	OD	-	-	-	IN	OD	IN
PTP313_4	IN	IN	+	+	-	+	OD	-	OD	OD	-	-	-	IN	OD	OD
PTP313_5	OD	IN	+	IN(O)	OD	OD	OD	IN(O)	OD	OD	OD	+	-	IN	OD	IN
PTP313_6	IN	IN	+	IN(O)	-	+	-	IN(O)	OD	OD	-	-	+	IN	OD	IN
PTP313_7	OD	IN	+	IN(O)	IN(O)	IN(O)	-	IN(O)	IN	OD	-	-	-	IN	OD	IN
PTP313_8	OD	IN	+	+	-	+(M)	-	IN(O)	OD	OD	-	OD	+	IN	OD	IN
PTP313_9	IN	IN	+	+	-	+	-	-	OD	OD	-	-	+	IN	OD	OD
PTP313_10	OD	IN	+	IN(O)	OD	OD	OD	IN(O)	OD	OD	OD	OD	OD	IN	OD	IN
PTP291_1	-	OD	+	IN(O)	-	IN(O)	-	IN(O)	+	OD	+	+	+	IN	IN	-
PTP291_2	+(M)	IN	IN(O)	IN(O)	-	+	IN(O)	+	-	IN(O)	+	+	-	+	+	-
PTP291_3	+(M)	IN	IN(O)	IN(O)	+	+	IN(O)	+	-	IN(O)	+	+	+	+	+	-
PTP291_4	-	IN	IN(O)	IN(O)	-	-	-	+	+	IN(O)	+	+	-	+	+	-
PTP291_5	-	IN	IN(O)	IN(O)	+	+	-	+	+	IN(O)	+	+	+	+	+	-
PTP291_6	-	OD	+	IN(O)	+	+	-	IN(O)	IN	OD	OD	+	OD	IN	IN	OD

Continue Table S 7

	QSAR genotoxicity and mutagenicity													QSAR ecotoxicity models		
	AOJ	A6A	A7S	A7T	A7U	A7V	A0D	ML	A08	A64	IVCA	MM	IVMN	BCF	AUG	AUE
PTP291_7	-	OD	+	IN(O)	-	-	-	IN(O)	IN	IN	OD	+	OD	IN(O)	IN	OD
PTP291_8	+(M)	OD	+	IN(O)	-	+	IN(O)	IN(O)	OD	OD	OD	+	OD	IN	IN	OD
PTP291_9	+(M)	OD	+	IN(O)	+	+	IN(O)	IN(O)	OD	OD	+	+	+	IN	IN	OD
PTP291_10	-	OD	+	+	+	+	OD	+	IN	OD	-	+	+	IN	IN	OD
PTP291_11	+(M)	OD	+	+	-	+	+	+	IN	OD	+	+	+	IN	IN	OD
PTP291_12	-	OD	-	+	-	-	OD	+	IN	IN	+	+	+	IN	IN	OD
PTP291_13	+(M)	OD	-	+	+	+	+	+	IN	OD	+	+	+	IN	IN	OD
PTP275_1	-	IN	+	+(M)	-	-	-	IN(O)	-	OD	+	+	+	IN	IN	-
PTP275_2	-	IN	+	IN(O)	-	-	-	+	-	OD	OD	+	OD	IN	IN	-
PTP275_3	-	IN	-	-	-	-	-	+	OD	+	OD	+	OD	IN	+	-
PTP275_4	-	IN	IN(O)	IN(O)	-	IN(O)	-	+	+	IN(O)	+	+	+	+	+	-
PTP275_5	+(M)	IN	IN(O)	IN(O)	-	+	-	+	-	IN(O)	+	+	+	+	+	-
PTP275_6	+(M)	IN	+	IN(O)	-	+	-	IN(O)	OD	OD	+	+	+	IN	IN	OD
PTP275_7	-	OD	+	IN(O)	-	IN(O)	-	IN(O)	IN	OD	OD	+	OD	IN	IN	OD
PTP275_8	+(M)	IN	-	+	-	+	OD	+	IN	OD	-	+	+	IN	IN	OD
PTP275_9	-	OD	-	+	-	IN(O)	OD	+	IN	OD	-	+	+	IN	IN	OD
PTP148	-	+	+	+	-	-	+	IN(O)	-	-	+	+	+	+	-	-
PTP259_1	-	IN	+	IN(O)	-	-	-	IN(O)	OD	OD	OD	+	OD	IN	IN	OD
PTP259_2	-	IN	-	+	-	-	OD	+	IN	OD	OD	+	OD	IN	IN	OD

*Positive (+), marginally positive (+(M)), negative (-), inconclusive (IN), inconclusive orange (IN(O)), out of domain (OD)

Table S 8. Predicted bacterial toxicity of TD and its PTPs calculated with four acute toxicity models for *Vibrio fischeri* [Microtox Toxicity to Environmental Bacteria (AUA, Case Ultra) and three acute toxicity vibrio *fischeri* models (Oasis Catalogic)]

Compounds	QSAR Models			
	AUA*	Acute tox 5min**	Acute tox 15min**	Acute tox 30min**
Thalidomide	+	4772	8452	22076
PTP129_1	-	92675	190620	867726
PTP 173_1	OD	32582	65946	243584
PTP 173_2	OD	30131	62966	228602
PTP 173_3	OD	1121726	2835106	17687038
PTP277_1	+	61705	135798	508310
PTP277_2	+	62610	136972	514351
PTP297_1	OD	143405	319377	1348079
PTP297_2	OD	2227087	6199375	38976000
PTP313_1	OD	165682	370706	1586430
PTP313_2	OD	375217	906459	4361442
PTP313_3	OD	369000	897552	4302719
PTP313_4	OD	383116	917690	4435801
PTP313_5	OD	711124	1753250	9301782
PTP313_6	OD	2622604	7277318	46582816
PTP313_7	OD	5684938	17340104	123596776
PTP313_8	OD	5797778	17542722	125583680
PTP313_9	OD	6180744	18218648	132273640
PTP313_10	OD	674733	1699652	8913655
PTP291_1	+	258017	629915	2885552
PTP291_2	IN	7429	13692	37419
PTP291_3	IN	1655	2708	5948
PTP291_4	+	33939	69973	238877
PTP291_5	+	7461	13728	37555
PTP291_6	+	7065	13064	35406
PTP291_7	+	32233	66704	225745
PTP291_8	IN	7053	13051	35354
PTP291_9	IN	1548	2559	5553
PTP291_10	+	7067	13130	35559
PTP291_11	-	7176	13248	36000
PTP291_12	+	32144	66917	226158
PTP291_13	-	1572	2594	5643
PTP275_1	+	97158	219631	880525
PTP275_2	+	14066	27275	82536
PTP275_3	+	47002	100010	360895
PTP275_4	+	12743	24356	72723
PTP275_5	+	2797	4774	11419
PTP275_6	+	2665	4560	10820
PTP275_7	+	12108	23224	68751
PTP275_8	+	2679	4596	10909
PTP275_9	+	12139	23371	69171
PTP148 (phthalimide)	-	146	200	343
PTP259_1	+	4541	8067	20896
PTP259_2	+	4516	8079	20888

*Positive (+), negative (-), inconclusive (IN), out of domain (OD)

**PTPs with lower IC 50 (mg/L) than Thalidomide are presented in colored bold. (orange is marginally lower and red is strongly lower).